

Union Schweizerischer Gesellschaften für Experimentelle Biologie
Berichte der 12. Jahresversammlung

Union des Sociétés Suisses de Biologie Expérimentale
Comptes rendus de la 12^e Réunion annuelle

Union of Swiss Societies of Experimental Biology
Abstracts of the 12th Annual Meeting

Basel, 13./14. März 1980

PHYSIOLOGIE – PHYSIOLOGY

Control of burst conductances in *Aplysia* neurone R15

W. B. Adams and I. B. Levitan, *Friedrich-Miescher-Institut, P.O. Box 273, CH-4002 Basel*

Bursting in *Aplysia* cell R15 is mediated by slow changes in membrane conductance. The conductance changes are, in turn, controlled by the cell's electrical activity to provide the feedback necessary to maintain regular bursting. We have studied 2 slow conductance pathways that are activated by action potentials: a sodium conductance that peaks 0.5 sec after the action potential; and an outward current, carried by an as yet unidentified ion, that peaks 2–5 sec later. Both currents are sensitive to changes in composition of the bathing medium and both are affected by synaptic inputs and by application of putative neurotransmitters. As a result, the bursting pattern of cell R15 can be modulated by direct control of the conductances that produce bursting.

Projections of precentral motor cortex (area 4) upon so-called association nuclei (MD, LP) of the thalamus in the monkey

K. Akert, K. Hartmann-von Monakow and H. Künzle, *Institut für Hirnforschung der Universität Zürich, CH-8029 Zürich*

The projections of area 4 (precentral) motor cortex upon thalamic association nuclei medialis dorsalis and lateralis posterior have been established by means of autoradiographic tracer methods in 8 monkeys (*Macaca fascicularis*). MD receives connections predominantly from the facial representation, while LP seems to have preferentially dense projections from limb areas. These pathways may be important cortico-thalamo-cortical links in a feedback control of motor command systems since MD and LP project in turn to prefrontal and posterior parietal cortex respectively.

Coupled stretch reflexes in human ankle flexor and extensor muscles

J. H. J. Allum, *Brain Research Institute, CH-8029 Zürich*

The timing of short and medium latency stretch reflexes in human ankle muscles was investigated during quiet standing. Rapid changes of muscle length were applied to tibialis anterior (TA) and triceps surae muscles (TS) by rotating a level platform, on which subjects stood with eyes closed, about the axis of the ankles. 3 distinguishable phases of EMG activity were observed which could be classified into 2 types of reflexes. At 40 msec, a short latency reflex was observed on TS stretch, but not when TA was stretched. Medium latency reflexes occurred at times dependent on the muscle stretched. On stretching TS muscles the TS reflex occurred at 90 msec followed 40 msec later by a time locked response in TA. On stretching TA the response ordering was reversed (90 msec in TA and 40 msec later in TS). The results demonstrate that stretch reflexes in ankle muscles are organized as a reciprocal couple producing first an excitatory response in the stretched muscle and then an excitatory response in the released muscle.

Cross-correlation analysis of connectivities between motor cortex neurons of the monkey

J. H. J. Allum, M.-C. Hepp-Reymond and R. Gysin, *Brain Research Institute, CH-8029 Zürich*

Pairs of cells were recorded within the hand region of the precentral motor cortex of monkeys trained to squeeze a

force transducer between the thumb and index finger. Neuronal discharges related to the task, were analyzed only during periods of constant isometric force. Each cell pair was recorded with a single electrode, thus recorded potentials are a linear summation of the individual action potentials. Prior to the cross-correlation analysis, computer programs separated the sampled potentials using a template technique. Cross-correlograms in the majority of the cases had a sharp peak or a sharp trough followed by a sharp peak at latencies suggesting monosynaptic causal relations between the cell discharges.

Membrane properties of solitary rod photoreceptors

C. R. Bader, P. R. MacLeish and E. A. Schwartz, *Département de Physiologie, Ecole de Médecine, CH-1211 Genève 4, Department of Neurobiology, Harvard Medical School, Boston, MA 02115, USA, and Department of Pharmacological and Physiological Sciences, University of Chicago, Chicago, IL 60647, USA*

Single, isolated rod photoreceptors were obtained by enzymatic dissociation of tiger salamander retina. These solitary cells retained the morphological and physiological features of rods in the intact retina and could be maintained in culture for several days. The properties of the current modified by light stimulation of rods was studied by voltage clamp. The maximum amplitude of the voltage-clamp current produced by a flash or step of light was a nonlinear function of membrane potential but no time dependence of this nonlinearity was observed. This current was nearly constant in the physiological range of membrane potentials. Thus, in this domain, the phototransduction mechanism behaves like a constant current generator.

Baroreceptors: do they also signal cardiac output?

A. J. Baertschi and J. D. Charlton, *Department of Animal Biology, University of Geneva, CH-1211 Geneva 4*

Previous work (J. Physiol., Lond. 273, 1, 1977) showed that atrial stretch receptors may signal venous return. To test the hypothesis that arterial baroreceptors are sensitive to cardiac output, single baroreceptor activity in rat left aortic nerves was monitored while sinusoidal aortic flow pulses were applied through the right carotid artery by a pump. Fibre impulse rate was largest during pump instroke (IS), although aortic mean and pulse pressures were lower than at begin of outstroke (OS). Descending aortic flow increased and decreased 20% during IS and OS, respectively. Nerve impulses, averaged together with aortic pressure on LSI-11 computer increased $29 \pm 6\%$ SEM ($n=15$) and decreased $32 \pm 12\%$ ($n=4$) with respect to control during IS and OS, respectively, with no significant differences in aortic pulse pressure. Nerve impulses were added (IS) or lost (OS) in early diastole. Results suggest that aortic baroreceptors signal changes in aortic flow even in the absence of aortic mean or pulse pressure changes.

Light adaptation in photoreceptors of the honeybee drone

F. Baumann, *Département de Physiologie, Ecole de Médecine, CH-1211 Genève 4*

Effects of local adaptation were studied in retinula cells of the honeybee drone by means of intracellular recording. The test stimulus was a narrow bar of light, positioned perpendicularly to the cell. After exposure to a white

adapting light, that stimulated a small fraction of the total length of the cell, the sensitivity was found to be decreased over the whole length of the cell. A similar reversible effect was observed with a violet adapting light. At the site of illumination with violet light however, the sensitivity remained depressed and recovered only after illumination with green light. These results are explained by the existence of 2 mechanisms responsible for light adaptation; one is diffuse, affects the whole cell and may be ionic in nature, the other is restricted to the site of adaptation and related to localized changes in the photopigment concentration.

Synaptic delays in fish spinal cord

I.R. Baumann, H.R. Lüscher, H.G. Goldscheider, N.G. Greeff and G.M. Yasargil, Department of Physiology, University of Zürich, CH-8028 Zürich

Excitatory and inhibitory delays (e.s.d.; i.s.d.) in synaptic transmission between Mauthner (M) axon collaterals and motoneurons (m.n.) were measured in tench spinal cord *in situ*, using extracellular recording as to define the arrival time of the impulses in the M-axons and the onset of the composite excitatory and inhibitory postsynaptic potentials. If either of the impulses in both M-axons arrived within an interval of less than 0.1 msec, their excitatory effects were mutually inhibited (minimum ipsilateral e.s.d.=0.8 msec; minimum contralateral e.s.d.=2.1 msec; minimum contralateral i.s.d.=1.1 msec (n:10) at 10°C). If the impulse in 1 M-axon arrived later than 0.1 msec, its excitatory effects being still suppressed, its inhibitory effects disappeared before the synaptic transmission of the excitatory effects of the earlier activated M-axon was completed. We conclude that the targets of the mutual inhibition are the m.n.'s with short e.s.d. and the internuncial excitatory interneurons, but not the m.n.'s with delayed minimum e.s.d.

Selective axonal transport of ³H-D-aspartate in the pigeon retinotectal pathway

A. Beaudet, A. Burkhalter, J.C. Reubi and M. Cuénod, Brain Research Institute, CH-8029 Zürich

Recent reports have suggested that amino acids can be selectively taken up and retrogradely transported in neurons where they normally serve as neurotransmitters. The present radioautographic study shows that D-aspartate (asp), which shares high affinity uptake properties with L-asp and L-glutamate (glu), can be both retrogradely and anterogradely transported in the pigeon retinotectal pathway. 6 h after intratectal instillation of ³H-D-asp, an important contingent of retinal afferent fibres can be traced back to their parent perikarya in the ganglion cell layer. Conversely, when ³H-D-asp is injected into the eye, retinofugal fibres are found to be labeled up to the optic tectum. These fibres originate from small, heterogeneously distributed ganglionic neurons. Biochemical measurements confirm that more than 80% of the radioactivity recovered in tectum corresponds to free D-asp. These findings are consistent with the hypothesis that glu and/or asp are involved in retinotectal neurotransmission.

Serotonin-induced increases in K⁺ conductance in *Aplysia* neurone R15 are mediated by cyclic AMP

J. Benson, A. Drummond and I. Levitan, Friedrich-Miescher-Institut, P.O. Box 273, CH-4002 Basel

In the bursting neurone R15, bath perfusion with serotonin (5HT) at concentrations between 0.05 μ M and 10 μ M produced a current measured under voltage clamp. The

reversal potential for this current was about -78 mV in normal medium, and varied in a Nernstian fashion with change in external [K⁺], suggesting that the current is carried largely by K⁺ ions. This effect was mimicked by bath application of the phosphodiesterase-resistant cAMP analog PCPT-cAMP at 0.7 mM. When 10 μ M 5HT was applied to the neurone during treatment with cAMP analog, no further increase in outward current was measured. Specific 5HT receptor antagonists blocked current produced by 5HT but not by cAMP analog. Previous studies have shown that 5HT stimulates adenylate cyclase activity in membranes from isolated R15 cell bodies. 5HT also causes cAMP to accumulate in R15 in intact ganglia. These and other observations lead to the conclusion that the K⁺ conductance increase induced in R15 by 5HT is mediated by cAMP.

Oxytocin: a major corticotropin releasing factor (CRF) of the diabetes insipidus (DI) rat posterior pituitary

J.L. Bény, M. Friedli and A.J. Baertschi, Department of Animal Biology, University of Geneva, CH-1211 Geneva 4

CRF released from normal rat posterior pituitaries (PP) *in vitro* is predominantly vasopressin (Neuroendocrinology, *in press*). DI rats lack vasopressin yet release ACTH in response to stress. Therefore, CRF released from DI rat PP *in vitro* was bioassayed with dispersed adenohypophyseal and adrenal cells. Following electrical stimulation of PP at 30 Hz for 15 min (5 sec on and off), CRF release increases $33 \pm 15\%$ SEM (n=4) over control. The concomitant oxytocin release is 3.2 ± 0.2 mU and can account for the CRF effect, since 3.2 mU oxytocin has CRF activity not different ($p > 0.45$) from that of stimulated PP media. CRF activities are abolished by treatment with thioglycollate. PP extracts from DI rats has $70 \pm 23\%$ (n=8) more CRF activity than can be explained by their oxytocin content. Although a CRF distinct from oxytocin can be extracted, oxytocin is the major CRF released from PP in the DI rat.

Insulin secretion following ventral brain stem stimulation

D.A. Bereiter, M. Brunsmann, H.R. Berthoud and B. Jeanrenaud, Laboratoires de Recherches Médicales, 64, avenue de la Roseaie, CH-1205 Genève

Unilateral electrical stimulation of the ventral brain stem in the region of nucleus ambiguus (Amb) caused a prompt rise in peripheral insulin levels (IRI) without significantly altering blood glucose (BG). Male rats anesthetized with α -chloralose/urethane (25 mg/kg:250 mg/kg) received unilateral electrical stimulation (50 μ A, 30 Hz, 0.2 msec, biphasic) for 3 min in one of several ventral brain stem structures. All blood samples were taken from a jugular catheter. Among the various brain stem structures stimulated, only the Amb group showed a consistent elevation in IRI during the stimulation period ($p < 0.01$). As previous anatomical studies have shown Amb to be one source of vagal efferents innervating the pancreas (Laughton and Powley, 1979), the present physiological experiments suggest that the observed rise in IRI following Amb stimulation reflects this vagal innervation of the endocrine pancreas.

Noise analysis at neuromuscular junctions formed by the N. vagus

H.R. Brenner and P. Breitschmid, *Department of Physiology, University of Basel, CH-4051 Basel*

In skeletal muscle, the gating of receptor channels in the endplate membrane is faster than that of extrasynaptic channels responsible for denervation hypersensitivity (Nehrer and Sakmann, *J. Physiol.*, Lond. 258, 705, 1976). Rapidly gating channels are also induced by motoneurons forming ectopic endplates in the extrasynaptic region (Brenner and Sakmann, *Nature* 271, 366, 1978). The question arises whether preganglionic autonomic neurons forming synapses on skeletal muscle can influence channel gating. Experiments were carried out on frog ectopic neuromuscular synapses formed de novo by fibres of the N. vagus and on denervated motor endplates reinnervated by the same nerve. Analysis of acetylcholine induced current fluctuations recorded from vagus junctions revealed channels with gating properties similar to those of normal endplate channels. Synaptic currents in response to indirect stimulation were abolished by α -bungarotoxin.

Changes in [^{14}C]-2-deoxyglucose labeling pattern in visual structures of monocularly deprived pigeons

A. Burkhalter and P. Streit, *Brain Research Institute, CH-8029 Zürich*

The [^{14}C]-2-deoxyglucose method was used to study changes in cerebral functional activity of visually deprived pigeons. Subjects were raised for 6–11 months with 1 eye occluded. At the end of deprivation 50 μCi [^{14}C]-2-deoxyglucose was injected in 3 groups of 2 animals: During 45 min both eyes were free (DBE) or 1 eye covered either the deprived (DDE) or the nondeprived one (DEE). Normal vision for 8 days prior to the injection was allowed in 2 other pigeons (DBE-8). Animals exposed binocularly (BE) or monocularly (ME) served as controls. In groups DDE, DEE and ME labeling of all known visual structures was heavier contralateral to the exposed eye. The asymmetry in DBE and weaker also in DBE-8 was restricted to the visual wulst, where labeling was stronger contralateral to the deprived eye. Symmetry in all the structures was found in BE animals. Present data suggest a functional change in an area of binocular convergence which consists in an increased glucose consumption of the deprived system.

Insulin sensitivity in man studied by indirect calorimetry during euglycemic glucose clamp

B. Burnand, M. Hurni, E. Maeder and E. Jequier, *Institut de Physiologie, Bugnon 7, CH-1011 Lausanne*

During continuous glucose infusion ($1 \text{ mmole m}^{-2} \text{ min}^{-1}$), insulin (I) was simultaneously infused, in 9 healthy young subjects, to maintain euglycemic levels. Glycemia was continuously monitored using an autoanalyzer. Under these glucose clamp conditions, endogenous I secretion was inhibited as reflected by the decrease in C peptide levels. I requirements were $30 \pm 2 \text{ mU m}^{-2} \text{ min}^{-1}$ for an average glycemia of $4.8 \pm 0.1 \text{ mmol l}^{-1}$. Carbohydrate oxidation rate, determined from nonprotein RQ, was 0.37 ± 0.04 and $0.81 \pm 0.04 \text{ mmol min}^{-1}$ before (fast of 12 h) and during glucose clamp respectively. The amount of glucose infused in 1 h was $109 \pm 3 \text{ mmol}$ and glucose oxidized was $49 \pm 3 \text{ mmol}$; the difference being assumed to be the net glucose stored. This procedure will allow to study 2 aspects of insulin resistance: a) the amount of insulin infused is inversely related to the sensitivity of the insulin-mediated

glucose uptake; b) the degree of impairment of glucose oxidized should reflect intracellular defect in glucose metabolism.

The localization of medial rectus motoneurons in the monkey oculomotor nucleus

J.A. Büttner-Ennever, M.A. Glicksman and W. Lang, *Brain Research Institute, University of Zürich, CH-8029 Zürich, and Department of Pathology, Universitätsspital, CH-8091 Zürich*

During an anatomical investigation of premotor inputs onto the oculomotor nucleus (III), it became necessary to verify the exact location of the medial rectus (MR) motoneurons in the macaque monkey. The following set of experiments show that the generally accepted organization of MR motoneurons is incomplete. Retrograde tracer substances: ^{125}I -labelled wheat germ agglutinin and horseradish peroxidase (HRP) were injected into eye muscles. The accidental uptake of tracer by other eye muscles was always carefully controlled. 3 clearly separate groups of MR motoneurons were found to be labelled in III: (A) the classical area described by Warwick (1953), (B) a large group lying more dorsal and (C) a third midline group lying on the dorsal medial border of the classical III. Group C was labelled almost exclusively if the injection only filled the outer (orbital) layer of the muscle. Structure and function of this layer differ from that of the inner, or global layer.

Descending afferent projections to the lateral reticular nucleus of the rat

C.E. Chapman and M. Wiesendanger, *Institut de Physiologie, Université de Fribourg, CH-1700 Fribourg*

Previous studies have indicated that the lateral reticular nucleus (LRN), a precerebellar relay nucleus, plays a role in motor control. The aim of this study was to investigate, by means of retrograde tracing methods, supraspinal inputs to the LRN. First, the LRN was identified electrophysiologically and then HRP was injected with a microsyringe or iontophoresed from a micropipette. Labelled cells were found in layer V of the contralateral cerebral cortex within the confines of the somatosensory cortex, especially in the face area. More rostrally (near the frontal pole) a dorsolateral strip of labelled cells was found which partially overlapped the facial motor area. It seemed unlikely that labelling of the cortical facial area was due to spread of HRP into the trigeminal nucleus since a similar distribution pattern was obtained in cases with reaction products confined to the LRN. Labelling was also found in the caudal two-thirds of the magnocellular red nucleus (contralaterally). Finally, labelling was seen in the transitional zone between the ipsilateral interposate and lateral nuclei of the cerebellum. Only sparse labelling was seen in the contralateral fastigial nucleus.

Secondary effects of stimulation and inhibition of active $\text{Na}^+ - \text{K}^+$ -transport on the heat production rate (\dot{E}) of mouse soleus muscle

A. Chinet, T. Clausen and R. Dubois-Ferrière, *Département de Physiologie, 20, rue de l'Ecole-de-Médecine, CH-1211 Genève 4, and Fysiologisk Institut, Århus University, Århus, Denmark*

In the isolated mouse soleus muscle, stimulation of active $\text{Na}^+ - \text{K}^+$ -transport with the β_2 -agonist salbutamol leads to a small transitory rise in \dot{E} , followed by a sustained

decrease. Conversely, inhibition of the Na^+ - K^+ -pump with ouabain produces a transitory drop in \dot{E} , followed by a sustained and progressive increase. These secondary changes in \dot{E} may be related to decreases and increases in the intracellular Na^+ concentration (Na_i^+). In Na^+ -substituted media, where Na_i^+ is decreased, a sustained drop in \dot{E} is observed, which cannot be accounted for by the diminished energy demand of the Na^+ - K^+ -pump only. Such changes in the basal metabolic rate, which can also be seen in other tissues (e.g. brown adipose tissue of the rat), could reflect Na_i^+ -dependent changes in the energy dissipation by the mitochondrial calcium cycle (Carafoli, FEBS Lett. 104, 1, 1979).

Pituitary receptor sites for LHRH: their relationship to regulation of gonadotropins secretion

B.S. Conne, S. Scaglioni, U. Lang, P.C. Sizonenko and M.L. Aubert, Department of Pediatrics, University School of Medicine, CH-1211 Geneva 4

Pituitary plasma membranes contain high affinity, low capacity binding sites for LHRH, that are likely to represent specific receptor sites for this hypothalamic hormone. The use of a highly potent analog of LHRH, DesGly¹⁰[DTrp⁶, (N-Et)Pro⁹]LHRH as radioiodinated tracer allows a specific and sensitive measurement of these receptor sites (Biochem. biophys. Res. Commun. 90, 1249, 1979). Castration of male rats produced a rapid and sustained increase of pituitary LHRH receptor concentration (LHRH-R) which paralleled the well-established augmentation of gonadotropins secretion and decrease of hypothalamic content of LHRH. Treatment during 7 days of chronically castrated rats (> 28 days) with either testosterone or estradiol allowed to fully restore normal levels of plasma gonadotropins but did not normalize either pituitary LHRH-R or hypothalamic content of LHRH. It is concluded that the rapid feedback action of sex steroids for the control of gonadotropins secretion is exercised mainly at the pituitary rather than the hypothalamic level in chronically castrated rats.

Na-free contractures in mammalian ventricular muscle

A. Coray, D. Miller, J. McGuigan and M. Boyett, Physiologisches Institut, B hlplatz 5, CH-3012 Bern

In cardiac muscle the Na gradient across the membrane maintains a low $[\text{Ca}]_i$ via a Na/Ca exchange mechanism (Reuter, Circulation Res. 34, 599, 1974). Thus Na removal by causing $[\text{Ca}]_i$ to increase should cause a contracture. However, in mammalian ventricular muscle Na removal does not cause a contracture in bundles with a diameter of around 0.8 mm. In such bundles Na removal is limited by diffusion, so to overcome this problem small strands of 200 μm were dissected from the larger trabeculae. In these strands Na-free contractures of greater than twitch height were obtained. These contractures were increased as the pH of the Na-free solution was increased. There was an s-shaped relationship between the contractures and $[\text{Na}]_0$. They depended on $[\text{Ca}]_0$ and were inhibited by Mg. Increasing the $[\text{K}]_0$ up to 40 mM increased the height of the Na-free contracture. A further increase in $[\text{K}]_0$ decreased the amplitude. In summary, Na/Ca exchange mechanism does operate in mammalian ventricular muscle but the exchange is not exclusive to these ions as other ions esp. H^+ play a role. The exchange may also be potential-dependent.

Identified isolated neurons from *Aplysia* CNS in culture

D. Dagan and I.B. Levitan, Friedrich-Miescher-Institut, P.O. Box 273, CH-4002 Basel

Events occurring on the somatic membrane of *Aplysia* neurons can be distinguished from synaptic events occurring in the neuropile by intracellular recordings from isolated neurons in culture. The following conditions were found most favorable for culturing: Incubation of ganglia in 0.25% trypsin at 37°C for 2-3 h followed by gentle mechanical separation and isolation of neuron somata with short axons. These neurons are transferred to a 5- μl drop of chick plasma (GIBCO) which is then clotted with 5 μl of thrombin (300 U/ml, Hoffmann-La Roche). Single and clusters of neurons are then cultured at 20°C in a Leibovitz-15 (GIBCO) medium supplemented with *Aplysia* salts and 2% fetal calf serum. Within 4-5 days some cells extend long processes up to 10 times their cell-body diameter in length. Intracellular recordings utilizing voltage clamp techniques show normal 1-4 M Ω input resistance and spiking activity in many of these neurons. We are attempting to induce and characterize synapse formation in vitro utilizing these cultures.

Regulation of Na-dependent phosphate (P_i) transport by 1,25(OH) $_2\text{D}_3$ in small intestine

G. Danisi, J.P. Bonjour and R.W. Straub, Department of Pharmacology, University of Geneva, CH-1211 Geneva 4, and Department of Pathophysiology, University of Bern, CH-3012 Bern

Animals treated with ethane-1-hydroxy-1,1-diphosphonate (EHDP), at doses inhibiting the production of 1,25(OH) $_2\text{D}_3$ (D), display a decreased net absorption of P_i . Changes in net transmural transport will appear as changes in the P_i influx across the brush border, if there is located the rate-limiting and regulated step in net absorption. Therefore, the effects of EHDP treatment and of EHDP treatment + D on P_i influx across the mucosal membrane, J_{mc} , in isolated rabbit intestine were investigated. The results showed that EHDP inhibits the Na-dependent, carrier mediated P_i influx in duodenum and that D overcomes this inhibition. These effects are apparent through changes in J_{mc}^{max} , which is decreased from 215, in controls, to 43 nmoles/cm 2 h by EHDP and increased to 404 nmoles/cm 2 h by D. These treatments do not affect the diffusional Na-independent P_i influx. The results suggest that 1,25(OH) $_2\text{D}_3$ modulates the number of carrier sites available on the mucosal membrane for Na-dependent P_i entry.

Orderly projection of the primary olfactory pathway in *Triturus cristatus*

M. Dubois-Dauphin, E. Tribollet and J.J. Dreifuss, Department of Physiology, Medical School, CH-1211 Geneva 4

The axons of olfactory neuroreceptors are known to synapse with mitral cell dendrites in the olfactory bulb, but previous studies failed to reveal a clearcut topological organization of this projection. We therefore injected 100-200 nl of HRP 50% into restricted areas of the olfactory mucosa in 53 adult tritons. The animals were perfused with glutaraldehyde 17 h later, the mucosa and brain were removed, serially cut (20 μm) and reacted with DAB to reveal a) the localization and extent of the injection and b) the areas in the glomerular layer of the bulb to which HRP had been transported by anterograde flow. The main olfactory mucosa was shown to project to the anterior half of the bulb, the dorsal mucosa occupying a more dorsal

region of the glomerular layer. The latero-posterior part of the ventral mucosa, i.e. the vomero-nasal organ, projected more caudally. It remains to be shown a) whether this somatotopic organization has a functional role or whether it results from ontogenetic considerations, and b) whether it can be experimentally altered in this system which regenerates.

Simultaneous measurements of short-circuit current and volume flow across bovine tracheal epithelium

J. Durand, W. Durand and P. Haab, Institute of Physiology, CH-1700 Fribourg

A method was developed for measuring simultaneously potential difference (PD), short-circuit current (i_0) and volume flow (J_v) across bovine tracheal epithelium in vitro. The tissue was bathed on both sides with Krebs-Ringer bicarbonate buffer, equilibrated with 95% O_2 -5% CO_2 , pH 7.4, 37 °C. The medium on luminal side was continuously renewed, PD and I_0 being identical as when medium was renewed on both sides. Electrodes were sealed into seringes filled with bathing medium, which gave identical results as by using KCl-agar bridges. Basal values were: PD 31 ± 2 mV, i_0 161 ± 8 $\mu A cm^{-2}$, resistance 202 ± 9 Ωcm^2 (mean \pm SEM, $n=50$). J_v was continuously recorded from serosal compartment with a direct volumetric method (sensitivity 60 nl). Basal J_v was not different from zero with no applied hydrostatic or osmotic pressure gradient. An osmotic gradient (20 mM sucrose, luminal) induced a constant J_v , with no effect on transepithelial PD (range 6–16 $\mu l h^{-1} cm^{-2}$, $n=5$).

Reversal of leaky states in toad skin by loop diuretics

Ch.-A. Favrod-Coune and R. C. de Sousa, Départements de Physiologie et de Médecine, Ecole de Médecine, CH-1211 Genève 4

Theophylline induced marked but reversible leaky states in amphibian skin, which were unaffected by inhibitors of Na transport acting at the external membrane (amiloride, triaminopyrimidine-TAP) or at the internal membrane (ouabain). Removal of Cl from the bathing media prevented the rise in conductance but no agents were found capable of inhibiting this effect of theophylline once established. We report here that loop diuretics (ethacrynic acid, furosemide, bumetanide) reduce the electrical conductance of skins pre-exposed to theophylline (10 mM) in Cl-Ringers. At 1 mM, ethacrynic acid induced a fall in conductance from 6.78 ± 1.28 to 1.42 ± 0.38 $mS \cdot cm^{-2}$ ($N=7$, $p < 0.005$). In contrast, the high conductance state elicited by external hypertonicity (mannitol, 200 mM) was not inhibited by the diuretic ($N=6$). These results are consistent with the Cl-blocking properties of loop diuretics and indicate that different mechanisms are responsible for the leaky states induced by theophylline and by hypertonicity.

Developmental changes of open field behavior differences in roman high- and low-avoidance rats

H. Fuemm and K. Bättig, Institut für Verhaltenswissenschaft, ETH, CH-8092 Zürich

In this experiment we used male and female RHA/Verh and RLA/Verh rats, bred for rapid versus slow acquisition of shuttle box avoidance. The development of several behaviors in the open field was investigated. The open field used (80×80 cm) was divided into 16 squares of equal size. Rats 16, 20, 24, 28, 32, 38, 44, 50, 60 and 72 days old were tested twice, for 10 min, with a test interval of 5 h. Activity increased in both lines with age, and from 44 days on

RHA/Verh females (but not males) were significantly more active than RLA/Verh females. RLA/Verh rats showed more rearing only until 32 days, whereas grooming time was higher, compared to RHA/Verh, until 72 days. There were no differences in defecation except for a higher number for RLA/Verh rats at 16 days. From 28 days on RLA/Verh rats entered the center of the open field more frequently than the RHA/Verh rats did. For both lines the values of most of the behaviors observed changed during the course of the study.

Sources of CO_2 in avian caudal air sacs

J. Geiser and J.R. Torre-Bueno, MPI für experimentelle Medizin, D-34 Göttingen, Federal Republic of Germany

To explain that caudal air sacs (CS) of birds contain more CO_2 than is reinspired with dead-space gas, we tested 2 hypotheses. 1. On inspiration, the first portion containing dead space gas would preferentially pass through neopulmo to CS and the rest of the V_T , composed of fresh air, would flow to the paleopulmo. 2. Stratification resulting from incomplete mixing of the CS leads to CO_2 retention. - The inspired V_T was labelled with Ar at different instants of V_T . F_{Ar} in CS was larger, the earlier in inspiration the breath was labelled. When after inspiration the breath was held for 20 sec, F_{Ar} was independent of the injection time, disproving hypothesis 1. Consequently the experimental results of higher Ar concentration following labelling early in inspiration indicate incomplete mixing of CS gas. This stratification makes the composition of caudal air sac tend towards dead space gas, richer in CO_2 than the whole V_T on the average. Hypothesis 2 could therefore qualitatively explain the 'excess' CO_2 in CS.

Stress susceptibility in individually- and group-housed rats: Plasma corticosterone levels in response to various stressful situations

C. Gentsch, J. Baumann, M. Lichtsteiner and H. Feer, Psychiatrische Universitätsklinik, CH-4025 Basel, and Kinderspital Basel, CH-4005 Basel

Male rats reared in isolation show in comparison with group-housed animals several behavioral differences (e.g. diverse activities in an openfield). To clarify if these differences are related to an uneven stress susceptibility, plasma corticosterone levels were determined in unstressed rats and after exposure to various stressful situations. Plasma concentrations in unstressed animals were not different in the 2 groups, neither at the beginning nor in the middle of the dark phase. After exposure to 'mild stressors' (novel cage, injection) no significant difference in corticosterone concentration was detectable. Immobilization provoked a high but even secretion in the 2 groups. Openfield exposure, a very stressful situation led in individually housed rats to less elevated hormone levels than in group-housed animals ($p < 0.05$). It is supposed that individually housed animals are less susceptible to only certain stress conditions.

Correlations between haemolymph ecdysteroids titer, multiplication of hypodermal cells and deposition of cuticle during the last larval instar of the tick *Ornithodoros moubati*

J.-E. Germond, M. Morici and P.-A. Diehl, Institut de Zoologie, Université de Neuchâtel, CH-2000 Neuchâtel 7

In order to grow, ticks like other arthropods have to molt between successive instars. The molting process involves a

series of modifications of the hypodermis (outermost cell layer secreting the cuticle), which lead to the typical renewal of the cuticle. One of the first cytological event of the molting process is the increase of the hypodermis surface by cellular division. It is followed by the detachment of the hypodermis from the old cuticle (apolysis) and the synthesis of new cuticle. At the moment of ecdysis, shedding of the old cuticle and stretching of the new soft cuticle allow an increase of volume. Those cellular events can be correlated to the ecdysteroids titer in the haemolymph. Detected by radioimmunoassay a small peak of ecdysteroids is associated with the mitotic event of the hypodermis and a larger peak with apolysis and the beginning of cuticle deposition. Preliminary results show that the ecdysteroid is mainly 20-hydroxyecdysone. The processes of molting in ticks and in insects are then very similar.

Sympathetic stimulation without concomitant activation of adrenal-medullary secretion during fasting in unrestrained, conscious dogs

L. Girardier, R. Benzi and J.F. Liard, Département de Physiologie, Ecole de Médecine, CH-1211 Genève 4, and Institut de Recherche cardio-angéiologique, CH-1700 Fribourg

Studies using norepinephrine turnover in rat heart as a mesure of sympathetic activity (L. Landsberg et al., *New Engl. J. Med.* 298, 1295, 1978) led to the conclusion that fasting suppresses and overfeeding stimulates the sympathetic nervous system. The problem was reinvestigated using well-adapted, unrestrained conscious dogs. Fasting for 108 h resulted in a gradual and significant increase in circulating norepinephrine whereas circulating epinephrine and dopamine remained to basal values. By contrast, insuline-induced hypoglycemia resulted in a large increase in circulating epinephrine, whereas norepinephrine increased to a lesser degree and dopamine was not altered. In conclusion, during fasting the sympathetic nervous system is stimulated in conscious dog but the adrenal medulla do not participate in the regulatory process. Hypoglycemia is most probably not the activating signal for the metabolic adjustments to fasting.

Recent advances in automatic respiration analysis

U. Gomez and U. Boutellier, Physiologisches Institut der Universität, CH-8028 Zürich

A new computer program is presented for on-line respiration analysis, based on pneumotachographic and gas analyzer data derived from both the inspiratory and expiratory phase of breathing. Tests with a program considering the expiratory phase of breathing only (Beaver et al.) made it appear unreliable for general use: 1. Calculating \dot{V}_{O_2} from $\int (F_{RO_2} - F_{EO_2}) \cdot \dot{V}_e \cdot dt$ by applying correction factors for water vapor and R presume an inadmissible simplification of F_{RO_2} conditions around the mouth piece. Correct computation was possible only when including inspiration for source data analysis. 2. Applying constant gas to airflow signal delays does not allow for variable response times of the mass spectrometer due to variable flow rates. Algorithms for breath-by-breath analysis of F_{O_2} and F_{CO_2} granted precise temporal correlations of \dot{V} and F_{O_2, CO_2} . 3. Breathing phase onset detection by fixed voltage levels fails in irregular and shallow breathing cycles. Low pass filtering and storing of airflow data enabled exact determination of inspiratory and expiratory onsets.

Pharmacological aspects of transepithelial osmosis

A. Grosso and R. C. de Sousa, Départements de Physiologie et de Médecine, Ecole de Médecine, CH-1211 Genève 4

Transepithelial osmosis was studied in a non-urinary epithelium, the ventral skin of the toad *Bufo marinus*. Net water flows (J_w) were monitored with an automatic technique having a time-resolution of 6 sec. 2 distinct types of receptors triggered an increase in J_w : receptors to neurohypophysial hormones and receptors to β -adrenergic agonists. The effects of vasopressin and of isoproterenol were competitive, differentially modulated by the epithelium and specifically inhibited by methohexital and by propranolol, respectively. Vanadate and Li^+ blocked the response to both agents, but only Li^+ decreased basal J_w . Psychotropic drugs, ethacrynic acid and Ag^+ induced vasopressinomimetic effects. The results suggest that of these 3 agents the first 2 interact with the cAMP system, while Ag^+ appears to act directly on the outer, rate-limiting barrier of the epithelium.

Mechanism of enkephalin action studied in hippocampal slices of the rat

H.L. Haas and R.W. Ryall, Neurochirurgische Universitätsklinik, CH-8091 Zürich

The actions of a synthetic enkephalin, H-Tyr-Gly-Gly-MePhe-Met(O)ol (FK 33-824, *Life Sci.* 24, 621, 1979), metenkephalin (ME) and morphine (MO) were analyzed on the hippocampal slice of the rat. Intra- and extracellular recordings from CA 1 and CA 3 pyramidal cells and from dentate granular cells lead to the conclusion that enkephalins cause excitation without blocking basket cell mediated recurrent inhibition probably at least in part by a presynaptic mechanism. Perfusion with FK, ME and MO (10^{-8} to 10^{-5} M) caused: 1. Appearance, enhancement and multiple firing of population spikes after stimulation of the perforant path, the mossy fibres and the Schaffer collaterals, respectively. Such effects were also obtained by ionophoretic application of FK to apical dendrites. 2. An increased amplitude of evoked epp's and repetitive firing. 3. No consistent changes in membrane potential, average spontaneous firing rate, D,L-homocysteic acid evoked firing, membrane conductance and recurrent inhibition.

Specific kainic acid binding in the human CNS

H. Henke and W. Lang, Brain Research Institute, University of Zürich and University Hospital, CH-8029 Zürich

Kainic acid (KA) effects in the CNS are likely mediated by specific KA-binding sites. Since these effects are very specific and can also mimic human neurological disorders (Huntington's disease), the KA-binding sites may play an important role in the CNS. Therefore, we have measured the KA binding in 21 regions of the human CNS using crude membrane preparations obtained 6–9 h postmortem from the brains of patients without neurological disorders. The binding ranged from 0 (e.g. pallidum, s. cord, lat. gen. body) to >100 fmoles/mg protein (e.g. frontal cortex, caudo-putamen, hippocampus). While in most regions only 1 type of binding site was found (K_d : 8–15 nM), in some area (e.g. cortex, caudo-putamen, hippocampus) 2 types of binding sites with app. K_d of 0.5–2 and 15–30 nM were measured.

Growth and differentiation of aggregating fetal rat telencephalic cells in a chemically defined medium: the effects of insulin

P. Honegger, D. Lenoir and M. Dolivo, *Institut de Physiologie, Université de Lausanne, CH-1011 Lausanne*

Rotation-mediated aggregating cell cultures of mechanically dissociated fetal (15–16 days gestation) rat telencephalon were grown in a chemically defined, serum-free medium (Honegger et al., *Nature* 282, 305, 1979). Insulin (0.1–5 µg/ml) caused a dramatic, concentration-dependent increase in [³H]thymidine incorporation at in vitro day 5, a marked increase in total DNA and protein content, as well as a great, permanent increase in glutamic acid decarboxylase specific activity, whereas choline acetyltransferase specific activity was decreased. The responsiveness of the cells towards insulin decreased with time in culture. These results, together with further circumstantial evidence, strongly suggest that insulin markedly enhances cellular proliferation in vitro, implying that GABA-ergic neurons, but not cholinergic neurons, were still dividing in culture.

Binding of ³H-GABA, (+)³H-bicuculline-methiodide and ³H-flunitrazepam in CNS cultures using autoradiography

E. Hösli, H. Möhler, J. G. Richards and L. Hösli, *Department of Physiology, University of Basel, CH-4051 Basel, and Pharmaceutical Research Department, F. Hoffmann-La Roche & Co. Ltd, CH-4058 Basel*

Autoradiographic studies in cultures of rat cerebellum and spinal cord have shown binding sites for ³H-GABA and (+)³H-bicuculline-methiodide (BCM) on many neurones but not on glial cells. In cerebellar cultures, both interneurons and Purkinje cells revealed binding sites for ³H-GABA and ³H-BCM, whereas in cultured spinal cord mainly small to medium-sized neurones, probably interneurons, were labelled. Binding of both radioligands was inhibited by excess unlabelled GABA and bicuculline. Similar results were obtained with ³H-muscimol (Hösli and Hösli, *Exp. Brain Res.*, in press, 1980). Our binding studies are consistent with electrophysiological investigations indicating that glial cells do not have receptors for GABA (Hösli et al., *Exp. Brain Res.* 33, 425, 1978). Binding sites for benzodiazepines using ³H-flunitrazepam were also found on cerebellar and spinal neurones but not on glial cells.

Carbon dioxide and potassium equilibrium in frog skeletal muscle

F. Huguenin, *Physiologisches Institut der Universität, Bühlpplatz 5, CH-3012 Bern*

Carbon dioxide (CO₂) influences resting potential (Meves and Völknner, *Pflügers Arch.* 265, 457, 1958), intracellular potassium activity (a_Kⁱ) and wet weight in frog skeletal muscle (Huguenin and Malachowski, *J. Physiol., Lond.*, in press). The aim of the present work was to analyze the mechanism of these effects. With recessed-tip pH-sensitive microelectrodes (Thomas, *J. Physiol., Lond.* 238, 159, 1974), the intracellular pH was determined in surface fibres of frog skeletal muscle at various P_{CO₂}'s (0–97 mm Hg) and external pH's (7.0–7.6). These data and our previous results on resting potential, a_Kⁱ and weight changes were confronted with a model predicting the steady-state effects of CO₂ in terms of a modified Donnan equilibrium. It is concluded that the effects observed might be largely accounted for by a shift of the Donnan equilibrium due to intracellular CO₂ buffering.

Facilitatory effects of some aminopyridines (AP) on the synaptic activity of the isolated frog spinal cord and the inhibition of these effects

H. Isler and C. G. Honegger, *Abteilung Neurobiologie, Departement Forschung, Kantonsspital, CH-4031 Basel*

We tested the effects of TEA, 2-AP, 3-AP, 4-AP and 3,4-DAP on the ventral root reflex responses (VRR), the spontaneous activity (SA) and the evoked ventral and dorsal root potentials (V/DRP). All drugs enhance these parameters and depolarize the VR and DR. The most potent was 3,4-DAP. An application of 10⁻⁵ M for 3 min elevated the VRR and the V/DRP, up to 300% and for 10 h or more. This was accompanied by strong spontaneous reflex discharges on the VR and the DR. The effects of 4-AP are clearly weaker but also potent, whereas those of 3-AP, 2-AP and TEA are only moderate and short lasting. From experiments with magnesium ions, EDTA and tetrodotoxin we conclude that the depolarization from AP is not mediated directly on motoneurons and primary afferents. We also tried to abolish this facilitated activity by inhibitory amino acids. Glycine and GABA have no effects, BALA inhibited the SA weakly, whereas taurine, like HA-966, abolished SA and VRR totally and the V/DRP partially.

The inhibitory effect of Lanthanum on phosphate efflux from nonmyelinated nerve fibres

P. Jirounek, M. Rouiller and R. W. Straub, *Département de Pharmacologie, Ecole de Médecine, CH-1211 Genève 4*

Previous studies in rabbit vagus nerve have shown, that both influx and efflux of phosphate are saturable and Na-dependent processes (Anner et al., *J. Physiol.* 260, 667, 1976). We have now observed that La³⁺ rapidly and completely inhibits the phosphate efflux in this preparation. The maximal effect is reached at a concentration of 5 µM. The inhibitory effect of La³⁺ can be partially prevented by increasing the concentration of Ca²⁺. The high affinity of La³⁺ for the extracellular Ca²⁺ sites and its inhibitory effect on the Ca²⁺ exchange in muscle and nerve fibres are well-recognized. Our findings thus raise the possibility that Ca²⁺ is implicated in the phosphate transmembrane movements.

Interdependence of breathing and pedalling rhythm in bicycle ergometry

J. Kohl and M. Jäger, *Physiologisches Institut der Universität, CH-8028 Zürich*

Mutual influence of respiratory rhythm and rhythm of body movement was investigated in 34 medical students and 10 competitive cyclists during exercise on a bicycle ergometer, work load being 50, 100, 150 and 200 W. Integer values of the number of pedal cycles per breath, and repeated phase coupling of breathing and pedalling cycles, were used as indices of synchronization of both rhythms. – The results showed a significant tendency to synchronization of both rhythms in the group of competitive cyclists. None of them was aware of this synchronization nor intended to adjust the breathing pattern to the rhythm of body movement. From the group of noncyclists about 50% of the subjects (mostly subjects with a regular breathing pattern), showed a significant tendency to synchronization. – It is concluded that the respiratory and cycling rhythms are neither entirely independent nor strongly coordinated and that some factors (training, regularity of breathing) increase the tendency to synchronization of both rhythms.

Interaction of respiratory reflexes arising from lung stretch (SR) and irritant receptors (IR)

J. Kohl and J. Kuoni, *Physiologisches Institut der Universität, CH-8028 Zürich*

Respiratory response to inhaled chemical irritants is known to be due to stimulation of IR. As the activity of SR changes under these conditions, the question arises whether and how these changes contribute to the resulting pattern of breathing. To answer this question, the effect produced by varying the lung volume (i.e. the levels of SR and IR activity) on the course of respiratory reaction to inhaled ammonia, was analyzed in anaesthetized rabbits, with SR intact or blocked by SO₂. – The results showed a significant influence both of changing lung volume and of SR block on some respiratory parameters during ammonia-induced tachypnoea. Although the increase of breathing frequency was comparable in all levels of lung volume both with SR intact and blocked, the degree of SR stimulation or inhibition affected significantly the inspiratory (t_I) and expiratory (t_E) duration and the ratio t_I:t_E. – It is concluded that SR activity permanently modifies the respiratory pattern primarily caused by stimulation of IR.

Ultrastructural and electrophysiological studies on a specialized area of the honeybee's eye

T. Labhart and E. Meyer, *Zoologisches Institut der Universität, CH-8057 Zürich*

The visual cells in the bee's compound eye are twisted around each other except in the dorsal rim area (DRA) where the retinula is straight (untwisted) (Wehner et al., J. comp. Physiol. 104). In addition, the cornea of the DRA appears opaque due to numerous small channels penetrating the cornea from the pigment cells. Only the central part of the facets is free of channels. Polarization sensitivity (PS) of the UV-receptors (which mediate e-vector detection) reveal strong PS in the DRA but poor PS in other eye regions. The visual fields are narrow in the latter areas as opposed to the DRA where in addition to a central peak, sensitivity is extended to $\geq 30^\circ$ off-axis, probably due to scattering of light in the opaque cornea. Behavioural experiments show that the DRA plays an important role in e-vector detection (Wehner, unpubl.).

Forearm blood flow in healthy subjects: dependence on hormonal state

V. Lacoste and M. Gastpar, *Psychiatric University Clinic, CH-4025 Basel*

To evaluate the influence of the hormonal state on 'basal' and 'stress' induced forearm blood flow, 13 healthy age matched male and female subjects (M = 32.2 years, range 21–46) and 28 women, divided according to Jaszman (in: The management of the menopause and post-menopausal years; Ed. Stuart Campbell; MTP Press, Lancaster 1976) in pre- (≤ 46 years), peri- (47–55 years) and post-menopausal (≥ 56 years) age classes, were studied. Male and female subjects showed similar 'stress' patterns of forearm blood flow, but the pre- and post-stress levels were higher in males ($p < 0.05$). In peri-menopausal women, there was an enhanced increase of forearm blood flow in response to mental 'stress' without a return to baseline levels after discontinuation of the stressing agent, whereas in post-menopausal women the 'stress' response was minimal. The results demonstrate a circulatory hyperactivity in peri-menopausal women and confirm the importance of hormonal state in modifying 'basal' cardiovascular parameters as well as their response to 'stress'.

Comparison of rheological properties of human red blood cells stored as whole blood or as red blood cell concentrates

S. Leuenberger, J.-P. Barras and K. Koerner, *Department of Physiology, University of Basel, CH-4051 Basel, and German Red Cross Blood Bank, D-7900 Ulm, Federal Republic of Germany*

The in vitro ageing of human red blood cells (RBC) stored either as whole blood or as buffycoatfree RBC concentrates in ACD-adenine was compared by measuring the viscosities of RBC suspensions at 20 °C, using a Contraves Low-Shear 30 rotational viscometer. At a hematocrit adjusted to 45% (RBC washed and resuspended in 0.9% NaCl), the viscosities of samples prepared from whole blood and from RBC concentrates were not significantly different. Likewise, packed cells (hematocrit 98%) derived from whole blood and from RBC concentrates showed similar viscosities, suggesting that RBC deformability was unaffected by the mode of storage. After incubation at 37 °C for 48 h, a marked decrease of ATP accompanied by an increase in viscosity was observed, indicating that blood viscosity was correlated to the ATP content of the RBC. Our results demonstrate that up to 35 days RBC concentrates can be stored equally well as whole blood.

Changes in cardiac output (CO) and skeletal muscle blood flow (SMBF) in dogs with salt-loading hypertension

J. F. Liard, *Institut de Recherche cardio-angéiologique, CH-1700 Fribourg*

We investigated regional blood flows with radiolabelled microspheres (3 isotopes) in chronically instrumented dogs, 8 receiving a salt and water load after renal mass reduction and 6 serving as controls. As previously described CO increased in the early stage of hypertension by 563 ± 124 ml/min (25%) whereas total peripheral resistance (TPR) did not change; 5–7 days later, CO was back to its control value, but TPR was increased by 15.7 ± 2.4 mm Hg/l min⁻¹ (35%). Most of the early CO increase took place in the skeletal muscle vascular bed, where the flow rose by 507 ± 153 ml/min (70%). Conversely, the secondary decrease in CO was paralleled by a return of SMBF to control. Other changes in regional blood flows took place, but there was an evident correlation between CO and SMBF changes ($r = 0.93$). Thus, TPR changes typical of salt loading hypertension did not reflect the resistance of single vascular beds but instead a more complex pattern with prominent early dilatation in skeletal muscle.

Release of α -MSH into blood and from hypothalamic slices: influence of circadian rhythm and stress

F. Monnet, J.-C. Reubi, A. Eberle and W. Lichtensteiger, *Institute of Pharmacology, University of Zürich, CH-8006 Zürich, Brain Research Institute, University of Zürich, CH-8029 Zürich, and Institute of Molecular Biology and Biophysics, ETH, CH-8093 Zürich*

The presence of an α -MSH-like peptide in central nervous system, particularly in the hypothalamus has been demonstrated by various authors (Barnea et al., 1977; O'Donohue et al., 1979; Swaab and Fisser, 1977). In investigations on the possible neuromodulator or neurotransmitter role of α -MSH, we studied the in vitro release of α -MSH from slices of hypothalamus. α -MSH was measured by radioimmunoassay (titer of the antiserum 1:10⁷, cross reaction with

ACTH: < 0.05%; limit of sensibility of the assay: 8 pg/ml). The average spontaneous release (30 pg α -MSH/min/hypothalamus) showed an approximately 100% increase in the presence of 47 mM KCl. This release was largely calcium-dependent. These observations indicate that hypothalamic α -MSH can be released in a transmitter-like way. - Parameters susceptible of influencing this release were analyzed. We observed circadian changes in the serum concentration of α -MSH with 2 peaks: one of them occurs 2 h before lights are turned off and the other one, 2 h before lights are turned on. Release of α -MSH from hypothalamic slices was measured in relationship to these circadian variations as well as in stressed animals (cold exposure).

Enkephalin-induced inhibition of hypothalamic paraventricular neurones in vitro

M. Mühlethaler and J.J. Dreifuss, Department of Physiology, Medical School, CH-1211 Geneva 4

To investigate the effects of various neuropeptides on the activity of presumptive endocrine neurones, we used 400–500 μ m thick coronal slices cut through the rat hypothalamus. The slices were laid on a nylon grid and their inferior side perfused with Yamamoto's medium. Long-term extracellular recordings were obtained from 102 paraventricular nucleus (PVN) neurones in 38 slices. 21 cells fired phasically, 22 were beating regularly, whereas the remainder fired more or less at random. Cell firing was altered in the predicted way by bath application of glutamate, GABA, nicotine and by changes in the external calcium concentration. Oxytocin 10^{-5} M produced a moderate excitation in 3 of 9 cells tested. A marked reduction in firing rate followed the application of D-Ala-Met⁵-enkephalin (6/7 cells) at concentrations as low as 10^{-8} M. This effect was naloxone-dependent. The data suggests that the enkephalinergic neurones and terminals present in PVN (Rossier et al., Nature 277, 1979) may have a functional role.

Effect of β -adrenergic and cholinergic blockade on the cardiac acceleration in response to short isometric and isotonic contractions

R. Nassehi, U. Gomez and E.A. Koller, Physiologisches Institut der Universität, CH-8028 Zürich

Heart rate (HR), blood pressure (BP) and respiration were recorded in young healthy volunteers with and without β -blockade (propranolol 2 mg/kg, oral) and/or atropine (0.02 mg/kg, i.v.) during standardized isometric handgrip (max. voluntary contraction: 10 sec) and repeated plantar flexion (20 sec). For the correlation control, R-R interval and respiration were monitored simultaneously. - The results show analogous increase in HR and BP in both groups, i.e. with and without β -blockade, the tachycardia, however, being essentially influenced by the depth of breathing. Atropine abolished the increase in HR due to muscular contraction and deep inspiration. - It is concluded that β -blockade, in contrast to McAllister (J. cardiovasc. Pharmacol. 1, 253, 1979), is without influence on HR during brief periods of muscular contraction, during which the tachycardia is mainly due to vagal withdrawal.

Electrooculography in isolated, perfused mammalian eyes

G. Niemeyer, Department of Ophthalmology, Universitätsspital, CH-8091 Zürich

Photic stimulation of the vertebrate eye not only elicits fast electrical signals (ERP and ERG) but triggers also slow

oscillations of the corneo-fundal potential. In man, 'light steps' of several log units trigger a positive, damped oscillation with a peak time of 7–10 min. These electrooculograms (EOG) are reduced or extinguished in various degenerative diseases of the retina. However, the generation of the EOG is not understood. A new approach to study the EOG of mammalian eyes is presented. The method of arterial perfusion has been shown by electrophysiological and morphological criteria to maintain the retina for several hours. We recorded EOGs from perfused cat and dog eyes by AgAgCl-saline-silk electrodes in dc mode; the signals, 1–3 mV in amplitude, were similar in configuration and time course to comparable in vivo recordings in various species. This provides an opportunity to study mechanisms of the generation of the EOG under controlled and biochemically modified conditions in vitro.

Pattern of exploratory behavior in Dashiell-type and Hebb-Williams mazes by 2 psychogenetically selected lines of rats

R. Nil, J. Schlatter and K. Bättig, Institut für Verhaltenswissenschaft, ETH, CH-8092 Zürich

8 RHA/Verh and 8 RLA/Verh rats were tested in a complex Dashiell-type maze and a Hebb-Williams swim maze. In the enclosed complex alley configuration of the Dashiell-type maze, the RHA/Verh rats exhibited greater activity, less locomotor complexity, a higher repetition index, a greater explored area, more maze center entries and a higher outward preference than did the RLA/Verh rats. In the 12 detour problems of the Hebb-Williams test, better overall maze performance was noted for the RLA/Verh rats. Possible explanations of these behavioral differences are discussed.

Ca-dependent dye fluorescence in presence of isolated components from skeletal muscle

H. Oetliker, Abteilung für Physiologie, Max-Planck-Institut, D-69 Heidelberg, Federal Republic of Germany, and Physiologisches Institut der Universität Bern, CH-3012 Bern

Muscle fibres stained with the 'potentiometric' dye, indodicarbocyanine, exhibit a transient decrease in fluorescence preceding tension, simultaneous with the early birefringence signal (Oetliker et al., Nature 257, 693). The 2 signals were suggested to reflect changes in SR potential or molecular structure or conformational changes of the contractile proteins (c.p.) during Ca release. Influence of pCa on dye fluorescence in presence of isolated SR or c.p. was tested to distinguish between these mechanisms. Changing pCa from 8 to 5 did not influence fluorescence in presence of c.p. while fluorescence in SR suspensions was decreased by 5 to 8% (ΔF in intact muscle fibres 1–3%) SR digested by PLA, SR treated with Ca-ionophore X517A and even the isolated transport protein exhibit similar Ca sensitivity in the presence of dye. The results support the 2nd hypothesis and show that these optical signals might be used as an indicator of fast changes in pCa and conformation of the SR-ATPase.

Oxygen deficit during concentric and eccentric work

P. Pahud, E. Ravussin, K.J. Acheson and E. Jequier, Institut de Physiologie, Bugnon 7, CH-1011 Lausanne

Aerobic ($\dot{M}R$) and anaerobic (\dot{M}_{an}) energy production was determined in 5 subjects during the first minute of concentric and eccentric work (steady state energy expenditure

approximately 415 W in both situations). M_{an} was obtained by solving the heat balance equation:

$$MR + \dot{M}_{an} - \dot{S} = (\dot{R} + \dot{C} + \dot{E}) \pm |\dot{W}|$$

all other variables of which could be measured. The size of the oxygen deficit was similar whatever the type of work (99 ± 19 W concentric and 102 ± 19 W eccentric). $MR + \dot{M}_{an}$ was lower than \dot{MR} during the steady state in both types of exercise (concentric work: 364 ± 19 W, 407 ± 24 W, respectively, and eccentric work: 346 ± 25 W, 430 ± 21 W, respectively). In conclusion, the size of the oxygen deficit during the first minute of muscular exercise is imposed by the steady state energy requirement whatever the type of work. The smaller energy expenditure during this phase is probably due to less energy being released when creatine phosphate is split without resynthesis (oxygen deficit) than during splitting and resynthesis of high energy phosphate bonds (steady state).

Asparagine as precursor of neurotransmitter aspartate: role in corticostriatal pathway

J. C. Reubi, G. Toggenburger and M. Cuénod, *Brain Research Institute, CH-8029 Zürich*

The metabolic pathway leading to the synthesis in the central nervous system of the putative neurotransmitter aspartate is not yet well-established; neither are the neuronal pathways using selectively aspartate as their transmitter. In order to investigate these questions, striatal slices were incubated with ^{14}C -asparagine which was converted to a large extent in ^{14}C -aspartate. Part of this aspartate could be released from striatal slices by 47 mM KCl. It represented 13 times the spontaneous release and was calcium-dependent. This suggests that asparagine is a valuable precursor for the putative neurotransmitter pool of aspartate in the rat striatum. – Furthermore, a fronto-parietal cortex ablation of 2 weeks produces a decrease of more than 70% in aspartate release in the striatum, whereas the GABA release, newly synthesized from glutamine, is not affected. This suggests that aspartate plays a transmitter role in some corticostriatal fibres.

The contractility recorded at the cellular level

Y. de Ribaupierre and P. Kucera, *Institut de Physiologie, Université de Lausanne, Bugnon 7, CH-1011 Lausanne*

The viscoelasticity of a given material is characterized by its mechanical impedance. The viscoelastic properties of the cytoplasm are closely related to the cell contractility and internal movements. Hence the cytoplasmic contractility can be measured by recording the changes of the mechanical impedance of the cell. For this purpose the tissue is mechanically coupled by a microneedle to an electromechanical oscillator which imposes to the tip of the needle a tiny vibration ($0.2 \mu\text{m}$ peak-peak outside the tissue). This vibration is attenuated because of the power dissipation in the tissue. The decrease of the amplitude of the oscillator, a measure of the impedance, is modified according to the contraction state of the cells situated in the immediate vicinity of the needle tip. Such local measurements have been performed at different places within the cardiac primordia of the intact chick embryos developing in vitro. The very first myocardial contractions have been detected and their evolution (synchronization, acceleration and amplification) has been followed. Records of the contractility in protozoa will also be shown.

Coding of click trains by neurons of the cat's medial geniculate body

E. Rouiller, A. Toros, Y. de Ribaupierre, C. Ivarsson and F. de Ribaupierre, *Institut de Physiologie, Bugnon 7, CH-1011 Lausanne*

Single unit responses to click trains were recorded extracellularly in the medial geniculate body (MGB) of nitrous oxide anesthetized cats. Clicks (40 dB SPL, 50 μsec) were presented in trains of different frequencies for 500 msec duration, at 1/sec. The responses of 193 units were classified in 4 categories as in the primary auditory cortex (AI) (F. de Ribaupierre et al., *Brain Res.* 48, 1972). One of these, the 'lockers' category represents 66% of the units studied. These cells are responding to the individual clicks of the trains with a precise latency up to a maximal frequency that varies between 10 and 800 Hz. The distribution of this upper frequency limit is similar in the pars lateralis (PL) and magnocellularis (mMGB): 43% of the cells are still locked to the clicks of the train for frequencies of 100 Hz and above (compared to 35% in AI). In PL, low characteristic frequency (CF) units tend to be better lockers than high CF units; this is the reverse in mMGB.

Reactivation of brown adipose tissue in obese hyperglycemic ob/ob mice by fasting and cold-adaptation

J. Seydoux, F. Assimacopoulos-Jeannet and B. Jeanrenaud, *Département de Physiologie et Laboratoire de Recherches Médicales, Université de Genève, CH-1211 Genève 4*

Ob/ob mice have impairment of thermogenesis. In small mammals, brown adipose tissue (BAT) is the main thermogenic effector which is controlled by its sympathetic innervation. 3 indices of BAT metabolic activity were measured: nicotinamide adenine redox state (NADP) during electrical nerve stimulation and noradrenaline (NE) addition, glycerol and heat output during NE addition. In control mice, nerve stimulation and NE induced increases of NADP redox state, glycerol and heat output. In fed obese mice, neither of these stimuli had any significant effect on BAT metabolism, indicating that in obese mice BAT is functionally disconnected from its nerve supply – 3 days fasting or cold adaptation (5°C) induced a partial functional nerve control recovery and NE-induced heat output but NE-induced glycerol release did not recover to the same extent due probably to a better free fatty acid oxidation since octanoate was also found to be oxidized.

Influence of thyroid status on β -receptor affinity of brown adipose tissue

J. Seydoux, J. P. Giacobino and L. Girardier, *Départements de Physiologie et de Biochimie Médicale, Université de Genève, CH-1211 Genève 4*

The effects of hypothyroidism on β -receptor response in rat brown adipose tissue have been studied. The β -receptor stimulation was induced by isoprenaline, noradrenaline and phenylephrine. The metabolic index was the NAD(P) redox state change, as measured by surface-emitted fluorescence. It was reported in *Experientia* 35, 927 (1979) that hypothyroidism induced a shift to the right of the dose-response curve by factors of 287, 87 and 1.8 for isoprenaline, noradrenaline and phenylephrine, respectively. To study the role played by β -receptors in this decreased response to catecholamine, stereospecific binding of $^3\text{H}(-)$

dihydroalprenolol to brown adipocyte purified plasma membranes was measured; its apparent K_D was found to be significantly higher in hypothyroid rats (941 ± 147 nM) than that of controls (276 ± 115 nM). The total binding capacity, however, was found to be identical in both groups. It can be concluded that the shift in catecholamine dose-response curves can be partly explained by a decreased β -receptor affinity in hypothyroid state.

Brain renin activity in distinct nuclei of spontaneously hypertensive rats

P. Schelling, D. Meyer, H.E. Loos and D. Ganten, Institut de Recherche Cardio-angéiologique, CH-1700 Fribourg, and Pharmakologisches Institut der Universität, D-6900 Heidelberg, Federal Republic of Germany

Renin concentrations were measured in distinct brain nuclei and in the hypophysis of 9-week-old stroke prone spontaneously hypertensive rats (SP-SHR) in comparison with age-matched Wistar Kyoto controls (WKY). A significant increase of brain renin content was found in the neurohypophysis and in noradrenergic brain stem regions such as A1, A2, A5 and locus coeruleus of 9-week-old SP-SHR as compared to WKY. Renin was decreased in frontal cortex, but was at control levels in all hypothalamic and thalamic nuclei investigated. The differences disappeared in 20-week-old animals. The renin content is elevated during the development of hypertension in noradrenergic brain stem areas known to participate in central blood pressure regulation and known to be stimulated in young SP-SHR. The brain renin-angiotensin system may influence the pathogenesis of hypertension in SP-SHR probably by modulating noradrenergic transmission.

Sympathetic nerve development in rat brown adipose tissue reevaluated with a functional test

G. Schneider-Picard, J. Seydoux and L. Girardier, Department of Physiology, CH-1211 Geneva 4

The sympathetic nerve development of rat brown adipose tissue (an effector organ in regulatory heat production in neonatal mammals) was evaluated in vitro with a spectrofluorimetric method on neuroadipose tissue preparations. Flavoprotein redox state, an index of the metabolic activity of the tissue, was continuously recorded; graded electrical stimulation of the tissue nerve supply showed a maximal increase of flavoprotein reduction at 4 Hz. With this stimulation frequency the shift in redox state was 23% of basal for < 12 h, 28% for 12–36 h, 26% for 14 day, 17% for 50-day-old animals – The frequency of stimulation required to produce half maximal response was found to be twice as high in newborns as that needed for 14- and 50-day-old animals. It is concluded that brown adipose tissue is functionally innervated at birth before any catecholamine content can be visualized by the Falk-Hillarp histochemical fluorescence method.

The activity of neurones in monkey midbrain during trained and untrained movements

W. Schultz and A. Ruffieux, Institut de Physiologie, Université de Fribourg, CH-1700 Fribourg

Monkeys were trained in a primate chair to perform a detection-reaching paradigm. The animal depressed a hold key. After a random period of several seconds the shutter of an apple-containing box opened and the monkey reached into it. The animals also accepted food from the hand of the experimenter. With the head restrained, single cell

recordings were performed in the midbrain. Cells in red nucleus were excited or inhibited during arm movements. Some of the neurones in substantia nigra were also related to movements, but more to the attentional or motivational aspects of goal-directed movements. Neurones in the perirubral mesencephalic reticular formation were tightly related to some aspects of movements similar to those of the red nucleus or were activated in a more 'holistic' way resembling substantia nigra neurones.

Input organization of nucleus gracilis in cats with an agenesis of the distal hindlimb

W. Schultz, R. Wiesendanger, M. Wiesendanger, B. Hess and A. Ruffieux, Institut de Physiologie, Université de Fribourg, CH-1700 Fribourg

Normally, the gracile nucleus (GN) represents to a large extent the distal portion of the hindlimb. In 2 cats from the same litter with unilateral absence of the distal hindlimb (congenital defect), the question arose whether the GN is reduced in size and in cell number or, if this were not the case, whether the remaining stump is 'overrepresented' in the GN. Anatomically, the sciatic nerve was smaller on the defective side as compared to the normal side matching the difference in peripheral neural inputs. GN cells were significantly smaller on the defective side. Micro-mapping of both GN revealed multi-unit responses to natural stimuli of the hindlimbs without any silent areas on the side of the stump. Neurones which normally represent the paw had small receptive fields within the distal stump area. Behaviourally, the defective hindlimb was used in locomotion, and it can be assumed that the medial lemniscus transmitted an equal amount of information from both hindlimbs to the brain in spite of a massively reduced peripheral input from the abnormal side.

Temporal separation of early large birefringence signal and latency relaxation in frog skeletal muscle

R.A. Schümperli and H. Oetliker, Physiologisches Institut, Universität Bern, Bülhlplatz 5, CH-3012 Bern

In single muscle fibres a birefringence signal (BS) has been demonstrated during the latent period between action potential and onset of positive tension, interpreted as a change in potential or molecular structure of the sarcoplasmic reticulum membrane during Ca-release. However, BS might simply reflect latency relaxation (LR). We have shown that several procedures have different effects on the amplitude of BS and LR (Experientia 34, 902, 1978). We now demonstrate that they are also well-separated in time: Under point stimulation the onset of BS precedes LR by 1.25–1.5 msec (corrected for apparatus delays). Field stimulation eliminates conduction time of the mechanical wave in the fibre and reduces the interval to 1 msec; in 2× hypertonic Ringer it is increased again by 50%. Cooling to 2°C increases the delay to about 6 msec and often introduces a plateau in LR (point stimulation). Our hypothesis is therefore supported that BS and LR represent different processes.

Variability of dietary induced thermogenesis (DIT) and sleeping energy expenditure (SEE) in young men

Y. Schutz, K. Acheson, P. Puhud and E. Jequier, Institut de Physiologie, Bugnon 7, CH-1011 Lausanne

The DIT responses over 4 h after standard evening meals (3470 kJ; 38 g protein) followed by an 8 h SEE were

continuously measured in a respiration chamber with $\dot{V}O_2$ reproducibility of $\pm 1.25\%$. 4 young healthy men (mean weight \pm SD, 69.2 ± 2.8 kg) were studied over 6 consecutive days. The last day was a control test without meal. Activity of the subjects was continuously monitored by a radar system using the Doppler effect. The DIT response was calculated as the excess energy expenditure over the control test and was expressed as percent of the food energy consumed. The mean (\pm SD) individual DIT responses were $4.8 \pm 1.0\%$, $6.8 \pm 1.0\%$, $10.0 \pm 0.4\%$ and $10.6 \pm 2.9\%$. The mean (\pm SD) individual SEE's were 4.3 ± 0.2 , 4.4 ± 0.1 , 4.0 ± 0.2 and 4.3 ± 0.1 $\text{kJ} \cdot \text{kg}^{-1} \cdot \text{h}^{-1}$. The variability of SEE within each subject was smaller than that of DIT. These results suggest that although DIT and SEE are variable between subjects their values are reproducible for a given individual.

Cardiac activity and the endogenous microvibrations (MV) of the body

R. Stürm and E.A. Koller, *Physiologisches Institut der Universität, CH-8028 Zürich*

The influence of the heart on the MV was studied in a total of 37 young healthy subjects under various experimental conditions. 27 subjects showed cardiac characteristics similar to the ballistocardiogram in the vertical force component (F_z). After isoprenaline inhalation or exercise, these cardiac characteristics were found in F_z of all 37 subjects; the maximal amplitudes as well as the rectified impulse values were increased in all directions, particularly, however, in the z-axis. The propagation of the MV through the body was independent of arterial pulsations. The increase in muscle tone due to cold stress led to a significant increase of the rectified impulse only in the sideward direction (S_y). – It is concluded that the triaxially recorded MV arise from cardiac activity, mainly reflected in the vertical (z) axis, and from skeletal musculature representing a mechanical oscillating system with varying material constants (muscle tension, inertial forces, etc.).

Norepinephrine contractions in arteries 'skinned' with saponin

S. Thorens, G. Haeusler and J. G. Richards, *F. Hoffmann-La Roche & Co. Ltd, CH-4002 Basel*

Rings of small rabbit mesenteric arteries (diameter ca. $300 \mu\text{m}$, wall thickness ca. $100 \mu\text{m}$) were 'skinned' for 5 min in a relaxing solution containing 0.5 mg/ml saponin. On the basis of morphological and physiological criteria, virtually all smooth muscle cells were shown to be rendered hyperpermeable by the saponin treatment. 'Skinned' arteries contracted upon addition of norepinephrine (NE) 10^{-5} M. This contraction was blocked by phentolamine but not by propranolol. It was diminished by depleting Ca pools with caffeine, FCCP or X-537A. The NE contraction in 'skinned' preparations was enhanced by loading the arteries with Ca in a high potassium solution before 'skinning'. However, NE did not elicit Ca release from membrane vesicles isolated from untreated arteries. These results would suggest that in vascular smooth muscle, a certain degree of structural integrity of the cell membrane, but not its selective permeability, is required for the coupling between the α -adrenergic receptor and the release of Ca from intracellular stores.

Oxygen consumption by drone photoreceptors in darkness and during repetitive stimulation with light flashes

M. Tsacopoulos, S. Poitry and A. Borsellino, *Experimental Ophthalmology Laboratory and Department of Physiology, University of Geneva, CH-1211 Geneva 4*

The steady-state O_2 consumption (QO_2) of the superfused honeybee drone retina was measured in darkness and under light stimulation. The back of the eye was sliced off and the exposed ommatidia were superfused with oxygenated Ringer's solution in a perfusion chamber in which the hydrodynamic behaviour of the flow was carefully controlled. Oxygen gradients were measured outside and inside the retinal tissue and oxygen consumption could be calculated. Light stimulation caused a 3-fold increase of QO_2 ($\Delta QO_2 = 0.040 \pm 0.004$ ml cm^{-3} tissue min^{-1}). This large and rapid change of QO_2 most likely occurred in the photoreceptor cells, which contain lots of mitochondria in contrast to the surrounding glial cells. On the basis of the data obtained by measurements of K^+ activity in the photoreceptors with microelectrodes as well as generally accepted stoichiometries, it has been calculated that the extra- O_2 consumed is at least sufficient for the work of Na^+ pump.

Blood tonometry with nonsaturating O_2 -CO-CO₂-N₂ mixtures

M. Tschopp, J. R. Haag, A. Tempini and P. Haab, *Institute of Physiology, CH-1700 Fribourg*

Equilibration of blood samples with O_2 -CO-CO₂-N₂ gas mixtures requires very long tonometry times if the concentrations of O_2 and CO are too low for complete saturation of hemoglobin at equilibrium. When conventional tonometers are used, this time may be so long that blood deteriorates before equilibrium is reached. In order to increase the surface-volume ratio of the blood sample, we devised a bubble tonometer similar to the one described by N.C. Staub (J. appl. Physiol. 15, 963, 1960). With such tonometers, relatively large amounts of blood (30 ml) could be equilibrated within 12 h at P_{CO} between 0.07 and 0.27, P_{O_2} between 6 and 140 and P_{CO_2} 40 Torr. After this time hemolysis was generally between 1 and 2%. This type of tonometry was found to be appropriate for determination of the whole blood relative affinity for CO and O_2 (Haldane's constant M). Values of M for sheep blood were found to lie between 110 and 200.

Activation of the hypothalamo-neurohypophysial system by hepatic portal vein osmoreceptors

P.G. Vallet and A.J. Baertschi, *Department of Animal Biology, University of Geneva, CH-1211 Geneva 4*

The decrease of antidromic compound action potentials (CAP) measured within the hypothalamo-neurohypophysial tract (HNT) was used as an index of increase of neural activity of the HNT. Superfusion of the hepatic portal vein (PV) of rats with hypertonic (1.2 osm) solutions (0.2 ml, 10 sec, 37°C) produced a CAP decrease of $18.7 \pm 1.7\%$ SEM ($n=16$). CAPs decreased $20.7 \pm 1.5\%$ in response to LiCl, $9.1 \pm 1.4\%$ to Na-isethionate, $10.2 \pm 0.8\%$ to choline-Cl, $6.0 \pm 2.9\%$ to glucose ($n=5-10$). Urea and isotonic NaCl had no effect. CAPs decreased significantly in response to prolonged superfusions (push-pull canula) with slightly

hypertonic (0.36–0.60 osm) solutions, but responses adapted completely after 2 min. Results suggest that PV osmoreceptors mediate neurohypophyseal hormone release to small transient increases in concentrations of low mol.wt substances within the i.p. fluid.

Kainic acid toxicity in the pigeon thalamus and consequent decrease in the hyperstriatal choline acetyltransferase and glutamic acid decarboxylase

A. Vischer, A. Fäh, A. Burkhalter and H. Henke, Brain Research Institute, CH-8029 Zürich

Kainic acid (KA) injections into the CNS lead to a specific destruction of neurons while afferent terminals and axons of passage are unaffected. Injection of 2.5–10 nmoles KA in 0.5 µl Krebs-Ringer solution into the dorsolateral thalamus (DL) caused a severe neuronal cell loss in DL. 4 weeks after injection choline acetyltransferase activity was reduced to $58 \pm 12\%$ in the ipsilateral hyperstriatum (HA) when compared to the contralateral side (55 ± 12 nmoles/h/mg prot.). Contralateral retinal ablation markedly attenuated the KA neurotoxicity in DL. In this case, no side differences were found in the HA. Similar results were obtained for glutamic acid decarboxylase activity. These data indicate that the retino-thalamic fibres may use glutamate as transmitter and the thalamo-hyperstriatal ones acetylcholine and GABA. However, at present, indirect effects or secondary degeneration in the HA cannot be excluded.

Effects of the early stages of paralysis on microcirculation of rat skeletal muscle

N. Wiernsperger and C. G. Honegger, Sandoz AG, CH-4002 Basel, and Departement Forschung, Kantonsspital, CH-4031 Basel

In rat gastrocnemius muscle (white), microelectrode determination of tissue pO_2 and morphometric analysis of capillary bed filling (also in red soleus muscle) were

performed during the early stages of paralysis in the following models: a) flaccid paresis caused by EAE, EAN (allergic autoimmune diseases) and denervation, b) spastic paresis caused by 6-aminonicotinamide. EAE and EAN had little effect on microcirculation during paralysis, but after recovery there was marked hyperoxygenation, not related to increased capillary perfusion. Denervation, in spite of a decrease in capillary filling, led to an immediate inhomogeneous pO_2 -distribution (shunt perfusion); after 1 week, the high O_2 content was accompanied by increased capillary perfusion in the white muscle but not in the red, where it was further reduced. 6-Aminonicotinamide had almost no effect on both parameters. The experiments indicate that for these models of paresis a) in contrast to b) induces a dysfunction in O_2 utilization by the muscle.

Circadian rhythms in brain receptors

A. Wirz-Justice, M. S. Kafka, D. Naber, P. J. Marangos and T. A. Wehr, National Institute of Mental Health, 4S-239/10, 9000 Rockville Pike, Bethesda, Maryland 20205, USA

Changes in the number of many rat brain receptor populations throughout the 24-h day are as great (ca. 30%) or greater (ca. 70%) than changes previously reported after chronic drug treatment. This is the case for specific binding in forebrain membranes to α -adrenergic (3H -WB4104 as ligand), cholinergic (3H -QNB), and opiate (3H -naloxone) receptors which are higher in the light phase than in the dark; β -adrenergic (3H -dihydroalprenolol) and benzodiazepine (3H -diazepam) receptors which increase at the end of the dark and beginning of the light phase, respectively. These are endogenous rhythms since they continue in the absence of time cues. In striatal membranes, both dopamine (3H -spiroperidol) and benzodiazepine receptors show bimodal rhythms with peaks in mid-light and mid-dark. The different wave forms, amplitude, phase and relationship to the entraining light-dark cycle of each of these receptor rhythms indicate a precision of temporal order with probable functional significance.

PHARMAKOLOGIE - PHARMACOLOGIE - PHARMACOLOGY

Quantitative analysis of theophylline metabolites by HPLC, after oral or i.v. administration

M.J. Arnaud and C. Welsch, Nestlé Research Department, CH-1814 La Tour-de-Peilz

No significant difference appeared in the elimination and metabolism of labelled theophylline (T) given orally to 6 rats or i.v. to 4 rats. After 24 h, $18 \pm 2\%$ of the dose was recovered in the feces, $70 \pm 7\%$ in the urine, $6 \pm 1\%$ in the CO_2 and less than 1% in the organs. About $\frac{1}{4}$ of the dose was secreted in the bowels. Urine metabolites were separated by HPLC and radioactivity was recorded and integrated. Unchanged T amounted to $35 \pm 3\%$ of urine radioactivity, 1,3-dimethyluric acid to $34 \pm 2\%$, 1-methyluric acid to $18 \pm 2\%$, 3-methylxanthine to $3 \pm 1\%$. 1-Methylxanthine, 3-methyluric acid and dimethylallantoin were detected ($< 1\%$). 2 unknown polar compounds, 2.5 and $2.3 \pm 0.3\%$, were found while the diaminouracil produced from caffeine, theobromine and paraxanthine was not found for T, showing the importance of the 7-methyl for this metabolic pathway.

 ΔPCO_2 in experimental renal tubular acidosis

E. Aubert and J.P. Guignard, Division de Néphrologie, Service de Pédiatrie, CHUV, CH-1011 Lausanne

The difference between urine and blood PCO_2 (ΔPCO_2) has been proposed to assess acidification defects in clinical patients. ΔPCO_2 was studied in 4 groups of pentobarbital-anesthetized rats during alkaline diuresis: a) control, b) rats with proximal tubular acidosis (PTA), c) rats with distal tubular acidosis (DTA), d) rats infused with amiloride, 0.5 mg/kg. PTA was induced by injecting the rats with 0.26 M Na maleate, 100 mg/kg i.v. DTA was induced by i.p. injection of 0.3 M lithium chloride, 3 mM/kg, for 3 days. Alkaline diuresis was induced, on the experimental day, by infusing the animals with 0.6 ml/kg · min of 140 mM NaHCO_3 . In control animals, plasma HCO_3^- was 31 ± 1 mM/l, urine pH 7.91 ± 0.01 , urine HCO_3^- 52 mM/l and ΔPCO_2 16 ± 2 mm Hg. In maleate-treated rats, plasma HCO_3^- was 28 ± 1 mM/l, urine pH 7.48 ± 0.04 , urine HCO_3^- 50 ± 7 mM/l and ΔPCO_2 26 ± 4 mm Hg. In lithium-treated rats, plasma HCO_3^- was 29 ± 1 mM/l, urine pH 7.56 ± 0.04 , urine HCO_3^- 51 ± 6 mM/l and ΔPCO_2 11 ± 2 mm Hg. Inhibition of distal H^+ secretion by amiloride also significantly depressed ΔPCO_2 , at all levels of HCO_3^- excretion. The difference between ΔPCO_2 in control or maleate-treated rats and lithium or amiloride-treated rats was highly significant ($p < 0.001$). Under well-defined conditions, ΔPCO_2 appears to be a valid tool in the assessment of acidification disorders.

Correlation of protriptyline serum- and myocardial concentrations and effects on ECG and heart mitochondrial functions

E. Bachmann and G. Zbinden, Institute of Toxicology, ETH/University of Zürich, CH-8603 Schwerzenbach

Rats were treated twice daily with 8, 16 and 32 mg/kg protriptyline per os. Serum- and heart-tissue homogenates were extracted with methylene chloride (giving minimal background interference) by extensive mixing. The drug was determined by fluorescence spectrophotometry (excitation at 300 nm, emission at 360 nm). Serum levels of protriptyline, measured 17 h after the last medication, rose rapidly to reach steady state levels after 2 doses of 32

mg/kg (0.5 $\mu\text{g}/\text{ml}$) and 6 doses of 16 mg/kg (0.1 $\mu\text{g}/\text{ml}$) and 8 mg/kg (0.05 $\mu\text{g}/\text{ml}$). Upon discontinuation of medication they fell rapidly to $\frac{1}{10}$ within 3 days. Heart-tissue levels exceeded serum levels by a factor of 10–20 (32 mg/kg = 8.1 $\mu\text{g}/\text{g}$) and 5 (16 mg/kg = 0.58 $\mu\text{g}/\text{g}$), decreasing also rapidly when treatment stopped. ECG changes, i.e. tachycardia, prolongation of QRS and PR intervals, elevation of T-wave amplitude and right deviation of electrical axis correlated well with serum and tissue concentrations. The same was true for the decrease in oxidative phosphorylation measured in mitochondria from hearts of protriptyline-treated animals.

Etude autoradiographique de la chlorpromazine- ^{14}C chez le rat et analyse des modifications ultrastructurales des stimulations induites par la chlorpromazine sur les cellules à prolactine de l'hypophyse

A. Benakis, Ch. Rey, J. Vitus, Y. Stefan, F. Rouais et P. Blanquet, Laboratoire du Métabolisme des Médicaments, Département de Pharmacologie, Université de Genève, CH-1211 Genève 4, Laboratoire d'Endocrinologie, Faculté des Sciences, Université de Genève, CH-1211 Genève 4, and INSERM, Unité 53, Domaine de Carreire, Bordeaux, France

L'étude autoradiographique de la chlorpromazine- ^{14}C chez le rat montre une distribution très générale de ce produit et de ses métabolites dans l'ensemble des tissus et organes, notamment aux niveaux du foie, des reins, des os, de la peau, de l'hypophyse et du cerveau. Dans ce dernier, la distribution n'est pas uniforme. Elle est plus prononcée au niveau du cortex cérébral tandis que le thalamus, l'hypocampe, le bulbe olfactif et le cervelet sont différenciellement imprégnés. L'analyse des coupes de microscopie électronique des hypophyses de rats mâles et femelles après administration répétée de la chlorpromazine (15 mg/kg) pendant 1–5 semaines montre des images d'hyperactivité sécrétrice au niveau des cellules à prolactine, déjà après 1 semaine de traitement. Les cellules à prolactine présentent un R.E.R. dilaté, un appareil de Golgi contenant des petits grains en voie de formation, le cytoplasme est pauvre en grains matures alors que les images d'exocytoses de grains parfois immatures sont fréquentes. La chlorpromazine provoque donc une stimulation de l'activité de synthèse et de la sécrétion au niveau des cellules à prolactine.

A rabbit model allowing access to portal vein, vena cava, aorta, and duodenum without anesthesia

H. U. Bieri, Th. Zysset, P. Probst and J. Bircher, Departments of Clinical Pharmacology and Radiology, University of Bern, CH-3010 Bern

In studies of hepatic first-pass elimination of drugs in experimental animals, gastric emptying, drug absorption and intestinal metabolism may be factors difficult to control. Access to the portal vein and to the duodenum without anesthesia could overcome this problem. A rabbit model was, therefore, developed with catheters, chronically implanted in the portal vein (through the inferior mesenteric vein), in the renal artery and vein (after left nephrectomy), and in the duodenum. Hepatic and renal function before and 10 days after the operation showed no difference with respect to serum GOT, GPT, K, Na, Cl, PO_4 , Urea-N and creatinine levels. Portal catheters were functioning for $42 \pm \text{SD } 22$, arterial catheters for $42 \pm \text{SD } 22$ and venous

catheters for $32 \pm \text{SD } 10$ days ($n=8$). Angiography showed open catheters. Autopsy after the catheters ceased functioning revealed no pathology other than minor spotty, calcified infarctions of the renal cortex and thrombosis about the catheters in situ. It is concluded that this model permits the separate study of hepatic and intestinal first-pass elimination of drugs in normal rabbits.

Backward locomotion in rats, a specific stereotyped behavior

E. P. Bonetti and G. Bondiolotti, Pharmaceutical Research Department, F. Hoffmann-La Roche & Co. Ltd, CH-4002 Basel

Backward running, walking and circling (backward locomotion, BL), a stereotypy proposed to result from concurrent dopamine (DA) and 5-hydroxytryptamine (5-HT) release (Curzon et al., 1979) occurred in all rats given D-amphetamine- SO_4 (D-AM) 10 (all doses in mg kg^{-1} i.p.). This stereotypy seen in addition to typical DA- and 5-HT-mediated signs was prevented by the synthesis inhibitors pCPA or α -MT. Simultaneous equimolar amounts of the DA agonist apomorphine and the 5-HT agonist quipazine also induced BL. The multiple agonist LSD (5) also induced BL, as did amfonelic acid (10) and methylphenidate (100), drugs claimed to act differently from D-AM. D-Methamphetamine (D-MA) and D-AM equipotently induced BL whereas their L-enantiomers were less active. L-Deprenyl, a MAO inhibitor metabolized to L-MA and L-AM, induced BL at high doses only (50–100). Cocain induced catecholamine-mediated signs but no BL. Nomifensine but not the new antidepressant mofenensine (Ro 8-4650) elicited BL. Thus, BL seems to result from a balanced DA and 5-HT receptor stimulation.

Wirkung von Parachlorophenylalanin (PCPA) und Tryptophan (TRP) auf den Schlaf der Ratte

A. A. Borbély, H. U. Neuhaus und I. Tobler, Pharmakologisches Institut der Universität Zürich, CH-8006 Zürich

Die Wirkung von PCPA und TRP auf Schlaf und motorische Aktivität der Ratte wurde mit telemetrischen Registriermethoden und automatischer Stadienauswertung untersucht. Im Vergleich zu den Kontrolltagen bewirkte PCPA (300 mg/kg i.p.) eine unmittelbare Erhöhung des Schlafes mit langsamen Wellen (SLW; ein Unterstadium des nonREM-Schlafes). Am 2. und 3. Tag nach PCPA waren dagegen der Gesamtschlaf sowie alle Schlafstadien reduziert und die motorische Aktivität erhöht. Am 4. und 5. Tag nach PCPA war der Schlaf weitgehend normalisiert mit Ausnahme einer Vermehrung des REM-Schlafes (REMS) über den Kontrollwert. TRP (150 mg/kg i.p.), 28 Std. nach PCPA verabreicht, erhöhte die Hirnkonzentration von Serotonin (5HT) und bewirkte eine temporäre Vermehrung von SLW und REMS. Die Resultate unterstützen die Annahme, dass die durch PCPA induzierte Schlafreduktion durch die Erniedrigung des 5HT-Spiegels bedingt ist, wobei jedoch weniger die absolute Hirnkonzentration als der 5HT-Abfall der entscheidende Faktor zu sein scheint.

Langzeitregistrierung der motorischen Aktivität beim Menschen

A. A. Borbély und H. U. Neuhaus, Pharmakologisches Institut der Universität Zürich, CH-8006 Zürich

Auf Grund polygraphischer Registrierungen im Schlaflabor lassen sich die verschiedenen Schlafstadien bestimmen.

Solche Untersuchungen des Schlafes haben jedoch den Nachteil, dass Versuchspersonen nur während einer beschränkten Zahl von Nächten unter ungewohnten Laborbedingungen erfasst werden können. Es wurde deshalb ein am Handgelenk zu tragendes Gerät konstruiert ($18 \times 49 \times 50$ mm, 58 g), das erlaubt, den Schlaf-Wach-Zyklus und die motorische Aktivität während des Schlafes unter den Normalbedingungen des täglichen Lebens über längere Zeit zu registrieren. Dabei werden die durch Armbewegungen ausgelösten Signale über Zeitintervalle von 7,5 Min. summiert und der Summenwert in einem Festkörperspeicher abgespeichert. In Abständen von 5 Tagen werden die Aktivitätswerte auf den Plattenspeicher eines Kleincomputers übertragen. Einige Anwendungsmöglichkeiten der Methode werden anhand von Langzeitregistrierungen von Versuchspersonen unter Normalbedingungen sowie nach pharmakologischer Beeinflussung illustriert.

H^3 -Spiperone binding in pre- and postnatal rat brain

A. Bruinink, M. Schlumpf and W. Lichtensteiger, Institute of Pharmacology, University of Zürich, CH-8006 Zürich

In order to obtain information on the ontogeny of central dopamine receptors and to further characterize prenatal drug effects, we are investigating H^3 -spiperone binding in relation to the development of fetal dopamine systems in the rat. H^3 -spiperone binding was measured in a crude homogenate of forebrain over the range of 0.05–20 nM; the binding characteristics were defined in tissue taken from immature rats. Scatchard analysis revealed the presence of a high and a low affinity binding site (30-day-old male rats). Binding was highly pH-dependent with a maximum at pH 7.4 (37°C). After intracisternal injection of 6-hydroxydopamine at postnatal day 5, increased binding was observed in postweaning rats. H^3 -spiperone binding was present in fetal forebrain in the last third of gestation. At embryonic day 19½, specific binding attained approximately 5–10% of the postweaning values. The topographical distribution of binding sites is currently being investigated by H^3 -spiperone autoradiography.

Behavioral and biochemical effects of mofenensine (MOX), nomifensine (NOM) and amphetamine (AMP): similarities and differences

M. O. Carruba, W. P. Burkard and M. Da Prada, Department of Pharmacology, University of Milan, Italy, and Pharmaceutical Research Department, Hoffmann-La Roche & Co. Ltd, CH-4002 Basel

NOM, like AMP, induced a marked anorexia in hungry rats along with an increase in motor activity and stereotyped behavior. These behavioral changes were antagonized by pimozide or αMPT indicating that the mechanism of action of both NOM and AMP is mediated by dopamine. MOX neither caused anorexia nor induced locomotor stimulation or stereotyped behavior. The compound only slightly reduced food intake, an effect which was not dose-related and insensitive to pimozide, αMPT , metergoline, propranolol or phentolamine pretreatment. Furthermore, MOX also behaved differently from NOM and AMP in its inhibition of monoamine uptake mechanisms in brain synaptosomal preparations. NOM and AMP, but not MOX, significantly increased plasma catecholamine levels. It is concluded that MOX has a different central and peripheral pharmacological profile to NOM and AMP.

Mutational basis for transformation of mammalian cells by chemicals

J. C. S. Clegg and F. Oesch, *Pharmakologisches Institut der Universität Mainz, D-6500 Mainz, Federal Republic of Germany*

2 cell systems have been developed in which both mutation at a specific locus and malignant transformation can be studied. In C3H10T1/2 mouse cells induction of both ouabain-resistant mutants and foci of transformed cells by nitroquinoline-N-oxide (NQO) follows a linear dose-response; transformation occurs 24 times more frequently than mutation. When caffeine (1 nM) is present in the 48 h immediately after treatment, induction of both mutation and transformation by high doses of NQO is inhibited, although there is little effect on induction by lower doses of NQO. – 7,12-Dimethylbenz(a)anthracene induces both azaguanine-resistant mutants and transformants able to grow in soft agar when BHK cells are exposed for 24 h in the absence of exogenous activation systems. The dose-response for both processes shows an initial rise up to a concentration of 1 µg/ml and a subsequent decrease. Thus data from both cell systems is consistent with a mutational origin for malignant transformation by chemicals.

Genetic influence on behavioral effects of pentobarbital-Na⁺

P. Driscoll, R. Stübi and K. Bättig, *Institut für Verhaltenswissenschaft, ETHZ, CH-8092 Zürich*

Our male Roman low-avoidance (RLA/Verh) rats are less resistant to the toxic effects of pentobarbital-Na⁺ (PB) than are our male Roman high-avoidance (RHA/Verh) rats (*Arzneimittel-Forsch.* 27, 1582, 1977). They also differ from RHA/Verh rats in that they show no posturing or fighting when paired and subjected to unavoidable shocks (*Experientia* 34, 897, 1978). The reactions of both strains (males) to nontoxic doses of PB (4, 8, 16 and 24 mg/kg) have been subsequently studied during like-pairing in an avoidable shock situation after either shuttle box-avoidance training or previous shock-induced fighting experience. Under these conditions, it was found that all RHA/Verh pairs preferred avoidance or escape to fighting, and that the RLA/Verh pairs consistently showed about 90% 'freezing behavior' and no fighting. With the higher PB doses the RHA/Verh rats escaped more and avoided less, being capable of these responses even at PB 24 mg/kg. All RLA/Verh rats slept at this dose, however, demonstrating their greater sensitivity to PB.

Radioreceptor assay for determination of β -blockers in serum and brain of rats

G. Engel, O. Wagner and H. Wagner, *Pharmaceutical Division, Preclinical Research, Sandoz Ltd, CH-4002 Basel*

A new highly sensitive radioreceptor assay (RIA) for β -blockers has been developed using purified turkey erythrocyte membranes and 2-cyano-¹²⁵I-hydroxybenzylpindolol as a ligand. The technique is analogous to RIA. The separation of bound from free label was performed by filtration through glass-fibre filters. For the determination of β -adrenoceptor blocking agents in blood and whole brain of rats treated with different drugs, the standard curves were run in serum or in the 30,000 × g supernatants of brain homogenate. Pindolol, 32-468, 21-009 and propranolol were given in the dose range 4–40 mg/kg p.o. to rats

30 min before taking blood (animal perfusion) and brain. All data are given in order to the above-mentioned substances for a dose of 10 mg/kg p.o. Serum, ng/ml (425, 155, 600, 340). Brain, ng/g (140, 35, 200, 3250). Ratio [brain]/[serum] by RRA (0.33, 0.23, 0.33, 9.6). Ratio [brain]/[serum] after distribution of ¹⁴C-labelled drugs (0.74, 0.23, 0.23, 5.6). Sensitivity of RRA, ng/ml (4, 1, 1, 4). Propranolol has a 10 times higher brain than plasma level and penetrates 30 times better across the blood brain barrier than the other drugs.

Failure of haemorrhage to stimulate renin release in renin-depleted rats

A. Essadki, N. Boillat and J. Atkinson, *Institut de Pharmacologie de l'Université de Lausanne, CH-1011 Lausanne*

Removal of the clipped kidney of a 2-kidney, 1 clip (2K-G) hypertensive rat leaves a normotensive renin-depleted rat (RDR). We have investigated whether such rats are capable of releasing renin in response to bleeding. The left clipped kidney was removed from 8 2K-G rats and the left untouched kidney from 4 unclipped controls (C). 24 h later the carotid artery was cannulated under pentobarbital anaesthesia. Haemorrhage (21 ± 0.7 ml/kg b.wt in 180 ± 16 sec) in RDR induced a fall of mean blood pressure from 108 ± 8 mm Hg to 32 ± 2 which recovered to 43 ± 5 (p < 0.05) within 15 min. In controls mean blood pressure fell from 105 ± 9 to 26 ± 1 (p < 0.001) but within 15 min recovered more effectively to 73 ± 8 mm Hg (p < 0.01 comparison with RDR). The plasma renin levels (PRL) rose in C following haemorrhage from 72 ± 11 ngAI · ml⁻¹ · h⁻¹ to 248 ± 37 (p < 0.05) and to 317 ± 60 (p < 0.05) at 15 min, whereas in RDR, PRL did not change following haemorrhage (45 ± 7, 53 ± 11 and 75 ± 14, respectively). – Our results show that the renin-depleted rats investigated were incapable of increasing their PRL in response to haemorrhage.

Steric, lipophilic and electronic factors influencing the biological properties of enkephalins

J. L. Fauchère, K. Q. Do, A. N. Eberle, V. M. Kriwaczek, M. Gillan, S. Paterson, H. Kosterlitz, P. Schiller and R. Schwyzler, *Institut für Molekularbiologie und Biophysik, ETH Zürich, CH-8093 Zürich, Unit for Research on Addictive Drugs, Marishal College, University of Aberdeen, Scotland, and Clinical Research Institute of Montreal, Montreal, Canada*

L-Carboranylalanine (Car), L-adamantylalanine (Ada) and L-t-butylglycine (Bug) are examples of 'fat' or 'super' amino acids. The van der Waals space occupied by their side chains is considerably greater than that of the corresponding amino acids Phe, Leu and Val. The lipophilicity constants π of their side chains are 324 (Car), 309 (Ada) and 3 (Bug) times greater than those of Phe, Leu and Val side chains, respectively. Whereas Ada and Bug are purely aliphatic, Car has some 'pseudoaromatic' character. Enkephalin analogues with fat amino acids in positions 4 and 5 were prepared and assayed in vitro for morphine-like activity, receptor binding and susceptibility to enzymatic degradation. The results indicate that 'pseudoaromatic' character in position 4 is essential for activity, that lipophilicities tend to overcompensate steric restraints on receptor binding, and that enzymatic degradation is markedly attenuated.

Dobutamine effects upon retina dopamine receptors: biochemical and binding studies

A. Forster and M. Schorderet, *Institut d'Anesthésiologie (Hôpital cantonal) et Département de Pharmacologie, Ecole de Médecine, CH-1211 Genève 4*

Rabbit retinae were used for testing in vitro potential activation of dopamine receptors by a new cardioactive sympathetic amine dobutamine. In biochemical studies, cAMP generation was measured in response to dobutamine, which stimulated dopamine receptors only at 10^{-4} M. The dobutamine-induced formation of cAMP was blocked by fluphenazine and not by α - or β -adrenergic receptor antagonists. When the test was performed at 10^{-6} M, dobutamine, in contrast with dopamine, epinine or apomorphine, cannot stimulate cAMP formation. Furthermore, only at 10^{-4} M, dobutamine was also found to display a weak displacing capacity of ^3H -spiroperidol binding in homogenates of bovine retina compared with dopamine or other dopamine-related drugs. In conclusion, despite the structure relationship of dobutamine with other dopamine analogs, the pharmacological action of the new sympathomimetic agent is more comparable to that of β -receptor stimulating agents, when it is used in therapeutic range of concentration.

Effects of a hashish extract on the behavior of thirsty mice in an exploration test

H. R. Frischknecht and P. G. Waser, *Institute of Pharmacology, University of Zürich, CH-8006 Zürich*

Adult mice, water deprived for 18 h, were tested during a 10-min exploration in a newly developed cage. 1.5 h after the first application of hashish extract (20 mg Δ^9 -THC/kg, p.o.), the frequencies of locomotion, scan object, rear, drink (all $p \leq 0.01$) and eat ($p \leq 0.05$) were decreased, whereas explore and body care were unchanged and immobility was increased ($p < 0.01$) compared to oil-treated controls. Mice tested for the first time after 4, 7, or 9 drug applications showed only a slow and partial tolerance to the sedative drug effects. Thus after 9 drug treatments, locomotion, scan, rear, drink and immobility were still significantly affected, but compared to initially drugged mice, the effects were significantly diminished (rear, immobility) or vanished (eat). When animals were tested repeatedly after 1, 4, 7 and 9 administrations, no differences were found after the last drug application compared to naive mice drugged 9 times. Repeatedly tested controls however, drank significantly sooner and more frequently than naive controls.

Generality and facility of 2-way avoidance behavior in the pharmacological testing of selectively-bred rats

A. Fuchs, J. Harting and P. Driscoll, *Medizinische Forschung, E. Merck, Postfach 4119, D-6100 Darmstadt 1, Federal Republic of Germany, and Institut für Verhaltenswissenschaft, ETHZ, CH-8092 Zürich*

Female Roman high-avoidance (RHA/Verh) and Roman low-avoidance (RLA/Verh) rats, selectively bred for rapid- vs nonlearning of 2-way avoidance in a shuttle box (door, CS: light) were compared to commercial Wistar (W) female rats in another 2-way avoidance test (hurdle jump, CS: buzzer). Both Roman lines maintained their characteristic divergent patterns of behavior in the hurdle test, and the RHA/Verh rats reached the learning criterion (80% avoidance) significantly quicker than the W rats. The

avoidance-latencies of the learners among the RHA/Verh and W rats, however, as well as the dose- and time-effect curves and ED_{50} s of several preparations (chlorpromazine, haloperidol, clozapine) were the same in both groups. Therefore, the savings in time and work engendered by the shorter training periods required for RHA/Verh rats further justifies their use in the testing of neuroleptics in this type of study.

Pharmacokinetics of ^{14}C -tauroline, a novel chemotherapeutic, in rats

A. J. Ganz, C. Steinbach-Lebbin and P. G. Waser, *Institute of Pharmacology, University of Zürich, CH-8006 Zürich*

In order to study the kinetics of tauroline (4,4'-methylene-bis-[tetrahydro-2H-1,2,4-thiadiazine-1,1-dioxide]) in rats, 2 differently ^{14}C -labelled drugs (I and II) were used. I contained 3 ^{14}C atoms/molecule, incorporated as methylene bridges, whereas II had 4 ^{14}C atoms within the taurinamide part. The radioactivity in biological materials was calculated by scintillation counting after p.o., i.p. or i.v. application. – Independently from the way of administration radioactivity of I was mainly exhaled. About 20% appeared in urine and little in feces. Concentration in blood showed a first fast and a second slower decrease. I.v. application of II resulted in a fast decrease of radioactivity in blood. Radioactivity was mainly excreted in urine, to a smaller extent in feces, but not by breathing. – It could be shown that ^{14}C -tauroline is well-absorbed after p.o. and i.p. application. The drug seems to be metabolized by forming CO_2 from the methylene bridges and a water soluble metabolite from the taurinamide part of the molecule.

The 'glucose effect' of porphyria: presence in cultured hepatocytes and relationship to cytochrome P450 (P450)

U. Giger and U. A. Meyer, *Division Clinical Pharmacology, University Hospital, CH-8091 Zürich*

Administration of glucose causes decreased induction of hepatic δ -aminolevulinic acid synthetase (ALAS) and clinical improvement in patients with drug precipitated porphyria. The biochemical basis of this 'glucose effect' is unclear. Drugs precipitating porphyria are inducers of P450. We studied the 'glucose effect' on drug-induced ALAS and P450 in chick embryo hepatocytes cultured 46 h in Williams E medium in the absence of glucose. Results: Phenobarbital (PB) (0.4 mM, present for 16 h) resulted in increased ALAS activity and P450 content (192 ± 8 and $199 \pm 18\%$ of control, respectively). Glucose (10–90 mM) completely or partially prevented PB induction of ALAS and P450 in a dose dependent way. By contrast, 2-deoxyglucose or 3-O-methylglucose (5–50 mM) markedly enhanced PB-induction of ALAS and P450 in culture, contrary to observations in vivo (rats) and in ovo. Increased inducibility also was observed with glucagon, theophylline or cAMP in the presence of 11 mM glucose. Insulin (10–100 nM) reduced induction of P450 but had little or no effect on ALAS. Conclusion: A 'glucose effect' occurs in vitro in the absence of hormonal and other extrahepatic factors. The effect on ALAS correlates with and may depend on changes in P450.

Bacterial mutagenicity of cell-activated benzo(a)pyrene metabolites correlates better with carcinogenicity than mutagenicity of metabolites activated by cell homogenates

H.R. Glatt, R. Billings and F. Oesch, Pharmakologisches Institut der Universität, Obere Zahlbacher Strasse 67, D-6500 Mainz, Federal Republic of Germany

Using homogenized hepatocytes and a NADPH generating system for metabolism benzo(a)pyrene (BP), its 7,8- and 9,10-dihydrodiols, 3-OH-BP and 9-OH-BP were strongly mutagenic with *S. typhimurium* TA 100. With intact hepatocytes, the 7,8-dihydrodiol and, at high doses, BP showed strong effects. The other metabolites were only very weakly mutagenic. The results with intact, but not those with broken cells correlate quite well with whole animal carcinogenicity studies. – In the 2nd part of this study we investigated if differences in metabolism can explain the different mutagenicity results. When broken cells are supplemented only with a NADPH generating system, monooxygenases which activate BP-metabolites are favored. Other metabolic routes, possibly important for inactivation, may occur to much smaller extents than in vivo, due e.g. to dilution of cofactors. Therefore, we added such cofactors to the homogenate. Very efficient inactivation mechanisms for the 3-OH-BP and BP-9,10-dihydrodiol-induced mutagenicity were found. The activity of the 7,8-dihydrodiol was reduced least.

Variation of epoxide hydratase activity in man

H.R. Glatt, E. Kaltenbach, J. Lorenz, F. Tegtmeyer and F. Oesch, Pharmakologisches Institut der Universität, Obere Zahlbacher Strasse 67, D-6500 Mainz, Federal Republic of Germany

Epoxide hydratase (EH) is an enzyme involved in the metabolism of many carcinogens. In this study its activity in several tissues was compared between human subjects. EH activity varied 17-fold in liver, 5-fold in lung, 3.6-fold in native lymphocytes, 1.5-fold in cultured lymphocytes and 2.3-fold in cultured fibroblasts. The much larger variation in organs such as liver and lung which are heavily exposed to foreign compounds, compared with that in cultured cells under uniform environmental conditions indicates that epigenetic factors are essential for the differences. Several parameters such as smoking habits, tumors in the lung and treatment with some drugs were found to correlate with altered activity levels. It remains to be seen if these effects are due to enzyme induction, enzyme activation or to alteration in the tissue composition. Genetic disposition appears less likely since our experiments with cells in culture indicate that genetically caused atypical EH activities do not exist or are very rare.

Methods for studying drug actions at the first synapse of the baroreceptor reflex (BR)

G. Haeusler and R. Osterwalder, Pharmaceutical Research Department, F. Hoffmann-La Roche & Co. Ltd, CH-4002 Basel

3 methods were used to study the effect of drugs on the first synapse of the BR in the nucleus of the solitary tract (NTS): a) recording of drug-induced changes in NTS-field potentials evoked by electrical stimulation of the ipsilateral carotid sinus nerve; b) reversible interruption of synaptic transmission by cooling of the superficially-located NTS with thermodes and c) monitoring of the decline in effectiveness of the BR after impairment of transmission by reduction of the temperature of the NTS. The centrally

acting antihypertensive clonidine reduced the amplitude of the field potential in the NTS. Cooling-induced interruption of transmission in the NTS abolished the sympatho-inhibitory effect of low doses of clonidine. Impairment of transmission through less intense cooling was partly antagonized by clonidine. It is concluded that clonidine facilitates transmission at the first synapse of the BR.

Is substance P (SP) the transmitter at the first synapse of the baroreceptor reflex (BR)?

G. Haeusler and R. Osterwalder, Pharmaceutical Research Department, F. Hoffmann-La Roche & Co. Ltd, CH-4002 Basel

SP (5–20 µg) injected into the lateral brain ventricle of anaesthetized rats caused dose-dependent increases in blood pressure (BP). By contrast, local application of SP to the region of the nucleus of the solitary tract (NTS), using small pieces of filter paper soaked in SP-containing (2×10^{-3} M) solution, resulted in hypotension and bradycardia. Similar results were obtained in cats. A combined cannula electrode with an uninsulated tip enabled identification of sites in the NTS of rats and cats where electrical stimulation elicited decreases in BP and heart rate, i.e. an activation of the BR. Subsequent microinjection of SP (10–15 nmoles) through the cannula into these defined areas produced similar cardiovascular effects. Release of SP from nerve endings through local application of capsaicin to the NTS also caused an activation of the BR. The results are compatible with the view that SP is the transmitter at the first synapse of the BR.

Effects of γ -amino-butyric acid (GABA), dopamine (DA) and norepinephrine (NE) on the transmembrane potential of cat hippocampal pyramidal cells in vivo

P. L. Herrling, Preclinical Research, Sandoz Ltd, CH-4002 Basel

The 3 neurotransmitters were applied by iontophoresis within 50 µm of the somata of pyramidal cells recorded by intracellular electrodes and identified by electrical stimulation of the fornix and fimbria. 8 neurons reacted to the ejection of GABA with a rapid hyperpolarization of their membrane which, in contrast to that reported with the same cells in vitro (B.E. Alger et al., *Nature* 281, 315, 1979), did not reverse to a depolarization with prolonged (> 1 min) ejection times. – DA and NE also hyperpolarized 10 and 6 cells, respectively, within 1 sec of the start of the application. Preliminary measurements indicated that during GABA-mediated hyperpolarizations, the apparent membrane resistance decreased, whereas during DA and NE application there was an increase.

Effects of carbachol on the membrane potential of cat caudate neurons

P. L. Herrling, Preclinical Research, Sandoz Ltd, CH-4002 Basel

Carbachol was applied by iontophoresis to the immediate vicinity (approximately 50 µm from the soma) of intracellularly recorded neurons. The effect was a slow and reversible depolarization (10–25 mV) of the resting potential causing the appearance of action potentials (APs) in 13 cells. The first APs occurred 10–20 sec after the onset of usually 20 sec long iontophoretic pulses. These effects lasted from 20 to 160 sec and were blocked by atropine. Glutamate on the same neurons had excitatory effects starting and ending much faster. – During carbachol-induced depolarizations, the amplitudes of the cortically evoked EPSPs and IPSPs

were reduced and increased, respectively. The effect on the IPSP is in contrast to earlier findings (G. Bernardi et al., *Brain Res.* 114, 134, 1976), where it was reported that the amplitude of this IPSP was reduced during the muscarinic action of acetylcholine on rat caudate neurons. - It was concluded that the here reported effects of carbachol were probably mediated by muscarinic receptors.

Differential effects of psychotropic drugs on central and peripheral β -adrenergic receptors

U. E. Honegger and M. H. Bickel, *Department of Pharmacology, Friedbühlstrasse 49, CH-3010 Bern*

The antidepressant, imipramine, as well as the neuroleptic, chlorpromazine (CPZ), reduce the β -adrenergic mediated cAMP-response in rat brain (Schultz, *Nature* 261, 417, 1976). In addition, Banerjee et al. (*Nature* 268, 455, 1977) showed a decrease in the number of central β -receptors after chronic desipramine (DMI) treatment of rats. We examined the effects of chronic DMI and CPZ treatments (10 mg/kg per day, i.p.) of rats on β -receptors of brain and of submaxillary glands as an example for a peripheral organ. Receptors were assessed by direct binding studies with the β -blocking agent ^3H -dihydroalprenolol. DMI treatment reduced the number of central and peripheral β -receptors to the same extent (26%). CPZ diminished central receptor binding capacity (24%) but caused no reduction in submaxillary glands. These data suggest that a decrease in the number of central β -receptors is not a specific effect of antidepressant drugs. The simultaneous determination of central and peripheral β -adrenergic transmission may be taken into consideration as a test system for psychotropic drugs.

Is desmethylinipramine (DMI) a lysosomotropic agent?

U. E. Honegger, A. A. Roscher and U. N. Wiesmann, *Departments of Pharmacology and Pediatrics, University of Bern, CH-3010 Bern*

In this study we investigated the uptake and intracellular localization of DMI in cultured human fibroblasts, obtained from normal skin biopsies. Confluent monolayer cultures were incubated with ^{14}C -DMI in Eagle's MEM with 0.25% BSA, buffered with bicarbonate/ CO_2 at pH 7.4. Intracellular uptake of ^{14}C -DMI was rapid, reaching half-maximal saturation within 15 min at 37°C. It was proportional to the extracellular DMI concentrations over a range of 0.5–500 μM . Intracellular concentrations were about 1000 times higher than in the culture medium. DMI uptake could be enhanced by rising extracellular pH. These results can be explained with intracellular trapping by protonation of the weak base in subcellular organelles of acidic pH. Fibroblasts chronically treated with DMI showed a typical granulation suggesting lysosomal localization. In addition, the degradation of ^{35}S -labelled glycosaminoglycans was inhibited, indicating lysosomal dysfunction. These kinetic, morphological and functional findings imply that DMI is concentrated within lysosomes.

A novel screening system for detection of cholestatic compounds

S. Hottinger, H. Wietholtz, G. Ris and R. Preisig, *Department of Clinical Pharmacology, CH-3010 Bern*

Since in animal experiments prediction of the cholestatic potential of new drugs is not yet feasible, we have developed a screening system in chick embryo hepatocyte monolayers (HM). HM were exposed during 24 h to the cholestatic model compounds (1–100 μM) ethinyl estradiol (EE),

lithocholate (Li), iproniazid (Ip) and - for comparison - to taurocholate (TC). Subsequently, ^{14}C -aminopyrine (AP) demethylation, conjugation of ^3H -cholic acid (CA), and P_{250} content of HM were measured. Whereas AP demethylation was uninfluenced by TC (V_{\max} 13.2 pmoles/min $^{-1}$ mg $^{-1}$ protein, K_m 1.3 mM), EE, Li and Ip resulted in decreased V_{\max} (by 70%) and K_m (by 80%). A reduced conjugation (by 70%) of ^3H -CA was also observed. In contrast, P_{250} content of HM remained unchanged after Ip, but was reduced after EE and Li. Thus, the application of cholestatic compounds, differing in their chemical structure, to HM results in uniform changes of phase I and II reactions, suggesting that HM may serve as a suitable screening system for new drugs prior to their use in man.

Somatostatin-induced cholestasis; inhibition of ductular bile flow

S. Hottinger, H. Wietholtz and R. Preisig, *Department of Clinical Pharmacology, CH-3010 Bern*

Since somatostatin (S) is known to inhibit gastrointestinal motility and pancreatic excretion, it is reasonable to suppose that it might affect bile formation (BF). Consequently we investigated the influence of S on BF in unanesthetized female boxer dogs, equipped with Thomas cannula. S was infused during 1 h (3.5 $\mu\text{g/kg}$ b.wt, a dose known to reduce hepatic blood flow) together with Na-taurocholate (24 $\mu\text{moles/min}$, to compensate for the interrupted enterohepatic circulation) and ^{14}C -erythritol (E). In all animals S caused a marked reduction of BF, while the E-clearance remained unchanged and the bile to plasma ratio of E was increased. In addition, biliary chloride and bicarbonate concentrations were diminished, suggesting that S had its effect at the ductular level. Since the secretin induced choleresis was unaffected by simultaneous administration of S, it is suggested that S causes cholestasis by inhibiting endogenous secretin release, rather than by a direct effect on ductular solute excretion.

Differential effects of the components of Co-dergocrine mesylate (BAN, dihydroergotoxine, Hydergine®) on Lashley maze acquisition in rats

A. L. Jatón, J. M. Vigouret and D. M. Loew, *Pharmaceutical Division, Preclinical Research, Sandoz Ltd, CH-4002 Basel*

Co-dergocrine (I) is composed of dihydroergocristine (II), dihydroergocornine (III), dihydro- α -ergokryptine (IV) and dihydro- β -ergokryptine (V) in the ratio of 3:3:2:1. Rats were trained in 4 consecutive trials to obtain a liquid reward. Drugs were given s.c. 4 h before each trial, and starting time (ST), running time (RT) and number of errors (NE) were recorded on trial 4 (Loew et al., in: *Dopaminergic Ergot Derivatives and Motor Function*, p. 129, ed. Calne and Fuxe, Pergamon Press, Oxford and London 1979). I (3 and 10 mg/kg) reduced ST, RT and NE. II and III (3 mg/kg) prolonged ST. IV (1.5 mg/kg) reduced NE, but V (1.5 mg/kg) showed no significant effect. At the doses investigated, none of the components exerted all of the effects seen after I. On the contrary, the actions of II and III on ST were opposite to that of I. These results confirm our earlier suggestion that effects on motor performance (RT) are independent of changes in cognitive performance (NE).

Hypermotility of the amphetamine type induced by a constituent of khat leaves

P. Kalix, *Département de Pharmacologie, Université de Genève, Rue Ecole-de-Médecine 20, CH-1211 Genève 4*

Khat leaves, widely used as a stimulant in East Africa and the Arab Peninsula, contain the alkaloid (-)-cathinone.

The effects of this substance on the locomotor activity of rats were compared to those of d-amphetamine. Both substances were found to induce a similar degree of hypermotility with (-)cathinone being approximately one third as potent as d-amphetamine. Furthermore, the effect of (-)cathinone on the locomotor behavior of hypophysectomized rats was analogous to that reported for d-amphetamine in such animals. The results support the claim that the symptoms caused by the chewing of khat are amphetamine-like.

Indirect sympathomimetic actions of the MAO inhibitor deprenyl at high doses

H. H. Keller, M. Pieri, R. Kettler and M. Da Prada, Pharmaceutical Research Department, F. Hoffmann-La Roche & Co., Ltd, CH-4002 Basel

L-Deprenyl (D), a type B MAO inhibitor, combined with L-DOPA has been proposed for the treatment of Parkinsonians (Birkmayer et al., *Lancet* **I**, 439, 1977). The MAO inhibition is probably due to D itself since the microsomal enzyme inhibitor proadifen (PRO) increased D-induced MAO inhibition in rat liver and brain and enhanced D-induced decrease of HVA in rat brain. However, D must also be considered a prodrug since it is metabolized to metamphetamine (MA, Reynolds et al., *Br. J. clin. Pharmacol.* **6**, 542, 1978). In rats with 6-OHDA-induced unilateral lesion of the nigro-striatal pathway, D (10 mg/kg i.p.) induced circling as seen with MA. Haloperidol antagonized both D- and MA-induced circling, but PRO only D-induced circling. In rats with low plasma noradrenaline (NA) after ganglionic blockade and MAO inhibition (pargyline) D increased plasma NA levels several-fold. Indirect sympathomimetic activity of D is also exerted in the CNS since D enhanced K^+ -induced release of 3H -NA from rat cerebral cortex slices.

Computer analysis of the rats' sleep stages

H. Kleinlogel, Research Institute, Wander Ltd, CH-3001 Bern

Simultaneous EEG recordings are made from 4 rats using a 16-channel Mingograph. From each rat EEGs of the cortex occipitalis and EMG are recorded. Since in paradoxical sleep (PS) signals of high frequency are superimposed on the characteristic θ -rhythm, one cortical EEG is additionally filtered above 10 Hz. The EMG is transformed into a frequency band of 1-32 Hz by an amplitude discriminating frequency-voltage converter. A Normalized-Slope-Descriptor computes the Hjorth parameters of activity (μV), mobility (Hz) and complexity (Hz) (Hjorth, *Electroenceph. clin. Neurophysiol.* **34**, 321, 1973) during a selected epoch duration of 8 sec. The parameters of each epoch are continuously stored on a digital magnetic tape and computer analyzed off line to determine the means and standard deviations of the parameters during the whole recording time. In a second step these values are used to attach to each epoch one of 6 different patterns of the Hjorth parameters associated with different stages of sleep and waking.

Early biochemical effects of a tumor promoting phorbol ester on mouse fibroblasts and their modulation by dexamethasone

R. Lanz and K. Brune, Department of Pharmacology, Biozentrum, University of Basel, Klingelbergstrasse 70, CH-4056 Basel

The phorbol ester 12-O-tetradecanoylphorbol-13-acetate (TPA) induces inflammation, proliferation and tumor pro-

motion. In addition, TPA is a potent releaser of prostaglandins in vitro. It has been suggested that prostaglandins might be initiators of a cascade of events finally causing increased cell proliferation. We have tested this hypothesis in cultures of confluent mouse 3T3 fibroblasts. We found that addition of 10^{-7} M TPA to the cells is followed successively by release of prostaglandin E_2 (PGE_2) induction of the enzyme ornithine decarboxylase (ODC), stimulation of 3H -thymidine incorporation into DNA and cell proliferation. Pretreatment of the cells with the anti-inflammatory steroid dexamethasone (10^{-6} M) inhibits TPA-induced PGE_2 release but enhances the other effects of TPA. Addition of PGE_2 to the culture fluid only at high doses (10^{-5} M) has a marginal stimulating effect on ODC induction and cell proliferation. These data suggest that the proliferative effect of TPA on 3T3 cells is not mediated by PGE_2 .

Blood platelets as models for neurons: receptor- and nonreceptor-mediated membrane effects

A. Laubscher, A. Pletscher and C. G. Honnegger, Departement Forschung, Kantonsspital, CH-4031 Basel

In human and rabbit platelets the shape change reaction (transition from discoid to spheroid form) caused by 5-hydroxytryptamine (5HT) agonists showed stereoselectivity and was specifically inhibited by 5HT-antagonists. Butanol (3%) which removes adhering plasma proteins from the cell membrane abolished this shape change. D-LSD a mixed 5HT agonist/antagonist showed saturable, high affinity binding to the platelet membrane. Various drugs, which counteracted the LSD- and 5HT-induced shape change also antagonized LSD-binding. Random coil basic proteins, e.g. myelin basic protein also caused a shape change reaction. This was enhanced after butanol treatment of the platelets and antagonized by the polyanion heparin though not by 5HT-antagonists. In conclusion, 5HT-agonists and antagonists, in contrast to basic proteins probably influence platelet function by interfering with specific membrane receptors. Both types of shape change inducers have been reported to act on neurons of the central nervous system.

5HT neurons in rat brain after acute and chronic treatment with p-chloro-amphetamine (PCA) and p-chloro-N-methylamphetamine (PCMA)

H. P. Lorez, A. Saner and J. G. Richards, F. Hoffmann-La Roche, PF/1, CH-4002 Basel

PCA and PCMA are classified as serotonin (5HT) neurotoxins since they induce e.g. a long-term decrease of brain 5HT. However morphological results showing neuronal degeneration are inconclusive. We hoped to find more marked (toxic) effects after 20-day PCA or 32-day PCMA treatment (increasing doses 5-30 and 5-40 mg/kg i.p., respectively) than after 1×35 mg/kg. However no further decrease of brain 5HT and no delay of 5HT recovery during 40 days was obtained. Formaldehyde-induced 5HT fluorescence accumulated in swollen axons 1-6 days after 1 dose, but similar axons were rare after chronic treatment possibly indicating acute degeneration and ongoing de- and/or regeneration of some 5HT axons. No signs of degeneration were revealed by either quantitative fluorescence-histo-chem. of metencephalic 5HT cells or by EM of n. suprachiasmaticus (rich in 5HT nerve terminals) and identified (supraependymal) 5HT terminals. Damage to other 5HT nerve terminals cannot be excluded.

Uptake and release of adenosine in rabbit vagus nerve, at rest and during activity

J. C. Maire, J. Médilanski and R. W. Straub, *Département de Pharmacologie, Ecole de Médecine, CH-1211 Genève 4*

In desheathed vagus nerve incubated at 37 °C in Locke with 0.2 μ M adenosine and trace amounts of 3 H-adenosine, the uptake of radioactivity was linear with time up to 2 h. Incubation with different adenosine concentrations showed that the uptake had a linear and a saturable component, with a K_m of 19 μ M. Most of the incorporated label was found in nucleotides. The uptake was partially inhibited by AMP, ADP and ATP, dipyridamole, colchicine and clozapine, and abolished by tubercidine. Adenine and D-ribose had no effect. – In labelled nerves, washed with Locke, the efflux of label had a rate constant of $0.5 \times 10^{-3} \text{ min}^{-1}$. Addition of adenosine (2 μ M) increased it to $2.1 \times 10^{-3} \text{ min}^{-1}$. Electrical activity caused an extra efflux of $1.8 \times 10^{-6} \text{ impulse}^{-1}$. The resting and the stimulated efflux consisted of adenosine (2%), inosine and hypoxanthine, showing that release of adenosine is not confined only to the nerve endings.

The effect of oxygenated water on alcohol metabolism in man

J.-A. Maring and J.P. von Wartburg, *Medizinisch-chemisches Institut, Postfach, CH-3000 Bern 9*

Besides alcohol-dehydrogenase, catalase and a microsomal system, both oxygen-dependent, oxidize ethanol to acetaldehyde in the liver of mammals. Hyvärinen et al. (Life Sci. 22, 553, 1978) demonstrated that drinking oxygenated water increased the pO_2 in the portal vein of macaque monkeys, resulting in a 1.6 times faster rate of ethanol elimination. Therefore, we carried out similar experiments with 5 human volunteers. The fasted subjects received 4 times 200 ml portions of tap or oxygenated water at 30-min intervals, the 2nd portion containing 0.5 g ethanol/kg of b. wt. 1 h after ethanol ingestion the mean breath ethanol concentrations in control and oxygen experiments were not statistically different (4.46 ± 0.33 and $4.74 \pm 0.53 \mu\text{M}$, corresponding to blood alcohol levels of 43 ± 3 and $46 \pm 5 \text{ mg}/100 \text{ ml}$, respectively). During the following 2 h the breath ethanol concentrations decreased linearly to 1.94 ± 0.29 and $1.89 \pm 0.15 \mu\text{M}$, respectively. After 1 h the breath acetaldehyde levels in oxygen experiments ($43.3 \pm 9.4 \text{ nM}$) were not significantly different from controls ($49.9 \pm 17.4 \text{ nM}$), confirming the lack of an effect of oxygenated water.

Comparison of the effect of several ergot derivatives on central pre- and postsynaptic α -adrenoceptors

R. Markstein, *Pharmaceutical Division, Preclinical Research, Sandoz Ltd, CH-4002 Basel*

Pharmacological and biochemical experiments with ergot derivatives suggest antagonistic effects at α -adrenoceptors. There are at least 2 types of central α -adrenoceptors, a presynaptic one controlling the NA-release and another one, mediating the postsynaptic effects of NA. In order to understand the possible net result of the interaction of ergot derivatives with α -adrenoceptors in a working noradrenergic synapse, the effects of dihydroergocornin (I), dihydroergocristine (II), dihydro- α -ergokryptin (III) and dihydro- β -ergokryptin (IV) on the NA-dependent cyclic AMP formation and the electrically stimulated NA-release from slices of rat brain occipital cortex were studied. All tested ergot derivatives potently antagonised the stimulating effect of NA on the cyclic AMP formation. However, all tested ergot

drugs at very low concentrations also increased the stimulated release of NA. The results suggest that for the understanding of the central effects of ergot drugs, presynaptic effects in noradrenergic systems must also be taken into consideration.

Cholinergic influences on maze patrolling

J.R. Martin, D.H. Overstreet and P. Driscoll, *Institut für Verhaltenswissenschaft, ETH, CH-8092 Zürich, and School of Biological Sciences, Flinders University, Bedford Park, 5042 South Australia*

Rats of 2 psychogenetically selected lines (RHA/Verh and RLA/Verh) received i.p. injection of scopolamine·HBr (SCO, 0.25, 1.0 or 4.0 mg/kg), pilocarpine·HCl (PIL, 3.0, 6.0 or 12.0 mg/kg) or oxotremorine (OXO, 0.2, 0.4 or 0.8 mg/kg) and were then tested once in a complex maze. Rats receiving PIL or OXO injection were pretreated with methscopolamine to counter their peripheral actions. Treatment with SCO, PIL or OXO depressed locomotion, reduced explored area and increased the time required to initially activate 24 different photocell units distributed throughout the maze. The SCO doses were equally effective in both rat lines, whereas only RHA/Verh rats were affected by the lowest PIL dose. OXO treatment elicited tremors only in the RLA/Verh rats. These results demonstrate the differential sensitivity of RHA/Verh and RLA/Verh rats to central cholinergic manipulation and the deleterious effect of treatment with SCO, PIL, or OXO on maze patrolling in both rat lines.

Solubility and cholestatic property of bile acids (BA)

U. Mathis, G. Karlaganis and R. Preisig, *Department of Clinical Pharmacology, CH-3010 Bern*

Administration of cholestatic BA, such as tauroolithocholate (TLi) or tauro-3 β -hydroxy-5-cholenoate (THC), is associated with dilatation of bile canaliculi and loss of microvilli. The mechanism responsible for these structural changes and their relationship to cholestasis is not understood. Since poor solubility of these BA may be an important factor, we have compared the effects of TLi and THC with those of sulfotauroolithocholate (STLi) on bile formation in rats with bile fistulae during pentobarbital anesthesia. Compared to controls (infused with 10% albumin in NaCl, used to solubilize TLi and THC), STLi (100 nmoles $\text{min}^{-1} 100 \text{ g}^{-1} \text{ b.wt}$) did not affect bile flow; although endogenous BA excretion was in part replaced by STLi, BA independent fraction (IF) and the amount of water 'obligated' by BA remained unchanged. In contrast, equimolar doses of TLi and THC produced complete abolition of BA-IF, suggesting that solubility may be the primary determinant for cholestatic potential of structurally similar BA.

Characterization of 2 opiate κ -agonists

R. Maurer and T.J. Petcher, *Pharmaceutical Department, Preclinical Research, Sandoz Ltd, CH-4002 Basel*

Classical pharmacology led to the proposal of different subgroups of opiate receptors: μ , σ and δ . More recently kappa (κ) opiate receptors have been added. We have compared 2 tritiated representative κ -agonists, ethylketazocine (E) and a benzomorphan derivative with a hydroxycyclopropylmethyl side chain at the nitrogen atom ([–]-Isomer of 14-707), using crude synaptosomal membranes from total rat brain for binding studies. – A single binding site can be detected with both ligands in the presence or absence of sodium, the apparent dissociation constants and the B_{max} vary considerably, however (K_D E: 1.90 nM, B_{max}

E: 96.8 pM, K_D 14-707: 0.48 nM, B_{max} 14-707: 156 pM). – A small number of selected opiate agonist/antagonists were chosen to further differentiate the 2 ligands by their IC_{50} values.

Methylation of rat liver DNA by the carcinogen dimethylnitrosamine (DMNA) formed in vivo from dimethylamine (DMA) and dietary nitrite or nitrate

A. Meier-Bratschi, W. K. Lutz and Ch. Schlatter, Institute of Toxicology, ETH/University of Zürich, CH-8603 Schwerzenbach

The nitrosation of amines by nitrite leads to nitrosamines which are then metabolized to alkylating agents. Methylation of liver DNA by DMNA can be studied with radioactive tracers and can be used for the measurement of the in vivo nitrosation of dietary DMA: Adult male rats received by gavage 50 mg/kg KNO_2 and 1.15 mg/kg ^{14}C -DMA-HCl. After 6 h liver DNA was isolated and its specific radioactivity was compared with that obtained after administration of either labelled DMA or DMNA. The results indicate that about 2–3% of the dose of DMA have been nitrosated to DMNA. The in vivo reduction of nitrate to nitrite was similarly determined; rats were pretreated with 0, 1000 or 3000 ppm KNO_3 in the diet for 1 week. They then received ^{14}C -DMA with an additional single dose (0, 100, or 300 mg/kg) of nitrate. The specific activity of liver DNA was increased only after the 3000 ppm pretreatment and corresponded to a value that was calculated for a 0–6% conversion of nitrate to nitrite.

Apparent incorporation of heme (H) into apocytochrome P450 (apo P450): requirement for GSH

P. J. Meier and U. A. Meyer, Division of Clinical Pharmacology, University Hospital, CH-8091 Zürich

Induction of cytochrome P450 requires coordinated synthesis of apoP450 and the prosthetic group H. After experimental dissociation of these 2 biosynthetic processes by concomitant treatment of rats with phenobarbital (PH) and $CoCl_2$, apoP450, determined by its in vitro reconstitution to functionally active holocytochrome with H, accumulated predominantly in rough endoplasmic reticulum closely associated with mitochondria (MITO-RER; Exp. Cell Res. 111, 479, 1978). We studied the in vitro conditions required for optimal incorporation of H into free apoP450 in MITO-RER from livers of rats treated with PH and $CoCl_2$. Results: 1. The in vitro incorporation of H into free apoP450 was dependent on the presence of a soluble, heat stable factor contained in the liver cytosol of $CoCl_2$ -pretreated rats. 2. Treatment with $CoCl_2$ resulted in a 6-fold increase in the hepatic concentration of GSH (29.10 ± 2.43 μ moles/g) over NaCl-pretreated rats (4.90 ± 1.55 μ moles/g). 3. GSH (2–4 mM) added to MITO-RER accounted for 78% of the effect on H-incorporation of the $CoCl_2$ -cytosol. Conclusions: GSH plays an important role in the in vitro incorporation of H into apoP450.

Determination of cholinergic quaternary ammonium (QA) and other amine salts using a new syringe micropyrolyzer with gas chromatography-chemical ionization-multiple ion detection (GC-CI-MID)

F. Mikeš and G. Boshart, Pharmakologisches Institut der Universität, CH-8006 Zürich

For the determination of QA and other amine salts by the sensitive GC-CI-MID method, these salts must first be

converted to a volatile form. We have developed a new flash filament syringe micropyrolyzer for use with every GC and with which these amine salts can be demethylated and deprotonated, respectively. The products are immediately carried with the carrier gas through the pyrolyzer needle into the GC. Acetylcholine and choline extracted from biological samples may be analyzed by pyrolysis (Pyr)-GC-CI-MID with a detection limit of 10 pg, and 8 determinations per h can be performed. Alkaloid (atropine, nicotine, morphine, etc.) salts may be deprotonated by pyrolyzing at 3.0 Amp on a 15×0.3 mm o.d. platinum wire. The potential of Pyr-GC-CI-MID with a computer system for the simultaneous determination of several amine containing neurotransmitters and pharmaca in various tissues is being explored.

Reduced sensitivity of cortical neurons to noradrenaline after chronic treatment with antidepressant drugs

H.-R. Olpe, Biology Laboratories, Pharmaceuticals Division, Ciba-Geigy Ltd, CH-4002 Basel

The sensitivity of cingulate cortical neurons to microiontophoretically administered noradrenaline and GABA was investigated in groups of rats treated either chronically or acutely with various antidepressant drugs or with the tricyclic antiepileptic carbamazepine. The chronically treated animals received one daily i.p. injection of either desipramine (10 mg/kg), clomipramine (10 mg/kg), maprotiline (25 mg/kg), tranlycypromine (1 mg/kg) or carbamazepine (30 mg/kg) during 4 weeks. The acutely treated rats obtained one daily injection of the vehicle during 4 weeks, followed by one single injection of one of the 5 drugs 24 h before the experiment. In chronically treated rats a statistically significant reduction in the sensitivity of cells to noradrenaline was observed with all 4 antidepressants. The chronic treatment with carbamazepine had no effect on the noradrenaline sensitivity of cortical neurons. The sensitivity of these neurons to GABA was unchanged following chronic administration of these antidepressants.

Rebound hypertension following single doses of clonidine in rats

M. Parker, R. Studer and J. Atkinson, Institut de Pharmacologie de l'Université de Lausanne, CH-1011 Lausanne

Rebound hypertension following abrupt cessation of treatment with clonidine has been observed in hypertensive patients as well as in hypertensive rats. Rebound peaks of blood pressure (BP) and heart rate (HR) have recently also been described after single doses of clonidine in normotensive rats. – We have compared the BP and HR effects of single doses of clonidine in unanesthetized rats or rats anesthetized with either ether or pentobarbital. Under *ether anesthesia*, BP measured by the tail cuff procedure, slightly but significantly decreased 1 h after 0.03 or 0.1 mg/kg i.m. clonidine, HR remained unchanged. No rebound BP peak was observed after 18 or 24 h. Under *pentobarbital anesthesia*, 0.05 mg/kg i.m. clonidine, within the 1st h, induced a significant fall in BP (carotid artery cannulation) (–28.3%) and of HR (–33.1%) followed by a rebound peak of BP (+23% above pre-drug level) at 14–20 h. In *unanesthetized* rats, 0.1 mg/kg i.m. clonidine induced no significant primary change in BP (chronic cannula in aorta) but in 4 out of 10 rats there was a significant rebound peak in blood pressure (+13 \pm 2 mm Hg above pre-drug level: 120 ± 5) 18 h later.

Uptake of catecholamines (CA) and their methoxy-derivatives by human platelets

G.B. Picotti, A.M. Cesura, M.D. Galva and M. Da Prada, *Institute of Pharmacology, University of Milan, Italy, and Pharmaceutical Research Department, Hoffmann-La Roche & Co. Ltd, CH-4002 Basel*

Upon aerobic incubation in plasma containing 10^{-7} to 10^{-4} M labelled normetanephrine, metanephrine or methoxytyramine (MT), human blood platelets accumulated these methoxy-derivatives against a concentration gradient until concentration ratios (platelet/plasma) of up to 300:1 were obtained. The uptake reached a plateau at 60 min and the substrate concentration curves showed a saturable and a nonsaturable component. Kinetics analysis revealed that the affinity of MT for the platelet uptake system was higher (K_m 2×10^{-6} M) than that of dopamine (K_m 50×10^{-6} M) but lower than that of 5HT (K_m 0.4×10^{-6} M). The uptake of the methoxy-derivatives was markedly reduced at 4 °C or in the presence of the metabolic inhibitors NaF and KCN. CA and their methoxy-derivatives seem to be, at least in part, stored in 5HT organelles since reserpine partially inhibited their accumulation in platelets.

Antagonism by caffeine and theophylline of diazepam effects on the cat spinal cord

P. Polc, *Pharmaceutical Research Department, F. Hoffmann-La Roche & Co. Ltd, CH-4002 Basel*

Caffeine and theophylline competitively inhibit diazepam binding in the brain (Marangos et al., *Life Sci.* 24, 851, 1979). A high density of benzodiazepine receptors in the substantia gelatinosa of the spinal cord (Young and Kuhar, *Nature* 280, 393, 1979) prompted a study of the interaction between diazepam and methylxanthines at the spinal level. In unanesthetized spinal cats, caffeine and theophylline ($1\text{--}30\text{ mg}\cdot\text{kg}^{-1}$ i.v.) reversibly and dose-dependently reduced the increase of segmental dorsal root potentials and dorsal root reflexes induced by diazepam ($0.1\text{--}1\text{ mg}\cdot\text{kg}^{-1}$ i.v.) without per se consistently affecting spinal cord activities. These findings support the evidence from binding studies by demonstrating the antagonistic effects of methylxanthines on a well-known action of diazepam on a particular synaptic event, i.e. enhancement of GABAergic presynaptic inhibition in the spinal cord (Polc et al., *Arch. Pharmac.* 284, 319, 1974).

Metabolic inhibition decreases β -adrenoceptor density in intact rat reticulocytes

H. Porzig and M. Baer, *Pharmakologisches Institut der Universität, Friedbühlstrasse 49, CH-3010 Bern*

We report experiments suggesting that the maintenance of steady state β -adrenoceptor density in rat reticulocytes requires metabolic energy. Receptor numbers were estimated from stereospecific binding of the β -antagonist (^3H)-(–)-dihydroalprenolol (DHAP). With saturating concentrations of DHAP fresh reticulocytes bound 10 ± 0.81 fmoles/ μl cells. When metabolic inhibitors were used to lower endogenous ATP to $\sim 1\text{ }\mu\text{M}$ or when fresh cells were incubated at 1 °C, specific DHAP binding decreased to 6.7 ± 0.6 and 4.2 ± 0.4 fmoles/ μl cells, respectively. The loss of β -adrenoceptors in the cold was partially reversible upon rewarming. The apparent dissociation constant (K_D) for DHAP was close to 1 nM and did not change significantly during metabolic inhibition. The K_D value for the agonist isoprenaline decreased from 440 ± 68 nM in controls to 120 ± 24 nM in starved cells and 41 ± 10 nM in cells at 0 °C.

Heme biosynthesis (HB) in rat brain cell culture (RBCC)

I. Reubi, P. Honegger and U.A. Meyer, *Clinical Pharmacology, University Hospital, CH-8091 Zürich, and Institute of Physiology, University of Lausanne, CH-1000 Lausanne*

Heavy metal poisoning, hepatic porphyria and tyrosinemia are disorders of HB characterized by heme precursor accumulation and nervous system dysfunction. The relationship between defects in brain HB and brain dysfunction is unknown. We evaluated, if HB can be studied in RBCC (Brain Res. 133, 329, 1977). Results: 1. The activity of δ -aminolevulinic acid (ALA) synthetase, ALA dehydrase and uroporphyrinogen I synthetase were 374 ± 38 , 1722 ± 560 , 217 ± 4 in RBCC and 480 ± 65 , 1800 ± 196 , 181 ± 14 in homogenate (HO) from adult rat brain (mean \pm SD, pmoles ALA equivalents formed or used mgprot^{-1} 90 min^{-1}). 2. RBCC and HO were incubated with 10^{-4} M ALA, porphyrins (P) extracted as methylesters and analyzed by HPLC: uro-P (37%), copro-P (18%) and proto-P (18%) accumulated in HO, while in RBCC there was almost exclusive accumulation of proto-P (85%). Conclusions: 1. 3 enzymes of HB have similar activities in RBCC and HO. 2. The difference in precursor accumulation suggests a relative deficiency of the final steps of HB in RBCC. 3. RBCC may provide an important tool to investigate defects of HB in vitro and their effect on brain cell function.

Localization of benzodiazepine receptors (BR) in rat brain by electron microscopy

J. G. Richards, H. Möhler and M. K. Battersby, *Pharmaceutical Research Department, Hoffmann-La Roche & Co. Ltd, CH-4002 Basel*

Flunitrazepam (FNZP), a potent benzodiazepine which binds reversibly and with high affinity to BR, can be used as a photoaffinity-label for the receptor. UV irradiation (at 4 °C) of brain slices from rats previously injected with [^3H]FNZP leads to its irreversible incorporation into the tissue; co-injection of other benzodiazepines prevented this with a potency corresponding to their affinity for BR. High resolution autoradiography was used to localize BR in brain slices photolabelled with [^3H]FNZP. In cerebral and cerebellar cortex 55% and 74%, respectively, of all radioactivity was present in nerve terminal regions, which occupied only 16% of the total slice area. This selective accumulation was markedly reduced in the presence of Ro 11-7800, a potent benzodiazepine. Among the nerve terminals labelled in the cerebellum (20% had symmetric synapses, 10% asymmetric, 60% nonsynaptic and 10% obscured by silver grains) were those believed to be GABAergic, e.g. Golgi terminals.

Drug induced β -adrenergic receptor regulation in different organs of rats

A.A. Roscher, U.E. Honegger and U.N. Wiesmann, *Departments of Pediatrics and Pharmacology, University of Bern, CH-3010 Bern*

Adaptive changes in the number of β -adrenergic receptors have recently been shown to be a self-regulating mechanism protecting the target organs from abnormal neurotransmitter levels. Therefore we studied the susceptibilities of different rat organs to changes in β -receptor characteristics induced by isoproterenol (ISO) and reserpine (RES). Male Sprague-Dawley rats (80–100 g) were daily injected with

5 mg/kg of ISO or 0.5 mg of RES for 12 days. β -adrenergic receptors were measured in crude membrane preparations from lung, brain, heart and submaxillary glands by a direct binding assay using the β -receptor blocking agent ^3H -dihydroalprenolol (DHA) as a high affinity radioligand. Both treatments changed the apparent numbers of specific DHA-binding sites, while binding affinities remained unchanged. Percentual changes in receptor numbers were highest in salivary glands, whereas the drug effects were less pronounced in the other organs investigated. The results suggest that the potency to compensate for changes in neurotransmitter levels is differently developed from organ to organ.

Testosterone: an antagonist of aldosterone in the urinary bladder of the toad

B. C. Rossier, H. P. Gaggeler and K. Geering, *Institut de Pharmacologie de l'Université, CH-1011 Lausanne*

In contrast to the well-characterized action of progesterone as an antimineralocorticoid, little is known about a similar role for testosterone. We have studied this question in the urinary bladder of the toad (*Bufo marinus*). The results indicate that: a) testosterone (up to 40 μM) had no agonist activity on Na^+ transport, b) testosterone (from 0.1 μM to 40 μM) antagonized the action of aldosterone on Na^+ transport in a dose-dependent manner, c) the antagonist action of testosterone was reversible upon further addition of an equimolar concentration of aldosterone, d) testosterone competed for ^3H -aldosterone binding sites in the cytoplasm at 0°C within the same range of concentrations which were effective in antagonizing aldosterone-dependent Na^+ transport, e) testosterone prevented the nuclear binding of the aldosterone-receptor complex at 25°C. We conclude that testosterone fulfills most of the criteria for a competitive antagonist of aldosterone both with respect to its action on Na^+ transport and its binding activity at the level of the putative mineralocorticoid receptor.

Interaction between local anesthetics and calcium on phosphate efflux

M. Rouiller, P. Jirounek and R. W. Straub, *Département de Pharmacologie, Ecole de Médecine, CH-1211 Genève 4*

In the presence of local anesthetics (e.g. tetracaine, 0.6 mM) the efflux of phosphate from rabbit vagus nerve is decreased and the transstimulation of the efflux by external phosphate is abolished (Rouiller et al., *Experientia* 35, 952, 1979). This effect of local anesthetics is not modified by an increase in the external Ca^{2+} concentration up to 10 mM, but it is completely abolished in Ca^{2+} -free Locke solution containing 0.1–1.0 mM EGTA. On the other hand, Ca^{2+} -free plus EGTA Locke does not modify the phosphate efflux in the absence of local anesthetics. Chromatographic analysis of membrane constituents shows that the application of local anesthetics increases the phosphorylation of membrane phospholipids. – These results indicate that the inhibition of the phosphate efflux by local anesthetics requires Ca^{2+} and that membrane phospholipids are involved in this effect of local anesthetics.

High affinity ligands for β -adrenergic receptors

P. Simons and M. Staehelin, *Friedrich-Miescher-Institut, Postfach 273, CH-4002 Basel*

An accurate method for measuring the number of β -adrenergic receptors is needed. ^3H -Dihydroalprenolol and ^{125}I -OH-benzylpindolol both exhibit considerable unspecific

binding in intact cells. The preparation of purified membranes, however, results in losses in the total number of receptors. In a search for more suitable ligands to be used in intact cells, ^3H -carazolol and ^3H -CGP 12177 were found to be 100 and 10 times more potent than ^3H -dihydroalprenolol on the β -adrenergic receptor of C-6 glioma cells. The potency is mainly due to a slower dissociation rate. Whereas the association rate for ^3H -CGP 12177 is about the same as for ^3H -dihydroalprenolol and 5 times greater for ^3H -carazolol the dissociation rates at 30°C are 15 and 50 times slower, respectively. This allows more extensive washing procedures which reduce the unspecific background to low levels.

GABA-induced depolarization of the superfused rat superior cervical ganglion (SCG) and its antagonism by various drugs

R. Schaffner, *Pharma Research Department, F. Hoffmann-La Roche & Co. Ltd, CH-4002 Basel*

Various drugs known to interfere with Cl^- -translocation mechanisms at different membrane sites were studied for their effects on the depolarization induced by GABA of the SCG. 1. Bicuculline (10^{-5} to 3×10^{-4} M) shifted the GABA concentration-response curve to the right in a parallel fashion as to be expected of a competitive antagonist. 2. A mixed competitive/noncompetitive antagonism was observed with picrotoxin (3×10^{-6} to 10^{-4} M), the convulsant benzodiazepine Ro 5-3663 (10^{-4} to 10^{-3} M) and strychnine (10^{-5} to 3×10^{-4} M). These drugs shifted the GABA curve to the right at low concentrations and depressed the maximal GABA response at high concentrations, findings which are consistent with the proposed action on the chloride channel. 3. A noncompetitive GABA antagonism was obtained with Na benzylpenicillin (10^{-5} to 10^{-3} M). 4. Furosemide (10^{-6} to 10^{-3} M) and ethacrynic acid (10^{-5} to 10^{-4} M), diuretics known to inhibit the active chloride transport, reduced the maximum of the GABA depolarization without displacing the GABA curve.

Uptake of urate and p-aminohippurate (PAH) into isolated, nonperfused proximal renal tubules of rabbits

Ch. Schäli and F. Roch-Ramel, *Institut de Pharmacologie de l'Université, CH-1011 Lausanne*

S_1 , S_2 and S_3 segments of rabbit proximal tubules were dissected and incubated (30 min; pH 7.4; 37°C) in oxygenated Ringer's solution containing bovine serum albumin, ^{14}C -urate or ^3H -PAH, and inhibitors at 10^{-3} M. Radioactivities were measured by liquid scintillation spectrophotometry and expressed as cpm per nl of tissue water (microphotographic tubular volume multiplied by tissue water content) or per nl of incubation medium. Uptake was expressed as tissue water/medium ratio (T/M). – Urate (9×10^{-5} M) and PAH (3×10^{-5} M) uptake was significantly larger in S_2 (T/M: urate 6.1 ± 0.4 [mean \pm SEM], 42 tubules from 11 animals; PAH 133.0 ± 18.9 , $n=24/8$) than in S_1 (urate 2.9 ± 0.3 , $n=15/7$; PAH 22.7 ± 4.6 , $n=19/8$) or in S_3 segments (urate 1.7 ± 0.3 , $n=14/7$; PAH 66.2 ± 15.3 , $n=20/8$). Addition of cold urate to ^3H -PAH, or cold PAH to ^{14}C -urate significantly depressed the S_2 T/M ratios to $15.1 \pm 3.7\%$, $n=15/6$, and $16.4 \pm 2.4\%$, $n=15/7$, of control values, respectively. In rabbits, urate and PAH appear to be transported by a common mechanism, mainly located in the S_2 segment of the proximal tubule.

Site-dependent facilitation and inhibition of learning by posttrial injection of substance P into the brain

Ursula Stäubli and J. P. Huston, *Institute of Pharmacology, University of Zürich, CH-8006 Zürich, and Institute of Psychology, University of Düsseldorf, D-4001 Düsseldorf, Federal Republic of Germany*

Posttrial injection of the neuropeptide substance P (SP) into the brain has profound effects on passive avoidance learning, facilitating or inhibiting learning, depending on the injection site. The influence of SP on learning exactly mimics the effects of posttrial electrical brain stimulation: In the lateral hypothalamus and the medial septum SP as well as electrical stimulation lead to facilitation of learning, whereas as in the substantia nigra and the medial amygdala both posttrial electrical stimulation and SP injection induce retrograde amnesia.

Wirkung von Delta Sleep Inducing Peptide (DSIP) und Arginin Vasotocin (AVT) auf den Schlaf und die motorische Aktivität der Ratte

I. Tobler und A. A. Borbély, *Pharmakologisches Institut der Universität Zürich, CH-8006 Zürich*

Die Wirkung von DSIP und AVT auf den Schlaf und die motorische Aktivität (MA) der Ratte wurde nach systemischer und intraventrikulärer (i.vent.) Verabreichung der Peptide untersucht. Während der 24 Std. nach DSIP (40–160 nmoles/kg i.p.) war die MA nicht erniedrigt und weder der Schlaf noch die EEG-Leistung im Deltaband (Delta-EEG) während der 2 Std. nach i. vent. Verabreichung (7–24 nmoles) erhöht. Nach AVT (10^{-15} bis 10^{-19} M i.vent.) waren ebenfalls weder der Schlaf noch das Delta-EEG erhöht. Folgende signifikanten Unterschiede wurden nach Peptidverabreichung festgestellt: Die MA war in den ersten 4 Std. nach DSIP (80 nmoles/kg) erhöht und während der gesamten Dunkelzeit 1 und 2 Tage nach 160 nmoles/kg erniedrigt. Eine Reduktion des Delta-EEG wurde nach i.vent. Verabreichung von DSIP (7 nmoles) und AVT (10^{-17} M) festgestellt. Wir schliessen aus den Resultaten, dass weder DSIP noch AVT bei der Ratte eine spezifische schlafinduzierende Wirkung ausüben, jedoch eine noch nicht näher definierte neurobiologische Veränderung bewirken können.

Biphasic action of dopaminergic (DA) stimulants on locomotion in mice

J. M. Vigouret, A. L. Jaton and D. M. Loew, *Pharmaceutical Division, Preclinical Research, Sandoz Ltd, CH-4002 Basel*

Treatment of mice with DA stimulants results in a biphasic alteration of locomotion. An initial inhibition is followed by a late enhancement. Di Chiara et al. (Adv. Biochem. Psychopharmac. 19, 275, 1978) suggest that this inhibition is due to a preferential stimulation of self-inhibitory dopamine receptors. In our study, groups of 5 mice were placed in activity cages immediately after s.c. drug administration. In the following hour, controls showed exploratory locomotion which was inhibited by 1 mg/kg apomorphine or N-Nor-propyl-apomorphine and 5 mg/kg bromocriptine. This inhibition was followed by stimulation. In contrast, when the same treatments were administered 1 h after caging, a strong enhancement of locomotion was seen which was not preceded by a latency or an initial inhibition. The results show that the biphasic changes seen after DA stimulants in non-habituated animals depend essentially on the behavioral state of the animal and are not due to an intrinsic property of the drug.

Monitoring of mebendazole plasma concentrations in the treatment of alveolar echinococcosis

F. Witassek, J. Eckert and J. Bircher, *Departments of Clinical Pharmacology and Parasitology, University of Bern, CH-3010 Bern, and University of Zürich, CH-8006 Zürich*

Mebendazole (M) given in standard laboratory chow (500 ppm) to experimentally infected rodents (jirds) leads to reduction in parasite weight at plasma M concentrations (PMC) of 700–1200 ng/ml. Therefore, M has been proposed for therapy in man. In 27 patients on oral doses of 16–60 mg/kg·day fasting PMC (measured by HPLC) varied widely ranging from 4 to 575 ng/ml (median=40; n=48) and were not correlated with the doses ($r=0.04$). 4 h after a single morning dose of 8–21 mg/kg PMC increased by 3–233 ng/ml (median=67; n=37). The relation between dose and increase in PMC suggested appearance of drug in systemic circulation only above an extrapolated dose of 5 mg/kg, a finding which is compatible with first-pass elimination. These results indicate that maintenance of PMC similar to those in experimental animals would require higher M doses and close monitoring of PMC.

Measurement of dopa in plasma (P) and cerebrospinal fluid (CSF) by a highly sensitive COMT radioenzymatic assay

G. Zürcher and M. Da Prada, *Pharmaceutical Research Department, Hoffmann-La Roche & Co. Ltd, CH-4002 Basel*

A newly developed single isotopic catechol-O-methyltransferase (COMT) radioenzymatic assay permits the measurement of fmole amounts of DOPA in min-tissue samples and μ l aliquots of body fluids (Zürcher and Da Prada, J. Neurochem. 33, 631, 1979). In man, the concentration of free (unconjugated) DOPA was about 3 times higher in P than in CSF (~ 1500 and 500 pg/ml, respectively). In SPF rats the DOPA level was also about 3 times higher in P than in CSF (~ 600 and 200 pg/ml, respectively). Benserazide (BZ), a peripheral decarboxylase inhibitor, elevated endogenous levels of DOPA in human P as well as in rat P and CSF. After BZ (10 mg/kg p.o. 3 h) the DOPA level in P was significantly higher ($p < 0.002$) in fed than in 24 h starved rats (14.24 ± 0.86 and 10.21 ± 0.50 ng DOPA/ml P, respectively). DOPA in P originates from multiple sources including the peripheral sympatho-adrenal system and possibly from unspecific hydroxylation of tyrosine by liver phenylalanine hydroxylase.

Ethanol induced reduction in first-pass elimination of clomethiazole in the rabbit

T. Zysset and J. Bircher, *Department of Clinical Pharmacology, University of Bern, CH-3010 Bern*

Clomethiazole (CZ) is widely used to treat symptoms of alcohol withdrawal although occasional overdoses have been observed. To study the interaction of CZ with single doses of ethanol, but avoiding risks to human subjects, studies were designed in rabbits with permanently implanted catheters in portal vein, vena cava and aorta. CZ was infused in a dose of 2 μ moles/kg·min for 90 min into portal vein or vena cava either together with i.v. saline or ethanol. Plasma CZ and ethanol concentrations were measured by GLC. When ethanol plasma concentrations ranged from 1.5 to 2 g/l mean CZ steady state concentrations resulting from portal CZ infusions on the average reached 212% ($12.5 \pm \text{SD } 2.8$ μ moles/l) of saline controls, and those resulting from i.v. infusions 130% (30.3 ± 2.5 μ moles/l). It is concluded that the ethanol induced decrease in hepatic first-pass elimination may explain instances of clinical toxicity in inebriated subjects.

BIOCHEMIE – BIOCHIMIE – BIOCHEMISTRY

Cathepsin D and renin-like activity in bovine pineal gland

A. de Agostini, A. Reinharz and M. B. Vallotton, Division of Endocrinology, University of Geneva, CH-1211 Geneva 4

Bovine pineal gland was found to contain much carboxyl proteinase activity. The goal of this study was to characterize this activity and to distinguish cathepsin D from other carboxyl proteinases. The following criteria were applied: relative hydrolytic rate with various natural or synthetic substrates, pH optimum and pepstatin inhibition. – Carboxyl proteinase hydrolyses the fluorogenic octapeptide Z8PNA (Z-Pro-Phe-His-Leu-Leu-Val-Tyr-Ser-naphthylamide) with an optimum of pH 3–4.5 and natural bovine renin substrate similarly at pH 4 and 5.5. The ratio of activities on BSA and hemoglobin (Hb) was 0.1. On gel-filtration the enzyme elution volume corresponds to a mol.wt of 45,000. Its activity is abolished by pepstatin. The different affinities for cathepsin D and renin (or renin-like) of various protein substrates (angiotensinogen human and bovine, Hb and BSA) and peptide substrates (tetradecapeptide angiotensinogen, Z8PNA, Z5PNA, Z4PNA) permits to distinguish between these 2 enzyme's activities. – The pineal gland appears to contain both cathepsin D and a renin-like enzyme which could play a role in activation of hormonal peptides.

Inhibition of phosphodiesterase affects dark current in retinal rods

C. Albani and S. Yoshikami, National Institutes of Health, NIH, Bld. 2, Rm 103, Bethesda, Maryland 20014, USA

When light bleaches rhodopsin molecules in the outer segment of photoreceptors, the current flowing inward in the dark is shut down and the cell hyperpolarizes. 2 mechanisms are currently under consideration to explain the link between photon absorption and changes in Na^+ permeability. The calcium hypothesis assumes that Ca^{++} is released from the photoreceptor discs by light and blocks the Na^+ conductance mechanism. In the cyclic GMP schema ion permeability is controlled by hydrolysis of cGMP through a light-activated phosphodiesterase enzyme (PDE). Isolated rat retinæ were superfused with Ringer containing 1 mM isobutylmethylxanthine (IBMX) or 1 mM SQ 20006. When 8% of the rhodopsin was bleached, the retinæ treated with the PDE inhibitors IBMX and SQ 20006 showed a faster recovery of the dark current as compared to control retinæ. Low Ca^{++} Ringer superfusion ($\text{pCa} \approx 7$) had a similar effect on the dark current. These results suggest that both cGMP and Ca^{++} control the Na^+ permeability of the photoreceptors membrane with a high intracellular cGMP level mimicking a low intracellular Ca^{++} .

Studies on the subunit composition and quaternary structure of glycinin

P. Amiguet, Research Department, Nestlé Products Technical Assistance Co. Ltd, CH-1814 La Tour-de-Peilz

Glycinin (mol.wt 350,000), the main storage protein of the soybean is composed of 2 types of subunits (acidics of mol.wt 32,000 and basics of mol.wt 22,000) which form disulfide cross-linked dimers and which appear to be packed in 2 hexagons (Badley et al., Biochim. biophys. Acta 412, 214, 1975). In this study the subunit composition as well as the nature of the disulfide bonds and their possible

role in the subunit assembly have been reinvestigated using 1- and 2-dimensional isoelectric focusing. There appear to be 14 different subunits (6 acidics and 8 basics). 2 of the basic subunits are not cross-linked with an acidic subunit. All basic subunits undergo a large shift in their pI of up to 3 pH units while at the same time the acidic subunits shift less than 0.5 pH units. Moreover, the acidic and basic subunits have distinct patterns of heterogeneity which suggests that each group is subject to a different type of selective pressure.

Characterization of the renal Na,K-transport system in phosphatidylcholine vesicles

B. M. Anner, Department of Pharmacology, Ecole de Médecine, CH-1211 Geneva 4

Vesicles containing functional renal Na,K-ATPase can be prepared with cholate, phosphatidylcholine and the purified enzyme (Anner, Lane, Schwartz and Pitts, Biochim. biophys. Acta 467, 340, 1977). The detergent/lipid/protein ratio is critical for obtaining a functional Na,K-transport system in the artificial membrane. By varying these parameters, a short procedure has been developed which yields highly efficient transport vesicles (Anner, Int. J. Biochem., 1980). – They are single-walled, their diameter is about 90 nm, and they contain several molecules of Na,K-ATPase spanning the lipid bilayer (Skriver, Maunsbach, Anner and Jørgensen, in preparation). – The incorporation of the Na,K-ATPase protein into the phosphatidylcholine vesicles decreases the turnover of the ATP-splitting site 5–10-fold, while the Na:K exchange activity of the enzyme is restored to a K-transport to ATP-splitting ratio of about one.

Cleavage of human IgM with human lysosomal elastase

A. Baici, M. Knöpfel, K. Fehr and A. Böni, Universitäts-Rheumaklinik, Gloriastrasse 25, CH-8091 Zürich

Lysosomal elastase (EC 3.4.21.11), a serine proteinase stored in the azurophil granules of human granulocytes, is able to degrade immunoglobulins G (IgG) and M (IgM), producing characteristic fragments. Monoclonal human IgM was subjected to proteolysis by elastase and the reaction products were separated by gel-filtration. The reaction occurred in 2 steps: a) a fragment (IgMe) was produced first; b) a fragment (Fab_u) was produced in a 2nd phase by proteolysis of IgMe. The Fc_u fragment was not recoverable since it was rapidly degraded to dialyzable peptides. IgMe was compared with the IgM subunit (IgMs) obtained by reduction and alkylation of IgM, and with the IgMp fragment obtained by papain proteolysis. IgMe had a smaller mol.wt and showed a partial immunochemical identity, when compared with IgMs and IgMp. The Fab_u fragment was practically identical to that obtained by papain digestion of IgM.

The immunogenicity of various forms of nicotinic acetylcholine receptor (nAChR)

N. A. Bersinger, R. W. James and B. W. Fulpius, Department of Biochemistry, University of Geneva, Sciences II, CH-1211 Geneva 4

As part of an ongoing study of the role of nAChR in experimental autoimmune myasthenia gravis (EAMG), the effects of various chemical and enzymatic modifications of

the receptor are being investigated in terms of its ligand-binding (α -bungarotoxin) and antigenic properties. Previous studies indicated that glycosidases modified toxin-binding properties of purified nAChR (Experientia 35, 931, 1979). This work has been extended to membrane-bound nAChR. Endoglycosidases reduce toxin-binding capacity by 23% after 72 h at 25 °C. With glucose oxidase, a much more dramatic effect was observed; toxin-binding capacity dropped 67% and 91% after 4 h and 72 h, respectively, at 25 °C. - Concomitant studies of the immunogenicity of modified forms of the receptor are under investigation. Present results indicate that purified, reduced-denatured nAChR is immunogenic, induces a high titre of antinative nAChR antibodies but does not provoke EAMG. Nonpurified, membrane-bound nAChR induces a lower titre of antinative nAChR antibodies but does provoke EAMG. The significance of these and other studies of receptor antigenicity will be discussed.

The coupling factor complex in membranes of a thermophilic cyanobacterium

A. Binder, M. C. Bohler, M. Wolf and R. Bachofen, Institute of Plant Biology, University of Zürich, Zollikerstrasse 107, CH-8008 Zürich

In isolated membrane particles of the thermophilic cyanobacterium (blue-green alga) *Mastigocladus laminosus* photophosphorylation and proton uptake were measured. The optimal temperature for these activities was 45-55 °C, depending on the growth temperature of the cells. The water soluble part of the complex (AF_1) was isolated and its structure, specificity and kinetics were characterized. The membranes depleted of AF_1 showing neither proton uptake nor photophosphorylation could be reconstituted with the soluble AF_1 , thereby bringing back the membrane activities up to 70%. The photophosphorylation as well as the Mg^{2+} -dependent ATPase of the membranes were inhibited by the energy transfer inhibitors DCCD and oligomycin. The DCCD-binding protein of the membrane part of the complex (AF_0) was isolated with chloroform methanol and characterized.

Biochemical and biological characterization of pregnancy associated plasma protein-A

P. Bischof, Departments of Obstetrics and Gynecology, University of Aberdeen, Scotland, and University of Geneva, CH-1211 Geneva 4

Pregnancy associated plasma protein-A (PAPP-A) is a placental product specific to human pregnancy. It is secreted in increasing concentrations as pregnancy progresses and almost exclusively into the maternal circulation. PAPP-A purified from late pregnancy plasma is a dimer, each monomere being composed of 2 polypeptide chains of around 200,000 mol.wt. - The amino-acid composition, the electrophoretic mobility and the molecular structure of PAPP-A are very similar to human α_2 -macroglobulin but no immunological identity between these 2 molecules could be detected. - Pure PAPP-A elicited in vitro a dose-dependent inhibition of the hemolytic activity of guinea-pig complement. Furthermore, PAPP-A produced an inhibition: of the caseinolytic activity of plasmin and of the urokinase-induced plasminogen activation. It is hypothesized that during pregnancy in humans PAPP-A participates to the maintenance of the conceptus by reducing the maternal immunological response and by increasing the fibrin deposits at the interface between trophoblastic and maternal tissue.

A monomeric bifunctional enzyme of the tryptophan pathway has two different, but independent active sites

H. Bisswanger, W. Cohn, K. Kirschner and C. Paul, Biozentrum, Abteilung Biophysikalische Chemie, Klingelbergstrasse 70, CH-4056 Basel

The enzyme that catalyzes the reactions phosphoribosyl anthranilate \rightarrow 1-(o-carboxyphenylamino)l'-deoxyribulose 5'-phosphate \rightarrow indoleglycerol phosphate is a monomer in *E. coli*. Reduction of the intermediate with borohydride affords a product analogue of the first reaction and a substrate analogue of the second reaction. N-phosphoribityl anthranilate binds to 2 different sites on the enzyme. Kinetic studies with fluorescence detection reveal 3 relaxation processes. These results indicate that the 2 sites are independent to the extent that a conformational change of one site is not transmitted to the other. Limited proteolysis yields 2 separable, folded fragments of the polypeptide chain. The enzymic and ligand binding properties of the putative domains are discussed.

Effect of cytochrome c oxidase on the conformation of lecithin in vesicle membranes

R. Bodmer and D. Walz, Biozentrum der Universität Basel, Klingelbergstrasse 70, CH-4056 Basel

It has been found that chlorophyll *a* incorporated into membranes of lecithin vesicles acts as a sensor for the conformation of lipids (D. Walz, J. Membrane Biol. 27, 55, 1976; 31, 31, 1977). By means of this tool, it can be shown that the incorporation of cytochrome *c* oxidase into vesicle membranes alters the conformation of the lipids. Changing the redox state of the oxidase from oxidized to reduced yields minor absorbance changes of chlorophyll *a* which, however, cannot unambiguously be related to an alteration of the lipids' conformation due to a possible contribution of an electric potential difference across the membrane. The spectral response of chlorophyll *a* upon addition of valinomycin to the vesicle suspension (see references given above) is substantially reduced in the presence of oxidase which is either due to a reduced solubility of the antibiotic in an oxidase containing lecithin matrix or results from a decreased effect of valinomycin on the conformation of lipids in the vicinity of the oxidase complex.

Size, stoichiometry and conformational features of glucagon bound to detergent micelles

C. Bösch, L. R. Brown and K. Wüthrich, Institut für Molekularbiologie und Biophysik, ETH, CH-8093 Zürich

To investigate possible conformations for glucagon bound to plasma-membrane receptors, micellar glucagon-detergent complexes have been studied. Ultracentrifugation and quasi-elastic light scattering measurements demonstrated that such micellar complexes have a well-defined size and stoichiometry. Evidence for very similar conformations for glucagon bound to detergent or phospholipid micelles and to phospholipid bilayers was obtained from circular dichroism measurements. High resolution 1H -NMR allowed a characterization of conformational features of glucagon bound to deuterated dodecylphosphocholine micelles. Particularly informative were measurements of truncated driven nuclear Overhauser effects (TOE) which indicated that although micelle-bound glucagon adopts a definite conformation, this conformation is extended rather than compact and globular.

Biosynthesis of some chloroplast components and activities in greening of streptomycin-bleached *Chlamydomonas*

A. Boschetti and E. Sauton-Heiniger, *Institut für Biochemie der Universität Bern, Freiestrasse 3, CH-3012 Bern*

The streptomycin-resistant mutant sr₃ of *Chlamydomonas reinhardtii* forms yellow cells, when cultivated in the dark and in the presence of streptomycin. The plastids are of normal size and contain starch granules, but only a few rudimentary lamellae, no pyrenoid and no prolamellar body. Upon illumination the cells become green, but do not divide within the first 72 h, offering therefore an ideal system for studying the development of chloroplasts. In the light, after a lag-phase of 24 h, simultaneously with the accumulation of chlorophyll, the appearance of proteins typical for thylakoid membranes is observed. Among these are found proteins synthesized on cytoplasmic and on chloroplast ribosomes. During dark cultivation photosystem I-activity as well as the carboxylase activity decrease with approximately the same rate as the chlorophyll content, but in the light PS I-activity starts immediately to recover.

Determination of polypeptide conformation by NMR: distance geometry algorithm for the structural interpretation of TOE data

W. Braun, N. Gö, C. Bösch, L. R. Brown and K. Wüthrich, *Institut für Molekularbiologie und Biophysik, ETH, CH-8093 Zürich*

A new systematic method for investigations of the conformations of lipid-bound polypeptide chains was developed. Measurements of truncated driven nuclear Overhauser effects (TOE) provide a list of constraints on through-space proton-proton distances. This list is used as input for a distance algorithm to elucidate conformations which would be consistent with the experimental data. The method was used for studies of glucagon bound to deuterated dodecylphosphocholine micelles. The resulting spatial structure is discussed in the light of the previously established structure for monomeric glucagon in aqueous solution and for glucagon single crystals.

Relation between extra- and intramitochondrial ATP/ADP ratios in rat liver mitochondria

F. Brawand and G. Folly, *Biochemisches Institut der Universität Basel, Vesalianum, Vesalgasse 1, CH-4051 Basel*

The dependence of the internal ATP/ADP ratio on the respiratory state was measured in incubations with rat liver mitochondria. ATPase or creatine/creatine kinase were used as acceptor systems in order to change the extramitochondrial ratio. Under all conditions tested, the intramitochondrial ratio changed in the same direction as the extramitochondrial one, except in the presence of atractylate where this correlation was not observed. Furthermore, it could be shown that the oxygen uptake and pyruvate carboxylase activity correlated with the intramitochondrial ATP/ADP ratio and not with the extramitochondrial one.

Binding of cytochrome *c* to *bc*₁ complex

C. Broger, M. J. Nałecz and A. Azzi, *Medizinisch-chemisches Institut der Universität Bern, P.O. Box, CH-3000 Bern 9, and Nencki Institute of Experimental Biology, Warsaw, Poland*

On the basis of kinetic and labelling experiments it was suggested that cytochrome *c*₁ (cyt *c*₁) is the reductant of

cyt *c* and might also be the binding site for cyt *c* at the *bc*₁ complex. We prepared radioactive azido derivatives of cyt *c* with the azido label at lysine 13 or lysine 22. Upon illumination of *bc*₁ complex in presence of these derivatives, the cyt *c* molecule is cross-linked to the nearest available subunit of the *bc*₁ complex. The polypeptide composition of the incubation mixtures was analyzed on polyacrylamide gels by dual wavelength scanning at 280–300 and 400–430 nm and by measuring the cyt *c* radioactivity distribution over the gel. It was found that only with the lysine 13 derivative a new high mol.wt band appeared while the quantity of band IV of *bc*₁ diminished. The mol.wt of the new band was approximately the sum of the mol.wts of band IV and cyt *c*. Band IV was shown to be cyt *c*₁. Only the lysine 13 derivative was able to produce changes in the polypeptide pattern. Thus, lysine 13 but not lysine 22 is included in the area of cyt *c* which interacts with the *bc*₁ complex.

A new approach for conformational studies of membrane proteins: high resolution NMR studies of polypeptide chains bound to deuterated micelles

L. R. Brown, C. Bösch, W. Braun and K. Wüthrich, *Institut für Molekularbiologie und Biophysik, ETH, CH-8093 Zürich*

Understanding of the functional properties of biological membranes is currently limited by the paucity of information on conformation of membrane-bound polypeptides or proteins. Complexation with deuterated detergent or lipid micelles provides a way to obtain high resolution ¹H-NMR spectra of lipid-bound polypeptide chains suitable for a many-parameter characterization of the molecular conformation. – The use of NMR data to study polypeptide conformation, orientation at a lipid-water interface and polypeptide-lipid interactions will be illustrated. For glucagon bound to fully deuterated dodecyl-phosphocholine micelles, the combined use of truncated driven nuclear Overhauser effects (TOE) measurements and of a distance geometry algorithm to obtain detailed molecular conformations will be described.

Head group and chain conformation in membranes of phosphatidylcholine and phosphatidylathanolamine as seen by neutron diffraction

G. Büldt, *Abteilung Biophysikalische Chemie, Biozentrum der Universität Basel, Klingelbergstrasse 70, CH-4056 Basel*

Neutron diffraction experiments on selectively deuterated lipids provide a new method of determining to a segmental resolution the mean conformation of a lipid molecule as projected along the bilayer normal, despite the high amount of disorder that exists in these bilayers. In addition a time averaged picture of the extent of the positional fluctuations of the individual segments in this direction can be given. Samples deuterated at different positions were measured in the gel phase *L*_β, and in the liquid crystalline phase *L*_α. The results show that the average orientation of the dipole in the head group is almost parallel to the membranes surface in the gel state (*L*_β) as well as in the liquid crystalline state (*L*_α). For the *L*_β-phase it was shown that the 2 hydrocarbon chains are axially displaced as seen in the crystal structures of these lipids. In the *L*_α-phase the width of the time averaged positional fluctuation of the methylene groups is found to be increased by more than a factor of 2 at the end of the chains.

Na⁺-coupled solute transport in renal brush border membrane vesicles studied by a fluorescent membrane potential probe

G. Burckhardt, B. Stieger and H. Murer, Max-Planck-Institut für Biophysik, Kennedyallee 70, D-6000 Frankfurt am Main, Federal Republic of Germany

Brush border membrane vesicles isolated by a calcium precipitation technique from rat or rabbit kidney cortex are equilibrated with 74 mmol/l Na₂SO₄ and 1 mmol/l K₂SO₄. The addition of K₂SO₄ to the vesicles in the presence of valinomycin leads to an increase in the fluorescence of 3,3'-diethylthiadicarbocyanine iodide indicating an inside positive K⁺-diffusion potential. The maximal fluorescence response is reached in less than 5 sec and is related to the magnitude of the K⁺-concentration difference. The addition of D-glucose as well as of different neutral L-amino acids leads only in the presence of sodium to a transient fluorescence increase. Fluorescence changes at different substrate concentrations show a saturation phenomenon. Simultaneous addition of 2 different substrates at saturating concentrations leads to a partial addition of the individual signals, if both substrates are transported by different systems, e.g. glucose and L-alanine. No additivity is observed, if both substrates have a common transport system, e.g. L-alanine and L-phenylalanine.

Synthesis and subcellular distribution of ³⁵SO₄-sulfatide in mouse brain

T. Burkart, H. P. Siegrist, N. Herschkowitz and U. Wiesmann, Department of Pediatrics, University of Bern, CH-3010 Bern

Synthesis and subcellular distribution of ³⁵SO₄-sulfatide were studied in brains of 17-day-old mice after a 2 h ³⁵SO₄-pulse-label-chase. At 1–24 h after i.p. injection of ³⁵SO₄ the brains were homogenized and fractionated according to Herschkowitz et al. (J. Neurochem. 16, 1049, 1969). A 17,000 g supernatant of microsomes was subfractionated on a continuous sucrose gradient (Siegrist et al., J. Neurochem. 33, 497, 1979). ³⁵SO₄-sulfatide was highest at 1 h after labelling in the crude microsomes, after 3 h in the presumptive lysosomes and synaptosomes and continuously accumulated in the small and large myelin up to 6 h. In the submicrosomal gradient, the earliest labelling of sulfatide was observed in the Golgi fractions after 1 h. From there, ³⁵SO₄-sulfatide rapidly moved to denser and lighter fractions of the gradient. Thus, sulfatide synthesized in the Golgi complex appears partly in light premyelin vesicles and partly in heavy vesicles, possibly primary lysosomes.

Rotational mobility of (Ca⁺⁺ + Mg⁺⁺)ATPase of sarcoplasmic reticulum

A. Bürkli and R. J. Cherry, Laboratorium für Biochemie, ETHZ, CH-8092 Zürich

Rotational mobility of the iodoacetamido-eosin labelled (Ca⁺⁺ + Mg⁺⁺)ATPase of rabbit hind leg sarcoplasmic reticulum was investigated by observing flash-induced transient dichroism. At room temperature and above, the initial absorption anisotropy is rather small indicating the existence of a fast motion which reduces the anisotropy in a time shorter than the resolution time of the measurement (20 μsec). The initial anisotropy decreases rapidly with increasing temperature over the range of –6 °C to 37 °C. Hence either the amplitude of this fast motion or its fractional contribution is strongly temperature-dependent. At times longer than 20 μsec, the absorption anisotropy

exhibits a slow decay characterized by a time constant of 50–100 μsec at room temperature. The decay is reduced by lowering the temperature and abolished by fixation with glutaraldehyde. One interpretation of the data is that the fast motion is due to segmental motion of all or part of the hydrophilic moiety of the ATPase, while the slow decay represents rotation of the protein in the membrane. Alternatively the fast and slow motions could be assigned to the rotation in the membrane of monomeric and aggregated ATPase, respectively.

Stoichiometric analysis of the interaction between cytochrome c oxidase and dicyclohexylcarbodiimide

R. P. Casey, M. Thelen and A. Azzi, Medizinisch-chemisches Institut der Universität Bern, Bülhstrasse 28, CH-3012 Bern

It has been shown recently that mitochondrial cytochrome c oxidase, the terminal enzyme of the respiratory chain may possess a H⁺-translocating activity. We have demonstrated that this activity is inhibited in both reconstituted vesicles and in mitochondria by dicyclohexylcarbodiimide (DCCD), a well-known inhibitor of ATP-linked H⁺ pumps. Furthermore, ¹⁴C-DCCD is bound covalently to subunit III of the reconstituted oxidase. Both binding and inhibition are time- and concentration-dependent. We report here that the inhibitory effects and binding of DCCD appear concomitantly. In addition we have carried out a stoichiometric analysis of DCCD binding and inhibition which indicates that there is one specific binding site for DCCD located in subunit III of the oxidase which has a position of central importance in the H⁺-translocating activity of the oxidase. Binding of DCCD to isolated cytochrome c oxidase occurs at subunits III and IV and in this case the maximal binding stoichiometry is 1.6.

Differential regulation of Cl in fluid and solid phase

R. M. Chapuis and R. G. Medicus, Université de Lausanne, CH-1011 Lausanne

Expression of Cl activity results from the balance of its activation and inactivation rates. Using purified native Cl, we have studied the rate of Cl formation and inactivation by Cl inhibitor (Cl-INH) when bound on activators as well as in fluid phase. Activation of Cl bound to EA (IgM) is unimolecular and concentration-independent, while fluid-phase activation is strongly concentration-dependent, indicating a bimolecular mechanism. Cl-INH quickly inactivates the Cl formed in fluid phase, but has no influence on the rate of Cl formation. The rate of Cl inactivation by Cl-INH when bound to solid phase IgG is 10–100 times slower than in fluid phase, depending on the species of IgG. With human IgG the rate is 10 times as fast as with rabbit IgG. At serum concentrations of Cl-INH, 50% of the human IgG bound Cl is inactivated in 12 min. Since the rate of Cl formation on activators is significantly slower, susceptibility of activator bound Cl to inactivation by Cl-INH may be of greater significance for regulation of the classical pathway than its intrinsic rate of activation.

Mouse P-815 mastocytoma antigens

K. J. Clemetson, M. Bertschmann and E. F. Lüscher, Theodor-Kocher-Institut, Freiestrasse 1, CH-3000 Bern 9

The P-815 murine mastocytoma has 2 tumor associated (TA) antigens which can be detected by allo- or xenotransfers rendered specific by absorption. The allo-TA antigen has a mol.wt and lectin binding properties similar to histocompatibility antigens (H-2). It is however immunologically distinct from H-2, as immunoprecipitation

removed the H-2 antigens while leaving the allo-TA antigen. After preparation of membranes from P-815 cells much less allo-TA antigen could be detected than on intact cells while the H-2 and xeno-TA antigens were unchanged. A particular conformation or association of the allo-TA antigen may be present on intact cells which is altered during membrane preparation. P-815 has been reported to carry H-2 specificities not present on the host DBA/2 mouse, in particular H-2.15, implying the presence of derepressed or mutant H-2 antigens. However when both the Berne and Sloan Kettering P-815 sublines were tested with monospecific antisera (N.I.H.) those H-2 specificities characteristic of the DBA/2 line were expressed normally.

Formation of hydroxypyruvaldehyde phosphate – a possible substrate of the glyoxalases – in human erythrocytes

M. Cogoli and P. Christen, *Biochemisches Institut der Universität Zürich, CH-8028 Zürich*

The dismutation of α -ketoaldehydes to the corresponding α -hydroxyacids is catalyzed by the glyoxalases, an ubiquitous enzyme system whose natural substrate has remained unknown till today. Radioactive hydroxypyruvaldehyde-P (HPAP), formed during incubation of human erythrocytes with [14 C]-glucose, was quantitatively detected by a 'diagonal' chromatographic procedure. If glycolysis was blocked by inhibition of glyceraldehyde-3-P dehydrogenase, 0.7 μ moles HPAP per l of packed erythrocytes was detected. Without inhibition, only 0.3 μ moles/l packed cells was found. The fact that more HPAP is formed if glycolysis is blocked after the aldolase reaction step is compatible with the hypothesis that this α -ketoaldehyde might be produced by the oxidative paracatalytic reaction of aldolase which has been observed in vitro and whose product has been identified as HPAP (J. Am. chem. Soc. 94, 7911, 1972). α -Ketoaldehydes react with proteins and nucleic acids and inhibit protein synthesis and cell division.

Physiological effects of liposomes-trypanosomes interactions

D. Coral, A.-L. Knupfer, J. Gruenberg and J. Deshusses, *Department of Pharmacy and Department of Biochemistry, University of Geneva, CH-1211 Geneva*

Positively charged fluid liposomes which undergo fusion with the plasma membrane show a very strong lethal effect on *Trypanosoma brucei* cultureform while neutral fluid liposomes do not have such toxicity. The relationship between the toxicity and the plasma-membrane functions will be discussed.

Sucrose uptake in lily pollen: a proton symport

J. Deshusses, S. Gumber and F.A. Loewus, *Department of Biochemistry, University of Geneva, CH-1211 Geneva, and Department of Agriculture Chemistry, Washington State University, Pullman, Wash. 99164, USA*

Germinated pollen of *Lilium longiflorum* is able to transport sucrose. The intake is driven by the H^+ gradient, with an optimum external pH of 5.0. The K_m , as calculated from the initial rate of pH variation induced by sucrose uptake or from [14 C]sucrose uptake was 1.7 mM. FCCP, a proton ionophore, is a strong inhibitor of [14 C]sucrose uptake at 3×10^{-6} M and abolishes the pH variation induced by sucrose. After 2 min incubation in the presence of labelled sucrose, 18% of the radioactivity is found as free sucrose,

the remaining part being free glucose (4.5%), fructose (3%), phosphorylated derivatives (39%) and high molecular products (35%). Interference with invertase will be discussed.

Yeast tryptophan synthase is a bifunctional enzyme

M. Dettwiler, K. Kirschner and K. Stöckli, *Biozentrum, Abteilung Biophysikalische Chemie, Klingelbergstrasse 70, CH-4056 Basel*

The enzyme has been purified for the first time from an overproducing strain of *S. cerevisiae* (R. Hütter 558). Undesirable proteolysis by yeast protease(s) was circumvented by using 0.5 M phosphate buffer in the first few steps. The crucial step is hydrophobic chromatography on pentyl Sepharose 4B, which appears to remove the protease(s)/SDS polyacrylamide gel-electrophoresis yields M_r 76,000. The M_r equals 160,000 as determined by equilibrium sedimentation, but equals 380,000 as determined by gel-chromatography. This discrepancy is due to an unusually large Stokes' radius (54 Å), which reflects an elongated shape of the native enzyme. These results indicate that yeast tryptophan synthase is a homodimer (γ_2), and confirm previous genetic evidence for the enzyme being encoded by a single, multifunctional gene (trp 5). Steady-state kinetics of the various enzyme-catalyzed reactions were performed. The kinetic parameters and other properties of the yeast enzyme are compared to those of the multienzyme complex from *E. coli*.

Functional groups at the active site of mitochondrial aspartate aminotransferase (mAATase)

G. Eichele, G.C. Ford, J.N. Jansonius, E. Sandmeier, U. Hausner, K.J. Wilson and P. Christen, *Abteilung Strukturbiochemie, Biozentrum der Universität Basel, CH-4056 Basel, and Biochemisches Institut der Universität Zürich, CH-8028 Zürich*

A Kendrew-Watson model of the active site of mAATase from chicken has been built based on a 2.8 Å electron density map. Both subunits in the α_2 dimer contribute to each of the 2 active sites. The coenzyme pyridoxal-5'-P lies at the back of the active site cleft. Lys 258 and Tyr 70* (from the other subunit) could function as H^+ -donor/acceptor in the aldimine-ketimine tautomerization. Arg 386 and Arg 292* are in proper positions for binding the α - and ω -carboxylate groups of the substrate. This suggestion is supported by chemical modification of the enzyme in solution. Peptide analysis of AATase, modified with [14 C]-phenylglyoxal yields a radioactive fragment which is not labelled under substrate protection. Determination of its amino-acid sequence identifies the substrate-protected residue as Arg 292. The enzyme with blocked Arg 292 is catalytically inactive and is unable to bind oxalacetate.

Age-related changes in dopamine metabolism and cholinergic enzyme activities in rat striatum

A. Enz, K. Reichle, A. Chappuis and W. Norfleet, *Preclinical Research, Sandoz Ltd, CH-4002 Basel, and University of Missouri, Columbia, USA*

The dopamine (DA) concentration and the levels of the 2 principal dopamine metabolites dihydroxyphenylacetic acid (DOPAC) and homovanillic acid (HVA), were determined in the striata of adult (1 year, n=10) and senescent (3 years, n=10) female rats. In the same structure, the activities of choline acetyltransferase (CAT) and acetylcholinesterase (AChE) were also measured. All parameters analyzed showed a significant age-dependent decline. The DA content decreased to 73% and the DOPAC and HVA

level to 72% and 63%, respectively. The turnover of DA was also reduced in the aged rats. The activity of CAT decreased to 71% and that of AChE to 72%. The results suggest that both dopaminergic and cholinergic systems might be involved in functional deficits observed in old age.

Phospholipid dependence of human red cell membrane acetylcholinesterase

C. Di Francesco and U. Brodbeck, *Medizinisch-chemisches Institut, Universität Bern, Postfach, CH-3000 Bern 9*

Human erythrocyte membrane acetylcholinesterase in presence of detergents exists as a dimeric protomer. Its activity depends on the presence of an amphiphile (T. Wiedmer, C. Di Francesco and U. Brodbeck, *Eur. J. Biochem.*, in press). The effects of phospholipids on activity were further investigated by diluting the enzyme into a suspension of phospholipid vesicles. 100% of enzyme activity was preserved by 3.9×10^{-3} M total erythrocyte phospholipids (EPL) and egg phosphatidylcholine (PC). Sphingomyelin preserved 80% and phosphatidyl serine only 12% of the activity. In absence of a vesicle suspension, no activity was obtained. Sucrose density gradient centrifugation revealed that in case of EPL and PC all the enzyme activity was associated with the liposomal fraction. These results suggest that a suitable amphiphilic environment is necessary for enzyme activity. This is provided by the polar lipids mainly associated with outer half of red cell membranes.

A bonemarrow-derived cell participates in the biosynthesis of human Transcobalamin II

M. Fräter-Schröder, C. Nissen, J. Gmür and W.H. Hitzig, *Department of Pediatrics, University of Zürich, CH-8032 Zürich*

Transcobalamin II (TC II) is an essential trace protein in plasma, which binds vitamin B12 (Cobalamin) and delivers it to cells and tissues. Studies concerning the site of origin of TC II have been conducted in mice, rats, dogs, guinea-pigs and rabbits, and indicate release or synthesis of TC II by liver, kidney, heart, intestine and cell cultures of fibroblasts, -hepatocytes and -mononuclear phagocytes. Human intestine has been shown to release TC II. However, data concerning the site of TC II biosynthesis in man are lacking. Polymorphic TC II variants in human serum express a genetic isoprotein system (*Experientia* 34, 909, 1978). This system was used to examine possible bonemarrow-induced changes of TC II-phenotypes in 9 patients (severe aplastic anemia: 3, acute leukemia: 6) with stable bonemarrow grafts from TC II nonidentical donors. After transplantation, the TC II-phenotype was unchanged in 5 patients and significantly, although incompletely changed in 4 patients. These 4 incomplete or split chimeras of TC II show that at least half of apo-TC II is bonemarrow-derived.

Conformation of the phospholipids in the *Escherichia coli* membrane

H. U. Gally, G. Pluschke, P. Overath and J. Seelig, *Biocenter of the University of Basel, CH-4056 Basel, and Max-Planck-Institut für Biologie, Tübingen, Federal Republic of Germany*

The dynamic conformation of phospholipid molecules in membranes of *E. coli* has been investigated by means of deuterium magnetic resonance. *E. coli* fatty acid auxotrophs

which were also deficient in the synthesis of cardiolipin were grown in the presence of selectively deuterated elaidic acid, oleic acid and palmitic acid. The spectra reveal a striking similarity between the phospholipid conformation in a biological membrane and that of pure lipid model membranes. If the deuterium label is attached at the C-2 segment of the fatty acyl chains or at the *cis*-double bond the deuterium magnetic resonance spectra are rather unique and can be considered as spectral fingerprints of the phospholipid conformation in the fluid membrane. Almost identical fingerprints are observed for native *E. coli* membranes, for liposomes formed from extracted *E. coli* lipids and for synthetic phospholipids. It can be concluded that the membrane proteins do not change the overall phospholipid conformation significantly.

A new diagonal procedure for isolating sulfhydryl peptides alkylated with N-ethylmaleimide

H. Gehring, *Biochemisches Institut der Universität Zürich, CH-8028 Zürich*

The alkylation product of N-ethylmaleimide is stable at acid pH but is hydrolyzed at alkaline pH to the corresponding N-ethylsuccinamic acid. Based on this behavior, a diagonal electrophoretic procedure for separating sulfhydryl peptides modified with N-ethylmaleimide from the bulk of unlabelled peptides was developed. After a first high voltage paper electrophoresis at pH 6.5 of a proteolytic protein digest, the paper strip is exposed to an ammonia atmosphere. Hydrolysis of the N-ethylsuccinamide moiety to succinamic acid generates a new negative charge. During electrophoresis in the 2nd dimension, the peptides with the additional charge move out of the diagonal toward the anode. The procedure offers the advantage of modifying the sulfhydryl groups prior to the first electrophoresis, thus avoiding problems which arise from their oxidation. Furthermore, prepurification allowing the application of a higher amount of labelled peptides onto the electrophoresis paper can easily be performed using [^{14}C] or [^3H] labelled N-ethylmaleimide.

Ambient temperature adaptation and nucleotide-triphosphate levels in erythrocytes of the goldfish

R. Geiser, K. H. Winterhalter and J. D. G. Smit, *Biochemie I, ETH, CH-8092 Zürich*

Nucleotidetriphosphates exert a similar effect on the oxygen affinity of fish hemoglobins as 2,3-DPG on mammalian hemoglobins, the latter being virtually absent in fish erythrocytes. In the goldfish (*Carassius auratus*) both GTP and ATP are physiologically allosteric effectors but GTP has a more pronounced effect on oxygen affinity than ATP. The molar ratios of these organic phosphates to hemoglobin in goldfish erythrocytes were determined as a function of the ambient temperature. For ATP this ratio (about 0.9 $\mu\text{moles ATP}/\mu\text{mole Hb}$) is independent of the goldfish's environmental temperature but the GTP/Hb ratio changes drastically from about 1.5 $\mu\text{moles GTP}/\mu\text{mole Hb}$ at 4°C to about 0.85 $\mu\text{moles GTP}/\mu\text{mole Hb}$ at 30°C. These observations are consistent with our hypothesis that changes in red blood cell GTP concentration are used to assure a sufficient oxygen supply of goldfish tissue at different environmental temperatures and thus O_2 solubility in water. In addition our data reveal that ATP and GTP are partly hydrolyzed to ADP and GDP during the usual preparation of protein-free extracts from hemolyzed erythrocytes with TCA. Thus, reported nucleotidediphosphate levels in fish erythrocytes might well be erroneously high.

Specific and nonspecific binding of

$^3\text{H}(-)$ dihydroalprenolol to brown adipocyte plasma membranes

J. P. Giacobino, Département de Biochimie Médicale, Ecole de Médecine, CH-1211 Genève 4

The binding of $^3\text{H}(-)$ dihydroalprenolol to brown adipocyte plasma membranes in the presence of increasing concentrations of both $(-)$ - and $(+)$ -propranolol was studied. The results indicate that the fraction of the total binding which is inhibited by propranolol can be divided into 2 parts; one which is stereospecific and represents 17% of the total binding and the 2nd which is nonstereospecific and represents 49% of the total binding at a propranolol concentration of 10^{-4} M. The results of the metabolic studies which showed that the $(+)$ -propranolol does not modify the norepinephrine-induced increase of the steady state NAD(P) redox value in brown adipose tissue suggest that only the stereospecific binding of $^3\text{H}(-)$ -dihydroalprenolol reflects an interaction of the ligand with the β -receptor. Thus the widely used technique of measuring the nonspecific binding of $^3\text{H}(-)$ -dihydroalprenolol to cellular membranes in the presence of an excess of $(-)$ -propranolol leads to the inclusion in the specific binding value of the part of the binding which is nonstereospecific.

Characterization of monospecific antibodies directed against Na-K-dependent ATPase and its subunits from toad kidney

M. Girardet, D. Geser, J. Frantes, K. Geering, C. Bron, B. Rossier and J. P. Kraehenbuhl, Institut de Biochimie et Institut de Pharmacologie, Université de Lausanne, CH-1011 Lausanne

The Na-K-dependent ATPase was purified from toad kidney. In order to study its organization and biogenesis, antibodies were raised against membrane ATPase, the catalytic subunit (Mr 116K), and the glycoprotein (Mr 62K). The antisera directed against each subunit were monospecific when tested by agarose immunoreplication, whereas the antitotal ATPase recognized the 2 subunits. Using a complement mediated cytotoxicity test and toad red cells as target, the 3 antisera were lytic indicating the presence of surface antigenic determinants. Appropriate absorption abolished lysis without altering ATPase binding suggesting the presence of internal antigenic sites. Morphometric analysis of red cells labelled with ferritin-coupled antibodies indicated a stoichiometric relationship between the 2 subunits with 7000 ferritin molecules per cell.

Partial primary structure of a 16s rRNA gene from *Euglena gracilis* chloroplasts

L. Graf, Zs. Schwarz, H. Kössel and E. Stutz, Laboratoire de Biochimie, Université de Neuchâtel, CH-2000 Neuchâtel, and Institut für Biologie III, Freiburg i. Br., Federal Republic of Germany

Restriction fragments derived from pEgcl1 plasmid DNA, and which code for structural parts of *E. gracilis* 16s rRNA, have been mapped (B. Jenni and E. Stutz, Eur. J. Biochem. 88, 127, 1978) and used for sequence analysis with the dimethylsulphate/lydrazine technique (Maxam and Gilbert). Identification of the 5' and 3' terminal portions of *E. gracilis* 16s RNA were achieved by comparison with the respective portions of 16s rRNA from *Escherichia coli* (J. Brosius et al., PNAS 75, 4801, 1978) and *Zea mays* (Zs. Schwarz and H. Kössel, Nature 279, 520, 1979). A comparison of the 3 sequences reveals extensive homology in

several domains, but also zones of evolutionary divergence. Possible hairpin structures are shown and compared and evolutionary aspects are discussed.

Interactions of liposomes with *Trypanosoma brucei* (culture form)

J. Gruenberg, D. Coral, A.-L. Knupfer and J. Deshusses, Department of Biochemistry and Department of Pharmacy, University of Geneva, CH-1211 Geneva

Fluid positively charged liposomes undergo fusion with the plasma membrane while negative solid liposomes only adsorb to the surface as shown by temperature dependence and trypsinization. These results are consistent with the subcellular fragmentation of broken trypanosomes previously exposed to liposomes. [^3H]concanavalin A and [^{35}S]diazobenzenesulfonate were used to label the plasma membrane.

Nanosecond relaxation in lipid bilayers

B. Gruenewald, W. Frisch and J. F. Holzwarth, Biozentrum, Klingelbergstrasse 70, CH-4056 Basel, and Fritz-Haber-Institut der MPG, Berlin, West

A laser-temperature jump method (J. F. Holzwarth et al., J. phys. Chem. 81, 2300, 1977) was applied for the study of nsec-relaxation processes in dipalmitoylphosphatidylcholine liposomes and vesicles. The solution turbidity was observed. The relaxation time (accuracy: $\pm 20\%$) did not show a significant dependence on the temperature in the range from 30°C to 50°C which includes the phase transition temperature. Amplitude measurements represent the variations in laser energy and are unsuitable for interpretation. - Objective for this work was to assist in the decision about the kinetics of the lipid phase transition. The lack of temperature dependence of the described process emphasizes the view that relaxation effects in the msec range (B. Gruenewald et al., BBA, in press) with a pronounced maximum of time constants at the transition midpoint temperature represent the total change of degree of transition. The above nsec effects are tentatively interpreted as temperature-induced rotation of lipid chains about C-C bonds. The existence of these 2 types of effects demonstrates an analogy with nematic liquid crystals.

Laser raman studies of the binding of calcium to human fibrinogen

C. M. H. Harrison, P.-C. Bugnon and C. W. Schlaepfer, Hämatologisches Zentrallabor, Inselspital, CH-3010 Bern, and Institut de Chimie inorganique, Route de Marly, CH-1700 Fribourg

Binding of calcium to the 2 high affinity sites in human fibrinogen produces a set of configurational changes precisely measurable by laser raman spectroscopy, which appear to involve the stabilization of a series of beta turns. The fact that these sites seem to be phenylalanine/tryptophan-rich, with indications of sharp changes at frequencies corresponding to a disulphide bridge, allow a sequence assignment to residues 316-328 in the gamma chains. Features in the spectrum suggest that calcium at these sites is coordinated to the carboxyl oxygens of Asp 316, Asp 318, Asp 320 and Glu 328, and the carbonyl oxygens of Phe 322 and Gly 324 in the gamma chains. Alterations at 400 cm^{-1} suggest that the third calcium stabilizes a proline-rich segment in the middle of the alpha chains. It therefore appears that the role of calcium binding in human fibrinogen is the stabilization of regions in the molecule which are involved in aggregation, and which become covalently cross-linked by Factor XIII as the final step in the clotting process.

Amino-acid sequence of mitochondrial aspartate aminotransferase from chicken; intra- and interspecies comparison of the mitochondrial and cytosolic isoenzymes from chicken and pig in the light of the spatial structure

U. Hausner, K.J. Wilson, P. Christen, G.C. Ford, G. Eichele and J.N. Jansonius, *Biochemisches Institut der Universität Zürich, CH-8028 Zürich, and Abteilung Strukturbiochemie, Biozentrum der Universität Basel, CH-4056 Basel*

The degree of interspecies sequence identity of the 2 mitochondrial (m) and cytosolic (c) isoenzymes of aspartate aminotransferase (AATase) from chicken and pig (87% and 82%, respectively) markedly exceeds that of the intraspecies identity between mAATase and cAATase from chicken (45%) and from pig (48%). Of the 412 amino-acid residues per chain, 40% are identical in all 4 isoenzymes. As expected, the greater part of these residues is located in the active site cleft and in the interior of the molecule. Residues that are invariant specifically in the 2 mitochondrial enzymes appear to cluster in certain surface regions. Most conspicuous in this respect is the N-terminal segment (up to residue 33) which bridges the active site cleft. In this stretch, there is only 1 amino-acid substitution in the 2 mitochondrial enzymes while their cytosolic counterparts differ in 11 positions.

Purification of spinach thylakoids and an investigation into their pigment/protein complexes after partial and selective solubilization

L.E.A. Henry and P.-A. Siegenhaller, *Laboratoire de Physiologie végétale, Université de Neuchâtel, 20, rue de Chantemerle, CH-2000 Neuchâtel*

We aim to study the polypeptide composition of thylakoids. The purified membranes (purity assessed by marker enzymes) were capable of rapid electron transport in the presence of added ferredoxin. Lipid hydrolysis and transformations were minimal. – Using different combinations of SDS and Triton X-100 the thylakoids were solubilized and electrophoretically fractionated into 6 distinct chlorophyll-protein complexes. The effects of storage, solubilization and electrophoretic procedures upon the pigmented and protein patterns in the electrophoretogram were determined. The different chlorophyll-protein complexes were characterized by spectral analyses and apparent mol.wt.

Identification of the product formed by human erythrocyte membrane galactosyltransferase

F.J. Hesford, E.G. Berger and D.H. van den Eijnden, *Medizinisch-chemisches Institut, Universität Bern, Postfach, CH-3000 Bern 9, and Vrije Universiteit Amsterdam, The Netherlands*

The products formed by human erythrocyte membrane galactosyltransferase (GT) using asialo-ovine submaxillary mucin or Tn-transformed erythrocyte membranes, obtained from a patient with permanent mixed-field polyagglutinability, as exogenous acceptors have been analyzed. Immobilized asialo-mucin, treated with solubilized GT and UDP-14C-gal was subjected to alkaline-borohydride treatment and the released oligosaccharides separated on a Biogel P2 column. Periodate treatment of the isolated disaccharide yielded theosaminol, confirming a gal 1→3 GalNAc linkage. Incubation of GT with solubilized Tn-transformed erythrocyte membranes resulted in the incorporation of labelled galactose into the asialo-agalactoglycophorin present in Tn-membranes, as evidenced by

fluorography of enzymatically labelled Tn-membranes resolved on SDS-polyacrylamide gel-electrophoresis. The Gal 1→3 GalNAc linkage formed in vitro and the incorporation of labelled galactose into asialo-agalactoglycophorin of Tn-membranes demonstrates that this galactosyltransferase is involved in the biosynthesis of the sugar side chains of glycophorin.

Lipid-protein interactions in phosphatidylcholine-bacteriorhodopsin vesicles

M.P. Heyn, N.A. Dencher, R.J. Cherry and A. Blume, *Biozentrum der Universität Basel, CH-4056 Basel, Laboratorium für Biochemie, ETH Zürich, CH-8092 Zürich, and Institut für physikalische Chemie der Universität Freiburg, Freiburg i. Br., Federal Republic of Germany*

Large DMPC-bacteriorhodopsin (BR) vesicles were prepared by a dialysis method. Above the temperature of the lipid phase transition (T_c) the proteins are monomeric, below T_c they are arranged in a hexagonal lattice. The effect of the protein on the lipid phase transition, as monitored by fluorescence depolarization and differential scanning calorimetry (DSC), is to broaden the transition and to reduce the cooperativity without affecting the transition temperature. Incorporation of BR leads to a large increase in the fluorescence anisotropy of a lipid soluble probe. This BR induced effect may be interpreted either as an increase in lipid order or as an increase in membrane viscosity. The formation of the hexagonal BR lattice and the accompanying immobilization of the protein were monitored by CD and protein rotational diffusion measurements. These methods indicate that the protein aggregation occurs a few degrees below T_c . This is consistent with the DSC curves which show a clear broadening on the low-temperature side.

Influence of EHDP and 1.25 (OH)₂ vit. D₃ treatment in vivo on sodium-dependent uptake of inorganic phosphate (P_i) by rabbit duodenal brush border membrane vesicles

B. Hildmann, C. Storelli, G. Danisi, J.P. Bonjour and H. Murer, *Max-Planck-Institut für Biophysik, Kennedyallee 70, D-6000 Frankfurt am Main, Federal Republic of Germany*

Male rabbits (California/New Zealand, 1.5–2.0 kg b.wt) were pair-fed (0.7 g% P_i, 0.8 g% calcium and 1200 IU vit. D₃/kg). 2 animals (A+B) received during 3 days 40 mg/kg/day EHDP s.c., 2 further animals (C+D) received sham injections. 9 h before sacrifice and brush border membrane isolation B and D received 600 ng/kg 1.25 (OH)₂ vit. D₃ i.v. – Sodium-dependent P_i transport was reduced after EHDP treatment (A vs. C). Treatment with 1.25 (OH)₂ vit. D₃ led to a stimulation of sodium-dependent P_i transport (B vs. A, D vs. C). Saturation experiments demonstrated that in a sodium-gradient medium a saturable component is apparently added to a diffusional component seen in a potassium medium. EHDP (A vs. C) abolished this saturable component, whereas after 1.25 (OH)₂ vit. D₃ treatment a saturable P_i uptake (B vs. A) or an increase in the saturable component (D vs. C) was observed.

Acetylcholinesterase kinetics

P. Hofer and U.P. Fringeli, *Laboratorium für physikalische Chemie, ETHZ, CH-8092 Zürich*

3 mechanisms have been suggested to explain the inhibition of acetylcholinesterase by excess acetylcholine. 1. Substrate inhibition occurs through reaction of acetylcholine with

acetylated enzyme. The deacetylation of this ternary complex is supposed to be completely inhibited (R.M. Krupka and K.J. Laidler, *J. Am. chem. Soc.* 83, 1448 (1961). 2. A ternary complex is formed as in mechanism 1. However, the deacetylation is not completely inhibited (literature see 1). 3. A 2-site mechanism is proposed. Acetylcholine binds either to the active site or to the modifier site. The binding to the latter changes the activity of the active site (T.L. Rosenberry and S.A. Bernhard, *Biochemistry* 11, 4308, 1972). Steady state treatment was applied to 1–3. A least squares fit leads to biochemical constants. It is demonstrated that mechanism 2 is the most simple one which can describe satisfactorily the experimental data. Limits for a set of kinetic constants are derived from the biochemical constants. Values of some kinetic constants have been refined by numeric integration and curve-fitting.

Synthesis and properties of 6-substituted phlorizin analogues as fully-competitive inhibitors and as potential photoaffinity labels of the small-intestinal D-glucose carrier

M. Hosang, Andrea Vasella and G. Semenza, *Laboratorium für Biochemie und Laboratorium für organische Chemie, ETHZ, CH-8092 Zürich*

A series of photoaffinity labelling phlorizin analogues, 6-azido-6-deoxyphlorizin, N-(2-nitro-4-azidophenyl)- β -alanyl-6-O-phlorizin (NAP- β -Ala-Phl), N-(2-nitro-4-azidophenyl)-6-amino-6-deoxyphlorizin (NAP-N-Phl) and N-(2-nitro-4-azidophenyl)- β -alanyl-6-amino-6-deoxyphlorizin-amide (NAP- β -Ala-N-Phl) were synthesized from phlorizin. Like phlorizin ($K_i \approx 8 \mu\text{M}$) these derivatives competitively inhibited D-glucose uptake into vesicles from brush border membrane of rabbit small intestine ($K_i \approx 10, 48, 36$ and $148 \mu\text{M}$, respectively). In addition they inhibited specific phlorizin binding to membrane vesicles to a similar extent ($K_i \approx 11, 60, 49$ and $103 \mu\text{M}$, respectively). Photolysis of NAP-derivatives with visible light led to the decomposition of the arylazido group, the half-time being 90 sec. In the presence of membrane vesicles the sensitivity of these compounds to irradiation was significantly increased, depending on the vesicle concentration. By comparing the K_i -values of the new phlorizin derivatives some indications as to their mode of interaction with the transporter were obtained.

Measurement of water exchange times through plant cell membranes by pulsed nuclear magnetic resonance

A. Hugi and J.-P. Zryd, *Institut de Chimie minérale et analytique, 3, place du Château, CH-1005 Lausanne, and Institut de Biologie et Physiologie végétales, Palais de Rumine, CH-1005 Lausanne*

Good measurements of the 'water diffusion permeability' (Pd) are scarce and some of them are limited in their efficiency by the existence of unstirred layers. Pulsed NMR measurement of water exchange time (τ_a) in presence of $2.5 \times 10^{-2} \text{ M}$ of Mn^{++} (see Conlon and Outhred, *BBA* 288, 354, 1972) allow good estimation of Pd. We have used cells of *Acer pseudoplatanus* L. cultivated in liquid medium: this material consisting of isolated cells and small cell aggregates has the advantage of being sensitive to hormonal treatments and close to equilibrium regarding water potential. Mean cell diameter of exponentially growing cell

suspensions is $38 \pm 6 \mu\text{m}$. We have used the relation $\text{Pd} = V/(A \cdot \tau_a)$ to calculate water permeability from cell dimensions and water exchange time. A slow influx of Mn^{++} ($8.8 \times 10^{-15} \text{ M cm}^{-2} \text{ sec}^{-1}$) is present and therefore τ_a has been calculated by extrapolation of the measured values to time 0 (Mn^{++} addition). The treatment of NMR data was completely computerized to allow rapid and unbiased estimation of τ_a . The mean Pd value of exponentially growing cells is $6.4 \pm 0.8 \times 10^{-3} \text{ cm sec}^{-1}$.

Clathrin from coated vesicles: improved isolation and reaction with nucleotides

B.A. Imhof, J.H. Lanz, M. Müller and W. Birchmeier, *Biochemie I, ETH, CH-8092 Zürich*

Bovine brain clathrin was isolated in a monomeric form with high yield and purity > 95%. A dissociating effect of ATP upon clathrin baskets has been found by Schook et al. (*PNAS* 76, 116, 1979). We have observed that ATP neither phosphorylated nor bound to our clathrin in a significant amount. A GTP-binding site on clathrin, however, was identified by photoaffinity labelling. The effect of GTP upon the assembly-disassembly cycle of clathrin baskets is presently studied.

Structural differences between polyclonal murine membrane and secreted IgM

J.-C. Jaton and P. Vassalli, *Department of Pathology, University of Geneva, 30, quai E. Ansermet, CH-1211 Geneva 4*

Membrane and secreted murine IgM, characterized as described elsewhere (Vassalli et al., *PNAS* in press, 1979), were biosynthetically labelled, their μ -chains isolated by SDS-PAGE and cleaved by CNBr. The CNBr peptides of these chains were analyzed by SDS or urea PAGE and characterized by partial N- and C-terminal sequence determination. They were shown to encompass residues 152–234, 235–397, 398–506, 507–576, according to mouse myeloma 104 E μ -chain sequence (M. Kehry et al., *PNAS* 76, 2932, 1979). 2 corresponding CNBr peptides from secreted and membrane μ -chains had different electrophoretic mobilities; the most striking discrepancy being observed for the C-terminal peptide, both by SDS- and urea-PAGE. The C-terminal peptide from membrane μ -chain had an apparent mol.wt and a net acidic charge higher than its counterpart secreted μ -chains. Sequencing and enzymatic cleavage of these peptides followed by HPLC analysis suggested internal structural differences between membrane and secreted μ -chains.

Properties and regulation of adenosine 5'-phosphosulfate sulfotransferase (APSSTase) from cell suspension cultures of *Nicotiana sylvestris* (Spegazz. et Comes)

B.E. Jenni, Chr. Brunold and J.-P. Zryd, *Pflanzenphysiologisches Institut der Universität Bern, CH-3013 Bern, and Institut de Biologie et Physiologie végétales de l'Université de Lausanne, CH-1005 Lausanne*

APSSTase catalyses the transfer of the activated sulfate of adenosine 5'-phosphosulfate (APS) to a carrier protein (Car-SH) thus forming Car-S- SO_3^- . Optimal APSSTase

activity (about 100 nmoles activated sulfate transferred per h per mg protein) were obtained when *N. sylvestris* cells were extracted with 0.1 M tris-HCl pH 8.0 containing 2 M MgSO₄ and 10 mM dithioerythritol. The K_m for APS was $11.1 \pm 0.96 \mu\text{M}$. – Addition of 0.1 mM cysteine to the culture medium decreased the extractable enzyme activity to about 10% of the initial value within 12 h without significant inhibition of growth. 0.5 mM cysteine gave an ultimately greater decrease, but inhibited growth completely.

Cytochrome oxidase rotates in the inner membrane of intact mitochondria and submitochondrial particles

S. Kawato, E. Sigel, E. Carafoli and R. J. Cherry, *Laboratorium für Biochemie, ETHZ, CH-8092 Zürich*

Rotational diffusion of cytochrome oxidase in the inner membrane of bovine heart mitochondria has been measured by observing flash-induced linear dichroism of the cytochrome oxidase-CO complex. A decay in the absorption anisotropy occurs and is characterized by a time constant of about 300–400 μsec in both intact mitochondria and submitochondrial particles. Since vesicle tumbling can be excluded in these experiments, it is concluded that cytochrome oxidase rotates in the mitochondrial membrane with a relaxation time of a few hundred μsec . However, it is likely that only a fraction of cytochrome oxidase contributes to the observed decay, the remainder being relatively immobile.

Interaction of phenylisothiocyanate with human erythrocyte band 3: competitive binding studies with the water soluble analogue p-sulfophenylisothiocyanate

Ch. Kempf, H. Sigrist and P. Zahler, *Institute of Biochemistry, University of Bern, CH-3012 Bern*

The 2 structurally related probes, the apolar phenylisothiocyanate and the polar, water-soluble p-sulfophenylisothiocyanate, are analyzed for their interaction with human erythrocyte band 3 protein. Competitive binding studies indicate that 3–4 binding sites are specifically modified by the hydrophobic phenylisothiocyanate. As analyzed in electrophoretically-separated band 3 and in the isolated 95,000 dalton protein, an additional interaction site can be occupied by both the polar p-sulfophenylisothiocyanate and the hydrophobic phenylisothiocyanate. The occupation of this common binding site by either probe results in effective inhibition of phosphate transport.

The driving forces in Na-dependent transmembrane transport systems of D-glucose and L-ascorbate in the small intestine

M. Kessler, G. Toggenburger and G. Semenza, *Laboratorium für Biochemie der ETH Zürich, Universitätstrasse 16, CH-8092 Zürich*

As shown by the effects of various anion and cation gradients, a) the driving force of D-glucose uptake and accumulation into brush border vesicles from small intestine is the gradient of electrochemical potential of Na⁺; the yield of energy conversion is better than 80–90%; b) the driving force of L-ascorbate uptake (and accumulation?) in human and guinea-pig small intestinal vesicles is the gradient in chemical potential of Na⁺.

Kinetics of Na⁺-dependent D-glucose transport in intestinal brush border vesicles: a) functional asymmetry, b) effect of the membrane potential $\Delta\psi$ on transport

M. Kessler and G. Semenza, *Laboratorium für Biochemie der ETH Zürich, Universitätstrasse 16, CH-8092 Zürich*

a) D-glucose transport is functionally asymmetric. Influx is strongly accelerated by $\Delta\psi$ (negative inside), efflux is insensitive to variation of $\Delta\psi$. In addition, influx is inhibited already at low concentrations of Na⁺ present in the trans-compartment, efflux is not. b) The effect of $\Delta\psi$ on influx may be explained in 2 ways: If the carrier itself is electrically neutral ($z=0$), the ternary complex carrier/glucose/Na⁺ is positively charged and its inward translocation is promoted. Alternatively, if the unloaded carrier is negatively charged ($z=-1$), it is the return of the empty carrier, which is accelerated. 2 tests are used to distinguish among these alternatives: 1. The $\Delta\psi$ -dependence of K_m and V_{max} . 2. The $\Delta\psi$ -dependence of the trans-inhibition by Na_{in}⁺ and glucose_{in}. It is shown in a general model, that increasing $\Delta\psi$ must lead to opposite effects: trans-inhibition increases if $z=0$, it decreases if $z=-1$.

A study of the conformation of thioredoxin fragments

A. Klaus, H. Reutimann, P. L. Luisi and A. Holmgren, *Technisch-chemisches Laboratorium, ETHZ, CH-8092 Zürich, and Department of Chemistry, Karolinska Institutet, S-104 01 Stockholm 60, Sweden*

Escherichia coli thioredoxin is split by trypsin into 2 fragments (1–73) and (74–108) (A. Holmgren et al., *Proc. nat. Acad. Sci. USA* 72, 2305, 1975) which are inactive. However, the recombination of the 2 fragments produces a fully functional protein; and therefore, this system is an ideal one to study the structural prerequisites for a fragment-fragment recognition. With this aim, we have synthesized the pentadecapeptide corresponding to the sequence 77–91 (other sequences are in preparation) and recombination studies between this synthetic fragment and the fragment (1–73) have been carried out. An investigation of the conformation of the synthetic and original protein fragments with CD techniques is in progress in order to assess to what extent each fragment is able to maintain the high degree of secondary structure which is present in the native protein.

Asymmetric insertion of the Na⁺-D-glucose Co-transport carrier in the small-intestinal brush border membrane

A. Klip, S. Grinstein, J. Biber and G. Semenza, *Laboratorium für Biochemie der ETH Zürich, Universitätstrasse 16, CH-8092 Zürich*

We have compared a) little permeant (p-chloromercuribenzylosulfonate) and permeant (p-chloromercuribenzoate) SH-reagents in their inhibition of phlorizin binding and of D-glucose transport into sealed, rightside out vesicles from small intestinal brush border membranes; b) little permeant (red. glutathion) and permeant (dithioerythrol) thiols in their capability to restore phlorizin binding to vesicles which had been pretreated with HgCl₂; c) various reagents (trypsin, chymotrypsin, papain, p-chloromercuribenzylosulfonate, etc.) in their inhibition of phlorizin binding to native vesicles or to deoxycholate-extracted membranes. The results show conclusively that one or more SH-group(s) located at the cellular side of the membrane is (are) essential for phlorizin binding to the carrier (although

not occurring at the substrate binding site: substrates do not protect from inactivation by SH-reagents) and that proteolytic inactivation of the carrier by the proteases tested is possible only from the cellular side (or after partial dislodging by deoxycholate). The asymmetric insertion of the carrier in the membrane agrees with its functional asymmetry (Kessler and Semenza, 1980).

Partial structural characterization of the Fc fragment of human IgD

H.P. Kocher and J.-C. Jaton, *Department of Pathology, University of Geneva, CH-1205 Geneva*

The tryptic Fc fragment of IgD myeloma protein Ho was cleaved with CNBr. 3 fragments, designated CB1C, CB2 and CB3 were obtained. CB1C was positioned to the NH₂-terminus of the Fc fragment based on sequence analysis. The peptide encompassed the entire intrachain disulfide loop of the C δ 2 domain. Fragment CB2 was cleaved beyond the first half-cystine residue of the C δ 3 domain and contained the second half-cystine of this domain. SDS-PAGE analysis of CB2 exhibited 2 bands, both of which were shown to have an identical NH₂-terminal sequence. This heterogeneity may be the result of a proteolytic degradation at the COOH-terminus and/or differences in carbohydrate content. The peptide CB3 was positioned between the 2 fragments CB1C and CB2. Its sequence had an uncommonly low homology to similar regions in heavy chains of other Ig classes. A relatively large number of hydrophobic amino acids was found which might be of interest in view of the known presence of IgD as membrane bound surface receptor on B lymphocytes.

Different α - and β -adrenergic receptor binding and adenylylase stimulation in the brain of isolated rats

K. Kräuchi and H. Feer, *Psychiatrische Universitätsklinik, Wilhelm-Klein-Strasse 27, CH-4025 Basel*

α - and β -adrenergic receptor binding (³H-WB4101 resp. ³H-DHA) was determined in different brain regions (cortex, cerebellum, striatum, hippocampus, hypothalamus, medulla-pons and thalamus) of socially reared or isolated rats (n=8–15 rats). Additionally, we measured c-AMP generation by noradrenaline- and isoproterenol-sensitive adenylylase (50 μ M and 10 μ M, respectively) in cortex- and medulla-pons-thalamus-slices. Compared to socially reared rats ³H-DHA-binding was diminished in all brain regions of isolated rats (maximally by 12–15% in medulla-pons and thalamus, $p < 0.05$) and ³H-WB4101-binding was constantly elevated (1–14%, n.s.). Isolated rats showed a reduced c-AMP formation by noradrenaline (16%, $p < 0.05$) and isoproterenol (11%, n.s.) in pons-medulla-thalamus but not in cortex. No differences in basal levels of c-AMP were found.

In vivo tracing of actin and α -actinin in stress fibres of nonmuscle cells and their possible involvement in cell motility

T.E. Kreis, J.H. Lanz, B.M. Jockusch and W. Birchmeier, *Biochemie I, ETH, CH-8092 Zürich, and EMBL, D-69 Heidelberg, Federal Republic of Germany*

Nonmuscle cells were microinjected with fluorescently labelled actin or α -actinin and visualized by video-intensified fluorescence microscopy. Actin incorporated homogeneously into stress fibres (Kreis et al., PNAS 76, 3814, 1979). The α -actinin tracer, however, exhibited a regularly striped arrangement (see also Feramisco, PNAS 76, 3967,

1979) morphologically resembling the striation pattern of skeletal muscle sarcomers. – The fluorescently traced stress fibres remained intact following Triton X-100 extraction of the cells, and furthermore, these cell models contracted upon addition of MgATP. It is currently investigated whether the striation pattern of α -actinin changes during cell contraction and whether these structures thus also functionally reflect the muscle sarcomers.

Kinetics of L-leucine transport in brush border vesicles isolated from rabbit small intestine

O. Kriech, R. Förster, M. Kessler and G. Semenza, *Laboratorium für Biochemie der ETH Zürich, Universitätsstrasse 16, CH-8092 Zürich*

Kinetic studies were done by using a short-time incubator which allows to determine true initial influx rates. L-leucine appears to be transported by a single transport system, which is Na⁺-dependent and electrogenic. At $\Delta\psi = 0$, sodium primarily modifies the K_m of leucine influx leaving the V_{max} unaltered, indicating that the carrier can be classified to be of 'affinity type'. On the other hand, leucine influx is strongly inhibited by Na⁺ present inside the vesicles (> 80% at 100 mM Na_i). This trans-inhibition cannot be reconciled with a simple 'affinity type' mechanism, since it must be assumed that – at least in the inward facing conformation – the binary complex 'carrier/Na⁺' is formed extensively at low concentrations of Na_i⁺, and that this binary complex cannot translocate across the membrane. Therefore, more complex models have to be designed to fit the experimental data.

Binding to fibrinogen and fibrin of plasminogen activator from pig heart tissue

E.K.O. Kruithof and F. Bachmann, *Laboratoire Central d'Hématologie, CHUV, CH-1011 Lausanne*

It has been shown that pig heart tissue activator (PHTA) of plasminogen binds to clotted blood, whereas urokinase does not. To elucidate if conversion of fibrinogen to fibrin makes available binding sites for the PHTA, a partially purified PHTA preparation was passed over fibrinogen-sepharose and fibrin-sepharose. The dissociation constant of the complex (around 10⁻⁹ M) and the number of binding sites were similar for either substituted agarose. Human and porcine fibrinogen and fibrin and reptilase treated fibrinogen (des AA fibrin) gave qualitatively similar results. No binding whatsoever of PHTA was noted on albumin or ethanolamine-agarose. – Binding of PHTA to fibrinogen was confirmed by gel-filtration on sephadex G-200 with and without 1.75 mg/ml bovine fibrinogen in the eluant. The apparent mol.wt changed from 80,000 to 150,000. This indicates that under these conditions, 40% of the tissue activator was reversibly bound to fibrinogen.

The reaction of L-tryptophan with tryptophan-synthase complex from *Escherichia coli*

A.N. Lane and K. Kirschner, *Biozentrum, Abteilung Biophysikalische Chemie, Klingelbergstrasse 70, CH-4056 Basel*

Using stopped-flow methods, 3 phases were resolved in the reaction of L-tryptophan with *E. coli* tryptophan-synthase complex (EC: 4.2.1.20). The first, fast process was observable only when monitoring quenching of enzyme bound PLP fluorescence and was followed by 2 poorly resolved slow decreases in fluorescence. Improved resolution of the 2 slow processes was obtained from measurement of increases in absorbance at 473 nm. – The effects on apparent rate constants and amplitudes of deuterating the α -carbon

of tryptophan or of changing the pH agreed with predictions based on a 3-step linear reversible mechanism, in which removal of the c_a proton occurs during the 2nd step. The values of derived rate constants suggest that reversal of these step (i.e. tryptophan release) is largely rate-determining in the synthesis of tryptophan from indole and L-serine.

The influence of growth on the plasma membrane ATPase of *Saccharomyces cerevisiae*

H. Lentzen, O. Käppeli, G.F. Fuhrmann and A. Fiechter, Department of Pharmacology, Philipps-University Marburg, Lahnberge, D-3550 Marburg, Federal Republic of Germany, and Chair of Microbiology, ETH-Hönggerberg, CH-8093 Zürich

In continuous cultures of yeast cells under glucose limitation a 'steady state' of growth can be obtained. At high rates of glucose supply a strong repressional effect on respiratory metabolism has been observed (A. Fiechter and H.K. von Meyenburg, Path. Microbiol. 29, 696, 1966). This study, in addition to the above repression, shows a derepressional effect on plasma membrane ATPase. At the onset of respiratory repression the specific plasma membrane ATPase activity increased from 1.2 to 2.8 $\mu\text{moles/mg protein/10 min}$. This result is in accordance with the observation that plasma membrane ATPase activity in commercial baker's yeast is usually high because these yeasts are grown under respiratory repression conditions. Finally, a change in ATPase activity has been found in synchronized *S. cerevisiae* cells. During the cell cycle ATPase activity increased from 1.3 at the beginning of the S-phase to 2.2 $\mu\text{moles/mg protein/10 min}$ at the end of the M-phase.

Boc-(L-Val-D-Val)₄-OMe: a conformational model of Gramicidin A

G.P. Lorenzi, L. Tomasic, E. Benedetti, B. Di Blasio and C. Pedone, Technisch-chemisches Laboratorium, ETHZ, CH-8092 Zürich, and Istituto Chimico, Università di Napoli, I-80134 Napoli, Italy

The particular types of conformation proposed for Gramicidin A, that might account for the transmembrane channel forming properties of this antibiotic, are based on limited experimental evidence. One of these conformational types has now been identified in Boc-(L-Val-D-Val)₄-OMe, a synthetic octapeptide that exhibits alternating D- and L-residues like Gramicidin A. An X-ray analysis of single crystals of this octapeptide has shown a double-stranded antiparallel β -helical structure in detail. In addition, ¹H-NMR, CD and IR-absorption measurements, combined with mol.wt determinations by vapor pressure osmometry, have provided strong evidence for a double-stranded antiparallel β -helix as a major component of the conformational equilibrium of the octapeptide in cyclohexane or chloroform solution. These findings on a model oligopeptide provide important support for the conformational species 3 of Gramicidin A postulated by W.R. Veatch, E.T. Fossel and E.R. Blout (Biochemistry 13, 5249, 1974).

Peroxide, calcium and pyridine nucleotide interactions in rat liver mitochondria

H.R. Löttscher, K.H. Winterhalter, E. Carafoli and C. Richter, Biochemie I, ETH, CH-8092 Zürich

Peroxides lead to an irreversible oxidation and loss of mitochondrial pyridine nucleotides (PN) in Ca^{2+} -loaded mitochondria concomitant with the release of Ca^{2+} (H.R.

Löttscher, K.H. Winterhalter, E. Carafoli and C. Richter, Proc. nat. Acad. Sci. USA 76, 4340, 1979). We have now investigated the fate of mitochondrial PN in the presence of Ca^{2+} and peroxide. Injection of radioactively labelled nicotinic acid brings about a specific labelling of mitochondrial PN in vivo. Exposure of these mitochondria to Ca^{2+} and peroxide in vitro causes a release of the radioactivity. Nicotinamide is identified as the radioactive compound formed during the breakdown of mitochondrial NAD(P)^+ . The oxidation and the loss of PN are accompanied with release of Ca^{2+} from the mitochondria. The release of Ca^{2+} is electroneutral and is not caused by irreversible structural or functional damage to the mitochondria.

A cell-age specific antigen of human red blood cells

H.U. Lutz and M.M.B. Kay, Department of Biochemistry, ETH Zürich, CH-8092 Zürich, and VA Wadsworth Hospital, Los Angeles, USA

Human serum IgG contains autoantibodies against old RBC. Triton extracts from surface iodinated RBC were incubated with autologous IgG. Immunoprecipitates from extracts of old RBC were purified on Protein A sepharose and revealed a ¹²⁵I-labelled protein that had an approximate mol.wt of 120K, while those from young RBC showed only traces of this protein. Iodination of purified precipitates from unlabelled old RBC by the technique of Bolton-Hunter indicated that the 120K protein was the only major protein in the precipitate originating from RBC. In replicas of SDS PAGE gels of precipitates, the 120K protein was labelled with ¹²⁵I-protein A following incubation of the replica with autologous IgG. In replicas from gels of intact membranes ankyrin was labelled in both young and old RBC, whereas label in the 120K region was almost exclusively found in replicas from old RBC. The data suggest the cell-age specific antigen to arise from ankyrin which is inaccessible to autoantibodies in young, but accessible in old RBC as its 120K fragment.

Relationship between calmodulin binding to synaptic membranes and activation of adenylate cyclase in bovine cerebellum

A. Malnoë and J.A. Cox, Department of Biochemistry, University of Geneva, P.O. Box 78, CH-1211 Geneva 8

Receptors for calmodulin (CDR) in crude synaptic membranes from bovine cerebellum have been characterized using ¹²⁵I-CDR. The binding of ¹²⁵I-CDR is saturable, temperature-dependent and reversible. The binding is specific since addition of excess troponin C can not displace the bound CDR. Scatchard analysis reveals 2 binding sites of K_d 's 5 and 30 nM. Both CDR binding and adenylate cyclase (AC) activation by CDR require μM concentrations of free Ca^{2+} . However unlike AC activity, CDR binding is not inhibited by mM concentrations of Ca^{2+} . The antipsychotic agents of the phenothiazine group which selectively inhibit the CDR-dependent AC display a similar order of potency in inhibiting ¹²⁵I-CDR binding to synaptic membranes. Our results suggest that the CDR-dependent activation of AC is directly related to the binding of CDR to specific sites in cerebellar synaptic membranes.

Functional reconstitution of Triton X-100-solubilized rat liver cytochrome oxidase

Marianne Mattenberger, G. Hugentobler and P. Gazzotti, *Laboratorium für Biochemie, ETH, Universitätstrasse 16, CH-8092 Zürich*

Rat liver cytochrome oxidase has been purified in the form of a Triton X-100 complex (J. Bioenerg. Biomembr. 9, 237, 1977). The enzyme has been reincorporated into phospholipid vesicles by substitution of Triton X-100 with the appropriate phospholipid on a Bio Beads SM-2 column. This reconstitution procedure is very fast and permits to obtain cytochrome oxidase vesicles with high respiratory control. The formation of vesicles by this technique is highly dependent on the initial detergent to phospholipid ratio. The respiratory control index observed with the reconstituted cytochrome oxidase vesicles depends strongly on the type of phospholipids used. With soya beans lipids, respiratory control indexes as high as 7 are obtained whereas with total mitochondrial phospholipids the index is only between 2 and 3. Using various mixtures of mitochondrial phospholipids we have found that cardiolipin is responsible for the 'uncoupling' of the cytochrome oxidase reconstituted with total mitochondrial phospholipids. The reconstituted cytochrome oxidase vesicles are also capable of energy-dependent cation uptake in the presence of neutral ionophores.

Structural and enzymatic properties of horse liver alcohol dehydrogenase (LADH) solubilized in hydrocarbons via reversed micelles

P. Meier and P. L. Luisi, *Technisch-chemisches Laboratorium, ETHZ, CH-8092 Zürich*

The anionic surfactant di(2-ethyl-hexyl)sodium sulfosuccinate (AOT) forms reversed micelles in hydrocarbon solvents. We have found conditions under which enzymes can be solubilized in the aqueous core of these reversed micelles without loss of activity, e.g. ribonuclease (R. Wolf and P. L. Luisi, *Biochem. biophys. Res. Commun.* 89, 209, 1979). LADH could also be solubilized in n-octane with 50 mM AOT and 1–5% v:v of water. At optimal pH-conditions and molar ratio (H₂O)/(AOT), the activity is comparable to that in water. The hydrocarbon enzyme solution allows spectroscopic studies such as UV, CD, fluorescence, IR and NMR for the elucidation of the protein's structure and the properties of water around it. The system also offers a technical interest, e.g. for the enzymatic transformation of water insoluble substrates. This is now under investigation.

Statistical description of phospholipid bilayers as complement to deuterium NMR data

J.-P. Meraldi and J. Seelig, *Biocenter, University of Basel, Klingelbergstrasse 70, CH-4056 Basel*

A qualitative understanding of a biological membrane is obtained through the quantitative description of a model system like a phospholipid bilayer. Since ²H NMR, even in conjunction with other techniques, cannot rigorously achieve this goal, a theoretical model has been devised to extend and complement this experimental method. The model has a close relationship with the experiment since some semi-empirical parameters are adjusted on the basis of accurate reproduction of the highly qualitative ²H NMR data. Examples of the extension of the model to problems not accessible experimentally are given by the computation of CH₂ monomers configuration probabilities as well as the

characterization of their motional anisotropy. Finally the model was applied to the qualitative interpretation of several biological problems.

In-vitro formation of glucose-6-phosphate (G6P) and α-glycerophosphate (α-GP) from 3-phosphoglycerate (3PG) by rat liver cytosol

S. Mörikofer-Zwez, F. B. Stoecklin and P. Walter, *Biochemisches Institut der Universität, Vesalianum, Vesalgasse 1, CH-4051 Basel*

Liver cytosols from 48-h starved rats were prepared by centrifugation of 1:6 liver homogenates at 150,000×g. They were incubated at a dilution of 1:15 at 30°C and pH 7.4 in media supplemented with various cofactors. In presence of 2 mM 3PG, 20 mM lactate and 2 mM NAD, the following rates of product formation (μmoles·min⁻¹·g liver⁻¹±SD) were observed: α-GP 1.34±0.12, G6P 0.45±0.12. Addition of 0.5 mM α-GP to the incubation system decreased net α-GP-formation more than 4-fold and increased G6P-formation to 0.90±0.13. When 5 mM α-GP was added, G6P-formation increased to 1.4±0.2. Experiments with added ¹⁴C-α-GP showed that under the latter conditions maximally 30% of the G6P formed is derived from α-GP. It is concluded that, in contrast to previous results in the literature, G6P can be formed from 3PG by liver cytosol at rates within the physiological range.

The charge density is not a driving force for red blood cell shape change and vesicle release

H. Müller, U. Schmidt and H. U. Lutz, *Department of Biochemistry, ETH Zürich, CH-8092 Zürich*

The release of spectrin-free vesicles from human RBC can be considered the final step of the RBC shape change to echinocytes. Its mechanism was studied. If the electrophoretic mobility of fresh RBC was doubled by treatment of RBC with phospholipase D, the release of vesicles from these RBC, upon ATP-depletion, was identical to that of the control. Thus, an increase of negatively charged PL in the outer monolayer does not promote vesicle release. Likewise, a decrease of negatively charged PL on the inner monolayer of the released vesicles is not necessary: EDTA did not inhibit vesicle release at 1 mM (106±5%, n=3), although the polyPI content of these vesicles was virtually the same and that of PA 2–3 times that of fresh RBC. On the other hand, the concentration of a potential driving force, diacylglycerol, was in all vesicles 10-fold higher than in fresh membranes and most likely originated from PC rather than polyPI. Its content was decreased when vesicle production was inhibited to 90% by 15 mM EDTA.

Lectin-binding studies indicate a unique carbohydrate structure for the human platelet bovine von Willebrand factor (BvWF) receptor

H. Y. Naim, K. J. Clemetson and E. F. Lüscher, *Theodor-Kocher-Institut, Freiestrasse 1, CH-3000 Bern 9*

Galactose-binding lectins such as peanut agglutinin (PNA), soybean agglutinin (SBA) and *Ricinus communis* lectin (RCL) aggregate neuraminidase-treated human blood platelets. In subagglutinating concentrations, PNA inhibits agglutination of such platelets by BvWF, SBA and RCL were less effective. Incubation of platelets in Ca⁺⁺ but not in EDTA-containing medium removes the surface protein glyocalicin (GL) and this is linked to loss of response to BvWF. When Ca⁺⁺-treated platelets were desialylated,

their agglutination with PNA was greatly impaired, there was some inhibition of SBA-induced agglutination and RCL reacted normally. EDTA-treated platelets behaved normally with all 3 agents. GL and GPIb are retained on PNA-Ultrogel chromatography suggesting that GL is derived from GPIb, which acts as the receptor for BvWF. The unique carbohydrate structure of GPIb is evident from the different effects of galactose-binding lectins on desialylated platelets.

Protein associations in erythrocyte membranes demonstrated by protein diffusion measurements

E. A. Nigg, C. Bron, M. Girardet and R. J. Cherry, Laboratorium für Biochemie, ETHZ, CH-8092 Zürich, and Université de Lausanne, Institut de Biochimie, Chemin des Boveresses, CH-1066 Epalinges

Rotational diffusion of band 3 can be measured by observing the transient dichroism resulting from excitation of a covalently bound triplet probe by a linearly polarized light pulse. Protein rotation is sensitive to protein interactions and hence these measurements can be used to investigate associations of band 3 in the membrane. Self-association of band 3 was investigated by measuring rotation before and after formation of covalent dimers by chemical cross-linking. No change in rotation was observed, thus providing direct evidence for the existence of band 3 dimers. In addition, the existence of a band 3-glycophorin A complex in the membrane could be demonstrated: Band 3 rotation is strongly reduced following binding of divalent antiglycophorin A antibodies, but not by monovalent Fab-fragments, antispectrin or nonspecific antibodies.

Regulation of a presynaptic adenylate cyclase from bovine cerebellum by beta-adrenergic receptors

I. Novak-Hofer, A. Malnoë and E. A. Stein, Department of Biochemistry, University of Geneva, P.O. Box 78, CH-1211 Geneva 8

Intact crude synaptosomes prepared in Krebs-Ringer buffer can synthesize cAMP from the membrane-permeating precursor adenine. This synthesis takes place within synaptosomes as control experiments show that an externally located (postsynaptic) adenylate cyclase is inactive in the Krebs-Ringer medium. [³H]adenine pulse labelling indicates that synaptosomal cAMP synthesis is not affected by depolarization-induced Ca²⁺ influx, but is stimulated by norepinephrine and isoproterenol. Propranolol inhibits this stimulation whereas phentolamine does not affect it, suggesting the presence of a presynaptic beta-adrenoreceptor coupled adenylate cyclase.

Stimulation of net glycogen production in rat hepatocytes by insulin

F. Nyfeler and P. Walter, Biochemisches Institut der Universität Basel, Vesalianum, Vesalgasse 1, CH-4051 Basel

Isolated liver cells from 24-h fasted rats were incubated in an unfortified Krebs-Ringer buffer containing 4% albumin. In the presence of 10 mM glucose, addition of insulin stimulated net glycogen production by 54 ± 6% (n = 18), and in the presence of 30 mM glucose by 22 ± 3% (n = 63). The minimal dose of insulin producing a significant effect was 2 × 10⁻⁹ M and the stimulation reached a plateau at insulin concentrations between 10⁻⁸ and 10⁻⁷ M. 10–20 min after the addition of insulin, glycogen synthase-a activity was significantly enhanced, and this increase was still observed after 1 h of incubation. Insulin antagonized the inhibitory

action of suboptimal doses of glucagon on glycogen deposition, whereby significant decreases of glucagon elevated cAMP levels were observed. Insulin also decreased basal cAMP levels by 24 ± 4% (n = 8).

Modulation of human erythrocyte membrane acetylcholinesterase (AChE) by lipids

P. Ott, E. Frenkel, B. Roelofsens and U. Brodbeck, Medizinisch-chemisches Institut der Universität, P.O. Box, CH-3000 Bern 9, and Biochemisch Laboratorium Rijksuniversiteit Utrecht, Padualaan 8, NL-2506 Utrecht, The Netherlands

Purified, detergent-depleted human erythrocyte membrane AChE showed a linear plot of log activity versus 1/T. When Triton X-100 was present in the assay medium a curved plot was observed with activation energies of 8.3 kcal/mole in the low-temperature range (below 15 °C) and 2.1 kcal/mole at higher temperatures (above 35 °C). For AChE incorporated into dimyristoyl-lecithin vesicles a clear discontinuity at 23 °C could be observed consistent with the phase transition of the lipid. The activation energies were 8.7 kcal/mole below and 2.1 kcal/mole above the phase-transition temperature. Incorporation of AChE into mixed dimyristoyllecithin-cholesterol vesicles (molar ratio 5:4) abolished the discontinuity. In ghost preparations again a linear plot was obtained. These results indicate that the activity of AChE is strongly modulated by its hydrophobic environment.

Calf rennet lysozyme

J.-J. Pahud, K. Schwarz, I. Meyer and F. Widmer, Nestlé Research Laboratories, CH-1814 La Tour-de-Peilz

A strong lytic activity against *Micrococcus lysodeikticus* cell walls was detected in calf rennet. Purification was carried out using ion exchange, electrofocusing and gel-filtration. Hydrolysis of the bacterial peptidoglycan by the isolated enzyme released only reducing groups, thus indicating true glycolytic activity. Comparative tests with hen egg white lysozyme suggested a similar mode of action. – Multiple enzyme forms were revealed, with mol.wts of ca. 15,000, pH optima of ca. 5.0, and pI's ranging from 6.5 to 7.8. The enzyme exhibited remarkable stability against heat and pH conditions ranging from 2 to 9. Significant chitinase activity was observed at pH 5.0. – Specific antisera revealed sharp precipitation arcs in the β- to γ-electrophoretic region, when diffused against the most acidic or basic molecular forms, respectively. – The rennet enzyme differs markedly from the bovine milk lysozyme described only by Chandan et al. (BBA 110, 389, 1965).

Simple test system for determination of the dead time of stopped-flow instruments

C. Paul, G. Haenisch and K. Kirschner, Biozentrum, Abteilung Biophysikalische Chemie, Klingelbergstrasse 70, CH-4056 Basel

Reaction of 5,5'-dithio-bis (nitrobenzoic acid) with excess thioglycerol proceeds in 2 exponential phases, whose rate constants differ 23-fold over a wide range of pH and temperature. The reaction is followed at 436 nm. Since the reaction proceeds via a mixed disulfide intermediate, the integrated rate equations define the ratio of the amplitudes of the 2 reactions in a straight-forward manner, beginning at the apparent zero time of mixing. Given the constant ratio of rate constants, a simple algorithm exists, which relates the measured ratio of the amplitudes to the time elapsed after the apparent zero time of mixing. Thus it is

possible to determine the 'dead time' of a stopped-flow instrument with a simple progress curve. By adding proflavine, the system can be used for determining the dead time of fluorescence detecting equipment.

ACTH-mediated phosphorylation of proteins in adrenocortical cells

E.J. Podesta and R. Neher, Friedrich-Miescher-Institut, CH-4002 Basel

ACTH or cyclic AMP stimulates rapidly the ^{32}P -incorporation into a cytoplasmic protein of about 150,000 daltons (APS_{150}) present in a steady-state equilibrium with a $1/2$ -life of about 10 min. Receptor-bound cyclic AMP, phosphorylated APS_{150} (APSP_{150}) and corticosterone rose in parallel with respect to both time and ACTH concentration. All 3 responses were dependent on extracellular Ca^{2+} . Kinetics and chase experiments showed that APSP_{150} is under simultaneous control of kinase and phosphatase activity. The stimulation of a protein (about 16,000 daltons, APS_{16}) in the particulate fraction was observed when incubations were carried out with at least 280 pM ACTH or 3 mM monobutyl cyclic AMP for more than 15 min.

Abnormal sulfate metabolism in a demyelinating neuropathy

J. Reigner, M. Rütli and J.-M. Matthieu, Service de Pédiatrie, CHUV, CH-1011 Lausanne

Trembler mice are affected by a dominantly inherited neuropathy. Total lipid content and sulfatides were decreased in peripheral nerves (PNS) from 15-day-old mutants. The proportion of sulfatides in percent of total lipids was similar in control and Trembler PNS. The *in vivo* incorporation of ^{35}S -sulfate into sulfatides and nonlipidic material from Trembler PNS was significantly increased. Cerebroside sulfotransferase (CST) activity in Trembler PNS was 257% higher than in controls. No activator or inhibitor of CST could be found. In Trembler PNS, CST had higher apparent K_m and V_{max} and its heat sensitivity was different. Low levels of substrate and high arylsulfatase activities (218% of controls) could explain the lack of sulfatide accumulation. The increased sulfate incorporation into nonlipidic material could play a role in the overproduction of connective tissue whereas the high turnover rate of sulfatides could be correlated with intense demyelination and remyelination observed in the PNS of these mutants.

Purification of a new insulinotropic peptide from porcine duodenum: first results

F. Rey and J.-P. Felber, Division de Biochimie Clinique, Département de Médecine, CHUV, CH-1011 Lausanne

A crude extract of porcine duodenal mucosa (Prof. V. Mutt, Department of Biochemistry II, Karolinska Institutet, Stockholm, Sweden), shown to be insulinotropic on an *in situ* rat pancreas preparation, was divided into fractions by ion exchange chromatography, organic solvent extraction, isoelectric focusing and high pressure liquid chromatography. - During purification procedure, biological activity was followed by the same bioassay. The fractions were injected into the portal blood flow. Simultaneously, blood samples were collected from the same point, near the junction of the portal with the pancreaticoduodenal vein, for insulin determination. - Comparing the activity of all fractions with that of fractions containing the well-known insulinotropic gastrointestinal hormones, it appeared that a new 'incretin' activity was present in this acidic extract, different from that of VIP, GIP, Secretin, CCK 33 and

CCK 39. - Its physiological properties, mol.wt and isoelectric point are however similar to those of the mentioned gastrointestinal hormones.

Lipid peroxidation in rat liver microsomes increases membrane microviscosity and decreases rotational mobility of cytochrome P-450

C. Richter, R.J. Cherry and S. Kawato, Biochemie I, ETH, CH-8092 Zürich

Peroxidation of membranes phospholipids leads to destruction of highly unsaturated fatty acid residues and appearance of malondialdehyde (MDA) as breakdown product (J.A. Buege and S.D. Aust, *Meth. Enzym.* 52C, 302, 1978). Loss of unsaturated fatty acid residues and production of the bifunctional reagent MDA, a potent cross-linking reagent, could conceivably lead to an increase of the microviscosity in membranes and therefore a decreased mobility of membrane proteins. - We determined the microviscosity in peroxidized rat liver microsomes with the fluorescence polarization technique using diphenylhexatriene as probe. MDA production is paralleled by an increase in microviscosity from 130 cpoise in control membranes (0.5 nmoles MDA/mg protein) to 400-500 cpoise in peroxidized membranes (about 50 nmoles MDA/mg protein). Rotational diffusion of cytochrome P-450 was measured with the flash photolysis technique (C. Richter, K.H. Winterhalter and R.J. Cherry, *FEBS Lett.* 102, 151, 1979). In control membranes the translational diffusion coefficient D_T is in the order of 10^{-9} to $10^{-10} \text{ cm}^2 \text{ sec}^{-1}$. Moderate peroxidation (9 nmoles MDA/mg protein) results in complete immobilization of cytochrome P-450.

Binding sites on cytochrome c for cytochrome c oxidase, cytochrome c reductase and cytochrome c_1

R. Rieder and H.R. Bosshard, Biochemisches Institut der Universität, Zürichbergstrasse 4, CH-8028 Zürich

By the method of differential chemical modification (H.R. Bosshard, *Meth. biochem. Analysis* 25, 273, 1979), the chemical reactivity of each of the 19 lysines of horse cytochrome c was compared in free and in complexed cytochrome c and binding sites were deduced from altered chemical reactivities of particular lysyl side chains in complexed cytochrome c. Virtually identical binding sites were found for oxidase and reductase implying that cytochrome c cannot bind to its electron donor and acceptor simultaneously. Further, cytochrome c binds to the c_1 -subunit of the reductase since the whole reductase and its isolated c_1 -subunit are shielding the same lysyl side chains of cytochrome c. Lysyl residues 8, 13, 72+73, 86 and 87 are located at the common binding site, whereas residues 5, 7, 25, 27, 79 and 88 are peripheral to it. All other lysyl residues are outside the binding site.

Regulation of respiration in *Saccharomyces cerevisiae*

M. Rieger, O. Käppeli and A. Fiechter, Chair of Microbiology, Swiss Federal Institute of Technology, CH-8093 Zürich

The respiration of *S. cerevisiae* is subject to glucose repression (glucose effect). In a chemostat culture with glucose as the limiting substrate it is possible to grow *S. cerevisiae* at derepressed conditions. At dilution rates $D < D_R$ the cells exhibit a purely oxydative metabolism of glucose meaning that besides the formation of biomass glucose is oxidized to CO_2 and water. - The aim of this study was the determination of the respiratory capacity of *S. cerevisiae*. This was achieved by determining the oxygen uptake rate after an

ethanol pulse at various dilution rates in the range of derepressed growth ($D < D_R$). A maximum oxygen uptake rate was observed and the velocity of ethanol utilization was correlated to the difference between this maximum value of oxygen uptake and the corresponding steady state value on glucose before the ethanol pulse. The respiratory capacity as assessed by ethanol pulsing was compared to that measured in a Clarke type oxygen probe and a possible implication of a limited respiratory capacity in the glucose effect is discussed.

Effects of various iron chelators on the growth of enteropathogenic *Escherichia coli*

D. Rivier, Université de Lausanne, CH-1011 Lausanne

E. coli 0111:K58 has been cultured in minimal medium of Davis and Mingioli deprived of citrate and of FeSO_4 . Ferrioxamine B (desferal) inhibits the growth of *E. coli* 0111 at a minimal concentration of 1 $\mu\text{g/ml}$. In presence of desferal (10 $\mu\text{g/ml}$), ferricrocine (obtained from Dr. J. Nuesch, Ciba-Geigy) at a minimal concentration of 10 pg/ml or supernatant of *E. coli* 0111 culture (containing presumably enterochelone) at a 400-fold dilution stimulate the growth of *E. coli* 0111. Furthermore, dihydroxybenzoic acid – the iron-binding component of enterochelone – exerts a growth-promoting activity on *E. coli* 0111 at concentrations as low as 10 ng/ml . It is proposed that the membranes of *E. coli* 0111 possess appropriate receptor proteins for iron transport by ferricrocine and enterochelone. On the other hand, *E. coli* 0111 appears to lack a specific receptor protein for desferal. This compound does not antagonize ferricrocine (and presumably enterochelone). Experiments to abrogate the growth of *E. coli* by antibodies to dihydroxybenzoic acid (or enterochelone) are in progress.

Papain digestion of rat renal proximal tubular and small intestinal brush border membranes

R. Rohn, G. Stange and H. Murer, Max-Planck-Institut für Biophysik, Kennedyallee 70, D-6000 Frankfurt am Main, Federal Republic of Germany

Right side out oriented brush border membranes were isolated by calcium precipitation methods. Papain digestion removed maltase, sucrase, alkaline phosphatase and leucine-aminopeptidase in intestinal membranes; in renal membranes maltase, leucine-aminopeptidase and γ -glutamyl transpeptidase were digested. In intestinal membranes γ -glutamyl transpeptidase and trehalase were not digested, whereas in renal membranes alkaline phosphatase was not affected. Transport of D-glucose and L-alanine – as measured under sodium gradient conditions, transstimulation conditions and inhibitor-sensitive transport (phlorizin, HgCl_2) – were only slightly affected by proteolysis. Transport of inorganic phosphate was abolished after papain digestion. The results demonstrate: a) differences in the arrangement of similar systems in intestinal membranes as compared to renal membranes; b) protection from proteolysis of transmembrane transport mechanisms; c) in renal membranes transport of inorganic phosphate can be dissociated from alkaline phosphatase activity.

The purification of NADP-dependent malate dehydrogenase from spinach chloroplasts

E. Roux and P. Schürmann, Laboratoire de Biochimie, Université de Neuchâtel, CH-2000 Neuchâtel

The NADP-dependent MDH of chloroplasts is part of a shuttle system that allows the exchange of reducing equivalents between the chloroplast and the cytoplasm. The

enzyme has been shown to be active in the light and inactive in the dark. This light activation is accomplished by the ferredoxin-thioredoxin system of chloroplasts. We have purified the NADP-dependent MDH using acid and $(\text{NH}_4)_2\text{SO}_4$ precipitation, gel-filtration, ion exchange and affinity chromatography. The enzyme has a mol.wt of approximately 96,000 daltons as determined by gel-filtration and consists of 2 equal subunits as indicated by a single band of mol.wt 43,000 daltons found with SDS gel-electrophoresis. Its isoelectric point is in the range of pH 5.25–5.35. The specific activity, after complete activation in vitro with dithiothreitol and thioredoxin was 118 U/mg, the K_m for oxaloacetate was 10^{-5} M and the pH optimum for activation and activity was 7.9.

Thermostability and primary structure of 3-allelic forms of *Neurospora* tyrosinase

Ch. Rüegg, D. Ammer and K. Lerch, Biochemisches Institut der Universität Zürich, Zürichbergstrasse 4, CH-8028 Zürich

The allelic forms of tyrosinase isolated from 3 wild type strains of *Neurospora crassa* (TL, TS and Sing) have the same specific activity (1200 ± 100 U/mg) and Arrhenius activation energy (12.0 ± 0.1 kcal M^{-1}). The 3 forms, however, differ in electrophoretic mobility and in the Arrhenius activation energy of heat inactivation (80 kcal M^{-1} for TL, 107 for TS and 106 for Sing). The amino acid sequences of the 3 enzymes are identical with the exception of: Asn₂₀₁ (TL) \rightarrow Asp₂₀₁ (TS); Asn₂₀₁ (TL) \rightarrow Asp₂₀₁ (Sing), Val₁₂₉ (TL) \rightarrow Thr₁₂₉ (Sing), Ile₃₇₀ (TL) \rightarrow Thr₃₇₀ (Sing). It is noteworthy that in both thermostable enzymes asparagine residue 201 of the thermolabile form TL is replaced by an aspartate. It is proposed that this aspartate causes the increase in thermostability by forming an intramolecular salt bridge to a positively charged group. The pH-dependency of the heat inactivation rates has an apparent pK of 6.6 suggesting a histidine residue as the most likely counterion for the carboxylate group of Asp₂₀₁.

Study of agents effective in solubilizing opiate receptors

U.T. Rüegg, E.J. Simon, J.M. Hiller and B.W. Fulpius, Department of Biochemistry, University of Geneva, Sciences II, CH-1211 Geneva 4, and Department of Medicine, New York University, New York, NY 10016, USA

Opiate receptors are membrane-bound proteins. They have been solubilized as receptor- ^3H etorphine complex by the nonionic detergent Brij 36T (Simon et al., Science 190, 389, 1975). Using rat brain membranes and a gel-filtration assay for detection of solubilized species, we have studied the effectiveness of other detergents to solubilize opiate receptors as active complex. Up to 60% solubilization of this complex was obtained with digitonin, deoxycholate and Triton X-114 at concentrations above the CMC. Crude bee venom 6 mg/ml was also effective in this respect, but only partially (20–25%) although none of its constituents (hyaluronidase, phospholipase A₂, melittin) used alone was active. Melittin (0.3 mg/ml) together with phospholipase A₂ solubilizes up to 86% of the receptor. According to the well-documented synergism of action of these 2 polypeptides, it is proposed that they release endogeneous lysophosphoglycerids which act then as detergents. This interpretation is supported by the action of exogenously added L- α -lysophosphatidylcholine (0.8%) which gives a similar degree of solubilization. The opiate receptor solubilized as radioactive complex has an apparent mol.wt of 450,000–500,000 as tested by gel-permeation chromatography.

Mitochondrial aspartate aminotransferase 27/32-410: partially active enzyme derivative produced by limited proteolytic cleavage of native enzyme

E. Sandmeier, Biochemisches Institut der Universität Zürich, CH-8028 Zürich

The N-terminal segments of the 2 polypeptide chains of aspartate aminotransferase (AATase) are located in exposed position (J. molec. Biol. 133, 161, 1979) and thus are potential targets for proteolytic attack. Treatment of the native enzyme (from chicken) with trypsin cleaves selectively the peptide bond after Arg 26 or after Lys 31, producing 2 shortened enzyme derivatives, AATase 27-410 and AATase 32-410. The split-off N-terminal peptides are spontaneously released. The molecular activity of AATase 27/32-410 is about 3% of that of the native enzyme. The K_m -values for aspartate and 2-oxoglutarate are unchanged, indicating an unaltered geometry of the binding site. A markedly diminished syncatalytic response of the reactivity of Cys 166 toward 5,5'-dithiobis-(2-nitrobenzoate) suggests that the decrease in catalytic activity is due to an interference with syncatalytic conformational changes observed previously to occur in AATase (J. biol. Chem. 253, 3158, 1978).

Binding of dantrolene sodium to sarcoplasmic reticulum and mitochondria

C. Sengupta and E. Carafoli, Biochemical Institute, ETHZ, CH-8092 Zürich, and Division of Clinical Pharmacology, University Hospital, CH-8091 Zürich

Dantrolene sodium (Dan) is a muscle-relaxing agent which seems to act primarily on intracellular membrane targets in skeletal muscle. Dan is particularly effective in the treatment of the Malignant Hyperthermia muscle disorder. We have measured the binding of ^{14}C -labelled Dan to pig heart and skeletal muscle sarcoplasmic reticulum (SR) and skeletal muscle (*M. gracilis*) mitochondria. The method used has been equilibrium dialysis. The results show that SR from skeletal muscle has 2 classes of binding sites for Dan. The high affinity class contains 6 pmoles/mg protein binding sites with a K_D of 5 nM. The low affinity class has 33 nmoles binding sites/mg protein with a K_D of about 10 μM . SR from heart has only the low affinity binding sites (0.8 nmoles/mg protein, K_D about 2.5 μM). Skeletal muscle mitochondria possess only low affinity binding sites (1.2 nmoles/mg protein, K_D about 2 μM). These data are consistent with the hypothesis that Dan acts on SR of skeletal muscle only. Moreover they have permitted to demonstrate a clear difference between SR from heart and skeletal muscle.

Zwitterionic dipoles as a dielectric probe for investigating head group mobility in phospholipid membranes in the presence of cholesterol

J. C. W. Shepherd and G. Büldt, Abteilung Biophysikalische Chemie, Biozentrum, Klingelbergstrasse 70, CH-4056 Basel

For phospholipid membranes with zwitterionic head groups, the dipole can be considered as a specific label for tracing the changes in the dynamic behavior of this region of the bilayer in its various phases. Measurements of the dielectric properties of fully hydrated 1,2-dipalmitoyl-*sn*-glycero-3-phosphocholine bilayers in the frequency range 1–50 MHz show a dispersion which is attributed to the motion of the phosphocholine dipoles in the plane of the bilayers. When cholesterol is added the abrupt change in the derived relaxation frequency f_0 observed for pure DPPC at the gel-to-liquid crystalline phase transition at 42°C reduces to a more gradual increase of frequency with

temperature as the cholesterol content is increased. In general the presence of cholesterol increases the DPPC head group mobility due to its spacing effect. Above 42°C, however, an initial decrease in f_0 at cholesterol content up to 20–30 moles 0/0 is found.

Comparison of mouse brain development in vivo and in cell cultures

H. P. Siegrist, L. Sandru, T. Burkart, U. Wiesmann and N. Herschkowitz, Department of Pediatrics, University of Bern, CH-3010 Bern

In order to study, whether dissociated mouse brain cell cultures can serve as a model for early brain development in vivo, we compared several metabolic activities of oligodendrocytes in the first 28 days of life in vivo and in culture. As a parameter of myelin lipid synthesis, the activities of either cerebroside-sulfotransferase and β -hydroxy- β -methylglutaryl-coenzyme A reductase, which is the rate limiting enzyme for cholesterol synthesis, were measured. As a monitor for oligodendroglial membrane development, cyclic nucleotide phosphohydrolase activity was determined. The sequential timing of the different enzyme activities in respect to the turning on, peak activity and turning off of the in vivo development closely fits the development in culture. This indicates that important enzyme activities involved in myelination are mainly regulated by intrinsic factors of oligodendrocytes.

Bacteriorhodopsin: identification of the phenylisothiocyanate-binding site and cross-linking by p-azidophenylisothiocyanate

H. Sigrist, N. G. Abdulaev, M. Yu. Feigina and P. Zahler, Institute of Biochemistry, University of Bern, CH-3012 Bern, and Shemiakyn Institute of Bioorganic Chemistry, Moscow, USSR

The hydrophobic probe phenylisothiocyanate interacts covalently at a single specific site in bacteriorhodopsin: Lysine 215 (Nomenclature FEBS Lett. 100, 219, 1979). The phenylisothiocyanate-binding site is not blocked by the polar analog p-sulfophenylisothiocyanate. The modification is therefore concluded to occur in a hydrophobic membrane domain. Preincubation of purple membranes with the apolar cross-linker p-azidophenylisothiocyanate reduces phenyl[^{14}C]isothiocyanate incorporation significantly. Since p-azidophenylisothiocyanate competes for the unique phenylisothiocyanate-binding site in bacteriorhodopsin, the probe can be qualified as a site-specific, hydrophobic, heterobifunctional photosensitive cross-linker. Photoactivation of the covalently-bound cross-linker results in the formation of homopolymers.

Reconstitution of the chloroplast DCCD-binding proteolipid serving to translocate protons

K. Sigrist-Nelson and A. Azzi, Medizinisch-chemisches Institut, Universität Bern, Postfach, CH-3000 Bern 9

The butanol-solubilized DCCD-binding protein was reconstituted in a liposomal system. Proton conducting activity of K^+ -loaded vesicles was monitored by 9-amino acridine fluorescence in the presence of valinomycin. Proteolipid vesicles rapidly conducted protons. Proton conduction was inhibited by addition of DCCD but not its water-soluble analog EDC. – Proton uptake into the proteolipid K^+ -loaded vesicles was also measured potentiometrically with a pH electrode. Upon addition of valinomycin external alkalization occurred, indicating movement of protons.

Proton translocation from the vesicle interior occurred after addition of K^+ to the external medium and generation of a membrane potential with valinomycin. A lack of directionality for the proton translocation process is thereby implied. - Neither addition of CF_3 nor limited protease digestion appeared to affect conduction properties. However, chemical modification of tyrosine with tetranitromethane and lysine with phenylisothiocyanate markedly reduced proteolipid-mediated proton translocation.

Crystallographic studies on liver-fluke hemoglobin

J. D. G. Smit, *Laboratorium für Biochemie I der ETH, CH-8092 Zürich*

Monomeric liver-fluke (*Dicrocoelium dendriticum*) hemoglobin is the evolutionary oldest globin-fold known to date. Crystals of the CN-Met form of this hemoglobin have been grown from polyethylene glycol 2000 solutions, containing 0.1 M potassium acetate and 5 mM KCN at pH 4-5. 2 crystal forms have been obtained: a) hexagonal, $P6_3$ or $P6_4$, $a=b=91.5$ Å, $c=28.3$ Å, $\gamma=120^\circ$, $Z=6$; b) triclinic, $P1$, $a=37.1$ Å, $b=39.95$ Å, $c=49.0$ Å, $\alpha=88.8^\circ$, $\beta=76.8^\circ$, $\gamma=64.6^\circ$, $Z=2$. The triclinic form has been selected for crystallographic studies because its diffraction pattern extends well beyond 2.2 Å $^{-1}$ and irradiation damage is low. Spectroscopic evidence for the triclinic crystals shows that in the presence of cyanide the molecules are still CN-MetHb at a pH as low as 4.5. Data to 3.3 Å $^{-1}$ have been collected on an Enraf-Nonius CAD-4 4-circle diffractometer and used to determine the shortest distance (about 29 Å) between iron atoms. - Structure determination by the molecular replacement technique is in progress.

Localization of reaction centers in the chromatophore membrane of the photosynthetic bacteria

Rhodospirillum rubrum

M. Snozzi, E. Odermatt, R. Meyer and R. Bachofen, *Institute of Plant Biology, University of Zürich, Zollikerstrasse 107, CH-8008 Zürich*

Reaction centers were extracted from the membrane with the detergent LDAO. The isolated pigment-protein-complex consists of 3 protein subunits. Iodination of chromatophores with lactoperoxidase showed that only the largest protein subunit (H) is exposed to the cytoplasmic side of the membrane, whereas the 2 smaller subunits (M+L) were buried in the lipid bilayer. This orientation is confirmed by a hydrophobic labelling with the photoactive marker I^{125} -5-iodonaphthyl-1-azide (INA). Besides labelling of the subunits L and M INA binds preferentially to the pigments, suggesting a lipophilic environment and a good reactivity of these functional lipids. - Freeze etch micrographs of chromatophores show particles on the outer fracture faces. The density of these particles decreases after partial extraction of the reaction centers. Liposomes with incorporated reaction centers showed similar structures, suggesting that the particles seen in intact membranes are the reaction center complexes.

Effect of glucose on carbohydrate synthesis from lactate or alanine in hepatocytes from fasted rats

K. Solanki, F. Nyfeler, U. Moser and P. Walter, *Biochemisches Institut der Universität Basel, Vesalianum, Vesalgasse 1, CH-4051 Basel*

The effect of glucose on the incorporation of labelled alanine or lactate into glucose and glycogen was measured in hepatocytes from fasted rats. 10 mM glucose suppressed

incorporation of 2 mM alanine into glucose + glycogen by more than 40%, whereas no inhibition was observed with lactate as substrate. At higher concentrations of glucose (20-30 mM), the incorporation of lactate into glucose + glycogen was also weakly inhibited. Addition of fructose instead of glucose gave similar results whereas glycerol had no effect. The glucose effect was rapid (15 min) and was not due to isotope dilution of gluconeogenic precursors generated by increased glycolysis. The inhibitory effect of glucose on carbohydrate synthesis from alanine could be confirmed in experiments without isotopes in which net changes of glucose and glycogen were measured.

Investigations on the primary structure of bovine plasminogen

J. Schaller, P. G. Lerch, P. W. Moser, K. Bill and E. E. Rickli, *Institut für Biochemie, Freiestrasse 3, CH-3012 Bern*

The polypeptide chain of bovine plasminogen (mol.wt approx. 90,000) was cleaved with CNBr. Using column chromatographic methods the NH_2 -terminal fragment (57 amino acids), a tripeptide, a dodecapeptide, a nonadecapeptide and a fragment originating from the $COOH$ -terminal half of the light chain (115 amino acids) were separated from the bulk of disulfide-bridged fragments. This latter fraction, after reduction and carboxamidomethylation yielded another 8 fragments in the mol.wt range 2000-20,000 daltons. The fragmentation pattern differs from that of human (and porcine) plasminogen due to a different distribution of Met-residues. The purified fragments were characterized by partial NH_2 -terminal and $COOH$ -terminal sequence analysis using the automated Edman method and solid-phase techniques, respectively. These data compared with the known primary structure of human (and porcine) plasminogen allowed the assignment and localization of the CNBr-fragments within the bovine plasminogen polypeptide chain. Besides homologous regions the partial sequence of bovine plasminogen shows distinct differences from the primary structure of human (and porcine) plasminogen.

Plasma levels of peptide hydrolases and protease inhibitors reflect activity of adjuvant-induced inflammatory disease in the rat

H. P. Schnebli, *Pharmaceuticals Division, Ciba-Geigy Ltd, CH-4002 Basel*

Both during the primary (localized) inflammation and the development of the secondary (generalized) inflammation in adjuvant-treated rats, the plasma level of functional α -macroglobulins increases while proteases (measured as peptide hydrolases) sharply decrease. The decreased peptide hydrolase levels during episodes when protease 'spillage' into the bloodstream is elevated, suggests a more rapid clearance of α -macroglobulin-protease complexes associated with inflammation.

Effect of low pH on anticomplementary activity (AA) of IgG

E. Schneider, T. Borsos and H. Isliker, *Université de Lausanne, CH-1011 Lausanne, and National Cancer Institute, Bethesda, MD, USA*

Human IgG (Cohn fraction II) contains aggregates which produce severe clinical reactions when given i.v. to patients

with agammaglobulinemia. This is attributed to the complement activating properties of these aggregates. The untoward effects can be avoided if the IgG is previously exposed to pH 4 at 37°C for 6 h. We have begun a systematic study of IgG aggregates and the conditions for reversing their AA. As a model, rabbit IgG was pretreated at pH 7.4, 4.0, 3.5 and 3.0 followed by dioxan aggregation at neutral pH. Lowering of the pH led to a 3-fold loss of C2 consumption in guinea-pig serum relative to the amount of C1 bound. Thus, a significant part of C1 may become fixed to IgG exposed to low pH without being activated. When IgG was first dioxan-aggregated and then treated at low pH, AA was also lost. Although low pH values abolish AA of aggregated IgG, the same procedure will only partially decrease activation of complement by immune complexes, as measured by the hemolytic activity of rabbit anti-Forssman IgG.

Introduction of alkylaminogroups into surface glycoproteins for the nearest neighbor analysis by cross-linkers

E. Schweizer, W. Angst and H.U. Lutz, Department of Biochemistry and Organic Chemistry, ETH Zürich, CH-8092 Zürich

Cross-linking experiments with bifunctional reagents failed to give information on the spatial arrangement of sialoglycoproteins in human RBC. A reason for this failure could be the lack of accessible alkylamino groups. We have developed a method to introduce amino groups into glycoproteins in situ. Upon oxidation of the sialyl residues by periodate, a ^{14}C -arylalkyldiamine forms a Schiff base that is trapped in the reduced state for substantial modification. The alkylamino group does not react and is available for cross-linking. At pH 6.4 and 4°C the proteins of intact RBC are modified to an extent of 2 $\mu\text{C}/\text{mg}$ protein (50% label incorporated). By means of SDS PAGE and fluorography the label was found primarily in sialoglycoproteins. Proteins from the cytoplasmic side were not labelled. Other components were labelled, among them the bands assigned to ankyrin. Cross-linking studies with DTSP suggest these proteins to be cross-linked to glycophorin A.

Detection of peptides and basic proteins in polyacrylamide gels

Germaine Steck, P. Leuthard and R.R. Bürk, Research Department, Pharmaceutical Division, Ciba-Geigy Ltd, CH-4002 Basel

A new method is described, that allows detection of low mol.wt and basic proteins and polypeptides not retained in polyacrylamide gels by standard acid fixation procedures. Using standard acid conditions certain of these proteins remain soluble or, if precipitated, are solubilized again during staining or destaining of the gel. In contrast to the acid fixation we use formaldehyde to covalently link proteins and polypeptides to the polyacrylamide gel. Testing this new method with a variety of gel systems and proteins, we showed that all the proteins seen in the standard method were retained, but additionally also low mol.wt and basic proteins and polypeptides that were lost in the standard systems, are observed. The formaldehyde method is therefore suitable to detect these substances in polyacrylamide gels.

Thermodynamic buffering by adenylate kinase and creatine kinase

J. W. Stucki, Pharmakologisches Institut, CH-3010 Bern

A theory of oxidative phosphorylation based on linear nonequilibrium thermodynamics has been developed to obtain insight into the energetics of oxidative phosphorylation in vivo. The efficiency of oxidative phosphorylation is maximal if the conductance of ATP utilizing loads L_1 is related to the conductance of phosphorylation L_p according to the condition of conductance matching: $L_1/L_p = \sqrt{1 - q^2}$, where q is the degree of coupling of oxidative phosphorylation. In the cell L_p and q can be assumed as being constant during short-time intervals whereas L_1 fluctuates. Consequently oxidative phosphorylation would hardly ever operate at maximal efficiency in vivo. However, in the presence of fluctuating loads, the reversible reactions catalyzed by adenylate kinase and creatine kinase were found to buffer the phosphate potential near the value permitting maximal efficiency of oxidative phosphorylation. This experimental observation has been generalized to the concept of a new bioenergetic regulatory principle called thermodynamic buffering.

A procedure for transferring proteins from polyacrylamide gels to nitrocellulose sheets and their immunological detection

H. Towbin, T. Staehelin, J. Gordon and H. Weideli, Friedrich-Miescher-Institut, Postfach 273, CH-4002 Basel, and Pharmaceutical Research Department, Hoffmann-La Roche & Co. Ltd, CH-4002 Basel

We devised a novel procedure for the electrophoretic transfer of proteins from various conventional polyacrylamide slab gels to sheets of nitrocellulose. Transfer proceeded without loss of resolution, took ca. 1 h and yields ranged between 30% and 100% depending on protein and gel system. After blocking excess binding capacity, proteins on the nitrocellulose sheet could be detected by immunological methods. The sheet was incubated with antibody containing solution and then with a 2nd, labelled antibody. This was either radioactively labelled or coupled to peroxidase. Antigen was thus revealed by autoradiography or by the colored insoluble peroxidase reaction product. This method was applied to screening hybridomas secreting antibodies against eukaryotic ribosomal proteins.

Assembly of the first component of complement C1 from its subcomponents Clq,Clr and Cls and mode of IgG binding

J. Tschopp, W. Villiger, H. Fuchs, E. Kilchherr and J. Engel, Department of Biophysical Chemistry and Department of Microbiology, Biozentrum, University of Basel, CH-4056 Basel

In the presence of Ca^{++} both zymogens form dimers $(\text{Clr})_2$ and $(\text{Cls})_2$ with mol.wts $M=170,000$ as revealed by sedimentation equilibrium. When Ca^{++} is removed by EDTA $(\text{Cls})_2$ dissociates into monomer ($M=85,000$) but $(\text{Clr})_2$ persists. The chain weight in 5 M Gu·HCl is 85,000 in both cases. Both dimers have an elongated shape. The sedimentation constants $s_{w,20}$ and the axial ratios a/b are 6.7 S and 8.9 for Clr and 5.8 S and 14.2 for Cls. When mixed in the presence of Ca^{++} Clr and Cls form a complex $[(\text{Clr})(\text{Cls})]$ with $M=340,000$. This complex associates with Clq to $\text{Clq}[(\text{Clr})_2(\text{Cls})_2]$ ($M=760,000$, $s_{20,w}=16.2$ S, $D_{20,w}=1.75 \times 10^{-7} \text{ cm}^2 \text{ sec}^{-1}$). Higher ratios of the zymogens to Clq were also formed probably due to a dimerization tendency of $(\text{Clr})(\text{Cls})_2$. In electron micrographs Clq had the normal

appearance of 6 heads connected by collagen stems. For Cl consistently 9–10 globular domains were seen per molecule. This is tentatively interpreted by a binding of $[(\text{Cl})_2(\text{Clr})]_2$ in the region of the Clq heads. Pictures of IgG dimers and dimers bound to Clq clearly revealed that binding of IgG takes place at the heads of Clq.

Antigen-independent binding and activation of the first component of complement C1 by IgG oligomers

J. Tschopp, K. Wright, J.-C. Jaton and J. Engel, Department of Biophysical Chemistry, Biozentrum, University of Basel, CH-4056 Basel, and Département de Pathologie, Université de Genève, CH-1211 Genève 4

Rabbit anti-SII pneumococcal polysaccharide IgG was cross-linked by dithiobis (succinimidyl propionate). The purified oligomers fixed complement with decreasing binding constants K in the order tetramer ($K = 10^9 \text{ M}^{-1}$), trimer ($K = 10^7 \text{ M}^{-1}$), dimer ($K = 10^6 \text{ M}^{-1}$). From the concentration dependence of the weight average mol.wt of mixtures of the subcomponent Clq and $(\text{IgG})_2$ it followed that 3 dimers can be accommodated at the Clq molecule. The value of K was again 10^6 M^{-1} . The subcomponents Clr and CIs in reconstituted C1 were activated by IgG oligomers in a sequential mechanism. The rate of activation increased with increasing oligomers size and paralleled the increase of the binding constants. Both binding and activation were independent of the ligandation of the antigen-binding site in IgG protomers with a specific SII nonasaccharide. The findings are at variance with an antigen-induced allosteric mechanism for the action of antigen in the activation of C1 by IgG-clusters. They support the association model according to which a multifunctional antigen acts by cross-linking several IgG monomers.

Activation volumes ΔV^\ddagger for the rotational flips of internal aromatic rings in globular proteins, determined by high resolution 360 MHz ^1H NMR at variable pressure

G. Wagner, Institut für Molekularbiologie und Biophysik, ETH, CH-8093 Zürich

High resolution 360 MHz ^1H NMR at variable pressure was used to measure activation volumes ΔV^\ddagger for the flipping motions of aromatic rings in the basic pancreatic trypsin inhibitor (BPTI) and cytochrome *c*. All the flip rates which could be measured by NMR decrease with increasing pressure. The positive activation volumes obtained indicate that the dynamic processes manifested in the rotational motion of the aromatic rings is not limited to a local compressible ring environment but involves a transient increase of the total volume of the protein. In a BPTI solution at p^2H 5.2 and 57 °C, activation volumes ΔV^\ddagger of $50 \pm 10 \text{ Å}^3$ and $60 \pm 20 \text{ Å}^3$ were measured for Phe 45 and Tyr 35, respectively. According to the X-ray structure these values correspond approximately to the volume of the atomic groups which occupy the sphere necessary for ring rotation.

Nonequilibrium thermodynamic treatment of mitochondrial processes

D. Walz and J. W. Stucki, Biozentrum der Universität Basel, Klingelbergstrasse 70, CH-4056 Basel, and Pharmakologisches Institut der Universität Bern, Friedbühlstrasse 49, CH-3010 Bern

The fundamental thermodynamic function for a system in which processes do not go along paths of local equilibrium

states' is the so-called dissipation function. It consists of the sum of the products of thermodynamic flows and forces of all processes running in the system but is invariable with respect to the definition of flows and forces as long as their products sum up to the same function. Due to this characteristics, it is possible to define, for each experimental system with given boundary conditions, a set of appropriate flows and forces which are directly related to the experimentally assessable parameters of the system. Using linear flow-force relations, the mutual dependence of these parameters is then worked out which allows to analyze the experimental data in terms of the thermodynamically relevant coefficients such as degree of coupling and phenomenological stoichiometry.

Energetic coupling of ligand binding with conformational fluctuations in dehydrogenases

Z. de Weck and J.H.R. Kägi, Biochemisches Institut der Universität Zürich, Zürichbergstrasse 4, CH-8028 Zürich

The effect of NAD-coenzymes, coenzyme fragments and inhibitors on yeast alcohol dehydrogenase (YADH) and pig-heart lactate dehydrogenase (LDH) has been probed by IR-spectrophotometric measurement of peptide hydrogen-deuterium exchange. Binding of NADH and NAD^+ to the 2 enzymes reduced the average exchange rate of the slowly exchangeable peptide hydrogens by a factor of 2 and 5, respectively. The coenzyme fragments AMP and ADP had an effect on YADH intermediate between NADH and NAD^+ while ADP-ribose was slightly more effective than NAD^+ . An even more pronounced retardation was seen in ternary complexes of YADH with NAD^+ and pyrazole (50-fold) and of LDH with NAD^+ and oxalate (10-fold) or with NADH and oxamate (8-fold). The observations are consistent with the view that both enzymes fluctuate between a variety of conformational substates (conformers) and that ligands alter their distribution by stabilizing conformers which interact with them most firmly. It is proposed that the coenzyme-specific changes of the conformer equilibria serve an important role in optimizing the free energy profile of the redox reactions catalyzed by these enzymes.

A functional arginine residue in NADPH-dependent aldehyde reductase from human liver

B. Wermuth, A. Forster and J.P. von Wartburg, Medizinisch-chemisches Institut der Universität Bern, Bülhstrasse 28, Postfach, CH-3000 Bern 9

NADPH-dependent aldehyde reductase from human liver, a monomeric pyridine nucleotide-dependent dehydrogenase, was reacted with phenylglyoxal and 2,3-butanedione. With both substances inactivation was observed which was dependent on the concentration of the reagent and the time of incubation. In sodium borate buffer pH 7 at 37 °C 10 mM concentrations of both reagents inactivated the enzyme to more than 90% within 60 min. At 25 °C butanedione inhibited the enzyme to about 50%, whereas phenylglyoxal gave only slight inactivation. The presence of 1 mM NADP^+ in the incubation mixture protected the enzyme against loss of activity. NADPH could not be tested because both reagents are good substrates for this enzyme. 1 mM phenobarbital, a noncompetitive inhibitor of aldehyde reductase, gave no protection. Our results suggest that, in addition to lysine residues (Wermuth et al., *BBA* 566, 237, 1979), arginine is present at the binding site of the coenzyme.

Nonallosteric transhydrogenase from *Pseudomonas aeruginosa*

F. Widmer and I. Meyer, Nestlé Research Laboratories, CH-1814 La Tour-de-Peilz

The allosteric transhydrogenase from *P. aeruginosa* (EC 1.6.1.1) acts as an essential link between carbohydrate catabolism and respiratory chain (Widmer and Kaplan, *Biochemistry* 15, 4693, 4699, 1976). The enzyme is a uni-directional catalyst which brings about the reduction of NAD⁺ by NADPH + H⁺. The potential substrate NADP⁺ acts as an allosteric inhibitor, whereas other 2'-P nucleotides are allosteric activators. There are 1 catalytic site and 1 regulatory site per protomer. – We now report the identification of a nonallosteric transhydrogenase isolated from a *P. aeruginosa* strain obtained from a hospital patient. No functional effector site appears to be present, and the catalytic site does not accommodate 2'-P nucleotides. Therefore, this enzyme form only catalyzes hydrogen transfers between NAD(H) and coenzyme analogs lacking the 2'-P group. It never constitutes the totality of the transhydrogenase activity detected in the bacterium, and its physiological role is still unclear. Its occurrence might be due to mutation and/or nutritional constraints.

The cooperative response to Ca²⁺ of myofibrils regulated by troponin C with a single Ca²⁺ site

W. Wnuk and E.A. Stein, Department of Biochemistry, University of Geneva, P.O. Box 78, CH-1211 Geneva 8

The onset of contraction is triggered by binding of Ca²⁺ to troponin C (TN-C) in muscles with actin-linked control. When monitored by tension development or myofibrillar ATPase activity, the response to Ca²⁺ is more sensitive than predicted for noncooperative Ca²⁺ binding to TN-C. This was explained (Weber and Murray, *Physiol. Rev.* 53, 612, 1973) by the presence of multiple Ca²⁺-triggering sites on TN-C (as found among vertebrates): all the sites have to be occupied by Ca²⁺ for activation to take place. Our recent studies on crayfish TN-C show that the latter possesses a single site for Ca²⁺. However, ATPase activity of crayfish myofibrils and of reconstituted rabbit actomyosin with crayfish troponin-tropomyosin displays a cooperative rise with Ca²⁺ concentrations ($n_H \sim 1.4$), as is the case for the rabbit system. Thus protein-protein interactions (probably between actin and myosin) rather than the presence of multiple Ca²⁺-binding sites on TN-C are involved in the cooperative effect of calcium on myofibrillar ATPase.

Regulation of the interaction of F-actin with the actin cross-linking protein filamin: inhibition by tropomyosin

W. Wnuk and J. Lisowski, Department of Biochemistry, University of Geneva, CH-1211 Geneva 8

Filamin-actin interactions are of particular interest for cellular mechanochemistry since they may be involved in microfilament dynamics. We have tested whether and how a physiologically relevant factor, tropomyosin (TM), can control these interactions. Purified filamin from chicken gizzard (smooth muscle), actin and TM from rabbit skeletal muscle were used. In the absence of TM, actin-activated myosin ATPase inhibition by filamin starts and reaches 50% at molar ratios of actin: filamin of 50:1 and 24:1, respectively. When TM is bound to F-actin, the inhibition is considerably weakened: the above ratios become 17:1 and 6:1, respectively. A similar effect of TM has been observed by measurements of sedimentation rates of fila-

min-actin complexes. Studies with radioisotope-labelled proteins will tell whether competition between TM and filamin for actin takes place, or whether inhibition of filamin-actin interactions is brought about exclusively by stabilization of actin filaments by TM.

Bilayers of phosphatidylglycerol. A deuterium and phosphorus NMR study of the polar head group region

R. Wohlgemuth and J. Seelig, Abteilung Biophysikalische Chemie, Biozentrum der Universität Basel, Klingelbergstrasse 70, CH-4056 Basel

The structural properties of the phosphoglycerol polar head group in bilayers of 1,2-dipalmitoyl-sn-glycero-3-phosphoglycerol have been studied with deuterium and phosphorus-31 NMR. For this purpose, 1,2-dipalmitoyl-sn-glycero-3-phosphoglycerol was deuterated chemically or biosynthetically at all 3 segments of the glycerol head group. Both the D- and L-configuration of the glycerol head group have been synthesized and the correct stereochemical configuration of the polar group was verified by an enzymatic assay. The deuterium quadrupole splittings and the phosphorus-31 chemical shielding anisotropy were measured as a function of temperature in the range of 20–60 °C (phase transition temperature 41.5 °C). The spatial anisotropy of motion and the segmental fluctuations of the negatively charged (at pH 7.0) phosphoglycerol are similar to those of the zwitterionic phosphocholine and phosphoethanolamine head group, but differ distinctly from those of phosphoserine which also carries a net negative charge.

DNA in hydrocarbon solvents via reversed AOT-micelles

R. Wolf and P.L. Luisi, Technisch-chemisches Laboratorium, ETH-Zentrum, CH-8092 Zürich

High mol.wt DNA can be solubilized in aprotic solvents such as isooctane with the aid of the anionic surfactant (typically 50 mM) di(2-ethyl-hexyl)sodium sulfosuccinate (AOT) and traces of water (typically 1% v:v). Most probably, the DNA molecule is contained in the water pool of the reversed AOT micelle and thus protected from the organic solvent. Clear solutions are obtained which allow spectroscopic analysis in the far UV-region. Important structural alterations must occur, as apparent from spectroscopic changes. A hypochromic effect at the UV-absorption maximum and a change in ellipticity indicate that a high degree of DNA packaging is present in the micellar system. DNA in reversed micelles could thus be used as a model for the phenomena accompanying the packaging of DNA in natural systems, e.g. in phages. Studies are in progress about the size and form of DNA-containing micelles and about the properties of the water bound to the biopolymer.

Phosphorylation of myelin basic protein: possible effect on permeability of myelin vesicles towards cations

C. Wüthrich and A.J. Steck, ISREC, CH-1066 Epalinges

Membrane vesicles were obtained from bovine myelin membranes by adapting a method used for erythrocyte ghosts. With a light scattering technique it was found that the vesicles behave as osmometers and therefore must be sealed. These vesicles were fractionated on a Ficoll density gradient (d: 1.000–1.065) in 2 main fractions with densities of 1.015 and 1.045. The uptake (trapping) and the release rate of 22 Na⁺ was greatly enhanced in the 'light' vesicle

fraction as compared with the more dense fraction. – It is well established, that the myelin membrane contains an endogenous protein kinase which phosphorylates preferentially the myelin basic protein (mBP) in vivo and in vitro. We found that phosphorylation of mBP is stimulated by Ca^{2+} in the range of 1–10 μM , but not by cyclic AMP. Since phosphorylation of mBP may regulate ionic fluxes through the myelin membrane, we are currently measuring the permeability of the vesicles for Na^+ and Ca^{2+} as a function of the phosphorylation state of mBP. Preliminary results suggest that the phosphorylation of mBP causes a slight decrease in Na^+ -permeability.

Regulation of adenosine 5'-phosphosulfate sulfotransferase by sulfur dioxide in primary leaves of beans (*Phaseolus vulgaris* L.)

H.-R. Wyss and Chr. Brunold, Pflanzenphysiologisches Institut der Universität Bern, CH-3013 Bern

Treatment of *P. vulgaris* with air containing low concentrations of SO_2 decreased the adenosine 5'-phosphosulfate sulfotransferase activity extractable from the primary leaves. The sulfate concentration was increased about 10-fold. – Since cultivation of excised leaves on medium containing high sulfate concentrations gave similar effects, it is concluded that sulfate is involved in the regulation of adenosine 5'-phosphosulfate sulfotransferase.

The phospholipase A_2 activity of the inner mitochondrial membrane

M. Zurini and P. Gazzotti, Laboratorium für Biochemie, ETH-Zentrum, Universitätstrasse 16, CH-8092 Zürich

Rat liver mitochondria are known to possess a phospholipase A_2 (PLA_2) activity which is associated mainly with the outer membrane. However, there is some evidence indicating that the enzyme is also present in the inner membrane (Biochim. biophys. Acta 274, 426, 1972). We report here on studies on the PLA_2 activity of mitoplasts completely freed of the outer membrane. The mitoplasts were prepared by digitonin treatment and sonication of intact mitochondria. At low ionic strength, mitoplasts can hydrolyze endogenous phosphatidylethanolamine at a rate which is almost twice that observed with intact mitochondria. Some of the PLA_2 activity of the inner membrane seems to be 'masked' in intact mitochondria, but becomes exposed upon rupture of the outer membrane. The PLA_2 activity of mitoplasts, measured at low ionic strength, is maximally stimulated by low Ca^{2+} concentrations (ca. 150 μM). Studies with inverted inner membrane vesicles, purified by affinity chromatography on Sepharose 4B-cytochrome *c*, seem to indicate that the enzyme is available also from the matrix side of the inner membrane. Changes in the energy state of mitochondria or mitoplasts do not cause large effect on the PLA_2 activity. However, ATP inhibits it. The inhibitory effect of ATP is due to Ca^{2+} chelation, rather than to stimulation of acylating systems.

ZELL- UND MOLEKULARBIOLOGIE BIOLOGIE CELLULAIRE ET MOLÉCULAIRE CELL AND MOLECULAR BIOLOGY

Ultrastructural characteristics of tuberous electroreceptors in a high frequency electric gymnotid, *Sternarchus albifrons*

K. Akert, C. Sandri and M. V. L. Bennett, Brain Research Institute, University of Zürich, CH-8029 Zürich, and Department of Neurosciences, Albert Einstein College of Medicine, New York, USA

Thin-section and freeze-fracture electron microscopy were applied to the tuberous electroreceptor organs of *S. albifrons*. Special attention was paid to junctional complexes defining extra- and intracellular current pathways, to the organization of neuroreceptor junctions and to the peculiarities of the cover cells which are characterized by a crystalline ER lattice and which seem to form a fluid barrier between external environment and receptor cavity. HRP (horse-radish peroxidase) studies reveal that cover cells take up tracer applied to the skin surface. S.c. injected HRP fails to reach the electroreceptor organ which is protected by an epithelial and neuroendothelial capsule whose cellular components are interconnected by multi-stranded tight junctions.

Glioma-conditioned medium affects ^{14}C -acetate incorporation into cholesterol of neuroblastoma cells

U. R. Andres and D. Monard, Friedrich-Miescher-Institut, Postfach 273, CH-4002 Basel

Serum-free medium conditioned by glioma cells has been shown to induce neurite extension in neuroblastoma cells.

We now present evidence that the same conditioned medium can also reduce the incorporation of ^{14}C -acetate into cholesterol of neuroblastoma cells. In opposite to the neurite extension which is induced by macromolecular factor(s), the de novo synthesis of cholesterol is influenced by low mol.wt substances. High amounts of different lipids, released by glioma cells, are found in the conditioned medium. Unexpectedly, these lipids have little effect on the de novo cholesterol synthesis. Results aiming at the characterization and isolation of this glioma-released substance(s), able to affect the cholesterol pathway, are presented.

Stability and contractibility of the tail sheath of phage T4

F. Arisaka and J. Engel, Abteilung Biophysikalische Chemie, Biozentrum der Universität, Klingelbergstrasse 70, CH-4056 Basel

There are 2 steps in the stabilization of the tail sheath of T4 phage during the formation of the phage particle. After reversible polymerization of P18 to core-baseplates (Arisaka et al., J. molec. Biol. 132, 369, 1979) and before head-tail joining, the tail sheath is reversibly stabilized by gP3 and gP15. These tails which can be isolated from head-deficient mutants (e.g. 23⁻) are not able to contract under conditions at which the sheath in the whole phage is readily contracted. These sheaths tend to dissociate before contraction. Only upon or after head-tail joining, the sheath is irreversibly

bly stabilized by a still unknown mechanism. It was shown that the *wac* protein which forms so-called collar and whiskers is not necessary for irreversible stabilization. The sheath in ghosts and necked tails which are obtained by CsCl osmotic shock can contract and the latter is especially suitable for studying tail contraction.

Sequence analysis of the spacer boundaries in rDNA of different *Xenopus* species

R. Bach, M. Crippa and B. Allet, Département de Biologie animale, 154, rte de Malagnou, CH-1224 Genève, and Département de Biologie moléculaire, 30, quai Ernest-Ansermet, CH-1211 Genève 4

2 independent EcoR₁ rDNA fragments of *Xenopus borealis* and one of *X. clivii* have been cloned and characterized. They contain the whole nontranscribed spacer, the externally transcribed spacer and parts of the 18S and 28S rRNA structural gene. In each case, the nucleotide sequences were analyzed across the 2 ends of the NTS region, with special emphasis on the part precedes the 40S precursor RNA starting site. In parallel, 40S precursor RNA of *X. borealis* was used in 2 types of experiments aimed at locating the putative transcription starting site. One involved specific protection, and the other, specific extension of particular restriction fragments hybridized to 40S RNA. Our results lead to the following conclusions: a) the part of the NTS region that we have sequenced includes repetitive elements which are not arranged regularly, but are interspersed in various combinations; b) in *X. borealis* nucleotide sequences present at the 40S precursor RNA starting site are also present at other locations in the NTS regions; c) although the *X. borealis* and *X. clivii* sequences in the NTS and ETS regions differ extensively from the corresponding *X. laevis* sequences, a short stretch of 13 bp around the 40S starting site is identical in the 3 species.

Plasma membrane differentiation in paramyxovirus morphogenesis

Th. Bächli and M. Büechli, Institute for Medical Microbiology, University of Zürich, CH-8006 Zürich

The process of assembly at the host cell surface of 2 paramyxoviruses, Sendai and Newcastle disease, has been monitored by electron microscopy. Budding of these viruses follows the insertion of viral glycoprotein spikes into the outer and the association of the nonglycosylated membrane (M) protein with the inner lipid leaflet of the plasma membrane. Virus-specific membrane particles arranged in a crystalline array were revealed on both the protoplasmic fracture face (by freeze-fracturing of cells) and on freeze-dried membranes exposing their cytoplasmic surface; this observation suggests an insertion of M-protein into the inner leaflet of the lipid bilayer system. We propose that the recruiting of virus-coded proteins to the site of budding depends on an intramembranal aggregation of M which then interacts with the external spikes and the internal nucleoprotein. The transient nature of this configuration is reflected by a loss of crystalline organization in the envelope membranes of aged virus particles.

Antigenic architecture of the photosynthetic membrane from *Rhodospseudomonas viridis*

B. Baumgartner, E. Wehrli and K. Mühlethaler, Institut für Zellbiologie, ETH, CH-8093 Zürich

The photosynthetically active membranes of *R. viridis* were isolated from the bacterium. The polypeptides of these

thylakoids were fractionated into 2 groups on the basis of their solubility with 2 different detergents. With the nonionic detergent LDAO the reaction centers could be purified from the membranes. Solubilization of the thylakoid membranes with SDS followed by 2 cycles of preparative SDS-polyacrylamide gel-electrophoresis resulted in purified SDS-polypeptide complexes. Isolated proteins were used as antigens and the antibodies obtained characterized by double immunodiffusion assays as well as by 2-dimensional crossed immunoelectrophoresis. To localize these polypeptides within the membranes, thylakoids were adsorbed to glass and labelled with antibodies, using ferritin as marker. Replicas of freeze-dried preparations were viewed in the electron microscope and the results compared with the membrane model proposed by Wehrli and Kübler (in: Proceedings in life sciences, Springer, in press).

An autoradiographic study of Gunn rat thyroid

M. Benathan, J. Fakan, A. Gautier and D. Gardiol, Centre de Microscopie électronique de l'Université et Institut de Pathologie du CHUV, CH-1011 Lausanne

In an earlier study (Benathan et al., Biol. cell. 35, 5a, 1978), analysis of thyroid extracts showed qualitative and quantitative differences in the pattern of iodocompounds derived from Gunn and Wistar rats. We have now examined the localization of sites of ¹²⁵I-labelled molecules by high resolution autoradiography. The isotope was injected i.p. in Gunn rats and animals sacrificed after 1 or 8 days. At 1 day, label is found concentrated in the follicular lumen and colloid droplets; in certain cases the labelling was more marked in the periphery of the colloid than in the central region which supports the hypothesis that thyroglobulin is iodinated in the apical zone. At 8 days, labelling in colloid is strongly decreased. However, appreciable label is found in the dense matter, typical of Gunn rats, situated in the lumen. These results suggest that in the Gunn rat there exist 2 separate metabolic pools of iodinated molecules.

Stop codons of eukaryotic messenger RNAs

M. Bienz, H. Grosjean, J. Kohli and E. Kubli, Zoologisches Institut der Universität Zürich, CH-8057 Zürich

Simultaneous injection of mouse β -globin mRNA (opal stop codon) and tRNA^{Ser}_{opal} suppressor (*S. pombe*) into *Xenopus laevis* oocytes with subsequent radioactive labelling produces a read-through protein as demonstrated by 1-d PAGE. An analogous result is obtained by injecting TMV-RNA together with either tRNA^{Tyr}_{amber} (*S. cerevisiae*) or tRNA^{Tyr}_{ochre} (*S. cerevisiae*) suppressors. Hence, the stop codons of an mRNA can be read by the corresponding yeast suppressor tRNAs in *X. laevis* oocytes leading to a read-through product. These results raised the possibility of measuring the frequency of the 3 stop codons UAG, UAA and UGA in *X. laevis* oocyte mRNAs. The oocytes were injected with the above mentioned suppressor tRNAs and after incubation in [³⁵S]-methionine the proteins were extracted and separated on 2-d O'Farrell PAA-gels. Injection of suppressor-tRNA produces read-through proteins from the oocyte mRNAs leading to either a shift or a deletion of a protein on the 2-d gel (i.e. a change) in comparison with the control gels. Looking at 150 strong spots, it was seen that 14 showed a change after amber, 17 after ochre and 23 after opal suppressor-tRNA injection. 9 changes are shared by amber and ochre suppressor-tRNA injections, suggesting that some of the ochre changes are a result of UAG suppression due to wobble. From this it follows that all 3 stop codons are used in *X. laevis* oocyte mRNAs with a clear predominance of opal codons.

Myosin isoenzymes in human skeletal muscle. Gel-electrophoretic analysis of in vitro labelled single fibres

R. Billeter, C. W. Heizman and E. Jenny, Institut für Pharmakologie und Biochemie, Universität Zürich, CH-8057 Zürich

Until now an unambiguous assignment of the different isoenzymic forms of myosin to the 4 (I, IIA, IIB, IIC) fibre types was not possible. Therefore, a more comprehensive approach was chosen. Single fibres (m.vastus lat.) were dissected out of freeze-dried biopsies and first typed by staining for their myofibrillar ATPase. The fibres (1–3 µg dry weight) were then [¹⁴C]-labelled in vitro and the proteins separated by 2-dimensional gel-electrophoresis. With this method the light chains can clearly be resolved. In addition, the myosin isoenzymes were separated on native pyrophosphate gels. The results obtained until now suggest that the myosin composition of single fibres can be analyzed.

Characterization of a ribosomal in vitro transcription system from *Physarum polycephalum*

G. Bindler, T. Seebeck and R. Braun, Institut für allgemeine Mikrobiologie der Universität, CH-3013 Bern

rDNA in *Physarum* exists as a homogeneous population of linear, extrachromosomal and palindromic molecules of 57.5 kb. 2 sets of genes (19S, 5.8S, 26S rRNA) are located symmetrically at the end of each molecule. This rDNA can be isolated in the form of a transcriptionally active deoxyribonucleoprotein particle (rDNP) with polymerase I as the sole active RNA polymerase. The in vitro transcription on the rDNP by the endogenous RNA polymerase I is asymmetrical. Using rDNA restriction fragments it was possible to roughly localize the starting and termination points of the in vitro transcribed RNA. In the presence of heparin, transcription proceeds further outwards on the rDNA, suggesting the elimination of termination factors.

Alternating fibronectin fibres and focal contacts at the attachment surface of human fibroblasts

Carmen Birchmeier, T. E. Kreis, K. H. Winterhalter, H. M. Eppenberger and W. Birchmeier, Institut für Zellbiologie, ETH-Hönggerberg, and Laboratorium für Biochemie I der ETH, CH-8092 Zürich

The patterns of both fibronectin (LETS, CSP) fibres and focal contacts, as viewed by fluorescence and reflection contrast microscopy, respectively, has been compared in freshly plated WI-38 human fibroblasts. These 2 patterns were similar in some aspects such as the overall direction of both structures. However, focal contacts did generally not contain fibronectin and furthermore, the fibronectin fibres were often seen to alternate with the focal contacts. In contrast, overlap was observed between focal contacts and the endings of actin or α -actinin containing stress fibres.

70S polysomes bound to thylakoid membranes of *Chlamydomonas reinhardtii*

R. Bolli, L. Morgenthaler-Mendiola and A. Boschetti, Institut für Biochemie, Universität Bern, Freiestrasse 3, CH-3012 Bern

With the aim to localize the synthesis of thylakoid-membrane proteins we isolated thylakoid-bound 70S polysomes. The isolation was achieved in 3 main steps: 1. Fixation of chloroplast polysomes at the membrane with chloramphenicol and degradation of cytoplasmic polysomes with

MDMP. 2. Isolation of a fraction of stripped chloroplasts on a Percoll step gradient. 3. Release of the bound polysomes with Triton X-100. The polysomes were 95% of chloroplast origin and active in puromycin reaction in vitro.

Activation of macrophages by soluble factors: IV

Y. Buchmüller and J. Mauël, Institut de Biochimie, CH-1066 Epalinges

Mouse peritoneal macrophages are able to destroy intracellular *Leishmania enriettii* parasites, upon activation with activating factor(s) (AF) released by Con A-stimulated spleen cells (*Experientia* 33, 814, 1977). The ability of activated macrophages to kill intracellular parasites is lost when cells are treated with 2 inhibitors of peroxidase, trypan blue and aminotriazole, and is increased by the addition of exogenous horseradish peroxidase (HRP). *L. enriettii* are destroyed when incubated with a mixture containing hydrogen peroxide, HRP and iodide. These results and others previously presented (increased superoxide production and hexose monophosphate shunt in activated cells [*Experientia* 35, 958, 1979, and *Experientia* 34, 935, 1978] suggest that hydrogen peroxide is involved in intracellular *L. enriettii* destruction by activated mouse macrophages.

Molecular cloning of cellular unintegrated DNA forms of mouse mammary tumor virus (MMTV)

E. Buetti, B. Groner, N. Hynes and H. Diggelmann, Institut Suisse de Recherches Expérimentales sur le Cancer, Chemin des Boveresses, CH-1066 Epalinges

Circular unintegrated MMTV DNA was extracted from the soluble nuclear fraction of the MMTV-infected rat hepatoma cell line HTC-M1. The linear 90–10 kb molecules produced by restriction digestion at the unique EcoRI site were isolated by preparative agarose gel-electrophoresis and cloned in λ gtWES. 6 clones were identified with MMTV cDNA (0.025% of total) which contained MMTV DNA of homogeneous length: approximately 10 kb (2 clones) or 9 kb (4 clones), corresponding to the 2 size classes of circular unintegrated molecules present in infected HTC cells. – Linear unintegrated MMTV DNA from the cytoplasm of the same cells was digested with Pst I and internal fragments were inserted into the Pst I site of the plasmid pBr 322. A recombinant plasmid was obtained which contained the largest (4 kb) internal Pst I fragment of MMTV DNA. – Restriction analysis and infectivity studies with these cloned DNA's are in progress and will be presented.

3-Dimensional structure of the adenoviral coat protein hexon at 2.9 Å resolution

R. M. Burnett, G. Grütter and Janice L. White, Biozentrum der Universität Basel, CH-4056 Basel

The icosahedral adenovirus shell is formed from 240 trimeric hexons at the faces and 12 pentons and fibres at the vertices. X-ray crystallography has been used to calculate electron-density maps from which the molecular envelope has been determined, and the polypeptide chain is being traced. Hexon has a solid pseudo-hexagonal 'base' and a less dense triangular 'top'. The hexagonal shape of the base permits packing of hexons to form the flat continuous surface seen on a face of the viral capsid. Long stretches of the chain, comprising over 80% of the 1050 amino acids in the hexon subunit, have been traced, and are currently being correlated with the chemical sequence. The flat faces of the hexon base, involved in hexon-hexon interactions, are composed of beta-sheet, but there is little other secondary structure.

Early adaptive response of pulmonary parenchyma after bilobectomy in the rat

P. H. Burri, L. C. Berger and H. B. Pfrunder, *Anatomisches Institut der Universität Bern, Bülhstrasse 26, CH-3000 Bern 9*

45 days after resection of 25% of the lung volume the remaining lung had fully compensated for the tissue loss (Burri and Sehovic, 1979). In order to analyze the timing of this adaptation we removed the right upper and middle lobes of rats aged 23 days and investigated the rest lung morphologically and quantitatively on the postoperative days 1, 4, 6, 9, 12, 18 and 30. Sham-operated and normal animals served as controls. On the first day after surgery the volume of the lungs was close to normal. Until day 6 they contained more air, the scanning pictures revealing large alveolar ducts on day 1 and larger alveoli on day 4. During the first week tissue volume increased steadily so that on days 9 and 12 lung morphology and all the quantitative lung parameters were back to normal. On day 18 a slight but significant backlog in lung volume and tissue mass was again detected. These findings indicate: the pulmonary parenchyma readapts rapidly and efficiently after tissue loss, but this effort may disturb the normal growth phases.

Advances in specimen preparation for electron microscopy. I. Novel low-temperature embedding resins and a reformulated Vestopal

E. Carlemalm, W. Villiger and J. D. Acetarin, *Department of Microbiology, Biozentrum der Universität Basel, CH-4056 Basel, and Ecole d'Application des Hauts Polymères, Strasbourg, France*

Embedding procedures using ethylene glycol or methanol at very low temperatures ($\sim -40^\circ\text{C}$) in conjunction with a polar embedding resin, usable at such temperatures, promise to preserve molecular details to at least 20 Å. We have constructed 2 embedding media and reformulated Vestopal. The new resins are polyester- and methacrylate-based polymers with variable fusion temperatures (-10°C to -50°C) dependent on the cross-linker used. These resins appear to have good stability during electron irradiation. Tests show that they are also usable for low-temperature embeddings. The specimen preservation with our low-temperature embedding method has been tested on protein crystals, cellular inclusions and other systems (see II, III and IV). – The new Vestopal formula, which improves the sectioning quality, is the mixture (for medium hardness): (17.5:82.5) Vestopal 120/Vestopal 310 (Chemische Werke, Hüls, Federal Republic of Germany), UV-cured (360 nm), with 0.6% Benzoin methylether, as initiator, at -20°C to $+25^\circ\text{C}$. The hardness is varied by changing the content of Vestopal 120 (0–20 parts); a higher content gives harder blocks.

Renin immunoreactivity in pituitary somatotrophs

M. R. Celio and T. Inagami, *Anatomisches Institut der Universität, Gloriastrasse 19, CH-8006 Zürich, and Department of Biochemistry, Vanderbilt University, Nashville, USA*

Renin is synthesized in the kidneys by the cells of the juxtaglomerular complex and catalyzes the first step in the formation of Angiotensin II (A II) from Angiotensinogen. – Renin activity has been demonstrated biochemically in various other organs particularly in submaxillary gland, brain and pituitary. Using affinity chromatography purified antibodies against mouse submaxillary gland renin we detected specific renin immunoreactivity occurring selectively in a peculiar cell population of the mouse anterior pituitary lobe. – These cells proved to be somatotrophic

cells as revealed by sequential staining of consecutive semithin epon sections with antirenin antibodies and anti-growth hormone antisera. – Pituitary renin could take part in the production of locally active A II. However, together with various indications from biochemical studies, our results are also compatible with the hypothesis of an active intervention of renin in the biosynthesis of growth hormone.

Actin-depolymerizing factor: purification and partial characterization

C. Chaponnier and G. Gabbiani, *University of Geneva, Department of Pathology, CH-1211 Geneva 4*

Immunofluorescent staining of cultivated fibroblasts or epithelial cells and of frozen sections of various organs (e.g. liver and skin) with human anti-actin antibodies results in different staining patterns according to whether the whole serum or the purified antibodies are used. These differences are due to the presence in plasma or serum of human or experimental animals of a powerful actin depolymerizing factor (Experientia 35, 1039, 1979). ADF was purified from human serum by a 5-steps procedure, using ammonium-sulfate fractionation, gel-filtration on Sephacryl S-200, chromatography on Blue Sepharose, DEAE cellulose and Con A-Sepharose. On SDS-PAGE its mol.wt is about 90,000. Using negative staining we have observed that ADF depolymerizes F-actin from skeletal rabbit muscle within 1 min in a 1:20 molar stoichiometric ratio. ADF is heat stable, not retained on an actin affinity column, on a Blue Sepharose column or on a Con A-Sepharose column. Its depolymerizing activity is inhibited by trypsin.

Replication, volume and permeability of rat aortic endothelial cells during different types of experimental hypertension

C. de Chastonay, G. Gabbiani, M. B. Vallotton and I. Hüttner, *University of Geneva, Departments of Pathology and Medicine, CH-1211 Geneva 4, and McGill University, Montreal, Quebec, Canada*

We have studied cell density and mitotic index of aortic endothelial cells during early (7–10 days) and late (40 days) phases of 3 models of hypertension in rats: a) aortic ligation between renal arteries; b) uninephrectomy and Na-rich diet, and c) uninephrectomy, 0.9% NaCl as drinking fluid and desoxycorticosterone acetate (DOCA) s.c. Mitotic index and/or cell density were increased compared to controls: a) early after aortic ligation, and b) early and late after DOCA. In these situations, circulating mineralocorticoids were high compared to controls and to the other models. The increase of mitotic index and/or cell density were associated with increase of endothelial cell volume and permeability to HRP suggesting that different mechanisms of hypertension produce different rates of endothelial cell replication which in turn result in morphologically and functionally different endothelial cell layers.

Late protein codons mapped on the vaccinia virus genome

M. Chipchase, F. Schwendimann and R. Wyler, *Institute of Virology, University of Zürich, Winterthurerstrasse 266A, CH-8057 Zürich*

Synthesis of vaccinia virus late proteins can be detected about 4 h after infection. We wished to determine which

regions of the vaccinia genome coded for the different late proteins. – The analysis was based on the SstI restriction map of vaccinia. Vaccinia DNA was digested with SacI, the isoschizomer of SstI; the restriction fragments were separated on an agarose gel and transferred to millipore filter strips. The filter-bound DNA fragments were used to select for specific mRNAs by hybridization to RNA prepared from cells infected 6 h previously with vaccinia virus. The mRNAs were recovered from the RNA-DNA hybrids, translated in vitro and the protein products analyzed by SDS-PAGE. About 40 different proteins were detected, each DNA fragment giving rise to a different set of proteins. Some proteins ran parallel with, and may represent, vaccinia structural proteins. A map was constructed showing the distribution of the protein coding regions on the genome.

Polyacrylamide gels in scanning electron microscopy (SEM): effects of dehydration methods

V.E. Colombo and P.J. Späth, F. Hoffmann-La Roche & Co. Ltd, Central Research Unit, CH-4002 Basel, and Institute of Medical Microbiology, Friedbühlstrasse 51, CH-3010 Bern

Until now there has been no fully satisfactory method for the preparation of polyacrylamide gels for SEM. It has been always necessary to freeze the gels which gave rise to a shrinkage of the structures. Furthermore, the observed structures of the dried gels did not explain the separation mechanism of the gels during electrophoresis. The possibility of trailing artifacts also existed. – In this study the structures of dried gels have been examined by SEM after a dehydration procedure according to one of the following methods: air drying, freeze drying, or drying with the aid of the compound 2,2-dimethoxypropane. – We suppose that the structures seen were essentially due to the various methods of preparation. The application of 2,2-dimethoxypropane showed the existence of several zones within the dried gel. One of these, the outermost layer, had extremely fine pores. We believe that inside of this region the dehydration process was directly due to a chemical reaction of 2,2-dimethoxypropane with the inherent water.

Characterization of cloned cDNA covering over 7000 nucleotides (95%) of avian vitellogenin mRNA

P.J. Cozens, A.C.B. Cato and J.P. Jost, Friedrich-Miescher-Institut, Postfach 273, CH-4002 Basel

Restriction mapping of 41 cDNA clones indicate that 80% of them came from a similar region of vitellogenin mRNA. R-loop mapping has shown that these clones are most probably covering the 3' end of the mRNA. – Detailed restriction mapping of 20 clones together with double R-loop studies showed that 6 clones cover partially overlapping sections of the mRNA. These 6 plasmids cover a total of about 95% of the 7500 nucleotides of the mRNA. Representatives of all but one class of restriction map could be proven to be derived from vitellogenin mRNA by in vitro translation of the mRNA which hybridized to each cDNA clone followed by immunoprecipitation of the radioactively labelled product by antivitellogenin. – Hybridization under stringent conditions of RNA prepared from individual estrogen-treated chicks with cloned cDNA immobilized on diazotized cellulose paper suggest that all individual chicks used in the experiment synthesized all types of vitellogenin mRNAs.

Structural analysis of 35S Rous sarcoma virus RNA

J.L. Darlix, M. Schwager and P.F. Spahr, Department of Molecular Biology, University of Geneva, 30, quai Ernest-Ansermet, CH-1211 Geneva 4

The structure of Rous sarcoma virus (RSV) RNA has been studied previously by means of specific nucleases (J.L. Darlix, P.F. Spahr and P.A. Bromley, *Virology* 90, 317, 1978). We are now pursuing this structural analysis using the methodology developed for MS2 RNA by Fiers and coworkers (*Nature* 237, 82, 1972). 35S RSV RNA is digested by small quantities of T₁ RNase at 0°C and in 0.1 M Tris-HCl buffer, pH 7.5. The generated RNA fragments are then purified by polyacrylamide gel-electrophoresis under nondenaturing conditions and each RNA fragment analyzed by polyacrylamide gel-electrophoresis in 7M urea and by the 2-dimensional fingerprinting technique. The results of such an analysis indicate that 7 regions of the RNA molecule are very resistant to nuclease digestion and that each of these results from the association of different portions of the primary structure of RNA being located 1000 to 3000 nucleotides apart.

Identification of early hemopoietic differentiation markers

J.M. Davis, J.-F. Conscience, S. Deslex and F. Fischer, Friedrich-Miescher-Institut, P.O. Box 273, CH-4002 Basel

The direct identification of cells at early stages of hemopoietic differentiation is difficult, since they are present in a heterogeneous bone marrow cell population and no suitable markers are available. To overcome this problem, rats were immunized with adult mouse bone marrow cells, and their spleen cells fused with a mouse myeloma cell line. The hybrids were cloned and selected in one step, by plating the cells from the fusion mixture in semi-solid medium containing the components of the H.A.T. selection system. Out of a number of fusions, several hundred clones were picked, grown in liquid culture, and the medium screened by immunofluorescence for the presence of antibodies reacting against mouse bone marrow cells. Several of these clones react with subpopulations of bone marrow cells. We are now characterizing the cells which are recognized, using antibody-mediated cell sorting and complement-mediated cytotoxicity, in association with colony assays for the various hemopoietic precursor cells.

A novel secretory organelle in human neutrophils

B. Dewald, U. Bretz and M. Baggiolini, Research Institute Wander Ltd, CH-3001 Bern

Human neutrophils contain 2 major enzyme storage compartments, azurophil and specific granules, which are discharged primarily during phagocytosis. Subcellular fractionation revealed a 3rd population of vesicle-like enzyme stores. We have exposed neutrophils to particulate and soluble stimuli, i.e. opsonized zymosan, PMA, fMet-Leu-Phe, and A 23187, and have measured the appearance of selected markers in the medium. These were β -glucuronidase (azurophil granules), vitamin B₁₂-binding protein (specific granules) and gelatinase (3rd particles). The soluble stimuli had no effect on azurophil granules but induced a moderate discharge of specific granules. The most striking effect, however, was the high rate of release from the gelatinase-containing particles. These results indicate that the neutrophils contain, in addition to the granules, truly secretory organelles. It is suggested that gelatinase and possibly other secretory enzymes may be involved in neutrophil adherence to endothelia and migration into the tissues.

DNA sequences preceding the rabbit β -globin gene are required for correct initiation of transcription

P. Dierks, A. van Ooyen, F. Meyer, N. Mantei and C. Weissmann, *Institut für Molekularbiologie I, Universität Zürich, CH-8093 Zürich*

L-cells transformed with a pBR322-linked 2.1 kb rabbit chromosomal DNA fragment containing the β -globin gene synthesize 50–2000 strands/cell of mature β -globin-specific RNA. About 60% of the 5' ends map at the cap site and the rest 45–50 nucleotides downstream, or more than 350 nucleotides upstream. Deletions extending up to 70 nucleotides before the cap site reduce the proportion of correct 5' ends to 25%; most 5' termini map downstream at positions 45–50 and some upstream (probably in the plasmid moiety). With deletions up to 14 nucleotides before the 'cap site' (removing the 'Hogness box') no correct 5' termini are found; most 5' ends map at the pBR322 moiety and the remainder at positions 45–50. Thus, sequences in the region 14–70 nucleotides preceding the 'cap site' are required for correct transcription. Moreover, we found that the large intron is not required for correct initiation of transcription.

Globulin synthesis in developing kernels of the opaque-2 mutant of *Zea mays*

C. Dierks-Ventling, M.-F. Tschopp and K. Cozens, *Friedrich-Miescher-Institut, P.O. Box 273, CH-4002 Basel*

In the wild type and in the opaque-2 mutant globulins are synthesized in the endosperm of developing corn kernels in an exponential fashion, the rate of synthesis being greatly increased at about 30 days post pollination. The latter half of kernel development is characterized by the rapidly growing embryo which itself also synthesizes globulins. The 2 globulin populations differ from each other as shown on SDS-PAGE. At maturity total globulins in the opaque-2 mutant were increased 2-fold compared to the wild type. In the mutant increases of certain specific polypeptides could be shown on SDS-PAGE. Since the total protein content in the mutant was the same as in the wild type at maturity, the increase in globulins compensates for the loss in zein in the mutant. These findings indicate that the regulation of globulin synthesis may be linked to that of zein synthesis.

Proliferation and differentiation of myogenic cells in a defined medium

P. Dollenmeier, D. C. Turner and H. M. Eppenberger, *Zellbiologie, ETH-Hönggerberg, CH-8093 Zürich*

A defined medium was developed for primary cultures of chick embryo muscle cells, which is also useful for studying neuromuscular interactions. It is based on the MCDB 201 medium of McKeehan and Ham (J. Cell Biol. 71, 728, 1976) and contains 10 additional factors. Myogenic cells divide in this medium. Cultures exposed to ^3H -TdR from 24 to 48 h after plating were fixed at 80 h, stained by immunofluorescence for M-creatine kinase and radioautographed. Over 40% of the nuclei in myotubes and other fluorescent cells were labelled, confirming that differentiated cells arise from the proliferating population in the new medium. Myotubes contract and are viable for at least 10 days. Within 24 h after addition of crystalline trypsin (1 $\mu\text{g}/\text{ml}$), myoblasts detach from the substratum and can be separated from attached fibroblasts; when replated in fresh medium they yield cultures with up to 99% myoblasts and myotubes. Nerve cells from embryonic chick spinal cord are viable in the same medium and show prominent neurite outgrowth.

Shape determination of the scaffolding core of phage T4 prehead

R. Van Driel, R. Driedonks and A. Engel, *Biozentrum, University of Basel, CH-4056 Basel, and Max-Planck-Institut für Biochemie, D-8033 Martinsried, Federal Republic of Germany*

Shape regulation of phage T4 is accomplished during assembly of the prehead which consists of a core and a shell. The prolate core is assumed to act as a scaffold for correct assembly of the shell. This is supported by self-assembly of cores from a mixture of solubilized prehead proteins deficient in shell proteins. Major core protein P22 assembles into filaments of 9 nm width and undefined length. From the filament mass per length (19.3 KD/nm), determined by STEM, we calculate that a filament assembled from the P22 molecules of one prehead covers a surface which corresponds to that of a prolate spheroid of core dimensions. A helical arrangement of P22 filaments is suggested by striations on freeze-dried shadowed cores (pitch = 35°, axial repeat = 11 nm, in agreement with the 6-start helical core structure of T4 giants). Ring-shaped oligomers formed by P20, the cap initiator, have a diameter of 18 nm and a 12-fold rotational symmetry. Based on these data a core model was built consisting of a distorted 6-start P22-helix held together by the P20 complex at one end. Intrinsically, this structure has appropriate shape and dimensions to act as scaffold for the assembly of the prolate shell.

Partial characterization of the chromoid structure of *Chlamydomonas*

M. Dron, *Département de Biologie moléculaire, Université de Genève, CH-1211 Genève 4*

Transcriptionally active chromosomes (chromoid) can be isolated from chloroplasts of plants and algae. The chromoid of *Chlamydomonas* is a DNA-protein complex sedimenting at 85S. It is isolated by passing an 80,000 \times g supernatant of a chloroplast lysate through a Sepharose 4B column. – The kinetics of the endogenous RNA polymerase activity of the chromoid and its sensitivity to DNase I as well as its sedimentation coefficient have been examined after dissociating the complex at various ionic strengths between 0.05 and 2 M NaCl. At most salt concentrations the transcription of the chromoid is inhibited by rifampicin suggesting that no transcription reinitiation occurs under these conditions. – The sensitivity of the complex to DNase I increases with the ionic strength. Most of the proteins of the complex are stripped off between 0.1 and 0.5 M NaCl, indicating that the proteins of the chromoid are not as tightly bound as the histones in chromatin.

Tissue preference and differentiation of malignant hybrid cells during mouse development

D. Duboule, C. M. Croce and K. Illmensee, *Département de Biologie animale, Université de Genève, CH-1224 Chêne-Bougeries, and Wistar Institute, Philadelphia, USA*

Malignant hybrid cells between mouse teratocarcinoma and rat hepatoma were injected singly into C57BL/6 mouse blastocysts bearing several genetic markers. Subsequently these blastocysts were transferred into the uteri of pseudopregnant ICR foster mothers. 4 out of 61 fetuses analyzed at various stages revealed hybrid-cell participation in their livers and some organs of endomesodermal origin only. Xenogeneic gene expression in vivo, which was demonstrated for 3 rat enzyme variants (GPI, LDH, GPD), showed tissue specificity and differed from the pattern in

vitro. After culturing the chimeric organs in vitro, the original hybrid-cell pattern reappeared, thereby indicating reversible gene activity. About one third of these chimeric tissues when injected s.c. into *nude* mice, formed tumors. We therefore conclude that reversion of malignancy to a normal cellular phenotype is not always a stable process, at least with respect to fetal development.

Characterization of a chimeric plasmid containing bacteriophage T4D gene 32

R. M. Duvoisin, H. M. Krisch and R. H. Epstein, *Département de Biologie moléculaire, Université de Genève, CH-1211 Genève 4*

The product of T4 gene 32, a DNA-binding protein, has an essential role in viral DNA replication. Control of gene 32 expression is unusual, being self-regulated at the level of translation. A viable gene 32 hybrid plasmid was not isolated until a gene 32 nonsense mutation was introduced into the DNA to be cloned. The T4 insert of this plasmid contains genes 59 and 32 intact as well as a part of gene 33. The efficiency with which this plasmid could transform various bacterial strains as well as the growth rate of the transformants was shown to depend upon the extent of suppression of the gene 32 amber mutation. Using antibody specific to gene 32 protein, expression of this gene from the plasmid in uninfected cells was demonstrated. A variant plasmid was also isolated in which gene 32 expression appears to be reduced by an IS1 inserted in the cloned DNA.

Melanoma cell tyrosinase stimulating activity of α -melanotropin, β -melanotropin and some analogues and fragments thereof

A. N. Eberle, V. M. Kriwaczek, W. Hübscher, U. Walty and R. Schwyzler, *Institut für Molekularbiologie und Biophysik, ETH, CH-8093 Zürich*

α -MSH, β -MSH and about 20 MSH fragments and analogues were investigated with a tyrosinase assay using mouse melanoma cells in culture. The ED_{50} values for α -MSH and β -MSH were 2.5×10^{-9} M and 1.6×10^{-8} M, respectively, thus α -MSH being about 7 times more potent than β -MSH. The C-terminal α -MSH fragments (9–13), (7–13), (5–13) and (3–13) were about as active in the tyrosinase as in the melanophore assay (relative molar potencies: 5×10^5 , 9×10^7 , 8×10^8 and 10^{10} , compared to α -MSH = 4×10^{10}). Modification of position 11 (Gly, Nle, Ser or D-Lys instead of Lys) impaired the hormonal activity to about the same extent as in the frog skin assay (see Eberle et al., *Bull. Schweiz. Akad. med. Wiss.* 34, 99, 1978). The C-terminal part of MSH may therefore be recognized through a similar mechanism by both melanophore and melanoma cell receptors. On the other hand, [Leu⁹] α -MSH, a potent agonist in the frog skin, displays only weak agonistic (1%), but remarkable antagonistic properties in the melanoma tyrosinase assay. Most probably the physicochemical interaction of the central part of the peptide chain with the 2 receptors is not identical.

Characterization of antibodies to the myoblast surface

R. Ehrismann, M. Chiquet, M. Tschudi, D. C. Turner and H. M. Eppenberger, *Zellbiologie, ETH-Hönggerberg, CH-8093 Zürich*

Homogeneous populations of postmitotic chick myoblasts (Mb) were injected into rabbits. Judged by immunofluores-

cence, all 6 antisera reacted with cell surfaces of Mb, myotubes and fibroblasts. Each serum precipitated a different pattern of proteins, resolved by SDS-PAGE, from extracts of ³⁵S-methionine-labelled cells. 2 of the 6 sera precipitated a 42K protein, not identical to creatine kinase or actin, from extracts of muscle cultures, but not of fibroblasts or BUdR-treated myogenic cultures. This putative Mb-specific protein was lost from cells treated with trypsin, suggesting a surface location, but was not iodinated with lactoperoxidase. – We isolated the 42K protein by sequential immunoprecipitation with 2 different antisera and injected the precipitate into rabbits to produce a specific anti-42K-antiserum. – The antibodies and Fab fragments were tested for ability to interfere with Mb-Mb- and Mb-substrate adhesion as a first step in identifying Mb surface molecules involved in these events.

Myofibrillogenesis in muscle cell culture: The 165K M-protein as marker of assembly

H. M. Eppenberger, E. Strehler, U. Rosenberg, D. Turner and J. C. Perriard, *Zellbiologie, ETH-Hönggerberg, CH-8093 Zürich*

Antibodies against chicken 165K M-protein were used in immunofluorescence studies of differentiating chicken skeletal muscle cells. M-protein is one of several components of the M-line structure in myofibrils. During myogenesis in vitro-M-protein is first detectable in postmitotic myoblasts while dividing presumptive myoblasts (BUdR blocked) show no M-protein staining. In postmitotic myoblasts and in immature myotubes M-protein is clearly organized in the cross-striation pattern known from adult myofibrils indicating the presence of organized myofibrils at this stage; cross-striations are also present in suspended or newly attached cells at the same stage but the myofibrils are wound about the nucleus. Fibroblasts do not stain. Measurements of 165K M-protein synthesis, carried out by immunoprecipitation of radiolabelled protein, correspond with the cytological observations: there is no measurable incorporation in undifferentiated cells but increasing synthesis is found as the cells differentiate.

Steroid receptors and cAMP in GH3-cells

D. Fabbro, W. Roos and U. Eppenberger, *Experimental Endocrinology, Department of Gynecology, University Clinic Medical School, CH-4031 Basel*

A close dose-dependent relationship could be observed between rPRL-release and the increase of cAMP-dependent protein kinase ratio (–cAMP/+cAMP), if cholera-toxin was used as a cAMP-probe. No stimulatory effect of TRH on cAMP-dependent protein kinase (PK) activity could be demonstrated. Most of the PK-activity (95%) was found in the cytosol fraction. These PK-activities were characterized by DEAE-chromatography, gel-filtration and polyacrylamide gel-electrophoresis. – A long-term effect of TRH can also be mimicked by progesterone (PG) and estradiol (E₂). The steroid actions are based on the presence of their respective receptors which have been characterized by Scatchard analysis, competition experiments and isoelectrofocusing. The E₂-receptor was present in the cytosol and nuclear fraction, whereas the PG-receptor could be found only in the cytosol. – Since the long-term effect of TRH and cholera-toxin seem to be identical with the steroid effect, a close relationship between these 2 systems is suggested.

Cloning of cDNAs for mouse complement proteins C3 and C4

G. Fey, K. Odink and H. Diggelmann, *ISREC, Chemin des Boveresses, CH-1066 Epalinges*

The ≥ 5 kb size fraction of mouse liver mRNA was copied into cDNA, which was inserted into the plasmid pBr 322. 310 transformed *Escherichia coli* colonies (clones) were obtained. Candidates for C3 and C4 clones were found in a 2-step procedure: 1. mRNA was electrophoresed in agarose gels and bands ≥ 6 kb were excised, eluted and translated. Bands of (8.4 ± 0.4) kb and (7.5 ± 0.3) kb directed cell-free translation into proteins comigrating in SDS-PAGE with prepro-C4 and prepro-C3, respectively. Aliquots of eluted RNAs were labelled and used to screen through the collection of clones. 6 candidates each for C3 and C4 were found. 2. The assignment was supported by the finding that individual candidate DNAs hybridized to 8.4 and 7.5 kb mRNA species immobilized on cellulose paper after gel-electrophoresis. For final identification candidate DNAs were coupled to cellulose and used for preparative hybridizations. Work is in progress on cell free translation of retained RNA species.

Effects of lymphocyte activation products on cultured glia cells

A. Fontana, A. Grieder, St. Arrenbrecht and P.J. Grob, *Department of Internal Medicine, University Hospital, Section of Clinical Immunology, CH-8044 Zürich, and Pharmaceutical Division, Preclinical Research, Sandoz Ltd, CH-4002 Basel*

ConA and antigen stimulated rat lymphocytes release soluble products, which activate astrocyte precursor cells as measured by an increase of RNA- and DNA-synthesis. Only an augmentation of ($5\text{-}^3\text{H}$)uridine incorporation was observed in dibutyryl cyclic AMP treated mature astrocytes, which showed intense fluorescent processes after staining with an antigial fibrillary acid protein antiserum. Preliminary characterization demonstrated the glia-stimulating factor to be nondialyzable and heat stable at 56°C for 30 min, but not stable at 80°C for 30 min. – Products of activated lymphocytes (lymphokines) play a prominent role in the development and modulation of the inflammatory response. – The new lymphokine detected could contribute to the astrocytic gliosis observed in vivo in the vicinity of inflammatory reactions of the central nervous system.

Induction of sister chromatid exchanges in vivo in somatic cells of rats by mitomycin C

K. Frei, P. Maier and G. Zbinden, *Institute of Toxicology, ETH/University of Zürich, CH-8603 Schwerzenbach*

Sister chromatid exchanges (SCE) are a sensitive cytogenetic parameter for the detection of mutagenic activity of chemicals in mammalian cells. – Growth of granulation tissue was initiated with croton oil on the inside of a s.c. air pocket in rats (Granuloma Pouch Assay). 48 h later a 250 mg bromodeoxyuridine tablet was implanted s.c. 2 h later the test compound (mitomycin C) was injected i.p. or into the pouch. After an expression time of 24 h in vivo, the granulation tissue was excised and single cells were isolated by enzymic dissociation. Subsequently fibroblast-like cells were cultured on cover glasses for 24–48 h in culture medium containing $1\text{ }\mu\text{M}$ bromodeoxyuridine. 2 h prior to harvest, metaphases were accumulated with $2.1\text{ }\mu\text{M}$ colchicine followed by a hypotonic treatment with 0.3% KCl for 10 min. Cells were fixed and then stained by the fluorescence plus giemsa (FPG) technique. From control animals

13.19 ± 5.05 (SD) SCE per cell were scored. Mitomycin C applied into the pouch caused a dose-dependent increase of SCE. 5 mg mitomycin C/kg b.wt (i.p.) induced SCE-frequencies 10-fold higher than control values. Simultaneously, the inhibition of cellular replication by the drug was determined.

Escherichia coli dnaAcos mutant: replication of the host chromosome and the plasmids pSC101, RTF-TC and λ dv

J. Frey, Grete Kellenberger-Gujer, M. Chandler and L. Caro, *Département de Biologie moléculaire, 30, quai Ernest-Ansermet, CH-1211 Genève 4*

Cold-sensitive *dnaAcos* mutants overinitiate replication at low temperatures but grow normally at 42°C . We have used pulse labelling and DNA:DNA hybridization to follow the effect of a shift in temperature, in such a strain, on the replication of the plasmids pSC101, RTF-TC and λ dv. In each case the replication of the chromosome was also monitored. Our previous results show that pSC101 replication is strictly dependent upon the *dnaA* gene product while RTF can replicate at nonpermissive temperatures in *dnaA_{ts}* mutants. The hybridization results show that after a shift from 42°C to 32°C the chromosome of a *dnaAcos* strain undergoes 2 waves of overinitiation at 5 min and 25 min after the temperature shift while pSC101 harbored in this strain undergoes a strong overreplication for at least 60 min after the shift. The plasmid RTF-TC does not undergo overreplication in a *dnaAcos* strain while chromosome overinitiation is identical to that of the *dnaAcos*/pSC101 strain. λ dv shows normal replication behavior after the temperature shift in this strain but its presence suppresses completely the second wave of chromosomal overreplication and significantly reduces the first wave at 5 min. The presence of λ dv also suppresses cold sensitivity.

The structure of the alamethicin pore in lipid membranes

U. P. Fringeli and M. Fringeli, *Laboratorium für physikalische Chemie, ETHZ, CH-8092 Zürich*

The conformation of the linear peptide antibiotic alamethicin was investigated by means of IR attenuated total reflection (ATR) spectroscopy. In dry membranes it was found to be predominantly helical. Addition of liquid water resulted in helix unfolding. Extended peptide molecules associated to multimers spanning the membrane. Pore opening is expected to result from electric field induced conformational changes of the aggregates (U.P. Fringeli and M. Fringeli, *Proc. nat. Acad. Sci. USA* 76, 3852, 1979). Distribution and transmembrane diffusion of alamethicin in lecithin/water membranes reveal that the equilibrium conditions are similar in ATR- and black film experiments, however, many of the latter experiments have been performed with nonequilibrated membranes (U.P. Fringeli, *J. Membrane Biol.* 40, 1980). A review on black film experiments is given by G. Boheim and H.-A. Kolb (*J. Membrane Biol.* 38, 99, 1978).

Integration sites of mobile elements in yeast

J. Gafner, H. Eibel, M. Brennan, A. Stotz and P. Philippsen, *Department of Microbiology, Biozentrum, Klingelbergstrasse 70, CH-4056 Basel*

A class of mobile elements in *Saccharomyces cerevisiae* nuclear DNA, called TY1, have been recently described by Cameron, Loh and Davis. These elements are flanked by direct short repeats, so-called δ -sequences. Such sequences

exist also elsewhere in the genome not connected to TY1 elements. We analyzed several δ -sequences and TY1 integration sites in different yeast strains. The results are as follows: 1. δ -sequences are 337 nucleotide pairs long. Those flanking TY1 elements have identical sequences. Those not connected to TY1 show up to 10% sequence divergence including small deletions. δ -sequences have many nonsense codons in all reading frames. – 2. The integration sites of TY1 elements consist of 75% AT pairs. The integration creates a 5 nucleotide pairs duplication like the integration of IS2 in *Escherichia coli*.

Advances in specimen preparation for electron microscopy. II. Structural preservation in crystalline biological material

R. M. Garavito, W. Villiger and E. Carlemalm, Department of Microbiology, Biozentrum der Universität Basel, CH-4056 Basel

An embedding procedure utilizing low temperature dehydration, infiltration and polymerization has been developed. Keeping the specimen at -35°C or below throughout the majority of the embedding process seems to minimize molecular disorder and denaturation. Quantitative measurements of structural preservation can be made using highly ordered specimens, like protein crystals, and diffraction techniques (X-rays, electron or optical). Tests on catalase and aspartate aminotransferase (AAT) clearly show that these low-temperature procedures preserve more structural detail than conventional techniques. For AAT, X-ray diffraction orders up to 7 Å are readily observable. The critical points in the embedding method appear to be dehydration and infiltration rather than polymerization. Work with sectioned material suggests that a significant amount of information is lost through sectioning, inadequate staining and irradiation.

Advances in specimen preparation for electron microscopy. III. Molecular organization of the mitochondrial crystalloid in *Drosophila melanogaster* spermatids

R. M. Garavito, W. Villiger and E. Carlemalm, Department of Microbiology, Biozentrum der Universität Basel, CH-4056 Basel

The individualized spermatids of *D. melanogaster* contain 2 cellular organelles which were formed by a condensation of mitochondria during spermatogenesis. Within the major mitochondrial derivative exists a paracrystalline body (PCB) which extends along about 75% of the length and occupies about 30% of the volume of the spermatid. Though its function remains unknown, the PCB appears to be composed of proteinaceous filaments that are close packed (B. Baccetti and B.A. Afzelius, The Biology of the Sperm Cell, Karger, Basel). In this study, we have looked at its molecular organization using varying conditions of fixation, dehydration, embedding and post-staining. In longitudinal sections an effective resolution of 25 Å can be reached. A major repeat of about 50 Å is observed along with supramolecular repeat of 172 Å. The amount and character of the information obtainable from sections depends heavily on the nature of the specimen preparation. As an internal control, the axoneme was used to discern the preparation induced changes and, thus, help in the interpretation of the optical reconstruction.

Towards the isolation of conditional lethal mutants with somatic cells of plants

C. H. Gebhardt and P. J. King, Friedrich-Miescher-Institut, Postfach 273, CH-4002 Basel

Hyoscyamus muticus has been chosen as a model system for somatic cell genetics because fertile plants may be regenerated from single somatic cells, usually from protoplasts. Using this system we are testing a procedure, which should allow the isolation of conditional lethal mutants: 1. We routinely obtain haploid plantlets by anther culture of diploid plants. 2. Protoplasts are isolated from the leaves of haploid plants. 3. The protoplasts are treated with the mutagen N-methyl N'-nitro N-nitrosoguanidine. 4. The surviving protoplasts are cultured to colonies in an enriched medium and cloned in microtest plates. 5. The clones are tested individually on enriched and minimal medium. Whilst the minimal medium contains only mineral salts, sucrose and hormones, the enriched medium also contains casein hydrolysate, purines, pyrimidines and vitamins. 6. Clones growing on enriched but not on minimal medium are retested. 7. Plants are regenerated from putative mutant clones. – So far we have prepared and are now testing ca. 10,000 haploid clones.

Characterization of high affinity nuclear binding sites for triiodothyronine (T_3) in an adult amphibian

K. Geering and B. C. Rossier, Institut de Pharmacologie, Université de Lausanne, CH-1001 Lausanne

In the urinary bladder of the toad, *Bufo marinus*, T_3 antagonizes the action of aldosterone on sodium transport. We have demonstrated specific nuclear binding sites for T_3 in this tissue which might mediate the hormonal response. The proteinic sites extracted from tissue which was incubated with physiological hormone concentrations show a mol. wt of 45,000–53,000 as determined by gel-filtration. In view of the metabolism of T_3 in intact tissue, further characterization of the sites was performed on nuclear extracts prepared by a method adapted from K. R. Latham et al., J. biol. Chem. 251, 7388. At 25°C , the hormone binding in these extracts reached a maximum around 30 min but the T_3 -protein complex was not stable during incubation. Scatchard analysis was performed at 0°C by incubation of nuclear extracts for 14 h with 0.01–1 nM (^{125}I) T_3 . Extracts contain a single class of binding sites for T_3 with a K_d around 0.065 nM ($n=3$) and a maximal binding around 6.4 pM ($n=3$). The very high affinity of the T_3 binding sites allows an occupation at hormone concentrations found in living animals.

Absence of myelin basic protein and major dense line in a myelin-deficient mutation

H. Ginalska, R. L. Friede, S. R. Cohen and J.-M. Matthieu, Service de Pédiatrie, CHUV, CH-1011 Lausanne

Myelin was studied morphologically and biochemically in a new myelin-deficient mutant, the 'mld' mouse. In young adults, mld brains contained only 4% of the myelin measured in controls. The morphological analysis showed a drastic myelin defect in the different myelinated tracts of the brain. Myelin basic protein measured by radioimmunoassay in mld brain homogenate was 3% of controls. In purified myelin from mld brains, myelin basic protein was absent, while other typical myelin proteins or the enzyme 2',3'-cyclic nucleotide 3'-phosphodiesterase were normal or increased. The electron microscopic investigation showed in mld mutants a lack of major dense line in the hypoplas-

tic myelin sheaths and an excessive proliferation of oligodendroglia. These findings give further support to the localization of myelin basic proteins at the major dense line.

Independent regulation of H-2K and H-2D

R. Gmür, B. B. Knowles and D. Solter, *The Wistar Institute, Philadelphia, PA, USA*

Fusing clonal (H-2 negative) embryonal carcinoma cells (ECCs) of the cell lines PCC4azal and F9 BUDR (both of H-2^{bc} genotype) with H-2^k positive cells from C3H/HeJ spleens or the T-cell lymphoma BW5147, respectively, we obtained 2 sets of hybrids with very differently affected H-2 expression: a) the ECC-like PCC4xspleen cell hybrids completely lacked H-2 antigens but could be induced to differentiate in vitro, leading to the (re)expression of both, H-2^k and H-2^{bc} antigens. Interestingly, one of the clones only (re)expressed H-2D but not H-2K coded antigens. b) The F9 × BW hybrid clones consistently revealed preservation of H-2D^k and strong induction of H-2D^{bc} expression. In some of the clones, however, H-2K^k expression was strongly suppressed and H-2K^{bc} expression barely induced. The data demonstrate that reexpression of previously extinguished traits can be the consequence of cell differentiation and furthermore suggest that the genetically, structurally and functionally very closely related H-2D and H-2K gene products have to be independently regulated.

Studies on the retrograde neuronal transport of various tetanus toxin fragments

P. Grob, K. Akert, M. A. Glicksman and B. Bizzini, *Brain Research Institute, University of Zürich, CH-8029 Zürich, and Institut Pasteur, Paris, France*

Purified tetanus toxin can be separated into different fragments. The nontoxic B-II_b tetanus toxin fragment has been shown to be transported retrogradely within neurons of the rat peripheral nervous system (Bizzini et al., 1977). In our experiment toxic ¹²⁵I-I_{bc} fragment injected into the medial rectus muscle of the rat is not transported retrogradely. However, the same experiment with ¹²⁵I-I_{bc} tetanus toxin fragment coupled to B-II_b by a disulfide bond gave positive results. In conclusion, B-II_b tetanus toxin fragment can be used as a retrograde tracer of neuronal connections and fragments like B-II_b may serve in addition as specific carriers for chemical and chemotherapeutic agents within peripheral and central nervous systems.

Mouse mammary tumor virus genes can be integrated adjacent to unique and reiterated host DNA sequences

B. Groner and N. E. Hynes, *ISREC, CH-1066 Epalinges*

The GR-3A mouse mammary tumor cell line contains 50–60 proviral MMTV copies per haploid genome. Since the GR mouse contains only 5 copies, 45–55 copies have been acquired exogenously. We have cloned 6 individual cell line proviruses including their flanking sequences and have used restriction fragments thereof as hybridization probes to analyze genomic DNA derived from GR, Balb/c, C3H and feral mice. By Southern blotting analysis we can conclude that: 1. The endogenous proviruses of GR, Balb/c and C3H mice have terminal repeats i.e. exhibit sequences complementary to the 3' and 5' end of the viral RNA on both ends of the proviral DNA. 2. A feral mouse has 1 proviral gene without terminal repeats. 3. The exogenous provirus can be integrated in the GR cell line adjacent to unique DNA and to host sequences reiterated at least 15 times. 4. The EcoRI fragment of unique DNA serving as integration site in the GR cell line can be identified and is identical in GR, Balb/c, C3H and feral mice.

Processing of ribosomal precursor RNAs in *Physarum*

U. Gubler, T. Wyler and R. Braun, *Institute of General Microbiology, University of Bern, Altenbergrain 21, CH-3013 Bern*

In *Physarum*, most rRNA genes (19S, 5.8S, 26S) reside on linear, extrachromosomal and palindromic rDNA molecules of 57.5 kb length. 1 gene copy for each rRNA is located symmetrically at the end of each rDNA-molecule. The gene for the 26S rRNA contains 2 insertions. Transcription starts in the central part of the rDNA and is directed outwards. – The processing of intermediates of *Physarum* rRNA has been investigated using 2 cloned rDNA restriction fragments as sequence specific probes. The largest stable pre-rRNA detected has a length of 11.8 kb. R-loop analysis with that precursor fraction demonstrates that in *Physarum*, pre rRNA splicing takes place. – In addition, the gene for the 5.8S rRNA has been mapped within the transcribed spacer.

Tissue specific expression of α -amylase genes in mouse

O. Hagenbüchle, R. Young, M. Tosi, L. Fabiani, A. C. Pittet, R. Bovey, P. Wellauer and U. Schibler, *Institut Suisse de Recherches Expérimentales sur le Cancer, CH-1066 Epalinges*

Cloned cDNAs to α -amylase mRNAs from pancreas, salivary gland and liver were used to study the transcription of α -amylase genes in these 3 tissues. The lengths of deadenylated α -amylase mRNAs are 1.6 kb, 1.7 kb and 1.8 kb for pancreas, salivary gland and liver, respectively. – The concentration of these mRNAs varies considerably between the 3 tissues. Whereas in the exocrine pancreas cell α -amylase mRNA represents the most abundant polyadenylated transcript (about 10⁵ copies per cell), its relative concentration is rather low in hepatocytes (about 10² copies per cell). Comparison of the primary structures of these mRNAs reveals that at least 2 different α -amylase genes are expressed in mouse, one in pancreas and one in liver and salivary gland. – Using the cloned α -amylase cDNAs as hybridization probes, we have recently cloned large genomic DNA segments in λ -vectors carrying portions of α -amylase genes. We are currently investigating the structural arrangement of these genomic α -amylase clones.

Evidence for the importance of contact between pancreatic islet cells in glucose-induced insulin release

P. Halban, C. Wollheim, B. Blondel and A. Renold, *Institut de Biochimie clinique, Université de Genève, CH-1211 Genève 4*

Since communication between pancreatic islet cells has been observed, its possible role in control of insulin (IRI) release was evaluated. Isolated adult rat islets, cells isolated from islets by trypsinization and reaggregated clumps of such cells were preincubated (2 h) then incubated (1 h) for measurement of IRI release (which was related to cellular IRI content). IRI release was also measured in neonatal rat pancreatic cells cultured in either suspension or monolayer. Basal [glucose (G) 2.8 mM] IRI release from isolated cells was elevated whilst glucose-stimulated (16.7 mM) release was markedly reduced relative to intact islets. Reaggregation lowered basal release and partially restored glucose sensitivity. Conversely, elevating cAMP with 5 μ g/ml glucagon (+ G 16.7 mM) resulted in a 40% increase in IRI release from islets (relative to G 16.7 mM alone) and a 100% increase from cells or clumps. Results with neonatal cells were similar: glucose elicited IRI release from cells

grown in monolayer and aggregates of cells grown in suspension, whereas cells detached from the monolayer or isolated suspension cells were insensitive to glucose and displayed elevated basal IRI release. Glucagon combined with glucose stimulated all the neonatal preparations. The altered sensitivity to glucose in the face of retained sensitivity to glucagon suggests that cell contact may be of importance primarily for glucose initiation of insulin release.

Occurrence and properties of a composite transposon TnA::r-det

C. Hänni, S. Iida and W. Arber, *Biozentrum der Universität Basel, Microbiology Department, CH-4056 Basel*

In studies on the transposition of the r-det of NR1-Basel from the *Escherichia coli* chromosome to phage P7, P7 hybrids were isolated which carry the r-det inserted in the transposon 902, a TnA which normally provides P7-lysogenic strains with resistance to ampicillin. The resulting 'composite transposon' Tn902bla::r-det determines the phenotype Ap^rCm^rSm^rSu^rHg^r. Using this phage P7::Tn902bla::r-det to infect at low multiplicity of infection a strain harboring RTF of R100-1, it was found that the composite transposon translocates as a unit and is remarkably stable: the Tn902 of 4.8 kb carries along the IS1 flanked transposon r-det of 23 kb. – Restriction cleavage analysis of the DNA of 4 independent RTF::Tn902bla::r-det plasmids showed insertion of the composite transposon at different sites near or within IS1 of RTF.

Nonhistone chromosomal proteins in differentiating brain cortex neurons

C. W. Heizmann, E. M. Arnold and C. C. Kuenzle, *Institut für Pharmakologie und Biochemie, Veterinärmedizinische Fakultät, Wintherthurerstrasse 260, CH-8057 Zürich*

Neurons of the rat brain cortex develop from rapidly proliferating precursor cells at late fetal stages via non-dividing neuroblasts at birth to terminally differentiated postmitotic neurons thereafter. During the first postnatal week differentiation is accompanied by shortening of the chromatin repeat length from 200 to 174 basepairs. The involvement of nonhistone chromosomal (NHC) proteins in these events is probable. Therefore, we have analyzed the nuclear proteins of rat cortex neurons from 3 days before birth to 30 days postnatal age. Neuronal nuclei were isolated and the following classes of proteins analyzed by 2D-gel-electrophoresis after labelling in vitro with iodo[1-¹⁴C]acetamide: total nuclear proteins, NHC proteins, high-mobility group NHC proteins, low-mobility group NHC proteins and nuclear DNA-binding proteins. Some developmental changes were noted. Most striking was a post-natal accumulation of a single-stranded DNA-binding protein of mol.wt 35,000 and pI > 8.

Involvement of calcium ions in neuroblastoma neurite extension

R. Hinnen and D. Monard, *Friedrich-Miescher-Institut, Postfach 273, CH-4002 Basel*

A dose-response relationship has been found between the morphological differentiation of neuroblastoma cells induced by glial factor(s) and the calcium concentration in the medium. – Low concentrations of the calcium ionophore A23187 mimic the action of glial conditioned medium implying that the mobilization of calcium is a significant event leading to the extension of neurites. – Furthermore, process formation is initiated by agents

known to depolarize the membrane potential. The interaction of glial conditioned medium with the cellular membrane is assumed to cause changes in ionic conductance and membrane potential, which could be involved in neuroblastoma neurite extension.

Antiviral state toward orthomyxoviruses elicited by a resistance gene and interferon

M. A. Horisberger, T. Meyer and O. Haller, *Research Department, Pharmaceuticals Division, Ciba-Geigy Ltd, CH-4002 Basel, and Division of Experimental Microbiology, Institute for Medical Microbiology, University of Zürich, CH-8028 Zürich*

Mice bearing the allele *Mx* are selectively resistant to orthomyxoviruses. After 3 weeks in culture, peritoneal macrophages from resistant mice are equally permissive for influenza virus replication as macrophages from susceptible animals. However, specific resistance can be induced in such cultures of *Mx*-bearing macrophages by treatment with doses of interferon which leave non-*Mx*-bearing cells susceptible. In resistant macrophages attachment and penetration of virions occur as in permissive cells, but influenza virus protein synthesis is completely blocked. Thus, analysis of viral uncoating and primary transcription should clarify the step(s) at which viral replication is arrested by the antiviral state elicited by interferon together with the resistance gene *Mx*.

Transitional fibres in middle distance runners

H. Howald, R. Billeter and E. Jenny, *Forschungsinstitut der ETS Magglingen, CH-2532 Magglingen, and Institut für Pharmakologie und Biochemie, Universität Zürich, CH-8057 Zürich*

In human skeletal muscle type I fibres contain slow myosin (SM), type IIA and IIB fibres fast myosin (FM) and the rare type IIC fibres FM and SM (Billeter et al., *Histochemistry*, in press). In the m. vastus lat. of untrained persons, about equal numbers of type I and II fibres are present. Long-distance runners, however, have more type I and sprinters more type II fibres. This distribution may be hereditary and/or caused by training. Our observation of stages intermediate between type I and II support the latter assumption. In biopsies (m. vastus lat.) taken 2–3 weeks after a change in the training program (long distance/interval), some type I fibres contained a small amount of FM and some type IIA fibres a small amount of SM. In addition, a high number (2–6%) of type IIC fibres was found. These results indicate a transitional stage of a muscle changing his fibre pattern due to a change in the training.

Induction by various immunostimulants of interferon and natural killer cell activity in mice

P. Huguenin, A. Brownbill, P. Dukor and A. R. Schuerch, *Ciba-Geigy Ltd, CH-4002 Basel*

Polyinosinic-polycytidylic acid (poly I:C) and tilorone have previously been shown to induce interferon (IF) as well as natural killer cell activity (NKA) in mice (Senik et al., *Cell, Immun.* 44, 186, 1979). – In our study, the time course of induction of IF and of NKA in spleen and peritoneal exudate (PEC) by 6 well-established immunostimulants was investigated in mice of different strain and age. We found a) in Balb/c mice best induction of IF and NKA in 8-week-old animals irrespective of sex, b) the highest increase of both IF and NKA in NZB and CBA/J mice (> Balb/c > A/J), c) peak IF serum levels preceding peak NKA in spleen by 16 h and more, and cytotoxic activity in

PEC by 40 h, d) increased NKA in spleen induced only by drugs which also markedly enhanced serum IF (poly I:C and tilorone, but not a synthetic alkylidiamine, 6-o-mycocoyl-MDP, β 1,3-glucan and levamisole). – The data suggest that increased NKA following treatment with immunostimulants reflects prior induction of IF.

Membrane stabilization of chondrocytes by RHT

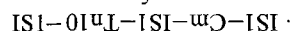
E. B. Hunziker, W. Herrmann and R. K. Schenk, *Anatomisches Institut der Universität Bern, Abteilung für Systematische Anatomie, CH-3000 Bern 9*

A major problem in chemical preservation methods for cartilage tissue is the stabilization of chondrocytic plasmalemmas, which exhibit numerous membrane ruptures with concomitant cell shrinkage. In order to stabilize these highly fragile membranes, we applied RHT (0.7%), an amine-complexed salt of ruthenium, to the cells. The small polyvalent cation of RHT is readily diffusible and has a high positive charge density. Thus it is able to interact with anionic groups (sulfate-, phosphate-, carboxyl-, sialyl-, etc.) of chondrocytic membrane surfaces ('glycocalyx'), as well as with pericellularly located polyanionic proteoglycans, by forming electrostatic cross-linkages and network junctions between these 2 interdigitating structural elements. At the same time proteoglycans are precipitated in situ. The RHT-stabilizing membrane effect is dependent on different physico-chemical conditions, which must be controlled: temperature +20°C, pH of 6.7 to 7.4, total measurable osmolarity 330 ± 15 mosmol. The application of RHT to chondrocytic membranes will allow the development of preservation methods for cartilage tissue which yield reproducible results.

IS1 mediated inversion observed in phage P1CmTc1 DNA

S. Iida, J. Meyer and W. Arber, *Microbiology Department, Biozentrum, University of Basel, CH-4056 Basel*

A P1CmTc genome can result from recombination between P1Cm1, which carries a Cm transposon (IS1-Cm-IS1) at the resident IS1 of P1, with P1Tc1, which carries Tn10 0.2 kb to the right of the IS1. Because of its large size, this genome is not packable into P1 phage particles. Plaque forming derivatives have nonessential genetic material deleted. In P1CmTc4, the right-handed IS1 of the Cm transposon caused a deletion which removed part of Tn10. P1CmTc1 lacks the P1 DNA between Tn10 and the C-loop about 9 kb to its right. Interestingly, P1CmTc1 has both Tn10 and the Cm transposon inverted while it still carries an IS1 at the original site. Thus it carries 3 IS1. We assume that this derivative arose by translocation of the left-handed IS1 of the Cm transposon into the C-loop causing the inversion of the DNA between the IS1 and its target. A subsequent deletion of inverted DNA may have led to the structure



A DNA-binding protein with specificity for a sequence associated with the major heat shock gene(s) of

Drosophila melanogaster

R. Jack, C. Brack and W.J. Gehring, *Basel Institute of Immunology and Biozentrum Basel, CH-4056 Basel*

Upon heat shock a dramatic change takes place in the transcriptional activity of *Drosophila* cells. Most genes are switched off and a small set of genes which code for the heat shock proteins are switched on. The major heat shock protein is encoded at 2 sites in the genome and structural genes from both sites have been cloned (Moran et al., Cell

17, 1, 1979). One of these clones has been used as a probe to detect sequence specific DNA-binding proteins in extracts from the nuclei of both *Drosophila* tissue culture cells and larvae. Using a filter binding assay a DNA binding activity has been demonstrated which binds to a short region lying about 0.5 kb upstream from the presumptive transcription start. The binding specificity has been confirmed by electron microscopy. The extract also shows specific binding to a short region on the sequence derived from the 2nd genetic locus and again the binding site lies upstream from the presumptive transcription start.

Ultrastructural study of intracellular proteinic cristals by optical filtration and computerized simulation

T. Jalanti, M.O. Soyer, J. Fakan and A. Gautier, *Centre de Microscopie Electronique, Université de Lausanne, CH-1011 Lausanne, et Laboratoire Arago, Université de Paris, F-66650 Banyuls-sur-Mer, France*

Prorocentrum micans E., a free-living primitive dinoflagellate, like many other protists, contains trichocysts. These extrudable organelles enclose a large, very regular prismatic core. Thin sections of the whole cell, after usual fixation, dehydration, embedding and sectioning, are examined using a transmission electron microscope fitted with a goniometer stage. – Optical Fourier analysis of the periodic information and optical filtration (T. Jalanti et al., Biol. cell. 35, 58a, 1979) permits us to propose a geometrical model for this proteinic cristal, characterized as a quadratic Bravais lattice of 9 nm unit mesh with a linear subunit decoration. Comparison between the micrographs and simulated pictures produced by a plotter interfaced with a minicomputer gives evidence of a small angle torsion deformation of the cristal.

The morphology of experimentally induced neural dysraphias in the chick embryo. A scanning and transmission electron microscopical study

R. C. Janzer, R. L. Friede, H. Walt and B. Walker, *Department of Neuropathology, Institute of Pathology, University of Zürich, CH-8091 Zürich*

Neural dysraphias induced by a single subgerminal injection of trypan blue in chick embryos of stages 6–8 were compared to normal neurulation. 3 h after injection, excessive blebbing occurred preferentially at the cervical level and affected selectively the neuroectodermal-ectodermal junction. These blebs formed zonulae adherentes with the underlying intact neural fold cells and consisted mostly of normal nonnecrotic cells and cytoplasmic fragments. After 20 h the neural tube was closed caudally and cranially to the dysraphias, while the same pattern of blebbing persisted. In addition, filopodia were found scattered between the blebs. These morphological changes, more subtle than cell death, were correlated with the failure of neural tube closure in our model. The described ultrastructural alterations might be the expression of disturbed mechanisms of cell recognition and adhesion during neurulation.

Characterization of retroviral and cellular gp70 glycoprotein on the surface of producer and nonproducer cells

F.A. Jay and C. Moroni, *Friedrich-Miescher-Institut, Postfach 273, CH-4002 Basel*

We have previously described (Moroni et al., Proc. nat. Acad. Sci. USA, in press) that serum directed against Friend leukemia virus is mitogenic for B-lymphocytes. As

normal fibroblasts from BALB/c, NFS/N and 129 mice absorb this activity, we have examined these cells for the presence of C-type viral components. Immune precipitation of surface-iodinated molecules followed by SDS-PAGE analysis revealed a component migrating to 70,000 daltons which showed homology by tryptic peptide analysis with viral envelope gp70 glycoprotein from infected cells and from purified Friend and xenotropic virions. These fibroblasts do not release complete virus. Thus, it appears that partial expression of an endogenous virus occurs in these cells.

Is there a size heterogeneity of *Euglena gracilis* chloroplast DNA molecules?

B. Jenni, M. Fasnacht and E. Stutz, Laboratoire de Biochimie, Université de Neuchâtel, CH-2000 Neuchâtel

E. gracilis Z chloroplasts contain multiple copies of apparently identical circular DNA molecules. However, recent results suggest that these molecules are heterogeneous in size. This postulate is based essentially on the observation that BglIII or HindIII digested ctDNA yields upon gel-electrophoresis a fragment pattern with a single diffuse band in addition to a defined number of sharp bands. The DNA fragments from these zones have an average mol.wt of about 6.7 kilobasepairs (BglIII diffuse band) or 5.7 kilobasepairs (HindIII diffuse band) with a size variation of approximately 300 basepairs. DNA from these zones were isolated and used for redigestion and hybridization experiments. The results obtained so far are best interpreted by assuming that ctDNA molecules carry variable deletions or insertions within a defined region.

Endogenous C-type viral protein expression in stimulated lymphocytes of a virus-inducible and noninducible mouse strain

J. Jongstra and C. Moroni, Friedrich-Miescher-Institut, Postfach 273, CH-4002 Basel

Stimulation of small resting B-lymphocytes in mice by the mitogen lipopolysaccharide (LPS) leads to expression of endogenous C-type viral genes. In many mouse strains this is followed by budding of mature viral particles from the plasma membrane. 129/J mice do not release viral particles although LPS stimulation results in normal levels of proliferation and differentiation. To define the defect in these mice we have investigated whether LPS stimulation leads to intracellular viral protein expression. Immunofluorescence studies using a broadly reacting antiviral serum showed induction of viral protein. The viral nature of the observed antigens was confirmed by absorption experiments.

Comparison of nitrogen mobilization and of proteolytic activities in leaves of annual and perennial plants

M. Keist and U. Feller, Pflanzenphysiologisches Institut, Altenbergrain 21, CH-3013 Bern

During senescence aminopeptidase activity always decreased, while carboxypeptidase and endopeptidase (hydrolysis of azocasein) activities peaked or remained high during nitrogen mobilization. Highest endopeptidase activities were measured in senescing leaves of annual crop plants (cereals, beans, rape), where most of the nitrogen was mobilized and translocated to the maturing fruits. While the rate of azocasein hydrolysis was higher at pH 5.4 until the onset of senescence, late in senescence the ratio

changed in favor of the pH 7.5 activity. An interference with exopeptidase – especially at pH 5.4 with carboxypeptidase – may be involved in this shift.

Noneukaryotic DNA-containing structures. I. Fundamental differences with eukaryotic chromatin as revealed by electron microscopy of thin sections

E. Kellenberger and A. Ryter, Department of Microbiology, Biozentrum der Universität Basel, CH-4056 Basel, and Institut Pasteur, Paris, France

Studies of the structure and conditions of fixation of different 'DNA-containing plasmas' have shown 2 distinct classes: Only the eukaryotic chromatin is apparently always fixed by aldehydes and/or OsO₄ and thus becomes relatively insensitive to dehydration. All the others, pools of replicating phage DNA, nucleoids of bacteria and of mitochondria, chromosomes of Dinoflagellates as well as solutions of DNA are sensitive and show finer and coarser aggregates. – On the nucleosomes of chromatin most of the DNA is bound to histones which are still accessible to chemical interfiber-cross-links. They become stabilized against aggregation during dehydration. Noneukaryotic DNA easily aggregates in ethanol, acetone, etc. because either the amount of protein as partners of DNA is too small for effective fixation or primary effects of fixatives induce their dissociation from DNA by changes of intracellular conditions (see communication II).

'Heat shock', glucose starvation and infection with SV40 or polyoma virus stimulate synthesis of specific cellular proteins

E. Khandjian, P. Arrigo, T. Rose and J.-M. Matter, Département de Biologie moléculaire, CH-1211 Genève 4

Infection with SV40 or polyoma virus stimulate in the host cells overall protein synthesis leading to a marked increase in cytoplasmic and nuclear proteins. Synthesis of several host proteins, particularly in the 94 and 77–72 kD range is considerably more stimulated than that of the other proteins (Khandjian et al., PNAS, 1980). We recently observed that exposure of uninfected monkey and mouse cell cultures to higher temperature (41 °C instead of 37 °C) or glucose starvation leads to the induction of the synthesis of proteins in the 94 and 77–72 kD range. Analysis in SDS-PAGE and 2-dimensional gels reveals an increase in amount and rate of synthesis of these proteins, as detected by Coomassie blue staining and autoradiography, by 15 min after transfer to 41 °C. In the cases of glucose starvation and viral infection, synthesis of these proteins are detectable only after 17–24 h. The biological significance of these findings is presently investigated.

The role of cyclic hydroxamates in the induction of cereal tissue cultures

P. J. King, Friedrich-Miescher-Institut, Postfach 273, CH-4002 Basel

Cyclic hydroxamates present in the supernatant of *Zea mays* coleoptile homogenates are known to drastically alter auxin-binding affinities of receptors on membranes isolated from the homogenates (M.A. Venis and P.J. Watson, Planta 142, 103, 1978). We have shown that such hydroxamates interfere with auxin-dependent processes, e.g. root

and shoot growth when added exogenously, and that the in vivo hydroxamate content of corn coleoptiles modulates their growth response to added IAA. Using genetic variation for hydroxamate content in corn we have further shown that tissue culture induction as an auxin-dependent process is also affected by intracellular hydroxamates and have proposed the hypothesis that the poor in vitro response of cereals is connected with the unique distribution of the cyclic hydroxamates in the Gramineae. We have investigated whether the exceptional in vitro response and the absence of hydroxamates in a mutant corn line are genetically linked characters.

In vitro transcription of mutant *SUP4* tRNA^{Tyr} genes of yeast

R.A. Koski, S.G. Clarkson, J. Kurjan and B.D. Hall, Département de Microbiologie, Université de Genève, Faculté de Médecine, 64, avenue de la Roseraie, CH-1205 Genève, and Department of Genetics, University of Washington, Seattle, WA 98195, USA

Mutant *SUP4* tRNA^{Tyr} genes of yeast which show a reduction or loss of suppressor activity in vivo have been tested for their ability to be transcribed in cell-free extracts of *Xenopus laevis*. Many mutant genes with point alterations in the mature tRNA^{Tyr} coding sequence are transcribed equally as well as the original *SUP* gene in vitro. In contrast, a mutation within the tDNA^{Tyr} intervening sequence results in shortened in vitro transcripts. Sequence analysis of these transcripts suggests that they terminate prematurely within the intervening sequence, and that this is due to the presence of a (dT)₅ tract in the noncoding strand of this mutant gene.

Mitochondrial distribution in skeletal muscles

R. Krauer, H. Hoppeler, H. Claassen, E. Uhlmann and E. R. Weibel, Anatomisches Institut Bern, CH-3012 Bern

This morphometric study on cat muscles was undertaken to examine whether random biopsies are reliable to estimate mitochondrial volume density (V_{vm}) and capillary numbers per fibre area (N_c/A_f). Large regional differences (> 100%) were found between various biopsy sites (deep, superficial; distal, proximal) in semitendinosus (ST); differences were less marked in longissimus dorsi (LD) and absent in diaphragm (D). Histochemical findings show more fibres of oxidative type at sites with high V_{vm} . We therefore conclude that, in order to estimate total mitochondrial mass, a sampling strategy must be applied which considers the possibly marked regional differences in V_{vm} . The capillary counts closely reflect the mitochondrial content, i.e. the oxidative capacity of the muscle fibres in the various samples.

The somatic DNA of *Ascaris lumbricoides* shows short-period interspersions

P. Landolt and H. Tobler, Zoologisches Institut der Universität Freiburg, Pérolles, CH-1700 Freiburg

DNA from 10-day-old larvae of *Ascaris lumbricoides* has been isolated, sheared to different fragment sizes (150–5100 NP) and labelled in vitro with ³²P using the slightly modified technique of Lillehaug and Kleppe (Biochemistry 14, 1225, 1975). 430 NP long unlabelled driver-DNA fragments were hybridized in excess to the tracer-DNA fragments of different lengths to Cot-values of 3.5. The results demonstrate that somatic DNA of *Ascaris lumbricoides* is composed of about 1% clustered repetitive sequences, about

12% single copy DNA sequences in short-period interspersions (530 NP) and at least 22% single copy DNA sequences in long-period interspersions (5100 NP). Thus, the somatic DNA of *Ascaris* is characterized by a short-period interspersions or 'Xenopus pattern'.

Transfer of highly resolved small DNA fragments to DBM-paper at high efficiency

A. Levy, E. Frei and M. Noll, Biozentrum der Universität, Klingelbergstrasse 70, CH-4056 Basel

A method that combines a good separation with a high efficiency of transfer to DBM-paper has been worked out for low mol.wt DNA. Small DNA fragments (10 to several hundred basepairs) were separated in a polyacrylamide gel consisting of a short upper gel of high percentage on top of a long 4% gel. Between 30% and 50% of the input DNA in the range of 10 to a few hundred nucleotides was transferred from the 4% gel and bound covalently to DBM-paper. Hybridization to a radioactive probe was specific and detectable down to 30 basepairs.

Chromatin fine structure of active and repressed genes

A. Levy and M. Noll, Biozentrum der Universität, Klingelbergstrasse 70, CH-4056 Basel

Chromatin structure of active and repressed genes was studied by digestion with micrococcal nuclease in the case of the genes coding for the major heat shock protein in *Drosophila melanogaster*. Transcribed genes are more, inactive genes less accessible than the bulk of chromatin. Both the accessible region of the active gene and the protected region of the repressed gene end at a site close to the termination of transcription. The protected region is larger than the mRNA-coding region and extends beyond its 5' end. The spacing of the nucleosomes is more homogeneous in the repressed gene than in the bulk of chromatin.

Heat-shock effects in *Chironomus* salivary glands

M. Lezzi, U. Riesen-Willy, B. Meyer and R. Mähr, Institute for Cell Biology, Swiss Federal Institute of Technology, CH-8093 Zürich

Incubation of *Chironomus tentans* larvae for 20–60 min at 35–40 °C leads to both regression of Balbiani rings and appearance of a number of new puffs in the salivary glands chromosomes. Among the newly puffed regions are IV-5-C, I-1-C, II-19-A and II-6-C. The same effect can be induced in vitro by incubating glands in an insect tissue culture medium at 37 °C. The appearance and size of the puffs seem to depend upon the duration and temperature of treatment, with the most consistent change found in IV-5-C. Within 30 min at 37 °C it extends to a measured size of 8 units (control: 3.5), which is a highly significant increase ($p \leq 0.001$). It is noteworthy that puffing in IV-5-C is known to be sensitive to the concentration of Mg^{++} . Autoradiography of the chromosomes and electrophoretic analysis of the newly synthesized RNA confirm that, upon heat-shock treatment, some active genes are inactivated, while other, previously inactive, regions become active.

Isolation of *pSC101* copy number mutants

P. Linder, G. Churchward and L. Caro, Département de Biologie moléculaire, Sciences II, 30, quai Ernest-Ansermet, CH-1211 Genève 4

In order to analyze replication and incompatibility functions of the *Escherichia coli* plasmid *pSC101* we have

constructed in vitro a derivative carrying an ampicillin resistance gene from a staphylococcal plasmid pI258 (A. C. Y. Chang and S. N. Cohen, Proc. nat. Acad. Sci. USA 71, 1030, 1974). Mutant plasmids conferring resistance to elevated levels of ampicillin have been isolated. The copy number of the mutant plasmids was analyzed by determining the fractions of DNA sedimenting as plasmid DNA in ethidium-bromide-CsCl gradients. Incompatibility properties of these mutant plasmids are being analyzed using a *pSC101* derivative carrying a streptomycin resistance gene in experiment designed to test whether the mutant plasmids can establish themselves in a cell already carrying *pSC101*, and whether they or the resident plasmids are preferentially lost from the cell carrying both plasmids.

A small RNA associated with large SV40 T-antigen

M. Loche and E. Khandjian, Département de Biologie moléculaire, CH-1211 Genève

When analyzed on 2-dimensional gels (IEF and SDS-PAGE), the single class of large SV40 T-antigen (88 kd) observed in SDS-PAGE consists of at least 4 differently charged molecules. To investigate the nature of the phosphate residues associated with large T-antigen, it was labelled in vivo with ^{32}P , and purified by immunoaffinity chromatography, followed by an SDS-PAGE step, and then incubated for 24 h in the presence of 0.3 N KOH. High-tension paper electrophoresis revealed in addition to phosphoserine, the presence of the 4 ribonucleotides (AMP, CMP, GMP and UMP). Large T-antigen could also be labelled in vivo with ^3H -uridine. From the 88-kd protein labelled with ^3H -uridine or ^{32}P we extracted and purified after digestion with proteinase K a small piece of RNA. Its migration in 7 M urea-PAGE suggests that its size corresponds to about 50 nucleotides. This RNA is presently characterized by oligonucleotide sequence analysis.

High metabolic activity of plant cell derived miniprotoplasts

H. Lörz, J. Paszkowski, I. Potrykus and Ch. Ventling, Friedrich-Miescher-Institut, Postfach 273, CH-4002 Basel, and Institute of Biochemistry and Biophysics, Polish Academy of Sciences, Warszawa, Poland

Isolated plant protoplasts can be fractionated by high-speed centrifugation in isosmolar density gradients into a) enucleated protoplasts or *cytoplasts* and b) nuclei containing *miniprotoplasts*. Subprotoplasts derived from cultured cells of *Zea mays* and *Nicotiana tabacum* have been characterized microscopically and studied biochemically by measuring uptake and incorporation of ^3H -leucine and ^{35}S -methionine. Cytoplasts had a very low activity which decreased rapidly within 24 h. In contrast, miniprotoplasts showed a manifold higher rate of uptake and protein synthesis than protoplasts. Considering the extremely reduced size of miniprotoplasts, which was determined to be about 10–15% of the original protoplast volume, the metabolic activity of this type of subprotoplasts is greatly increased.

Minute virus of mice: genome structure and the infection of differentiated cells

G. McMaster, K. Truong and P. Beard, ISREC, CH-1066 Epalinges

One strain of the minute virus of mice, MVM(B), grows in the lymphocytic cell line EL4 and inhibits the generation of cytotoxic lymphocytes in mixed lymphocyte cultures. An-

other strain, MVM(T) grows in mouse L-cells and was not found to inhibit mixed lymphocyte cultures. We are studying the differences in viral genome structure responsible for these distinct differences in biological properties. The major form of intracellular DNA of both virus strains is an approximately 5 kb linear duplex with a hairpin structure at both ends. In a comparison of restriction nuclease digestion products of the 2 DNAs the only obvious difference between them was a deletion of 50–100 bp near one end of MVM(B) DNA (the end believed to correspond to the 3' end of viral mRNA). After molecular cloning of parts of the viral genomes we will look in more detail at the nature and site of this deletion, and for other possible differences between the 2 strains. We are also studying intracellular viral nucleoprotein complexes.

Measuring error and sampling variation in morphometry

O. Mathieu, H. Hoppeler and E. R. Weibel, Anatomisches Institut, University of Bern, CH-3010 Bern

Several procedures are available to obtain stereological estimates. Point counting is known to be superior to lineal integration for estimating volume fractions. On the other hand, semi- or fully automated image analyzers are now available which permit a) to evaluate pictures with a much greater density of test points than is feasible by conventional point counting, b) to measure several features of different objects from one single trace of their profiles. – We evaluated the efficiency (accuracy and precision per unit time) of 3 methods (Point counting with different densities of test points; MOP AMO3, Kontron AG, Zürich; Quantimet 720, Cambridge Instruments) to estimate volume and surface density of a structure in models with different sampling variation. We show that the overall error is mainly determined by the sample variation so that measuring a single picture with very high precision is irrelevant.

Behavior of target antigens on tumor cell surfaces during lysis by allogeneic cytotoxic T lymphocytes (CTL)

A. Matter and L. Müller-Salamin, Pharmaceutical Research Division, F. Hoffmann-La Roche & Co. Ltd., CH-4002 Basel

Monovalent heterologous antibodies against the P-815 mastocytoma tumor of H-2^d origin were purified according to established techniques. Fab fragments thereof were produced by papain digestion and subsequent purification by repeated passages on ion exchange and gel chromatography columns. This resulted in homogeneous preparations as judged by SDS-polyacrylamide gel-electrophoresis. Such fragments lost their activity in complement-mediated lysis of P-815 cells whereas the titers of original antisera varied between $1/500$ and $1/2000$. These fragments retained, however, the ability to bind to tumor cell surfaces as shown in fluorescence (direct rhodamine coupling) and EM autoradiography (iodination). They also inhibited partially – though to a much smaller degree than the undigested antibody – lysis by CTL. – The binding of such Fab fragments was shown to be homogeneous and could not be induced to form either patches or caps by prolonged incubation at 37°C. Capping was only achieved when a second antibody – directed against the Fab fragments – was bound on top of the latter. – CTL lysis did not involve any sort of patch or cap formation but resulted in the progressive loss of target antigens during the later stages of the lytic process.

Comparison of cellular RNA and protein synthesis in growing and in polyoma- or SV40-infected resting mouse kidney tissue culture cells

J.-M. Matter and R. Weil, *Département de Biologie moléculaire, Université de Genève, CH-1211 Genève*

Abortive ('transforming') and lytic infection with SV40 and polyoma virus of resting mouse kidney tissue culture cells leads to synthesis of viral T-antigen which is rapidly followed by a mitogenic response of the host cells; it begins with the overall stimulation of cellular RNA (rRNA, hnRNA, 4S and 5S RNA) and protein synthesis with a pattern similar to that observed in uninfected resting control cells. In this study we compared cellular RNA and protein synthesis in growing (nonconfluent cultures) and in polyoma- or SV40-infected mouse kidney cells. Cultures were labelled with [³H]uridine or [³⁵S]methionine. Nuclear and cytoplasmic RNA was analyzed (OD and radioactivity) by electrophoresis in tubular nondenaturing polyacrylamide-agarose gels. Nuclear and cytoplasmic proteins were examined in 1-dimensional NaDodSO₄-polyacrylamide slab gels and in 2-dimensional gels. The results reveal marked differences in the pattern of RNA and protein synthesis in growing and virus-infected mouse kidney cells.

Membrane fractionation by affinity-density perturbation

A. Maurer, B. Baumgartner and K. Mühlethaler, *Institut für Zellbiologie, ETH, CH-8093 Zürich*

Latex spheres (synthesized by aqueous emulsion copolymerization of methacrylate derivatives) were coated with antibodies against conA. These immunolabelled spheres have a diameter of 600 Å and a density of 1.32 g/cm³ and are well-suited as density perturbation reagents. Yeast protoplasts were labelled with conA and as shown by freeze-etching the hexagonal arrays of the plasmalemma react with the lectins. After isolation the membrane was solubilized with 0.1% SDS at 6°C. 70% of the proteins were solubilized and 94% of the conA remained bound to the glycoproteins. The solubilized membrane proteins were mixed with the immunolabelled spheres and after reaction they were fractionated by density gradient centrifugation. The spheres were banded at 1.28 g/cm³ while the unlabelled proteins remained in the supernatant. SDS-PAGE showed that 2 glycoproteins with apparent mol.wts of 160,000 and 240,000 daltons were isolated. The immunological and ultrastructural characteristics of those glycoproteins are being investigated.

Integration and expression of exogenously acquired mouse mammary tumor virus sequences in cells not normally expressing endogenous MMTV

D. Mayor, N. Hynes, B. Groner and H. Diggelmann, *Institut Suisse de Recherches expérimentales sur le Cancer, Chemin des Boveresses, CH-1066 Epalinges*

In mink lung cells infected with MMTV stable acquisition of MMTV proviral DNA sequences could be demonstrated. Analysis of restriction fragments of cellular DNA showed colinear integration of these sequences with respect to viral RNA. Transcription of proviral DNA was stimulated by steroid hormone. Attempts to demonstrate virus-specific protein synthesis or virus particle production have so far been unsuccessful. Mouse L-cells lacking thymidine kinase activity have been used as recipients in cotransfection of

cloned genomic MMTV DNA fragments with plasmid containing a thymidine kinase gene. We have obtained clones of cells which have acquired thymidine kinase activity. These will be tested for the presence of new MMTV DNA sequences, virus-specific RNA and ultimately, virus-specific proteins.

Activation of 2 Balbiani ring genes in *Chironomus tentans* salivary gland cells

B. Meyer, T. Hertner, H.M. Eppenberger and R. Mähr, *Institute for Cell Biology, Swiss Federal Institute of Technology, CH-8093 Zürich*

Pilocarpine, an alkaloid from *Pilocarpus striatus*, causes in *Chironomus* larvae an almost complete expulsion of secretion from the salivary gland lumen. This effect is due to a pilocarpine-induced contraction of smooth muscles near the duct of the gland, which control the delivery of secretion. Emptied glands are able to refill their lumen after withdrawal of the drug or after cultivation of the glands in vitro. There is substantial evidence that the mRNA for the most abundant secretion proteins, which constitute the main part of the secretion, is synthesized in the Balbiani rings (BR). We therefore investigated the effect of pilocarpine on the BR genes, BR-RNA synthesis and on the synthesis of secretion proteins. We were able to show that the emptying of the glands induces decondensation of both, BR1 and 2, 15-fold stimulation of BR-RNA synthesis parallel to an enhanced level of secretion protein synthesis.

Expression in eukaryotic cells of SV40-DNA-linked rabbit β -globin cDNA carrying deletions in the 5' nontranslated region

F. Meyer, H. Weber, C. Weissmann, R. Mulligan and P. Berg, *Institut für Molekularbiologie I, Universität Zürich, CH-8093 Zürich, and Stanford University Medical Center, Stanford, Cal. 94305, USA*

Rabbit β -globin is synthesized in monkey kidney cells transfected with SV40 DNA in which the gene for capsid protein VPI is replaced by rabbit β -globin cDNA (Mulligan et al., *Nature* 277, 108, 1979). Several globin cDNA inserts carrying deletions in the leader region (Meyer et al., *Experientia* 35, 972, 1979) were tested in SV40 vectors. SV40 recombinants carrying the different modified globin inserts, in particular one in which the deletion reached up to the 3rd nucleotide preceding the initiator triplet, all elicited rabbit β -globin synthesis similar (within a factor of 2) to the one carrying the original wild type insert. The results indicate either that almost all of the 5' nontranslated region of the rabbit β -globin mRNA is expendable or that its function can be substituted with similar efficiency by adjacent SV40 specific sequences.

Organization of the modification and restriction genes of bacteriophages P1 and P15

J. Meyer, S. Iida, S. Hadi, B. Bächli, P. Caspers, M. Stålhammar-Carléalm, S. Schrickel, T.A. Bickle and W. Arber, *Department Microbiology, Biozentrum der Universität, CH-4056 Basel*

The results from transposition mutagenesis, DNA restriction cleavage analysis, electron microscopic heteroduplex and in vitro transcription mapping, and studies on the purified EcoP1 and EcoP15 restriction endonucleases taken

together allow the following conclusions to be drawn: 1. Both genes are contained in a DNA segment of about 5 kb, 2 kb specifying modification (Mod) and 3 kb coding for restriction (Res) function. The DNAs of P1 and P15 are homologous in the Res gene, while nonhomologous for about 1 kb at 1 end of the Mod gene. This sequence difference must account for the different DNA specificity of the 2 endonucleases. 2. The purified, *EcoP1* and *EcoP15* enzymes are composed of 2 subunits, of which the smaller one (mol.wt 75,000) determines specificity and is alone responsible for modification and the larger one (mol.wt 110,000) is necessary for restriction. These protein sizes correspond well to the coding capacity of the respective gene regions. 3. Transcription starts at the 'nonhomologous' end of the Mod gene and proceeds into the Res gene.

Are viral T-antigens involved in regulation of protein synthesis?

M.R. Michel and M. Schwyzer, Université de Genève, Département de Biologie moléculaire, 30, quai Ernest-Ansermet, CH-1211 Genève 4

Infection with SV40 or polyoma virus leads, shortly after appearance of viral T-antigen, to a stimulation of host cellular RNA and protein synthesis (Khandjian et al., PNAS, in press). We therefore tested the hypothesis that T-antigens interact with translational initiation complexes and modify the regulation of protein synthesis. Nuclei and cytoplasm of SV40-infected CV-1 cells were separated. The cytoplasmic fraction, which contained 5–10% of total large T-antigen, was analyzed by zonal centrifugation in sucrose gradients. Substantial amounts of cytoplasmic large T-antigen were found to sediment in the 40S, 60S, 80S and disomal region. Further analysis of these regions showed that T-antigen was associated with ribonucleoprotein, and that this association was salt-resistant: upon resedimentation through sucrose gradients containing 0.5 M KCl, large T-antigen cosedimented with the 40S ribosomal subunit. This finding implies a possible involvement of T-antigen in regulation of protein synthesis.

Noneukaryotic DNA-containing structures.

II. Induced loss of intracellular alkalis and polyamines affect the shape of bacterial nucleoids

M. Moncany, F. Borle and E. Kellenberger, Department of Microbiology, Biozentrum der Universität Basel, CH-4056 Basel

Strong changes of shape are induced by radiations, antibiotics and changes of growth conditions. Our results show that they are induced by modifications of the intracellular concentrations of alkalis and likely also of other small molecules. Fixation by glutaraldehyde or OsO₄ 0.01% induce nuclear dispersion, which we show to be correlated with an induced loss of K by studies which flame photometry (with H. Seiler and H. Jütte). Because of its high protein content the cytoplasm is fixed faster than the nucleoids and thus determine the shape of the latter. Fixation induced permeability modify the intracellular conditions and the shape of the nucleoids before the cytoplasm becomes fixed. Loss of K induces a dispersion (unfolding) of the initially more confined nuclear material into the cytoplasm. Agents which produce dispersed nuclei, as e.g. sublethal doses of UV- and X-rays are thus checked for a possible investigated in the above contexts.

Distribution of filipin-sterol complexes at sites of endocytosis and exocytosis. A freeze-fracture study

R. Montesano, P. Vassalli and L. Orci, Institutes of Histology and Pathology, CH-1211 Geneva 4

The distribution of membrane cholesterol was studied with the ultrastructural probe, filipin (Elias et al., J. Hist. Cyt. 27, 1247) in endocytosing macrophages and degranulating mast cells. Macrophages were induced to phagocytosis (with opsonized erythrocytes) or pinocytosis (with Con A or BSA), fixed in glutaraldehyde-filipin and freeze-fractured. Filipin-sterol complexes (FSC) (recognizable as 30 nm protuberances) were plentiful on the plasma membrane, on the membrane of erythrocyte-containing phagosomes, on the large vacuoles induced by Con A and on the smooth membrane invaginations and vesicles induced by BSA, but were absent from coated endocytotic pits. In purified mast cells, FSC were uniformly and densely distributed on plasma and secretory granule membranes, both in intact cells and during polymyxin B-induced degranulation. These results suggest that: a) different types of endocytotic membranes may have a different cholesterol content, b) sites of exocytotic membrane fusion appear not cholesterol-deprived.

High-pressure freezing: application to the freeze etching of nerve tissue

H. Moor, G. Bellin and C. Sandri, Department of Cell Biology, Swiss Federal Institute of Technology, CH-8093 Zürich, and Institute for Brain Research, University of Zürich, CH-8029 Zürich

Small blocks (0.5–1.0 mm in diameter) have been treated with the high-pressure (2000 bar) freezing method which obviates the use of aldehyde fixation and glycerol cryoprotection. The freeze-fracture replicas obtained with this method compare favorably with those prepared in the conventional manner from Freon frozen material. The formation of large ice crystals is prevented, deep etching is facilitated. Intra- and extracellular structures such as microtubules, filaments, mitochondrial cristae and collagen fibres (and their periodicity) appear clearly against a finely granulated background. An additional advantage is the applicability of freeze substitution to unfixed tissue which opens the way for the further improvement of cytochemistry.

Maturation of Parvovirus LuIII in a subcellular system

D.E. Müller and G. Siegl, Institute of Hygiene and Medical Microbiology, University of Bern, CH-3010 Bern

An in-vitro system prepared by lysis of LuIII-infected cells with Brij-58 was recently described by M. Gautschi and P. Reinhard (J. Virol. 27, 453, 1978). In this system progeny single-stranded DNA is synthesized and subsequently packaged into virus particles. The same system was now used to study both the sequence of events and the structural intermediates in the maturation of Parvovirus LuIII. Under optimal conditions viral DNA pulse-labelled for 15 min could be chased into mature virus particles at a constant rate during at least 60 min. Cautious extraction of nucleoproteins and centrifugation in linear sucrose gradients revealed that pulse-labelled DNA is associated with several distinct structures sedimenting between 70 and 150S. From there it can be chased into mature 110S virions. The isolated and fixed nucleoprotein complexes band at a medium density of 1.37 g/ml in CsCl and, according to electron microscopical observations, consist of nucleic acid molecules and viral capsid structures.

Circadian (daily) rhythm of liver cell membranes.

A morphometric study

O.M. Müller, Anatomisches Institut der Universität Bern, CH-3012 Bern

36 male Wistar rats were kept under standardized conditions in a climate chamber. They had light from 7.00 to 19.00 h and darkness from 19.00 to 7.00 h. Food and water was available ad libitum. After a period of 3 weeks for adaption all animals were sacrificed in one uninterrupted 24-h-period, 4 animals every 3 h. After exsanguination a small piece of liver was processed for light and electron microscopy. – The morphometric evaluation of the hepatic parenchyma showed, that the surface area of the smooth endoplasmic reticulum and the Golgi vesicles increase significantly during the dark period, in which the animals are more active. The surface is reduced during the first hours of the resting period, when the light was turned on. A similar behavior is found in the surface of mitochondrial membranes and the rough endoplasmic reticulum, although to a lesser extent. Possible circadian changes of the plasmalemma are covered by great individual changes. The morphological findings fit very well to circadian changes in mitochondrial activity and hexobarbital degradation as already reported.

Recombination between redundant tRNA genes in

Schizosaccharomyces pombe

P. Munz, R. Aebi, C. Gysler, J. Kohli and U. Leupold, Institut für Allgemeine Mikrobiologie, Universität Bern, Altenbergrain 21, CH-3013 Bern

In *S. pombe* 4 opal suppressors code either for a mutated serine tRNA (*sup3*, *sup9*) or a changed leucine tRNA (*sup8*, *sup10*). The frequency of suppressor active revertants among meiotic spores obtained from selfings involving inactive double-mutant alleles at the *sup3* and *sup9* loci is up to 75 times higher than in a control selfing involving the suppressor inactive wild-type allele. Similar but less pronounced results were obtained with *sup8* and *sup10*. We believe that a vast majority of these prototrophs are generated by a mechanism of heterologous recombination rather than mutation. Supporting this notion is the fact that no corresponding increase is found in parallel experiments with vegetative cells. Additional support comes from the selfing of a strain carrying 4 mutations in the *sup3* gene. The frequency of suppressor active revertants is comparable to the one found in selfings between double mutant strains.

Transient peaks of cyclic AMP following chemotactic stimulation of human neutrophil granulocytes

A. Naef and H. U. Keller, Department of Pathology, University of Bern, CH-3010 Bern

Several purified cytotoxins such as chemotactic serum peptides (CAT 1.6.1., C5a_{desArg}) or the synthetic peptide f-Met-Leu-Phe induce a transient increase in intracellular cAMP levels within the first min following stimulation. Chemokinetic agents such as HSA or immune complexes have no such effect. The peak is observed regardless whether or not the medium contains human serum albumin. While a primary stimulation with C5a_{desArg} (6.7×10^{-8} M) induced a clear-cut peak, a second exposure of washed neutrophils with the same agent had a smaller or no such effect. Unlike C5a_{desArg} f-Met-Leu-Phe (5×10^{-8} M) produced also a second peak upon secondary stimulation. The relationship between cAMP levels and chemotaxis is discussed.

Isolation and characterization of the messenger RNAs for the mouse complement components C3 and C4

K. Odink and G. Fey, Institut Suisse de Recherches expérimentales sur le Cancer, Chemin des Boveresses, CH-1066 Epalinges

Mouse liver mRNA was size-fractionated by sucrose gradient centrifugation and the ≥ 5 kb fraction was shown to contain mRNA for C3 and C4 by in vitro translation and subsequent direct immunoprecipitation. The immunoprecipitated material migrates by SDS-PAGE as 175 kdaltons and 185 kdaltons for prepro-C3 and prepro-C4, respectively. Mouse liver mRNA, when fractionated by electrophoresis on agarose gels containing MeMgOH, shows several discrete RNA-species ≥ 6 kb. Bands containing these species were cut out and the RNA was eluted and translated in vitro. Cell-free synthesis of proteins, comigrating with prepro-C3 and prepro-C4, was detected with RNA from bands of 7.5 kb and 8.4 kb, respectively.

Junctional combinations in the arachnoidea of the meninges

F.X. Omlin and A. Bischoff, Department of Neurology, University of Bern, Inselspital, CH-3010 Bern

The arachnoidea represents a barrier for the cerebrospinal fluid between the dura and subarachnoid space of the meninges (Nabeshima et al., J. comp. Neur. 164, 127, 1975). In order to elucidate the relation of functional and morphological aspects, mice optic nerves have been investigated by application of 3 different EM-methods. Thin sections and scanning preparations served as resource for orientation and layer identification. Only freeze-fractured tissue exhibits fibrils of tight junctions which are juxtaposed to hexagonally packed particles and pits of gap junctions (Mc Nutt et al., Progr. Biophys. molec. Biol. 26, 47, 1973). About 90% of these gap junctions are surrounded and/or crossed by the fibrils of occludens junctions. Therefore the arrangement of these particles and pits depends on the course of the corresponding tight junction. These perijunctional insulations could be responsible for the high efficacy of the seclusion mechanism of this barrier.

Structural studies on λ -exonuclease from bacteriophage λ

J. van Oostrum, Janice L. White, Barbara Wernli and R. M. Burnett, Biozentrum der Universität Basel, CH-4056 Basel

λ -Exonuclease is a deoxyribonuclease which is induced by bacteriophage λ of *Escherichia coli*. Mutations affecting genetic recombination are located in the structural genes for the protein. An improved purification procedure has provided sufficient material for characterization of the protein and the growth of crystals suitable for X-ray diffraction. SDS polyacrylamide gel-electrophoresis and equilibrium ultracentrifugation have shown that the molecule is a tetramer of mol.wt 108,000. Morphologically perfect crystals show no birefringence when inspected with a polarizing microscope indicating cubic symmetry, which has been confirmed from preliminary diffraction patterns ($a=208$ Å). Our long-term goal is to investigate at an atomic level the fine discrimination displayed by λ -exonuclease, in its interactions with DNA, in order to further our understanding of the mechanism of genetic recombination.

Heterogeneous distribution of filipin-sterol complexes on the luminal plasma membrane of toad urinary bladder granular cells

L. Orci, R. Montesano and D. Brown, *Institute of Histology, CH-1211 Geneva 4*

Cholesterol was localized on the membranes of granular cells from freeze-fractured toad bladders stretched by injection of fixative containing the sterol specific probe, filipin (Elias et al., *J. Histochem. Cytochem.* 27, 1247, 1979). While the luminal membrane of some cells had a heavy, homogeneous labelling, others had clusters of filipin-sterol complexes scattered on an otherwise poorly labelled membrane. The clusters were seen to overlie cytoplasmic granules, whose membranes were heavily labelled. In tissue fixed without filipin, many images of presumed granule exocytosis were seen. It is possible, therefore, that the clusters of complexes represent sites of interaction between granule and luminal membranes. In addition, complexes were absent from vasopressin-induced particle aggregates, even when the rest of the membrane was heavily labelled. This study pinpoints a heterogeneous distribution of sterols which could be important in the chain of events leading to permeability changes in this tissue.

Identification of a glycoprotein involved in cell adhesion during the latter stages of *Dictyostelium* differentiation

R. W. Parish and C. Steinemann, *Institut für Pflanzenbiologie, Universität Zürich, Zollikerstrasse 107, CH-8008 Zürich*

Univalent antibodies were used to identify a glycoprotein participating in the adhesion of *Dictyostelium discoideum* cells. This glycoprotein has an apparent mol.wt of 95 kdaltons, is first synthesized during the latter stages of differentiation (tip stage to culmination stage) and incorporates labelled fucose and glucosamine. It apparently replaces another glycoprotein ('contact sites A') which is involved in cell adhesion during the earlier aggregation stages.

Calcium-induced discharge of melanosomes from iris epithelial cells

L. Patmore and T. Yamada, *ISREC, CH-1066 Epalinges*

Fully differentiated iris epithelial cells (IECs) of adult newts can be converted into lens cells when they are induced to proliferate by lens removal in situ or by putting into culture. During cell-type conversion melanosomes disappear from IECs before lens differentiation starts. In culture discharge of melanosomes can be induced by increasing the intracellular calcium ion concentration. This is achieved by microinjection of calcium into the cytoplasm, fusion of calcium-containing phospholipid vesicles with the IEC membrane or by exposure to the calcium ionophore A23187. Calcium ions may provide a stimulus to initiate exocytosis similar to a stimulus-secretion coupling action, or be involved in a membrane-microfilament interaction which results in melanosome expulsion. – Another effect of raising the intracellular calcium ion level is a modification of cell shape similar to that observed when cAMP is injected into IECs (T. Yamada, *Mono. Dev. Biol.* 13, 1977). This suggests that calcium may be acting in association with cAMP.

Sendai virus stimulates chemiluminescence in mouse spleen cells

E. Peterhans, *Microbiology Department, The John Curtin School of Medical Research, Australian National University, Canberra A.C.T. 2601, Australia*

Nonadherent C57BL/6 mouse spleen cells were infected with purified egg grown Sendai virus, and chemiluminescence (CL) was monitored in a Liquid Scintillation Spectrometer operated in the out of coincidence mode. CL increased within 30 sec, reaching a peak at 6–8 min post-infection and declining thereafter. CL induction was independent of the virus genome (UV-irradiation of virus). In contrast, the spike envelope glycoproteins were essential, as CL could not be stimulated by Pronase-treated virus while reconstituted viral envelopes possessing the HN and F glycoproteins were effective in CL induction. The removal of F from the virus resulted in a marked decrease of CL with a shift of the peak from 6–8 to 2–4 min. CL with the latter kinetics was also induced by Sendai virus grown in MDBK cells, known to possess the inactive precursor of F, F₀. Cleavage of F₀ into F by trypsin resulted in an increase of CL and shifting back of the peak to 6–8 min. The biochemical reactions leading to light emission occur both in B- and T-lymphocytes.

Tn2301 transposition: in vivo isolation of a λ cosmid carrying the resistance plasmid pPJ3a and Tn2301

J. Cl. Piffaretti, *Département de Microbiologie, FM, Université de Genève, 22, quai Ernest-Ansermet, CH-1205 Genève*

Tn2301 is a transposon closely related to TN3 and specifying ampicillin resistance; pPJ3a is a resistance plasmid conferring resistance to streptomycin and sulfonamide; pPJ3b is a derivative of pPJ3a carrying Tn2301. We have constructed a λ cosmid carrying pPJ3b sequences by Tn2301 mediated transposition in vivo. Heteroduplex analysis and restriction enzyme digestions showed that pPJ10 is composed of pPJ3a adjacent to Tn2301, flanked by 14.9 kb and 8.4 kb λ DNA. Genetic and biochemical experiments have shown that: a) the presence of pPJ10 in the cell does not confer immunity to λ ; b) pPJ10 replicates using the replication system of pPJ3a; c) pPJ10 can be packaged in λ head and transduced, provided the cell contains a λ helper; d) pPJ10 can dissociate in *recA*⁺ or *recA*[−] hosts and give rise to smaller plasmids close or identical to pPJ3a or pPJ3b. This excision is probably mediated by transposition mechanism.

Involvement of carbohydrate and protein functional groups in cell-cell adhesion

P. Pippia, A. Cogoli and G. Ivaldi, *Istituto di Fisiologia generale, Università di Sassari, Sassari, Italy, and Laboratorium für Biochemie, ETH Zürich, CH-8092 Zürich*

The mechanisms localized on the cell membrane which regulate recognition, cellular adhesion and mitotic control have probably a common molecular basis. The objective of our study was to identify by chemical and enzymatic modifications carbohydrates and functional groups involved in the adhesion of neoplastic cells (SGS-2). The variations of the adhesion induced by degradation with neuraminidase, by oxidation with periodate, and by treatment with periodate followed by reduction with NaBH₄ indicate that sialic acid plays a regulatory role, without being a ligand, in the adhesion process. The decrease of adhesion either by treatment with fucosidase or by simul-

taneous exposure of single labelled cells to neuraminidase and galactose oxidase suggests the involvement of fucose and galactose in the process. SH-groups may be needed for adhesion since iodoacetamide is a strong inhibitor. The inhibition is lower with carbodiimide and imidoesters which specifically react with COOH and NH₂ groups, respectively.

Properties of single-strand DNA-binding proteins involved in mammalian DNA replication

P. Reinhard, B. Müller and R. Schindler, Department of Pathology, Freiburgstrasse 30, CH-3010 Bern

Semiconservative DNA replication in CHO cells partially lysed with the detergent Brij-58 is stimulated by cell extract. DNA replication in this system is inhibited by single-strand (ss) DNA (50% of molecules shorter than 5×10^4 daltons) due to formation of complexes with factor(s) present in the cell extract. Complex formation is not observed with pronase-digested cell extract indicating that the responsible factor(s) are proteins. They protect ss DNA (but not ds DNA) against digestion by DNase I. Protecting activity is decreased by preincubation of cell extract at 60 °C for 5 min, whereas preincubation at 42 °C for 30 min has little effect. At least in part, protecting activity is bound to ss DNA-cellulose and eluted with a buffer containing 800 mM KCl. The observation that ss DNA of approximately 1.5×10^6 daltons exhibits template activity if incubated with cell extract also suggests a functional role of ss DNA-binding proteins in DNA replication.

Characterization of polyoma virus T-antigens present in hamster tumor cells

V. Rey-Bellet and H. Türlér, Department of Molecular Biology, University of Geneva, 30, quai Ernest-Ansermet, CH-1211 Geneva 4

In a cell line derived from a polyoma-induced hamster tumor small (23 kdaltons) and middle (58 kdaltons) but no large (100 kdaltons) polyoma T-antigens were detected. Instead a protein of about 61 kdaltons was observed both in the nuclear and cytoplasmic fraction of these cells. Different clones derived from the original cell line and cells isolated from tumors induced by the original cell line or by cloned cells always gave the same result. Furthermore, 2 new cell lines isolated independently from polyoma virus-induced tumors, also lacked large T-antigen. Analysis by 2-dimensional gel-electrophoresis and by ³²P-labelling suggest that the 61 kdaltons protein is a truncated form of large T-antigen. Our observations and similar results obtained simultaneously in other laboratories (NIH and McGill University) indicate that large T-antigen and part of the early region of the viral genome are not required for tumor formation. Experiments are done in vivo and in vitro to get information on the selective pressure leading to the partial elimination of viral genetic information in hamster cells.

Electron microscope study of duck globin mRNA precursor cross-linked in situ

C. Raymond, A.M. Agliano, A. Nacci and G. Spohr, Embryologie moléculaire, Université de Genève, CH-1211 Genève 4

In duck erythroblast nuclei a significant fraction of globin mRNA precursor is hydrogen-bonded within structures of high mol.wt and fast turnover. The hydrogen-bonded structures were cross-linked in situ with aminomethyltrioxalene

and UV-light. The precursors were then hybridized with globin cDNA and spread for electron microscopy. – The observed hybrids display double-stranded segments the length of the globin mRNA and frequently 2 single-stranded tails located within the coding regions (cross-like structures) or single-stranded loops. One of the globin pre-mRNA appears to have only 1 intron. The other seems to contain 3 introns located close to each other or 1 or 2 introns folded into 3 loops. These introns do not appear to be removed in an orderly manner during processing. It can be postulated that endonucleolytic cleavages occur within the intron resulting in cross-like structures as intermediate steps in mRNA processing.

Identification of supra-ependymal 5-HT nerve fibres in human brain

J.G. Richards, H.P. Lorez, V.E. Colombo, R. Guggenheim and D. Kiss, Pharmaceutical Research Department, Hoffmann-La Roche & Co. Ltd, CH-4002 Basel, SEM Laboratory, University of Basel, and Institute of Pathology, CH-4410 Liestal

Transmission and scanning electron microscopy of the ventricle surface of human postmortem brain reveal varicose nerve fibres traversing between cilia and microvilli of ependymal cells. The varicosities, containing numerous small electron-lucent vesicles and frequent large opaque vesicles, are anchored to the surface by desmosomes. Supraependymal nerve fibres were observed in the lateral ventricles (n.caudatus), 3rd ventricle (habenula), interventricular foramen (stria medullaris) and floor of the 4th ventricle in brains of 5 cases. In one of these, a yellow formaldehyde-induced fluorescence was observed on the floor of the 4th ventricle. Its discrete granular aspect, rapid fading and color were typical of 5-HT nerve fibres observed in rat brain. The unique localization of this nerve plexus, in direct contact with the cerebrospinal fluid, raises the question of the target for the impulse-released 5-HT. Are the desmosome-like junctions between the varicosities and ependymal cells truly functional synapses at which 5-HT exerts its effect or does the released amine act, like a neurohormone, on more distant targets?

Sequence organization of nuclear and cytoplasmic 5S RNA genes in *Chlamydomonas*

J.-D. Rochaix, B. Allet and J.-L. Darlix, Département de Biologie moléculaire, Université de Genève, CH-1211 Genève 4

3 distinct protein synthesizing systems exist in the unicellular alga *Chlamydomonas*. They are located in the nucleocytoplasm, chloroplast and mitochondria. In order to examine the relatedness of these systems, we have compared the sequence organization of the genes coding for cytoplasmic and chloroplast 5S RNA. The chloroplast 5S RNA genes are present twice in each chloroplast DNA molecule and they are located very close to the other rRNA genes in the order 16S-7S-3S-23S-5S. Fine structure mapping and DNA sequencing have shown that the beginning of the 5S RNA gene is located 35 bp away from the end of the 23S rRNA gene. A large portion of the chloroplast 5S RNA has been sequenced and correlates well with the DNA sequence. 4 helical regions can be recognized and the region between residues 30–60 shows a striking similarity with the corresponding *Escherichia coli* 5S RNA sequence. The cytoplasmic 5S RNA sequence has also been established and differs considerably from the chloroplast sequence. In addition the nuclear 5S RNA genes are not closely linked to the other rRNA genes.

Computer-assisted reconstruction of the mitotic spindle of the cellular slime mold *Dictyostelium discoideum*

U.-P. Roos, J. R. McIntosh, K. L. McDonald and B. Neighbors, *Institut für Pflanzenbiologie, Universität Zürich, CH-8008 Zürich, and Department of Molecular, Cellular and Developmental Biology, University of Colorado, Boulder, CO 80309, USA*

Flat-embedded amebae of *D. discoideum* were examined with the light microscope and cells in selected stages of mitosis were processed for thin-sectioning. We used computer graphics technology (McIntosh et al., *J. Cell Biol.* 83, 428, 1979) to reconstruct mitotic spindles from profiles of microtubules (MTs) in electron micrographs of serial cross sections. The central spindle consists mainly of 2 sets of MTs, each of which originates in one of the spindle pole bodies (polar MTs). In metaphase, some MTs appear to extend from pole to pole (continuous MTs). A variable number of fragment-MTs, having neither end at a pole, occur in all the stages investigated. From anaphase to telophase, the region of overlap of the 2 sets of polar MTs decreases in length, a result that is compatible with a sliding mechanism during spindle elongation.

Extracellular control of cell development in *Dictyostelium discoideum*

C. Rossier, *Abteilung Zellbiologie, Biozentrum der Universität Basel, CH-4056 Basel*

Fluctuation of cAMP production is a prerequisite for optimal stimulation of development in strain Ax-2 of *D. discoideum* (Gerisch et al., 1975). Steady cAMP concentrations in the nanomolar range delay differentiation. In contrast, pulsatile as well as continuous addition of cAMP stimulates extracellular phosphodiesterase (ePD) and inhibits the production of its inhibitor (PDI). Steady levels of stimulant can be obtained by use of a slowly hydrolyzed cAMP analogue, 3',5'-cyclic phosphorothioate (cAMP-S). Like cAMP, the analogue seems to act via cell surface receptors. Effects of extracellular stimulants are under genetic control. Mutants resistant to the inhibitory effects of cAMP-S on development (cAMP-S^r) are partially independent of the periodic cAMP signals with respect to differentiation. One class is characterized by minute fruiting bodies ('fruity' phenotype, Sussman, 1955). cAMP-S resistance is not due to ePD overproduction. One cAMP-S^r mutant secretes low amounts of ePD and overproduces PDI.

Advances in specimen preparation for electron microscopy. IV. Immunocytochemistry on thin sections with the protein A-gold (pAg) technique

J. Roth, M. Bendayan, E. Carlemalm and W. Villiger, *Institute of Histology and Embryology, University of Geneva Medical School, CH-1211 Geneva, and Department of Microbiology, Biocenter, University of Basel, CH-4056 Basel*

The pAg technique (Roth et al., *J. Histochem. Cytochem.* 26, 1074, 1978) allows the localization of antigenic sites in thin sections of Epon-embedded tissue. In the present study we have assessed the feasibility of using a low temperature embedding procedure with a polar mixture of methacrylates for the pAg technique. Amylase was localized in thin sections of rat pancreatic tissue embedded in methacrylate at low temperature or in Epon. A quantitative evaluation showed a more specific labelling of the rough endoplasmic

reticulum, Golgi apparatus and zymogen granules for methacrylate-embedded tissue than for Epon-embedded tissue due to a significant decrease of the background staining. Moreover, the better preservation of the general cellular ultrastructure, particularly of the Golgi apparatus allowed a more precise localization of the labelling.

Cyclosporin A: specific binding to mouse thymocytes

B. Ryffel, U. Goetz, M. Tschopp and Ch. Hodel, *Preclinical Research, Sandoz Ltd, CH-4002 Basel*

Cyclosporin A (CS-A) is a cyclic endecapeptide known to suppress thymus derived lymphocyte functions (J.F. Borel et al., *Immunology* 32, 1017, 1977). In addition CS-A induces morphological changes in the thymus characterized by cellular depletion and signs of cell death in the cortex (B. Ryffel and H. Deyssenroth, *Int. Meeting on Inflammation, Verona 1979*). The results of binding studies employing ³H-CS-A revealed the presence of a single population of high affinity binding sites on mouse thymocytes which show a maximum capacity of 2.5 pmoles/10⁶ cells and a K_D of 7.5 × 10⁻⁸ M. The characteristics of the specific component of CS-A binding (K_D, threshold concentration at which maximum binding occurred) all correlated well with the equivalent parameters obtained for the inhibitory effect of the drug on mitogen induced (Con A) thymocyte proliferation. Together this data suggest that, in addition to the established effect of CS-A on peripheral lymphocytes, there is an interaction of the drug with specific receptors located on thymic lymphocytes.

Structure and in vivo transcription of *Xenopus* vitellogenin genes

G.U. Ryffel, T. Wyler, D.B. Muellener, W. Wahli, I.B. Dawid and R. Weber, *Zoologisches Institut, Sahlistrasse 8, CH-3012 Bern, and Laboratory of Biochemistry, National Cancer Institute, Bethesda, Maryland 20014, USA*

We have isolated from a *Xenopus* DNA library genomic DNA clones of about 16 kb of the 2 closely related vitellogenin genes A1 and A2. By electron microscopic analysis of R-loops of these genomic DNA clones with the vitellogenin mRNA we discovered 33 introns within the A1 and the A2 genes which measure 19 and 15 kb respectively. Analysis of heteroduplexes between A1 and A2 specific genomic clones revealed a hybrid structure indicating that the introns do not pair since they differ in length and sequence whereas the exons form hybrids since they are similar in sequence. From R-loops between RNA enriched for the presumed vitellogenin pre-mRNA and a cloned vitellogenin cDNA we established that at least the 12 major introns at the 3' end of the A1 gene are present in the presumed vitellogenin mRNA precursor.

Analysis of polyoma tumor antigens

C. Salomon and H. Türlér, *Department of Molecular Biology, University of Geneva, CH-1211 Geneva 4*

At least 3 distinct proteins called tumor (T)-antigens react specifically with antipolyoma T-serum and can be isolated in this way from polyoma-infected cells. The 3 T-antigens have a common amino terminal sequence and their complete amino acid sequence can be deduced from the known nucleotide sequence of the viral genome. Previously we had shown that large polyoma T-antigen (100 kdaltons) undergoes posttranslational modification in permissive cells. To get more information on modifications of the T-antigens we have analyzed wild-type and tsA mutant T-antigens by

2-dimensional gel-electrophoresis. In isoelectric focusing gels abnormal migration of all 3 T-antigens was observed without alkylation. After exposure to N-ethylmaleinimide the T-antigens showed considerable charge heterogeneity.

Gap junctions between pancreatic B-cells may increase independently of insulin secretion

M. S. Sheppard and P. Meda, *Institute of Histology and Embryology, University of Geneva, CH-1211 Geneva 4*

An increase of gap junctions between insulin-producing cells (B-cells) was observed during stimulation of insulin secretion (P. Meda et al., *J. Cell Biol.* 82, 441, 1979). However it is uncertain whether these 2 events are obligatorily linked. We have assessed B-cell gap junctions in freeze-fracture replicas of isolated rat islets of Langerhans incubated for 90 min with tetraethylammonium (TEA, 20 mM), a K^+ conductance blocker shown to enhance insulin release from islets (J.C. Henquin, *Biochem. biophys. Res. Commun.* 77, 551, 1977) and to increase gap junctions in smooth muscle cells (M.S. Kannan and E.E. Daniel, *J. Cell Biol.* 78, 338, 1978).

The results show that TEA significantly increases the median number of particles per gap junction at both 2.8 and 6 mM glucose but augments insulin release only in the presence of the higher glucose level. Thus B-cell gap junctions can be modified in absence of altered insulin release.

Cloning of genes transcribed in the oocyte of *Xenopus laevis*

G. Spohr, *Département de Biologie animale, Université de Genève, Embryologie moléculaire, 154, route de Malagnou, CH-1224 Chêne-Bougeries*

The overall aim of our study is to identify and characterize genes which are expressed coordinately during development of *X. laevis*. Embryonic DNA from *X. laevis* was cloned in Charon 9 coliphage. To identify recombinants containing DNA sequences which are transcribed in the oocyte and possible regulatory DNA segments, the *X. laevis* library was screened by hybridization with hnRNA from oocytes labelled in vitro with polynucleotide kinase and with repetitive DNA labelled by nick translation. 103 clones containing DNA segments ranging from a few hundred bases to 10 kb were selected. Of 75 clones containing repetitive DNA sequences 57 also contained sequences which hybridize with hnRNA.

Formation of planar membranes from natural liposomes and from lipid-protein vesicles

H. Schindler, *Biozentrum der Universität, Department of Biophysical Chemistry, Klingelbergstrasse 70, CH-4056 Basel*

Planar bilayers were formed via the transformation: vesicle → monolayer → bilayer. Monolayer formation from vesicles occurs spontaneously at the surface of any vesicle solution. Monolayer properties and conditions for bilayer formation from 2 such monolayers have been traced down to properties of the vesicles (H. Schindler, *Biochim. biophys. Acta* 555, 316, 1979, and *FEBS Lett.*, in press). This transformation of vesicles to bilayers via monolayers allows a combined study of the same lipid-protein sample in these 3 organizations including vesicle-monolayer transfer. Application to natural liposomes (from Torpedo electric organ and from the outer membrane of *Escherichia coli*) provided a characterization of the electrical membrane activity without having removed membrane components from their

native environment. Bilayer formation from reconstituted vesicles was used to assign this activity to properties of certain components of the natural membranes.

Establishment of a liver cell line with differentiated liver functions

Susanna E. Schlegel-Haueter, W. Schlegel and Janice Y. Chou, *NICHD, National Institutes of Health, Bethesda, MD, USA, and Fondation pour Recherches Médicales, 64, avenue de la Roseraie, CH-1211 Geneva*

Fetal rat liver cells were transformed by a temperature-sensitive mutant (*tsA255*) of simian virus 40. A permanent cell line (*RLA255-4*) which showed transformed features at 33 °C (permissive temperature) and nontransformed features at 40 °C (restrictive temperature) was isolated. The cells retained differentiated liver functions. They produced albumin and transferrin with low production rates in cells with transformed features and enhanced rates in cells with nontransformed features. These protein productions were also stimulated by 8Br cAMP, methylisobutylxanthin and by cortisol. The *RLA255-4* cells grown at either temperature contained functional specific receptors for glucagon which were measured by cAMP accumulation in response to glucagon. Cortisol added to the culture medium enhanced the glucagon response selectively in cells grown at the restrictive temperature.

A plasmid allowing preparation of phage Q β RNA containing lethal mutations

A. Schmid, M. Palmieri and M. Billeter, *Institut für Molekularbiologie I, Universität Zürich, CH-8093 Zürich*

The complete Q β sequence, transcribed into DNA and flanked by AT-regions (Taniguchi et al., *Nature* 234, 223, 1978; Billeter et al., *Experientia* 34, 957, 1979) was integrated into a plasmid containing the λP_L promoter, the Amp R of pBR322, the ori of col E1 and the Kan R of pCRI (kindly provided by W. Fiers). The Q β insert substitutes for part of the Amp R gene, and its transcription is under P_L control. In a host producing ts λ repressor this plasmid is maintained at 28 °C, but at 42 °C Q β plus strand RNA is made at a rate 10% that of total RNA synthesis, and the cells lyse, producing about 20–50 infectious particles per cell. Oversize Q β RNA isolated from the cells by chromatography on oligo(dT) cellulose under appropriate conditions has a specific infectivity about 1/6 that of normal Q β RNA, suggesting that the regions flanking the Q β sequence are removed efficiently in spheroplasts. Thus, it is now possible to produce Q β RNA containing lethal mutations and to study its properties.

Macrophage activation: correlation of enzyme levels and secretion rates with cellular RNA

J. Schnyder, B. Stadler, M. Baggiolini and A. de Weck, *Institute of Clinical Immunology, CH-3010 Bern, and Research Institute Wander Ltd, CH-3001 Bern*

Activation of mouse peritoneal macrophages results in a marked increase in cellular protein, lactate dehydrogenase and alkaline phosphodiesterase. In addition, activated cells secrete high amounts of lysosomal glycosidases and plasminogen activator. In macrophage populations which were obtained from stimulated mice or which were exposed to stimuli in culture, the percentage of cells with high RNA content as determined by cytofluorimetry is also increased (*Eur. J. Immun.*, 8, 243, 1978). – We have

now assayed the above enzymes and determined the RNA frequency distributions in macrophage populations of different degrees of activation. Increase in enzyme levels correlated closely with an increase in the proportion of cells with high RNA contents. Similar assays in macrophage subpopulations showed that plasminogen activator is secreted exclusively by cells with high RNA content. RNA cytofluorimetry, therefore, appears to qualify as a rapid test for macrophage activation.

The interaction of melittin and ACTH₁₋₂₄ with planar lecithin bilayers

P. Schoch, D. Sargent and R. Schwyzer, *Institut für Molekularbiologie und Biophysik, ETH, CH-8093 Zürich*

The capacitance minimization technique (J. Memb. Biol. 46, 71, 1979) was used to measure the membrane surface potential following the addition of charged molecules to 1 side ('cis') of the bilayer. The bee venom melittin shows simple binding behavior. No charges appear on the trans side of the bilayer, showing that no part of the molecule crosses the membrane. A quantitative analysis of the binding curve requires allowance for discrete charge effects. ACTH₁₋₂₄ shows a more complex interaction. The transmembrane potential depends on ionic strength and pH on the trans side, indicating that some of the charges move across the lipid core. As complete ACTH₁₋₂₄ molecules do not cross the membrane, we conclude that a limited region – probably the N-terminus – is inserted through the bilayer. The kinetic data are consistent with a fast adsorption followed by a slower insertion step. The significance of the penetration of pure lipid membranes for hormone action and receptor function will be discussed.

Insulin binding and insulin action adipocytes of hypophysectomized rats

E. Schoenle and E. R. Froesch, *Stoffwechsellabor, Medizinische Klinik, Universitätsspital, CH-8091 Zürich*

The number of insulin-binding sites on fat cells of hypophysectomized rats is decreased to about 65% although serum levels of insulin are low in such rats. Furthermore, insulin does not stimulate glucose transport and metabolism in fat cells of hypox rats. Whereas lipogenesis from glucose is almost abolished, glucose transport is maximal already in the basal state and not further stimulated by insulin. These defects can be restored by administration of hormones *in vivo* in the following manner: a) administration of growth hormone normalizes the glucose carrier system, i.e. basal glucose transport is again low and insulin sensitive but lipogenesis is not affected; b) lipogenesis is normalized after administration of ACTH together with T₃. These results suggest a factor in fat cell membranes which is induced by GH *in vivo*. This factor restricts the glucose transport in the basal state and is acutely inhibited by insulin, resulting in an enhanced glucose transport. Other hexose carrier systems which are not stimulated by insulin, e.g. the fructose carrier, are not changed in fat cells of hypox rats. The characteristics of this GH-dependent, insulin-sensitive glucose transport-limiting factor are under investigation.

Lysozyme-induced lysis of bacteriophage T4 infected cells is the consequence of arrested phage synthesis

H. Scholer and E. Kellenberger, *Department of Microbiology, Biozentrum of the University of Basel, CH-4056 Basel*

Phage coded lysozyme accumulates in cells early after infection. We have shown that it acts on the rigid layer of

the cell envelopes, the peptidoglycan, as soon as phage governed protein synthesis is arrested (syn⁻). The phenotype syn⁺ is dependent on the host and on several phage genes some of them known, others suspected, to be membrane proteins. With the phenotype syn⁻, phage synthesis is arrested 30 min after infection, whether lysozyme is produced or not. Mutants syn⁻ reflect also in large plaque sizes. The well-known r-mutants ('rapid lysis') have the phenotype syn⁻ on *Escherichia coli* strain S/6 but not on others. For other hosts syn⁻ mutants are selected for the purpose of studying the functions of the membrane of phage infected cells.

Membrane properties of cultured rat sympathetic neurons during adrenergic or cholinergic differentiation

M. E. Schwab and S. Landis, *Department of Neurobiology, Harvard Medical School, Boston, MA 02115, USA*

Neurons from the newborn rat superior cervical ganglion were grown in cultures under conditions allowing either adrenergic or cholinergic differentiation. Lectins and toxins were used for the light and electron microscopic detection of transmitter- and age-related differences in the composition of the cell membrane. The densities of binding sites for concanavalin A, ricin₆₀ and wheat germ agglutinin increased dramatically with age in culture on both adrenergic and cholinergic cells. Soybean agglutinin binding increased 3-fold on adrenergic axons, but failed to increase on neurons induced to become cholinergic by medium conditioned by rat heart cells (CM). Tetanus toxin binding remained low on adrenergic and cholinergic cells at all ages. Cholera toxin binding decreased with age on adrenergic axons but increased on cholinergic ones. – These results suggest, that CM provokes a fundamental change in the phenotype of developing sympathetic neurons involving the cell membrane as well as transmitter synthesis.

Posttranslational control of repressible acid phosphatase in yeast

A. M. Schweingruber, H. Gmünder and M. E. Schweingruber, *Institut für allgemeine Mikrobiologie, Altenbergrain 21, CH-3013 Bern*

Acid phosphatase (a.pase) of *Saccharomyces cerevisiae* is a glycoprotein located mainly at the cell surface. It may be used as a model system to study regulation of a cell surface glycoprotein. A.pase is 'derepressed' upon inorganic phosphate starvation. At least 9 genes are known to take part in the regulation. A model involving repressor-operator mechanisms has been proposed (Toh-E et al., MGG 162, 139, 1978). – *In vitro* translation and immunoprecipitation studies indicated a substantial posttranslational regulation of inactive preexisting a.pase (M. E. and A. M. Schweingruber, MGG 173, 349, 1979). – We succeeded to isolate and identify a larger inactive form of a.pase. The inactive a.pase is cross-reacting to rabbit antibodies raised against active a.pase. Tryptic fingerprint analysis shows a closely related elution profile from a cation exchange column. The main structural changes seem to occur in the glycosylated portion of the protein. One important step in the regulation of a.pase may be the activation of this inactive form to active a.pase.

Two specific phosphorylation sites in simian virus 40 large T-antigen

M. Schwyzer and E. W. Khandjian, *Université de Genève, Département de Biologie moléculaire, 30, quai Ernest-Ansermet, CH-1211 Genève 4*

Limited enzymatic proteolysis of SV40 large T-antigen and amino-acid sequence analysis of the resulting fragments (Schwyzer et al., *Experientia* 35, 67, 1979) led to the construction of a cleavage map that permits to localize posttranslational modifications. T-antigen was labelled in vivo with [32 P]orthophosphate or in vitro with γ [32 P]ATP and cleaved into fragments which were analyzed by SDS gel-electrophoresis and isoelectric focusing. Using the cleavage map, we showed that T-antigen contains not only one phosphorylation site as reported previously (Tegtmeier et al., *J. Virol.* 21, 647, 1977) but at least two, located near both termini of the molecule. The dissection of T-antigen described here will facilitate chemical analysis of the different phosphorylated residues and should contribute to an understanding of their function.

Chromatin structure of globin genes in chicken

J. Stalder and H. Weintraub, *Hutchinson Cancer Research Center, Seattle, WA 98104, USA, and Institut für Hygiene und medizinische Mikrobiologie, Universität Bern, CH-3000 Bern*

We have taken advantage of the differential digestion of specific genes by DNase I to investigate the chromosomal structure of the ovalbumine gene and of the adult and embryonic globin genes during erythropoiesis in chicken embryos. The results show that at a given time there are at least 3 chromosomal states corresponding to 3 levels of DNase I sensitivity: the insensitive state corresponds to a structure inactive for expression, like the ovalbumine gene in red blood cells; a moderate sensitivity is found for structural genes potentially available for expression as well as for the chromatin domains surrounding the globin genes; and a high sensitive state – also within a moderate sensitive domain – corresponds to regions of the DNA that are or have been expressed lately. With respect to Hb gene switching, we conclude that this phenomenon appears to operate after a determinative event required to alter the domain structure of the chromatin.

Specific DNase I cutting sites in chromatin are correlated with the gene activity

J. Stalder and H. Weintraub, *Hutchinson Cancer Research Center, Seattle, WA 98104, USA, and Institut für Hygiene und medizinische Mikrobiologie, Universität Bern, CH-3000 Bern*

In chicken red blood cells, transcribed globin genes or genes potentially active for expression are located in chromosome domains moderately sensitive to DNase I digestion; the actively transcribed structural genes themselves show a very high sensitivity. In addition, mild digestion of chromatin with DNase I leads to a restricted number of specific cuts in the chromosome. In erythroblasts, transcribing embryonic B-globin mRNA, specific cutting sites are observed close to the corresponding gene. In erythrocytes, transcribing only adult B-globin mRNA, other cutting sites are found. The DNase I sensitive sites map close to the initiation site of transcription. In contrast, similar specific DNase I cutting sites are detected near the 2 α -globin genes, irrespective of the state of the development stage. In the same regions of the genome, no specific DNase I sites are detected in other types of cells.

Interaction of bromodeoxyuridine (BrdU) and B-lymphocyte mitogens in endogenous virus induction

J. Stoye and C. Moroni, *Friedrich-Miescher-Institut, Postfach 273, CH-4002 Basel*

Mitogen-induced terminal B-cell differentiation is accompanied by endogenous xenotropic C-type virus expression. Virus production requires both cell proliferation and differentiation BrdU, even though it partially inhibits the latter processes increases virus production 10 \times and 100 \times as measured by reverse transcriptase and infectious centres, respectively. BrdU incorporation into cellular DNA is required for virus enhancement. Genetic and biochemical experiments to determine whether BrdU amplifies mitogen induction or induces a different viral genome will also be presented.

The use of disc methods in physiological and genetical studies on plant cell cultures

A. Strauss, F. Bucher and P. J. King, *Friedrich-Miescher-Institut, Postfach 273, CH-4002 Basel*

Growth inhibition zones are formed in agar-plated plant cells (e.g. *Rosa*) when discs with high concentrations of some drugs are applied. For some drugs a quantification of the growth inhibition is possible under strictly standardized conditions. Parameters like cell density, growth rate, diffusion constant and moment of drug application, strongly affect the halo size. We attempt to find a mathematical function for these processes. This method can be applied for isolation and testing of drug-resistant variants and for testing the effect of drugs and antidotes on plant cells. – Growth *exhibition* zones are formed when plant cells are plated in agar medium containing a toxic drug and a disc bearing an antidote is later applied. We are examining if this method can be used for antidote screening and determination of the growth factor requirements of auxotrophic mutants. The drug cycloheximide alone also causes an exhibition zone as cells recover from transient growth inhibition at only very high concentrations.

Activity and stability of some key enzymes of inorganic nitrogen metabolism in bean leaf extracts

L. Streit, U. Feller and K. H. Erismann, *Pflanzenphysiologisches Institut, Altenbergrain 21, CH-3013 Bern*

Nitrate reductase (involved exclusively in assimilation of nitrate taken up) was most active in developing leaves. Glutamine synthetase (involved in assimilation of ammonium produced by nitrate reduction, allantoinic acid degradation, photorespiration or other deaminating processes) was active from leaf development until senescence. Glutamate dehydrogenase (presumably deaminating glutamate during nitrogen mobilization) showed highest activities in senescing leaves. In crude extracts nitrate reductase was least stable, glutamine synthetase remained longer active and glutamate dehydrogenase showed an excellent stability. The time course and the stability of glutamate dehydrogenase are consistent with its role in nitrogen mobilization.

High resolution shadowing of freeze-fracture faces and freeze-dried surfaces of purple membrane

D. Studer, H. Gross, S. Ruchti and H. Moor, *Institut für Zellbiologie und Institut für Kommunikationstechnik, ETH, CH-8093 Zürich*

The purple membrane of *Halobacterium halobium*, from which significant periodic details down to 7 Å are known

(Henderson, Unwin, *Nature* 257, 1975), was chosen as test specimen for assessment of methodological progress. The resolution of a shadow-cast film is limited by its granularity (grain size and density), which is dependent on its own characteristics, the evaporation parameters (vacuum, deposition rate, film thickness, surface temperature), and the interaction of the specimen surface with the shadowing material (decoration phenomena). By optimizing these parameters for Ta/W-shadowing we achieved image processed significant periodic details of 20–15 Å both on fracture faces produced at -196°C under UHV ($p \leq 10^{-9}$ Torr) and on adsorbed and freeze-dried membrane surfaces. The visualization of single bacteriorhodopsin molecules on the surfaces in the same arrangement as in the total mass projection (Henderson, Unwin) proves that the intrinsic protein molecules reach the membrane surfaces.

Partial dissociation and reassembly of chromatin

F. Thoma, S. Sütterlin and Th. Koller, *Institut für Zellbiologie, ETH-Hönggerberg, CH-8093 Zürich*

Structural effects of partial dissociation, fractionation and reassembly of soluble rat liver chromatin are studied by electron microscopy and DNA gel-electrophoresis after micrococcal nuclease digestion. As a morphological assay, the ionic strength dependent folding of H1-containing and H1-depleted chromatin is used (F. Thoma, Th. Koller and A. Klug, *J. Cell Biol.* 83, 403, 1979). – Elimination of nonhistone proteins (NHP) at 300–350 mM NaCl results in a slight shift towards higher ionic strengths of the ionic strength dependent folding. Furthermore, at very low ionic strength, a destabilization of the nucleosomal structure is observed. After elimination of histone H1 and NHP at about 500 mM NaCl no folding into definite higher order structures occurs; the nucleosomes unfold at very low ionic strength. – Conditions have been found to reconstitute the regular morphology of chromatin fibres by readdition of H1 and/or NHP to partially protein-stripped chromatin samples.

Effect of serum stimulation on cellular RNA and protein synthesis in resting 3T3 fibroblasts

J.-M. Tiercy and R. Weil, *Département de Biologie moléculaire, CH-1211 Genève*

3T3 mouse fibroblast cultures were kept in a resting state by incubation for 1 week in 0.5% bovine serum. The addition of 10% serum induces the transition to a growing state. This is characterized by an increase in total cellular RNA, followed by induction of cellular DNA synthesis. We quantitated cellular RNA, protein and DNA by colorimetric methods. [^3H]uridine-labelled nuclear and cytoplasmic RNA was analyzed by sedimentation in sucrose density gradients and by electrophoresis in tubular nondenaturing polyacrylamide-agarose gels. [^{35}S]methionine-labelled nuclear and cytoplasmic proteins were examined by electrophoresis in 1 or 2 dimensions. The results show that the addition of serum stimulates within less than 2 h synthesis of 4-7S RNA's and of rRNA. This is paralleled by the stimulation of overall cellular protein synthesis and is followed by a net increase in total cellular RNA and protein. The effects of serum stimulation are thus reminiscent of those induced by the infection of mouse and monkey tissue culture cells with SV40 or polyoma virus.

Tissue specific expression of α -amylase genes in the mouse: isolation and characterization of cDNA clones

M. Tosi, U. Schibler, L. Fabiani, A.-C. Pittet and P. Wellauer, *Institut Suisse de Recherches expérimentales sur le Cancer, Chemin des Boveresses, CH-1066 Epalinges*

α -Amylase isoenzymes are synthesized by the acinar cells of the pancreas and the salivary glands and to a lower extent also by liver cells. We have identified the α -amylase precursor proteins produced in a cell-free translation system stimulated by pancreatic or salivary mRNA. We have constructed full length cDNA clones to each tissue specific α -amylase mRNA. The structures of these clones were compared by restriction endonuclease mapping, S1 Berk and Sharp mapping and electron microscopy of heteroduplexes and of RNA-DNA hybrids. These studies have established that mouse pancreatic and salivary α -amylase mRNAs are transcribed from different genes. In contrast, the liver α -amylase mRNAs is indistinguishable from the salivary type mRNA within the coding region but contains additional nontranslated sequences.

Polypeptide composition of hepatitis A virus particles

J. D. Tratschin, G. Siegl, G. G. Frösner and F. Deinhardt, *Institute of Hygiene and Medical Microbiology, University of Bern, CH-3010 Bern, and University of Munich, Munich, Federal Republic of Germany*

Particles of hepatitis A virus (HAV) were purified from a series of stool samples and disintegrated in the presence of SDS. Subsequently viral proteins were labelled with ^{125}I . Electrophoretic analysis of the proteins revealed that the polypeptide composition of particles isolated from individual samples could be correlated with their density and sedimentation characteristics: HAV particles banding at 1.34 g/ml and sedimenting with 160S showed a spectrum of 4 polypeptides comparable to the pattern reported for enteroviruses. 2 of these polypeptides, however, were either completely absent or present only in traces in particles banding around 1.33 g/ml and sedimenting with less than 160S. Yet, the latter particles contained at least one additional polypeptide of between 43,000 and 50,000 daltons. This polypeptide possibly corresponds to a precursor protein also present in immature virions and empty capsids of enteroviruses. Therefore, the variation in the polypeptide pattern is assumed to indicate differences in infectivity and antigenicity between individual HAV samples.

Evidence that a naked core is the first precursor particle of the phage T4

F. Traub and M. Maeder, *Department of Microbiology, Biozentrum der Universität, CH-4056 Basel*

The phenotype of the mutants T2 23 (am 94), T4 23 (am H11) and T4 23 (am E1236) is represented by naked core-like structures. The strictly membrane-bound particles are identical in size and staining properties to prehead cores. They appear in ideal cross and central longitudinal sections as pentagons or hexagons, which would be in agreement with an icosahedral symmetry of these bodies. A central cavity contains a dense kernel which again is seen in prehead cores. The number of particles formed is highest at an incubation temperature of 30°C , where it corresponds 90 min p.i. to an expected yield of phage precursors. The naked cores do not seem to contain DNA, as revealed by Gautier's DNA-staining technique (A. Gautier, *Int. Rev. Cytol.* 44, 170, 1976). The formation of naked cores is dependent on the active head gene products 20, 21 and 22,

but not on 23, 24 and 31. This dependency and all data mentioned above are suggestive for a true precursorship of these particles.

Chromosome aberrations and cell death

J. Tremp, Strahlenbiologisches Institut der Universität Zürich, Postfach, CH-8029 Zürich

Compared to untreated controls, irradiated cells show on the one hand more chromosome aberrations and on the other hand a reduced proliferation capacity or are killed. The correlation between these 2 radiation effects was investigated. – Synchronized Chinese hamster fibroblast cells were irradiated in early G₁. The rate of chromosome aberrations was determined in the first post-irradiation division at 2-h intervals. The highest rate of chromosome aberrations occurred in cells with a first cell cycle of medium length. – In parallel samples we measured the colony-forming ability of mitotic cells. The proportion of cells forming macrocolonies decreased with increasing cell cycle length, whereas the number of non-colony-forming cells, i.e. cell death, increased. Irrespective of various cell cycle lengths and different rates of chromosome aberrations, the number of cells forming microcolonies remained constant. There was found a correlation between cells without chromosome aberrations and the ability to form macrocolonies, except for cells with a long first cell cycle, which formed less macrocolonies than expected.

The early functions of polyoma virus

H. Türlér, Department of Molecular Biology, University of Geneva, 30, quai Ernest-Ansermet, CH-1211 Geneva 4

The early region of polyoma virus DNA codes for at least 3 related proteins having a common amino-terminal sequence and being terminated at different sites in different reading frames. 2 genetically defined classes of mutants map in different parts of the early region. The hr-t (host range, transformation negative) mutants have either deletions of 2–4% or small insertions. The ts A mutants are defective in initiation of viral DNA replication and initiation of cell transformation at high temperature (39 °C). Polyoma virus induces a broad spectrum of biological effects, i.e. tumor formation, cell transformation, induction of mitosis, cell surface alterations, progeny virus production, etc. These facts suggest that there are multiple interactions between the early viral proteins and the host cell. An attempt is made to correlate the wild-type and mutant proteins with the biological effects. Eventually, this should allow us to find biological assays for the viral proteins and to distinguish between primary, i.e. directly virus-induced effects and secondary, cell-mediated effects.

Reconstruction of the 2-dimensional lattice structure of the photosynthetic membrane of *Rhodospseudomonas viridis*

E. Wehrli, I. Wildhaber, H. Gross, O. Kübler and K. Mühlethaler, Institut für Zellbiologie und Institut für Kommunikationstechnik, ETH, CH-8093 Zürich

The photosynthetic membrane of the bacterium *R. viridis* is largely crystalline (Giesbrecht and Drews, Arch. Mikrobiol. 54, 297, 1966). The structural units are arranged in a hexagonal lattice with a repeat of 130 Å. In previous work we studied the general architecture and the lattice structure of this membrane (Wehrli and Kübler, Proceedings in Life Sciences, Springer, in press). We are now studying the substructures of the repeating elements of the hexagonal

lattice by using high-resolution, low-dose electron microscopy and digital image processing. The membranes were treated with glutaraldehyde or various detergents to preserve or to increase crystallinity. After specific adsorption to various supports they were either embedded in negative staining solution or in glucose for direct observation, or freeze-dried for Ta/W-shadowing (see also Studer et al., this meeting). From these data a 3-dimensional model of the hexagonal lattice unit is derived and its functional implication discussed.

Stereological estimates of cellular membrane surface density are magnification-dependent

E. R. Weibel and Dagmar Baumgartner, Anatomisches Institut, Universität Bern, CH-3012 Bern

If surface density (S_V) of subcellular membranes is estimated by stereological methods at various EM magnifications (18,000–170,000 \times) it is found to increase systematically up to 130,000 \times and to remain constant above that magnification. S_V of endoplasmic reticulum and inner mitochondrial membranes increase 3–4 times, S_V of outer mitochondrial membranes by 20% only. This effect explains in part the differences in estimates for hepatocyte membrane surfaces obtained in different studies. – Magnification dependency of S_V measurements is interpreted in terms of Mandelbrot's concept of 'fractals' which allows resolution correction factors to be derived. A magnification of 130,000 \times is thought to offer critical resolution requiring no correction.

Effect of homocysteine (Ho) on cultured bovine (BEC) and human (HEC) endothelial cells

B. J. Weimann, H. Kuhn and H. R. Baumgartner, Pharma Research 3, F. Hoffmann-La Roche & Co. Ltd, CH-4002 Basel

Patients with homocystinuria, a disease of cystathionine synthetase deficiency, develop arteriosclerosis early in life. Arterial damage can also be produced in animals by infusion of Ho. BEC and HEC were used to study the influence of Ho and various pharmacological agents. Cells were identified by the presence of factor VIII antigen, silver precipitation at areas of cell contact and Weibel-Palade bodies in HEC. Cell damage induced by Ho was followed by [⁵¹Cr] release, [³H]adenine uptake and cellular growth. Confluent monolayers were treated with different amounts of Ho for various times with and without sulfinpyrazone (SP). 0.1–2.5 mM Ho had only a small, higher concentrations a rapidly increasing cytotoxic effect. However, using repeated treatment for 3–5 days, Ho was cytotoxic already at 0.5 mM; 5–10 mM of methionine was necessary to produce similar effects. In addition, similar results were obtained with Balb/c 3T3, Hela and smooth muscle cells. SP did not protect the cells. Conclusion: Chronic administration of Ho damages cultured cells at concentrations similar to those found in patients.

Single-strand specific DNA-binding protein from calf brain cortex

G. Winkler, C. W. Heizmann and C. C. Kuenzle, Institut für Pharmakologie und Biochemie, Veterinärmedizinische Fakultät, Winterthurerstrasse 260, CH-8057 Zürich

In a survey of the nonhistone chromosomal proteins of rat cortex neurons we have detected multiple single-stranded DNA-binding proteins. Among these, one prominent pro-

tein attracted our interest because it accumulates postnatally during a period where the neuronal chromatin undergoes unusual conformational changes. Lack of material prevented its isolation from rat neurons. Therefore we isolated a homologous protein from calf brain cortex. An extract of this tissue was treated with 2 M NaCl and Polyethylene glycol and was centrifuged. The supernatant was chromatographed sequentially on double- and single-stranded DNA immobilized on cellulose. A protein with strong affinity for single-stranded but not for double-stranded DNA was recovered in purified form. It had subunit mol.wt 35,000 and $pI > 8$. On 2D gel-electrophoresis the protein exhibited several forms differing in basicity. This same microheterogeneity was also a characteristic of the homologous helix destabilizing protein from rat cortex neurons.

Chromatin in living cells decondenses with an increase in the nuclear ionic strength

P. Wuhrmann and M. Lezzi, *Institut für Zellbiologie, ETH-Hönggerberg, CH-8093 Zürich*

Isolated chromatin decondenses, recondenses and decondenses again when exposed to increasing ionic strengths. In the living cell chromatin is also partially decondensed. Is it in the first (I) or the second (II) state of decondensation? In order to answer this question we determined the K^+ - and Na^+ -activities in the nuclei of salivary glands of *Chironomus tentans* larvae by means of ion selective microelectrodes. With oligopausing larvae the total monovalent cation activity is 50 mM, and the polytene chromosomes are compact with very few and small puffs. After a 24 h in vitro cultivation of the glands the ion activity is increased by a factor of 3. The chromosomes of such cultivated glands are elongated by approximately 20% and show wider interbands, many small and some large puffs. – This observation suggests that in the living cell chromatin is on the verge to the decondensation state II because an increase in ionic strength enhances decondensation. Were it in decondensation state I a transient condensation would be observed.

Structural organization of chromatin. I. Structural role of a preferentially digestible group of proteins in interphase chromatin

H. Wunderli and R. Hancock, *ISREC, CH-1066 Epalinges*

Interphase chromatin of P815, a mouse mastocytoma cell line, is isolated in a low salt, one step lysis procedure (Hancock et al., *Meth. Cell Biol.* 15, 127, 1977) as a nonaggregated, morphologically discrete structure which is then purified on a sucrose gradient. Although the nuclear membrane is removed under these conditions the chromatin structures are not unfolded and stay morphologically intact even after removal of histones and some nonhistone proteins (2 M NaCl). The particles are extremely fragile and their yield and sedimentation pattern vary in different ionic conditions. We optimized the method to yield 70–80% intact particles. Pronase digestion with increasing concentrations of enzyme reveals that below a critical concentration a few preferred proteins (mol.wt 86 K, 68 K, 56 K, 35 K) are gradually digested and only after their removal the structures fragment, whereas at higher concentrations the proteins are randomly digested and the structures disintegrate. The possible identity of the 68-K protein with the lamina protein (Gerace et al., *J. Cell Biol.* 79, 546, 1978) is being tested with antilamina antibodies.

Structural organization of chromatin. II. Comparison of protein patterns of metaphase and interphase chromatin in CHO cells

H. Wunderli, M. Westphal and R. Hancock, *ISREC, CH-1066 Epalinges*

Interphase and metaphase cells were harvested from colcemid-treated CHO cultures. Metaphase chromosomes and interphase chromatin structures were isolated by a low salt, 1-step lysis procedure and purified on sucrose gradients. After dehistonization (2 M NaCl) they were further purified by metrizamide density centrifugation. Both interphase and metaphase show a complex protein pattern when analyzed by SDS gel-electrophoresis. Qualitative as well as quantitative differences are found. The 3 major bands in interphase are in the range of 60–75 K mol.wt, whereas the 3 major bands in metaphase have mol.wts between 35 and 55 K. The possible identity of the latter with tubulin (55 K), actin (45 K) and tropomyosin (34 K) is being studied by antibodies. The 68 K protein present in interphase but not in metaphase probably corresponds to lamina proteins (Gerace et al., *J. Cell Biol.* 79, 546, 1978); this will also be tested by antibodies.

The flattening of biological structure during specimen preparation

M. Wurtz and M. Häner, *Department of Microbiology, Biozentrum der Universität, CH-4056 Basel*

Proteins of supramolecular structure are functional only in the presence of water. Its removal for microscopy leads to artefacts of the specimen, mainly flattening. We have measured flattening of naturally hollow cylinder, T4 phage contracted polysheath (prepared by J. Tschopp). By the length of shadow of platinum at 10, 20 or 30° the height of the particle is calculated. Using the goniometerstage of the Zeiss-10 electron microscope, allows to construct a model of the particle cross section. Assumably unflattened latex spheres are used as reference. The results are the following: 1. Air-dried; glow-discharged air-dried; amylin glow-discharged stained: flattening ratio 1.1–1.2. 2. Agar filtration, stained or unstained; ratio 1.4–1.5. 3. Glow-discharged, negative stained; ratio 1.9–2. These results are unexpected and contrary as the general believe. We thus continue the experiments and extend them to other specimen and preparation methods.

Tissue specific expression of α -amylase genes in the mouse: sequence analysis of α -amylase isoenzyme mRNAs

R. Young, R. Bovey and O. Hagenbüchle, *Institut Suisse de Recherches expérimentales sur le Cancer (ISREC), Chemin des Boveresses, CH-1066 Epalinges*

We have determined the nucleotide sequence of α -amylase mRNA from the mouse pancreas and salivary gland; different α -amylase genes are expressed in these tissues. These mRNAs exhibit 11% sequence heterogeneity. Nucleic acid residues are less conserved in the untranslated regions, which account for only 3.4% (pancreas) and 7% (salivary gland) of the total mRNA. While most mRNAs studied thus far contain AAUAAA in the 3' nontranslated region, the pancreas α -amylase mRNA does not. – Only one frame can encode the 58,000 dalton α -amylase protein – the other 2 contain numerous termination triplets – and this predicts an amino-acid sequence whose composition is essentially identical to that determined for rat α -amylase (Sanders and Rutter, *Biochemistry* 11, 130, 1972). Although the amino-

acid composition is highly conserved, the sequence predicted for the 2 proteins differs by 12%. One striking difference is the appearance of an additional 3 contiguous amino-acids in a region of high sequence variability located near the middle of the salivary gland α -amylase.

Growth factors and the proliferation of cells in semi-solid media

A. Zumbé and R. R. Bürk, *Friedrich-Miescher-Institut, Postfach 273, CH-4002 Basel*

The state of inhibited cell growth in suspension culture was examined by supplementing semi-solid agar with growth factors, proteases and adhesion proteins. The cell lines (Balb/c 3T3, BHK21/13, NRK, WI38) and their trans-

formed derivatives (SV3T3, SV28, NRK-MSV, VA13), respectively, can all be shown in monolayer culture to be responsive to growth factors, fibroblast growth factor (FGF) and epidermal growth factor (EGF) in a thymidine incorporation assay and/or a migration assay. BHK21/13 and SV3T3 could be induced to grow in agar suspension with FGF; SV28 grew without added growth factors. Viral transformation of BHK21/13 was not a prerequisite for growth in agar when FGF was present. Also, the virally transformed SV3T3 did not grow in agar without added FGF. Fibronectin, trypsin, fibrinogen and collagen (I-IV) had no effect on the inhibition of the growth of BHK21/13 in agar. The effect was nongenetic as cells stimulated to grow in agar lost their ability to do so if replated in agar without FGF. The mechanism by which FGF induces these cells to proliferate in agar is being further investigated.

ERNÄHRUNGSFORSCHUNG RECHERCHES SUR LA NUTRITION NUTRITION RESEARCH

The mayor acid soluble proteins of the soybean

P. Amiguet, *Nestlé Products Technical Assistance Co. Ltd, P.O. Box 88, CH-1814 La Tour-de-Peilz*

The bulk of soybean protein (80-90%) consists of the high mol.wt complexes glycinin and conglycinin which precipitate selectively at pH 4.5. The remaining protein, referred to as acid soluble fraction (ASF) is known to have antinutritional properties in mice and may therefore have long-term effects also in man. ASF was separated by gel-chromatography in 6 mayor fractions which after further purification and characterization by SDS-electrophoresis, isoelectric focusing, amino-acid analysis and selected tests for enzymatic activity were shown to consist each of a single protein species. These are a) a glycoprotein (6% N, mol.wt 200,000), b) a multisubunit complex of mol.wt 150,000 (subunits of mol.wts 49,000, 30,000 and 18,000), c) lipoxylase (mol.wt 100,000), d) β -amylase (mol.wt 61,000), e) lectin (subunits of mol.wt 30,000) and f) trypsin inhibitor (mol.wt 21,000). Protein a could be detected in polyacrylamide with the Schiff stain only. Protein b focused at pH 9, all others between pH 6.5 (lipoxylase) and pH 4.5 (trypsin inhibitor).

Antibacterial activity of skim milks fermented with lactic bacteria

H. Amster and R. Jost, *Nestlé Research Laboratory, CH-1814 La Tour-de-Peilz*

Whey concentrates from milk cultures of *L. acidophilus*, *L. bulgaricus*, *S. thermophilus* and others, inhibited growth of *E. coli*, *P. fluorescens* and *S. aureus* in the disk diffusion assay. Inhibition was due to the presence of high concentrations of lactic acid in the fermented wheys. *L. acidophilus* whey had an acidity of 72°SH corresponding to 0.18 M lactic acid. In a defined medium lactic acid strongly inhibited growth of *E. coli* at pH 5-5.3 compared with acidification by HCl inhibitory only at pH 4.5. This confirms the important role which lactic acid plays in the protection of fermented foods against bacterial spoilage. Above pH 5 lactic acid showed little inhibitory activity, and no antibiotic activity was observed with whey concentrates in a buffered medium at pH 6.8. There was no evidence of antibiot-

ic production by the lactic bacteria as suggested by several authors and the growth inhibition they observed with fermented wheys was probably due to lactic acid.

Effects of dietary fats on polyenoic fatty acids in membranes and tissues

M. Blum, C. Richter and A. L. Prabucki, *Institut für Tierproduktion, Gruppe Ernährung, and Laboratorium für Biochemie I, ETH, CH-8092 Zürich*

Rat experiments were conducted to investigate the effects of plant oils rich in linoleic acid and animal fats on membrane and tissue levels of polyenoic fatty acids. Feeding fats derived from animal sources led to substantial increases of ω 3 docosaenoic acids and to corresponding decreases in linoleic acid in complex lipids isolated from the heart and liver. Similar effects were observed in heart mitochondria, liver mitochondria and liver microsomes. - When mitochondrial and microsomal membranes were assayed for membrane fluidity (DPH), no significant differences could be detected between membranes rich in ω 6 and ω 3 polyenoic fatty acids. Possible physiological consequences of these findings are discussed.

Glycogen utilization in exercise after increased plasma fatty acids or ketone bodies

J. Décombaz and L. Roux, *Research Department, Nestlé Products Technical Assistance Co. Ltd, LABIOR, CH-1350 Orbe*

Depletion of muscle glycogen (Gn) can be a major factor contributing to exhaustion during prolonged strenuous exercise. The rate of fatty acid oxidation by muscle is roughly proportional to the concentration of circulating FFA. Hence, we investigated the influence of elevated plasma FFA or β -hydroxybutyrate (OHB) on Gn utilization. Rats trained for 5 weeks to run on a treadmill were given 4 oral treatments: maize oil (+ heparin s.c.) (MO), medium-chain triglycerides (MCT), glucose (G) or water (W). Plasma FFA in MO was raised from 0.60 to 1.91 mM, while MCT had OHB elevated from 0.67 to 2.34 mM. Basal liver Gn was higher in G (57 ± 4 [9] mg/g) than in MO (42 ± 3). The rats were then exercised for 40 min (25 m/min, 10% grade).

Gn utilization in liver (26%) and muscle (soleus 73%, gluteus supf. 12%, red vastus lat. 60%) was essentially the same (mg) in all groups, as were running times to exhaustion (MO: 168 ± 12 min, MCT: 168 ± 13 , G: 189 ± 13 , W: 180 ± 9 , $\bar{x} \pm SE$ [12]). These results do not support the view that elevation of plasma FFA or ketones has a sparing effect on Gn utilization during endurance exercise.

In-vitro effects of cafestol, a diterpene compound, on respiration-linked functions of isolated rat liver mitochondria

R. Guidoux, Biological Laboratories, Nestlé Products Technical Assistance Co. Ltd, CH-1350 Orbe

The respiration rate of isolated mitochondria, incubated in a HEPES-buffer solution at 25°C (pH 7.4 or 7.6), was monitored with an oxygen electrode. At concentrations 10^{-5} to 10^{-4} M, cafestol exerted a dose-dependent inhibition of both State 3 and DNP-uncoupled respiration, when supported by glutamate and malate. The respiratory burst which is linked to Ca^{2+} loading of mitochondria, in the presence of Pi, was also slowed down, but was substantially prolonged by cafestol. When added after Ca^{2+} loading, cafestol also triggered a transient activation of the respiration rate. – With succinate as substrate, no inhibition of mitochondrial respiration was induced by cafestol in the metabolic conditions indicated above, but a secondary and here persisting activation of respiration, subsequent to Ca^{2+} loading, was again produced by the substance. These data suggest that cafestol causes both a rotenone-like inhibition of the respiratory chain and a release of Ca^{2+} from loaded mitochondria.

Effects of a mixed and of a very low-fat diet on substrate utilization in man, measured in a calorimetric chamber

M. Hurni and Ph. Pittet, Institut de Physiologie, Bugnon 7, CH-1011 Lausanne

11 normal-weight subjects (6 females [F], 5 males [M]; %ideal weight: 106 ± 2 [mean \pm SEM]) were fed for 7 days, with an interval of 2 weeks: a) a mixed diet (food quotient [FQ]=0.84): Protcal% (PROT) 17 ± 0.3 ; Lipcal% (LIP) 42 ± 1 ; CHOcal% (CHO) 41 ± 1 , providing 1883 ± 78 and 2112 ± 60 kcal/day for F and M, respectively; b) isocalorically, a very low-fat diet (FQ=0.94): PROT 19 ± 0.4 , LIP 6 ± 0.2 , CHO 75 ± 0.4 . Subjects spent the last 24 h of each dieting period in a calorimetric chamber for continuous gas exchange measurements and performed an exercise on bicycle: 30 W for 2.5 h. Composition of fuel oxidized during 24 h for FQ=0.84 was: PROT 15 ± 1 and 16 ± 2 , LIP 65 ± 6 and 64 ± 6 , CHO 20 ± 4 and 20 ± 1 for F and M, respectively. Values obtained with FQ=0.94 were: PROT 14 ± 2 and 15 ± 2 , LIP 28 ± 5 and 32 ± 5 , CHO 58 ± 2 and 53 ± 4 . – Substrates utilized for exercise only were, for FQ=0.84 and 0.94, respectively: LIP 57 ± 8 and 53 ± 5 , CHO 42 ± 8 and 46 ± 5 for F and LIP 47 ± 6 and 48 ± 6 , CHO 53 ± 8 and 52 ± 8 for M. Thus, although diets modified fuel utilized for daily metabolism, they had no influence on substrates oxidized for exercise.

Plastein synthesis as a new approach to supply essential amino acids in product fortification

R. Jost, J.C. Monti and R.S. Temler, Nestlé Research Department, CH-1814 La Tour-de-Peilz

Plastein synthesis can be used to incorporate essential amino acids into peptide bond. By achieving this, their

chemical stability is enhanced and thus, organoleptical problems in product fortification are less severe. With papain as catalyst, we prepared soy-based plasteins with up to 40% of covalently linked methionine. Substrates of this reaction were DL-methionine ethyl ester and soy protein. The resulting plastein, a water-insoluble and tasteless product, was equivalent to L-methionine in compensating the methionine deficiency of experimental diets (soy isolate and amino-acid mixture) for growing rats.

Synthesis and toxicology of 3 naturally occurring cyanoepithioalkanes

J. Lüthy, A. von Däniken, B. Manthey, U. Zweifel, Ch. Schlatter and M.H. Benn, Institut für Toxikologie der ETH und Universität Zürich, CH-8603 Schwerzenbach, and Chemistry Department, The University of Calgary, Calgary, Alberta, Canada

(\pm)-1-cyano-2,3-Epithiopropene (1), (\pm)-1-cyano-3,4-epithiobutane (2) and (\pm)-1-cyano-4,5-epithiopentane (3), 3 compounds naturally occurring in cruciferous vegetables, were synthesized and completely characterized by elemental analysis, as well as IR-, MS- and 1H - and ^{13}C -NMR-spectroscopy. The single-dose LD₅₀ of 1, 2 and 3 in mice were in the range of 100–500 mg/kg b.wt. 1 was tested for mutagenicity in the 'salmonella/mammalian microsome' test and gave positive results in the strains TA-100 and TA-1535 at a dose level of > 1 mg/plate. (^{35}S)-labelled 1 was found to bind covalently to DNA of rat liver, colon and stomach in vivo. 4-(p-Nitrobenzyl)-pyridine was slowly alkylated by 1, 2 and 3 in vitro. These results suggest that cyanoepithioalkanes are weakly mutagenic compounds.

Oral starch degradation and its influence on acid production in human dental plaque

Jeanette E. Mörmann-Buchmann, Zürich University Dental Institute, Department of Cardiology, Periodontology and Preventive Dentistry, P.O. Box 167, CH-8028 Zürich

Starch degradation by salivary α -amylase, its time dependence and influence on plaque acid production was investigated in vitro and in vivo. Analysis of the composition and fermentability of starch digests included gel-filtration chromatography and intraoral plaque pH-telemetry. Both in vitro with conditions similar to those of the oral cavity and in vivo cooked wheat starch, whole-wheat bread and wheat starch biscuit were hydrolyzed rapidly to maltose, maltotriose and limit dextrins. Oral α -amylolytic degradations of wheat starch products, studied in 4 volunteers, initiated significant drops in interdental plaque-pH. In vivo degradation and fermentation were influenced by salivary flow rate, amylase activity as well as by physical properties of the starch products.

24 h-energy expenditure (24-EE) and resting metabolic rate (RMR) in control (C) and obese (O) subjects

E. Ravussin, B. Burnand, Ph. Pittet and Y. Schutz, Institute de Physiologie, 7, Bugnon, CH-1011 Lausanne

7 C (103% id wt) and 10 O (150% id wt) were investigated. 24-EE and RMR (postabsorptive state) were obtained by continuous gas exchange measurements in a metabolic chamber (5×2.5 m) and for 1.5 h with a hood open system, respectively. In the chamber, spontaneous activity only was allowed and monitored by a radar system; a 2490 kcal diet was fed to each subject. – 24-EE and RMR were respectively 1960 and 1426 kcal/day in C and 2359 and 1756 kcal/d in O. Although 24-EE and RMR, when expressed on a b.wt

or total body fat basis, were significantly different between C and O, these differences disappeared once results were standardized for surface area or lean body mass. When expressed on the basis of sleeping metabolism, the percent increase in diurnal energy expenditure was significantly greater in O (+55%) than in C (+36%). This difference was due to both a higher diurnal and a lower sleeping energy expenditure in O. - Although 24-EE standardized for lean body mass or surface area was similar in C and O, the 2 groups showed a difference in the pattern of 24 h-energy metabolism.

Alcohol consumption and vitamin B₆ status in 20-40-year-old Heidelberg men

B. Schellenberg, L. Arab, P. Oster and G. Schlierf, Klinisches Institut für Herzinfarktforschung an der Medizinischen Universitätsklinik, Bergheimer Strasse 58, D-69 Heidelberg, Federal Republic of Germany

In contrast to studies showing alcohol intake causally associated with a decrease in serum parameters of vitamin B₆ status, we have seen, in an epidemiological study of 20-40-year-old normal men, a positive correlation between alcohol intake and pyridoxal 5 phosphate (P5P) on one hand and a negative association with erythrocyte glutamic oxaloacetic transaminase reactivity (α EGOT) on the other. - The men with an alcohol intake < 40 g/day had a lower mean P5P (5.17 mg/dl) than those drinking > 60 g/day (7.30 mg/dl). α EGOT values confirmed these findings, with

differences (1.64, 1.79) significant at a $p < 0.01$ level. - These surprising results may be explainable in terms of source of alcohol, as German beer contains 0.5 mg B₆/l. Comparison showed wine drinkers to have mean vitamin B₆ values like those of nondrinkers (P5P=5.16, 5.18; α EGOT=1.81, 1.80). In contrast beer drinkers showed significant differences (P5P=6.3, α EGOT=1.72).

Alterations in pancreas of rats fed on different levels of soya flour and casein

R. S. Temler, Nestlé Research Department, CH-1814 La Tour-de-Peilz

8 groups of rats were fed on either 10, 20, 30 or 40% soya containing active trypsin inhibitor (T.I.) or casein for 21 days. - The average pancreatic wt/100 g b.wt of the casein and soya fed rats were: 313±14, 577±15, 611±16, 622±16 and 487±29, 623±24, 774±28, 979±16, respectively. DNA and protein analysis showed that the increase in pancreatic size due to casein was a result of both hypertrophy and hyperplasia. - Trypsin and chymotrypsin activities increased and amylase activity decreased with increasing protein level. Pancreatic proteases of the soya group were 30% higher than in the casein group and amylase 2-3 times lower. Thus high protein diet and soya containing T.I. have a similar action on the pancreatic enzymes levels. T.I. is a potent stimulator of proteases and very potent inhibitor of amylase synthesis.

Instructions to authors

Experientia is published on the 15th of every month and can be obtained in any country through booksellers or from the publishers. All communications to the editors should be addressed to the publishers. All manuscripts for publication in a given number must be in the hands of the editors 3 months before publication.

Articles of general scientific interest, of interdisciplinary character: briefly stated and hitherto unpublished original reports of sufficient novelty value.

Experiments Papers in which animal experiments have been conducted without using the appropriate anaesthesia will not be accepted.

Manuscripts (including all figures and tables) should be submitted in duplicate.

Text should not exceed 2-3 typewritten pages (50-60 lines). 1-2 relevant figures or tables. English summary of maximum 4 lines. Abbreviations should be properly explained. References should be numbered consecutively and be presented on a separate page. Name and address have to be placed directly under the title. Linguistically inadequate manuscripts will be returned. Manuscripts in languages other than English should be supplemented by an English translation of the title. Footnotes should be avoided.

Figures Illustrations should be separate from the text, with the author's name on the back in soft pencil. The desired labelling should be shown on a second set of figures, which will be used as a model for

inscriptions. Drawings for reproductions should be on good paper in Indian ink, photographs should be supplied as glossy positive prints. The illustrations should be at least one and a half times as large as the definitive size desired. Over-large figures can be easily damaged in the mail. Captions should be selfexplanatory, without reference to the text.

Tables should be provided with a title and with selfexplanatory captions.

Headings In submitting their manuscript to *Experientia*, authors are requested to indicate one of the headings mentioned below, under which they would wish to place their short communication:

1. Mathematics and Physics; 2. Cosmology, Astronautics, Cosmonautics; 3. Mineralogy, Geophysics, Oceanography; 4. Inorganic and Physical Chemistry; 5. Organic Chemistry; 6. Biophysics; 7. Molecular Biology, Cellular Biology; 8. Genetics; 9. Botany; 10. Zoology; 11. Ecology; 12. Biochemistry (analytic and synthetic); 13. Biochemistry (Enzymes, Metabolism); 14. Physiology; 15. Neurology; 16. Pharmacology, Toxicology, Pathology; 17. Experimental Gerontology; 18. Anatomy, Histology, Cytology, Histochemistry; 19. Embryology; 20. Endocrinology; 21. Circulation, Cardiology, Angiology; 22. Nutrition, Gastroenterology; 23. Hematology, Serology; 24. Immunology, Allergy; 25. Microbiology, Parasitology, Chemical Therapeutics; 26. Oncology, Carcinology, Cytostatics; 27. Radiology.

Reprints The authors receive 50 reprints, without cover, free of charge. Price-list for further reprints is available.